UNIVERSITEIT VAN PRETORIA
UNIVERSITY OF PRETORIA
YUNIBESITHI YA PRETORIA

Predicting the development of weather phenomena that influence aviation at Abu Dhabi International Airport

by

Michael Pierre de Villiers

Submitted in partial fulfilment of the requirements for the degree

DOCTOR OF PHILOSOPHY

in the

Faculty of Natural and Agricultural Sciences

University of Pretoria

February 2010

SUMMARY

Predicting the development of weather phenomena that influence aviation at Abu Dhabi International Airport

Researcher: Michael Pierre de Villiers

Supervisor: Professor Johan van Heerden

Department: Geography, Geoinformatics and Meteorology

Degree: Doctor of Philosophy

Faculty: Natural and Agricultural Sciences

University: University of Pretoria

Keywords: Abu Dhabi, United Arab Emirates, Shamal, Nashi, fog, sand storm, dust storm, thunderstorm, rain trough, tropical depression, land and sea breezes.

The United Arab Emirates is a new country that has had little time to accumulate a scientific heritage. Meteorologically researched and documented weather material for forecasters is virtually non-existent and that available is fragmented and anecdotal.

The thesis tackles this problem by identifying weather phenomena significant to aviation in the Emirates and particularly at Abu Dhabi International Airport (ADIA). Mechanisms responsible for their development are described and applicable forecasting rules and principles are derived. Surface and upper air observation data at ADIA from 1983 to 2002 were analysed to identify the weather phenomena, their associated weather systems and for statistical analyses. When relevant, observation data at Al Ain was also used. Post-processed numerical weather prediction Global Forecast Service Eta model data are used and when and where possible radar and satellite imagery. A secondary aim is to provide information of the general seasonal climate. This was achieved by means of a literature study of the dominating weather systems and the presentation of surface and upper air mean circulation charts.

Fog is the most important weather phenomenon and serious disrupter of aviation at ADIA throughout the year. It does not occur during Shamal conditions, but fog can form well inland on the edge of the Empty Quarter at the Liwa Oasis when the Shamal wind becomes light. Contrary to local belief, fog is unlikely to occur on two, or more, consecutive nights. The Shamal can last for several days and disrupt helicopter flights to the oil rigs, while anabatic and katabatic effects often make it gustier and stronger inland at Al Ain than ADIA. While dust storms occur in strong southerly winds off the desert, the Shamal can bring dust from further afield from the north as can the previously unreported Nashi wind. The sea breeze can extend about 150 km inland to Al Ain and the Liwa Oasis. Thunderstorms associated with winter upper air troughs from the west, are the main producers of rain, while occasional thunderstorms off the Hajar Mountains in the east bring some rain in summer. Tropical depressions are a rare event.

SAMEVATTING

Voorspelling van die ontwikkeling van weerverskynsels wat lugvaart by die Abu Dhabi Internasionale Lughawe beinvloed

Navorser: Michael Pierre de Villiers

Studieleier: Professor Johan van Heerden

Department: Geografie, Geoinformatika en Meteorologie

Graad: Doktor in Filosofie

Fakulteit: Natuur- en Landbouwetenskappe

Universiteit: Universiteit van Pretoria

Die Verenigde Arabiese Emirate (VAE) is ‘n nuwe land min tyd gehad om ‘n wentenskaplike erfnis op te bou. Weerkundige navorsing sowel as die dokumentasie van weervoorspelling-tegnieke en kennis bestaan amper nie en dit wat wel bestaan is, is gefragmenteer en in is hoofsaaklik anekdoties (van aard).

In hierdie theses word die problem aangespreek deur die identifisering van belangrike weer-verskynsels asook die gepaardgaande weerstelsels wat ‘n invloed het op lugvaart in die Emirate en veral by Abu Dhabi Internasionale Lughawe. Die meganismes verantwoordelik vir hul ontwikkeling word beskryf sowel as die reëls en beginsels toepaslik vir die voorspelling van hierdie weerstelsels. Weerkundige waarneemings, te Abu Dhabi en wat oor twintig jaar (1983 tot 2002) strek, oppervlak asook bolug, was nagevors om hierdie weer-verskynsels en die weerstelsels wat hulle veroorsaak te identifiseer. Hierdie data is ook vir statistiese doeleindes aangewend. Waar van toepassing was die oppervlak waarnemings te Al Ain ook benut. Data afkomstig van die Numeriese Globale Voorspellingsdiens Eta Model was ook gebruik, wanneer en waar moontlik, asook radar en satelietbeelde. ’n Tweede doel van die projek was die opstel van ’n algemene klimatolgie vir die Emirate. Dit is bereik deur ‘n literatuurstudie van die dominante weerstelsels en aangevul deur die opstel (voorsiening) van oppervlak en bolug gemiddelde sirkulasiekaarte.

Die voorkoms van mis is die heel belangrikste weerverskynsel en het ’n ernstige en nadelige invloed op lugvaart by die Abu Dhabi Internastionale Lughawe. Mis kom nie voor gedurende Shamal toestande nie, maar dit kan vorm in die binneland veral in die omgewing van die Liwa Oase wanneer die Shamal wind swak word. In stryd met plaaslike (opvatting) mening, is die voorkoms van mis onwaarskynlik op twee of meer opeenvolgende aande. Die Shamal kan vir etlike dae lank duur en helikopter vlugte na die oliebore ontwrig. Anabatise en katabatise effekte maak dit dikwels meer turbulent and sterker in die binneland by Al Ain. Sandstorms kom voor wanneer ‘n sterk suidelike wind uit die woestyn waai. Die Shamal kan ook stof van ver in die noorde bring en so ook die Nashi wind wat nog nie vantevore beskrywe was nie.. Die seebries kan so ver as 150 km die binneland indring en word waargeneem by Al Ain en die Liwa Oase. Donderstorms, geassosieer met winter bolug troë vanuit die weste, is die belangrikste bron van reën, maar in die somer kom reën af en toe voor uit donderstorms wat ontstaan oor die die Hajarbege in die ooste. Tropiese laagdrukstelsels (tropiese werwelstorms) kom baie selde voor.

ACKNOWLEDGEMENTS

The author wishes to express his appreciation to the following organisations and persons for their assistance and contribution to make this thesis possible:

- Meteorological Office, Abu Dhabi International Airport, Abu Dhabi Directorate for Civil Aviation, United Arab Emirates, for the observation and computer model data.
- The South African Weather Services library and in particular Karin Marais and Anastasia Demertzis.
- The support of Weather Services International, Andover, United States of America and Birmingham, United Kingdom.
- Professor Doctor Johan van Heerden, my supervisor, for his many years of guidance, support and in particular his kindness.
- Professor Doctor C. J. (Hannes) de Wet Rautenbach for his kind assistance and support.
- My wife Roz for her support and encouragement.

DECLARATION

I, Michael Pierre de Villiers, declare that the thesis, which I hereby submit for the degree Doctor of Philosophy at the University of Pretoria, is my own work and has not previously been submitted by me for a degree at this or any other tertiary institution.

SIGNATURE: ……

DATE: ……

TABLE OF CONTENTS

LIST OF TABLES

LIST OF FIGURES

LIST OF SYMBOLS

°	Degree.
°C	Degrees Celsius, previously Centigrade.
θ_e	Wet-bulb potential temperature.
≥	Equal to, or greater than.
>	Greater than.
≤	Equal to, or less than.
<	Less than.
ω	Vertical motion in the pressure coordinate system.

LIST OF ABBREVIATIONS

ADIA	Abu Dhabi International Airport.
AGL	Above ground level.
AMS	American Meteorological Society.
AVN	Aviation NWP model product.
BLDU	Blowing dust.
BR	Mist.
CAPE	Convective available potential energy.
CAT	ILS category level.
DALR	Dry adiabatic lapse rate.
dBZ	Radar reflectivity unit. The reflectivity is related to the number of drops per unit volume and the 6^{th} power of their diameter. Rainfall rate can be determined using an empirical formula called the Z-R relationship.
DU	Dust.
ECMWF	European centre for medium range weather forecasting.
FG	Fog.
ft	Feet
GFS	Global Forecast Service.
gpm	geopotential metres.
GRADS	A type of NWP model post-processing product
hPa	Air pressure in hectoPascals. Previously millibar(s) was used.
HZ	Haze.
ICAO	International Civil Aviation Organization.
ILS	Instrument landing system.
KT	Knots.
m	Metres.
ms^{-1}	Metres per second
MSL	Mean sea level.
NWP	Numerical weather prediction.
NWS	National Weather Service (USA).
PCRGIDDS	Personal Computer based Gridded Interactive Display and Diagnostic System.
PPI	Plan position indicator.
RVR	Runway visual range.
SALR	Saturated adiabatic lapse rate.
SAWS	South African Weather Service, formally the South African Weather Bureau.
UAE	United Arab Emirates.
UK	United Kingdom.

UKMO	United Kingdom Meteorological Office.
UTC	Universal Time Corrected. The same as Greenwich Mean Time (GMT).
VCFG	Fog in the vicinity.
WAFS	World area forecast system.
WBPT	Wet bulb potential temperature.
WMO	World Meteorological Organization.

CHAPTER 1

INTRODUCTION

1.1 GENERAL

Although people have lived in the region since time immemorial, the United Arab Emirates (UAE) is a new country. Its existence as a federation of emirates dates back to 1971. The people of the region were mostly nomadic with small fishing and pearl diving villages at the coast and small settlements, at oases inland, provided the only forms of permanent residence. The discovery of oil and its exploitation changed this (United Arab Emirates Yearbook, 2001).

Today the UAE is a developed country with all the trappings and infrastructure of a modern country. With development comes the need to know the weather for aviation, oilrig operation, fishing and other day-to-day activities. Historically, it has had little time to accumulate a scientific heritage. Meteorologically, this is evident by the dearth of detailed forecasting knowledge and material for forecasters in the UAE. What little information is available is fragmented and often anecdotal. This lack of published information became apparent when the author (de Villiers 2003) did background research on wind towers in the UAE. Knowledge of the area had to be gleaned from books which discuss the climate and weather in generalised form by authors such as Taha, Harb, Nagib, and Tantawy (1981) and Martyn (1992).

Taha, et al (1981), although describing the climate of the countries in the Arabian Peninsula, do not even mention the UAE although the country was formed in 1971. They broadly mention the prevailing northerly to north-westerly winds in summer due to the monsoon trough over north-western India to the Arabian Gulf and winds from “different directions” in non-summer months. Apart from drawing attention to the hot desert climate in the Arabian Peninsula they also mention the importance of passing troughs in the upper westerlies in winter and spring as an important source of rain as well as thundershowers. This is discussed in more detail by Membery (1997) when such a system passed over the Middle East during December 1995. It brought persistent and heavy rain to the UAE and the Musandam Peninsula, as well as heavy snow on the Zagros Mountains in Iran. Membery (1985) also draws attention to the occasional influence of tropical depressions when, in a case study, he cites such a system that moved from the Arabian Sea across Oman and the UAE to the Rub Al Khali (Empty Quarter) of eastern Saudi Arabia.

Martyn (1992) discussing the “Levant and the Arabian Peninsula” also uses a broad brush to cover the weather in the region. He also makes mention of passing depressions in winter months as being a source of precipitation. But he is more specific in mentioning the persistent summer wind over the Gulf Sea known locally as the Shamal (meaning northerly) and its cooler more north-easterly winter Nashi wind. Once again, there is no specific mention of the UAE. More recently there has been published work by Membery (1983) about the Shamal wind at the Gulf State of Bahrain and by Rao, et al (2001 and 2003) in nearby Qatar. Further to the north Safar (1985) published a booklet on dust and dust storms in Kuwait.

More UAE specific studies by Zhu and Atkinson (2004), Eager et al (2005) and Eager and Raman (2005) draw attention to the high annual consistency of the sea and land breeze across the UAE coast. Of a more maritime nature, Jackson (1987) discusses the occurrence of waterspouts known to occur within sight of the UAE coast and Davey (1987) documents the destruction caused to the Jebel Ali Sailing Club by a tornado waterspout and Western (1997) gives a synopsis of forecasting for offshore sport fishing. As is to be expected in such an arid area considerable weather modification research, supported by a lengthy cloud physics study has been carried out to investigate the feasibility of hygroscopic seeding to enhance the precipitation in the hyper-arid zone of the Arabian Peninsula. This is joint venture between the UAE, Sultanate of Oman and the National Center for Atmospheric Research in Boulder, Colorado, USA (Breed et al 2005, Breed et al 2002, Jensen et al 2005 and Bruintjes and Yates 2003). Consideration has also been given to the effect of sodium chloride aerosols due to the proximity of the Gulf Sea (Salazar et al 2003) and ground water recharge (Yates et al 2005). Most recently, Al-Brashdi (2007), after a 9 day study of convective activity over the Western Hajar Mountains in the Sultanate of Oman, proposed an improved technique for forecasting the occurrence of seedable clouds, the aim being to improve precipitation in the area. To do this he suggested the Oman Convection Index (OCI), an improved locally effective derivative of the K-index (KI).

In 1996 the United Arab Emirates Department of Meteorology published a statistical book on the "U.A.E. Climate." As the title suggests, this concentrates on climatic tables of temperature, wind speed, cloudiness, humidity and precipitation. It is pointed out that in the summer months the monsoon dominates the area. Rising air over the Assam area of India, results in a subsiding column over the Arabian Gulf. So, although there is a "shallow semi-permanent trough of low pressure" over the region, the subsidence sub-tropical anticyclone above it prevents cloud growth and therefore rainfall. As a result of this and the mostly light northerly winds off the Gulf Sea, the UAE is very hot and very humid during the summer months. Occasionally hot and dry winds blow from the south and disrupt the more persistent hot and humid Shamal from the north off the Gulf Sea. These are more likely during March and April and are "accompanied by sand storms." During the winter months the UAE comes under the influence of the Asian anticyclone with occasional cold and dry surges from the east. And, as mentioned above, occasional rain bearing troughs pass through.

All this is very interesting, but to the author's knowledge no researched and/or published aviation meteorological literature exists for Abu Dhabi International Airport (ADIA) and the UAE. Therefore, a greater understanding of the mechanisms of local significant weather processes in the UAE and a methodology for forecasting them, combined at one source, is important. An attempt is made to address this lack of knowledge in the various chapters that follow and deal specifically with weather phenomena such as fog, dust and dust storms, thunderstorms, land and sea breezes, the Shamal and the Nashi winds.

1.2 SCOPE OF THE STUDY

Meteorological aviation activity in the Emirates is primarily confined to providing a service for helicopter operations to the offshore oilrigs and onshore drilling sites, as well as the more critical take-off and landing information at the international airports for commercial airlines. General aviation activity is very limited. Internationally, the normal spectrum of information is provided to commercial airlines operating to and from the UAE. The World Area Forecast Service at Exeter in the United Kingdom provides most of the en-route information for international flights. This information is merely relayed to the airlines by the meteorological

offices at the UAE international airports. Consequently, this study is confined to those meteorological phenomena peculiar to, and most important to, aviation in the region. Examples are fog, dust storms and dust, thunderstorms, rain bearing troughs, the Shamal (northerly wind) and (briefly) the Nashi wind, as well as land and sea breezes. In particular this study relates to ADIA, for which the observation data and numerical weather prediction (NWP) model data were obtained. By way of an introduction to weather in the region, the general atmospheric circulation and the seasonal sequence of the weather in the UAE is also presented. Although it gets very hot at ADIA, with summer maximum temperatures routinely reaching 45°C to 49°C (U.A.E. Climate, 1996), air temperature has not been included in this study. High temperatures decrease air density, increase aircraft take-off and landing speeds and considerably increase the runway length required (UKMO, 1994). However, at ADIA, and the UAE in general, this is not a problem, because the runways are suitably long and near to sea level.

1.3 METHODOLOGY

The lack of previous research dedicated to the UAE has meant that a method similar to that used by Taljaard (1985) in the ground breaking study of South African upper air cut-off lows has had to be adopted. This method relies on case studies and statistical analyses of limited data records when and where available. Taljaard (1994-1996) also relied on case studies in his 5 part series on South African weather phenomena, atmospheric circulation systems and synoptic climatology.

Observation data, both surface and upper air, at Abu Dhabi International Airport (ADIA) for the 20 years from 1983 to 2002 were analysed to identify significant weather phenomena and their associated weather systems as well as for statistical purposes. Included in this was the use, when and where possible, of radar and satellite imagery and when relevant, surface observation data at Al Ain were also used.

The most interesting and representative weather phenomena events from 2002 to 2004 were identified. Examples were then selected for analysis and presented in the form of case studies. Where the case studies were not fully representative they were supplemented with brief references to other events and statistical evidence.

Post-processed numerical weather prediction Eta model data, was also used to identify, analyse and present case studies as examples of situations that are likely to arise. Eta model versions used are the World Aviation Forecast System Aviation model (WAFS AVN) 1° horizontal resolution version, now called the Global Forecast Service (GFS) model, and the finer resolution 22 kilometres, 20 vertical levels version. Post-processing processes available were PCGRIDDS for the WAFS AVN/GFS 1˚ model and GRADS for the finer resolution model. These are powerful analysis systems facilitating analysis and research of the thermo-dynamical and circulation features of weather systems.

PCGRIDDS macros were developed by the author during 2002 to 2003 for operational use by the aviation forecasters in the ADIA Meteorological Office. These macros were also used in obtaining numerous charts that are used in this thesis. These can be made available on request.

After analyses and the presentation of case studies for each of the weather phenomena, a forecast methodology, or in aviation parlance a forecast checklist, is presented.

Note: Standard International (SI) metric units are used. However, the aviation industry still uses some non-metric units and will use them for a long time to come, as they still construct aircraft with altimeters in feet and air speed indicators in knots. It therefore makes sense to use these units, that is, feet (ft) for altitude instead of metres (m), or kilometres (km) and knots for the measurement of speed instead of metres per second (ms-1). The SI abbreviation for knot is kn, but in aviation and the International Civil Aviation Organization (ICAO) abbreviation is KT (ICAO 2004, WMO 1995 and UKMO 1994). Having said this, in order to conform as far as possible to SI practice, metres have been used instead of feet and where pertinent, measurements in feet have been provided in brackets. The measurement of wind speed is more complicated. All original operational observation and model data graphs and charts are produced in knots. To have changed these to metres per second would have been an impossible task. Therefore, in this thesis, knot(s), or KT, have been used. A rough conversion factor for knots to ms^{-1} is to divide by 2 and for feet to metres divide by 3. For the fastidious, conversion tables for these two units of measurement to metres (m), or metres per second (ms-1) have been provided in Appendix B.

1.4 OBJECTIVES OF THE RESEACH

The objectives of the research detailed in this thesis are:

The primary objective is the identification of significant weather phenomena and their associated regional weather systems that affect aviation in the UAE and ADIA in particular. Describe the forcing mechanisms responsible for their development and derive forecasting rules and principles applicable to these systems.

This has been achieved by the presentation of statistical analyses, case studies, a summary of the weather conditions to be expected and finally a forecast checklist to work through before issuing a forecast with respect to the relevant weather phenomena is suggested.

A secondary objective is to provide background information of the general seasonal climate sequence in the UAE.

This has been achieved by means of a literature study of the dominating weather systems and the presentation of surface and upper air mean circulation charts.

1.5 ORGANISATION OF THE DOCUMENT

General information about the UAE, such as historical and political background, geographical position, topography and airports is provided in chapter 2.

Chapter 3 outlines the major weather producing circulatory systems over the region through the use of mean circulation charts, January circulation, April, July and October, wind divergence at sea level, 850 hPa, 700 hPa, 500 hPa, 300 hPa and 200 hPa. Brief mention is also made of the effect of 200 hPa wind divergence, water vapour flux and sea temperature on the weather. A summary is provided.

After discussing fog dynamics, chapter 4 investigates the weather conditions under which fog occurs at ADIA. Fog statistics, such as when, why and how often it occurs, have been gathered. Meteorological phenomena that were observed during the 551 fog events at AIDIA, for the 22 years from 1982 to 2003, were collected and comprise the statistical data base. The selected 31 fog events, during 2002 to 2003, were researched, in detail. Data from these events include the analysis of 56 atmospheric soundings taken on the afternoons prior to, as well as on the morning of, the fog. During the two years of 2002 and 2003, 20 events, when fog was not predicted and in fact did not occur were also analysed for comparative purposes. The research also investigated the validity of several fog forecasting rules (of thumb) in general use prior to this research. The research results are summarised and a fog forecast methodology (or checklist) is presented.

The synoptic scale weather conditions that occur during the Shamal wind, at ADIA, are described in chapter 5. UAE Shamal statistics for the years 1992 to 2003 have been gathered. Due to the number of helicopter operations from the airport to the offshore oil rigs, the effect of the Shamal on the sea state in the Gulf Sea is explored. An example event is presented and discussed. A summary is presented and a forecast methodology is proposed.

Chapter 6 deals with dust storms. Dust storm dynamics are discussed, followed by a statistical analysis of their occurrence at ADIA from 1994 to 2003, including all events when the visibility was reduced to 5000 metres, or less. The dust storm case studies presented includes one event caused by the so called Nashi wind. Chapter 6 concludes with a summary and a forecast methodology.

In chapter 7 the dynamics, frequency of occurrence and general characteristics of UAE land and sea breezes are discussed. Their effect further into the desert, reaching Al Ain, the Abu Dhabi Emirates second international airport, is described. Case studies, including a brief discussion on inland anabatic and katabatic wind effects, are briefly investigated. The chapter concludes with the customary summary and a forecast methodology.

Winter rain bearing trough systems with imbedded thunderstorms as well as summer thunderstorms are detailed in chapter 8. This chapter briefly examines the rare tropical depressions that reach the UAE and present a summary and forecast methodology.

Chapter 9 deals with the conclusions and identifies topics for further research.

Appendix A provides definitions of the meteorological terms that frequently occur in the text.

Conversions factors: Knots to metres per second, feet to metres as well as the meaning of the term microbar are provided in appendix B.

Finally, appendix C explains the two fog point calculation methods mentioned in chapter 4. (UKMO Source Book to the Forecaster’s Reference Book (1997))

CHAPTER 2

THE UNITED ARAB EMIRATES

2.1 GENERAL

The United Arab Emirates (UAE), often simply referred to as the Emirates, is a federation of seven Emirates, formed in 1971 when the British withdrew from the region. The seven Emirates are; Abu Dhabi, Ajman, Dubai, Fujairah, Ras al-Khaimah, Sharjah, and Um al-Qaiwain. Collectively they form and area of about 77,700 square kilometres (UAE Climate, 1996). Obviously it is not a big country, but very wealthy due to oil deposits offshore and on land in Abu Dhabi. Abu Dhabi is the largest and most wealthy Emirate, while Ajman and Um Al Qaiwain are the smallest (Abu Dhabi Explorer, 2001, Callan and Robison, 2000). The capital, Abu Dhabi (the city) is situated on one of the larger islands and is reached by crossing one of two bridges from the mainland. What is often confusing to visitors is the fact that the capital city, or town, of each emirate has the same name as the emirate.

2.2 POSITION

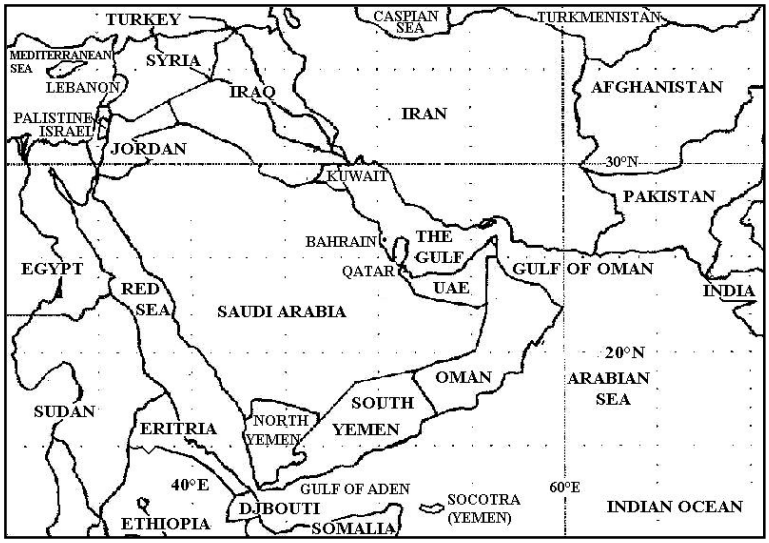

Figure 2.1. Political map of the Middle East.

The Emirates lie in the arid tropical zone extending across North Africa and into the Middle East. It is situated south-east of the Arabian Gulf (or simply The Gulf, or the Gulf Sea) on the Arabian Peninsula (figure 2.1) between 23°N to 25°N and 52°E to 57°E and extends to the east coast at the Gulf of Oman where the Fujairah Emirate is situated (figure 2.2). It is incorrect to refer to the Persian Gulf. If you are in the region it is wisest to refer to The Gulf, or the Gulf Sea. The Tropic of Cancer passes through the desert in the southern part of the country. To the south-east is the Sultanate of Oman, while to the south and west is Saudi Arabia. Qatar in the west, on its own peninsula is close enough to be a neighbour. The extreme north-eastern part of the land, at the Strait of Hormuz, is known as the Musandam Peninsula, which belongs to the Sultanate of Oman (United Arab Emirates Yearbook, 2001). There is also another enclave of the Sultanate of Oman in the Fujairah Emirate and an enclave of the Sharjah Emirate and Dubai as well.

2.3 TOPOGRAPHY

Over 90% of the UAE consists of sandy desert lowland with an elevation below 300 metres above mean sea level (MSL). From the low lying coastal plain, with large dry salt pans and isolated hills up to 40 metres above MSL, the land rises gently inland and quickly changes to sand dunes which are up 250 metres above sea level in the south. This southern portion of the UAE forms the beginning of what is known as the Rub al Khali (Empty Quarter) and extends into adjacent Saudi Arabia. Along the coast, the inshore area of the Gulf is very shallow, with literally hundreds of islands and coral reefs (Abu Dhabi Explorer, 2001, UAE Climate 1996).

In the extreme east, oriented from north to south is a mountain range that rises up to 1500 metres MSL. These are the Hajar (Rocky) Mountains (also known as the Western Hajar Mountains), but are known as the Musandam Mountains in the north. They extend to the south-east into the Sultanate of Oman, where they are known as the Eastern Hajar Mountains. The mountains are higher in Oman, the highest peak being Jabal al Sham (Mountain of the Sun) at 3075 metres (figure 2.2). Extending into the mountains and criss-crossing them are networks of wadis, which are valleys, usually very steep and narrow and which are prone to flash flooding when there is rain on the mountains (Abu Dhabi Explorer 2001, United Arab Emirates Yearbook 2001).

Figure 2.2. Map of the United Arab Emirates. The Hajar Mountains extend from the Musandam Peninsula at the Strait of Hormuz, south and south-eastward into Oman. The Empty Quarter is the area to the south and south-west of the U.A.E.

2.4 AIRPORTS

Considering the small size of the UAE, it has a high proportion of International Airports, but due to the small size of the UAE, nearly all flights to and from the airports are cross-border international flights.

The airports are listed below. The year in brackets is the date from which climate records are available at the modern airports. The metre readings are the altitudes of the airport's reference level above mean sea level.

Abu Dhabi International Airport (1982)	24° 26'N	54° 39'E	27 metres
Al Ain International Airport (1994)	24° 15'N	55° 36'E	265 metres
Dubai International Airport (1974)	25° 15'N	55° 20'E	8 metres
Fujairah International Airport	25° 06'N	56° 20'E	28 metres
Ras Al Khaimah International Airport (1977)	25° 37'N	55° 56'E	31 metres
Sharjah International Airport (1977)	25° 20'N	55° 31'E	33 metres

The first international airport at Abu Dhabi was on the island at Al Bateen, but had to give way to development on the island and it is now situated slightly inland of the coast, but about 32 kilometres from the city centre (figure 2.3). Climate records at the old Abu Dhabi Al Bateen airport date back to 1971 (figure 2.3), but were not used in the research.

Most of the present airports are virtually on the Gulf coast. Fujairah airport is on the narrow Gulf of Oman coast while Al Ain, which about 150 kilometres inland from Abu Dhabi differs from them all in that it has a continental desert climate. Al Ain is also close to and west of the Hajar Mountains, while Fujairah airport is on the eastern side of these mountains.

Airports have existed in the UAE from the late 1920's and early 1930's when they were constructed for use by British Imperial Airways flights from the United Kingdom to India and later on to Australia (Kay 1995). The oldest probably being Sharjah airport that was originally situated where the city centre is today. The earliest record of a landing strip at Abu

Figure 2.3. Location of Abu Dhabi International Airport. The airport is bottom, right of the picture, showing the two 4,100 metres (13,452 feet), runways oriented 310°/130° (ADAC 2009a). The island city of Abu Dhabi is to the left of the picture and the open sea toward the left and upper left off the picture. The old international airport (Al Bateen) is visible bottom/centre of the picture on the north-east corner of the Abu Dhabi Island (Photograph courtesy of Google–Imagery 2009 TerraMatics).

Dhabi dates back to 1935 when, after protracted negotiations, Sheikh Shaikhbut bin Sultan agreed to allow the British Royal Air Force (RAF) to build an emergency landing strip. It had to be 4 miles (6.4 kilometres) from the town and RAF personnel were not allowed in the town. The British paid an initial lump sum of 5000 Rupees and thereafter 400 Rupees per month rental (Tuson 1990). The airports are still not only important stopover points to the east and west, but also to other points of the compass.

To conclude, a comparative idea of the traffic through Abu Dhabi airport, both in terms of passenger and cargo, with other airports in the U.A.E. and others in the Middle East, is given in the list below, the statistics being for the 12 months up to September 2004 versus 2003 (Aviation Business, January 2005). ADIA is the second busiest in the U.A.E. and a close fifth to Kuwait in the Middle East.

	Passengers	Change (%)	Cargo (tonnes)	Change (%)
Abu Dhabi	5 032 390	+23.4	157 567	+13.7
Dubai	21 121 009	+21.6	1 123 467	+22.0
Fujairah	57 665	-42.6	28 703	-19.4
Ras Al Khaimah	150 468	- 8.8	8 198	+ 4.4
Sharjah	1 581 081	+34.0	472 776	+ 2.5
Amman (Jordan)	2 963 788	+26.8	98 097	+24.6
Bahrain	4 975 187	+17.9	276 243	+23.9
Beirut (Lebanon)	3 301 140	+19.7	66 100	- 1.1
Jeddah (Saudi Arabia)	12 304 650	+ 8.9	219 405	+ 7.5
Kuwait	5 051 076	+20.6	161 632	+14.9
Muscat (Oman)	3 503 970	+28.3	64 050	+36.1
Riyadh (Saudi Arabia)	10 185 554	+ 7.7	188 681	+11.9

CHAPTER 3

GENERAL ATMOSPHERIC CIRCULATION IN THE ARABIAN PENINSULA

3.1 INTRODUCTION

The Arabian Peninsula is approximately between 35°E to 60°E and 12°N to 30°N. It is bounded by the Gulf Sea and the Gulf of Oman in the east, the Arabian Sea in the south, the Red Sea in the west and to the north by Jordan, Iraq and Kuwait. It consists of the countries of the Bahrain, Kuwait, Oman, Qatar, Saudi Arabia, the United Arab Emirates and Yemen.

Topographically, the Arabian Peninsula is an inhospitable and vast sandy plateau with no permanent rivers, or streams. It is bordered by mountains in the west along the Red Sea and in the south and east along the Arabian Sea

This chapter outlines the major weather producing circulatory systems over the region.

3.2 DOMINATING WEATHER SYSTEMS

The dominating pressure systems are the winter cold Siberian anticyclone over central Asia, the summer monsoon Asiatic and India low (Glen 1954) and secondary depressions that migrate eastward from the Mediterranean (Kendrew 1961).

In winter, polar continental air masses form over central Asia. Characteristically the air mass has very low temperatures in a shallow surface layer with a marked inversion at about 1500 metres (5000 feet). When this stable air is advected over a warm moist surface, such as the Gulf, heating from below destroys the inversion and moisture absorption results in widespread cloudiness (Taha, Harb, Nagib and Tantawy 1981). Satellite imagery shows that frontal cloud patterns frequently extend from middle latitudes to the southern-most edge of the Arabian Peninsula, particularly in non-summer months. Their rainfall potential decreases from north to south and west to east (Taha, et al 1981). Maritime polar air follows transitory Atlantic low pressure systems across Europe and by the time the lows reach the Emirates they are considerably modified, but are still moister than the polar continental air mentioned above.

In summer the area is a meeting place of converging air masses forming a type of inter-tropical front. To the north the air mass, of moderate temperature and moisture content circulates in the sub-tropical anticyclone, while to the south very hot and dry air circulates in the monsoon trough. Maritime tropical air that loses its moisture over northern India infrequently arrives over the region as a very hot and dry air mass. Furthermore, the nearby water surfaces of the Gulf Sea, the Gulf of Oman and the Arabian Sea act as sources of moisture and heat (Taha, et al 1981).

In the pre-monsoon spring period of May and June and the post-monsoon autumn period of October and November, the Arabian Sea is invaded by tropical disturbances, some of which may intensify into tropical storms, but development into a full blown tropical cyclone is a rare event.

The majority of tropical cyclones occur in the post-monsoon period, but their influence is limited to the southern part of the Arabian Peninsula. The most frequent disturbances are easterly troughs, or easterly waves, moving from east to west (Taha, et al 1981) with the zone of convergence and convective activity on the eastern, or leading edge, of the trough axis.

During late spring to early autumn very dry and hot continental tropical air from the Sahara reaches the region (Taha, et al 1981).

3.3 MEAN CIRCULATION CHARTS

The charts used in the following sections on the seasonal flow, were obtained from the South African Weather Service (SAWS) publication "Charts of the mean circulation over the monsoon region of the world" (Triegaardt and Landman 1992). The mean charts were based on the 12h00 UTC initialised analyses of the European Centre for Medium Range Weather Forecasts (ECMWF) for the 8 years from 1980 to 1987.

In using these charts it must be borne in mind that there are limitations to their accuracy. Due to operational constraints and a cut-off time for inclusion of incoming observations, it is estimated that about 30% of a total observations are usually not available. Two other limitations are due to the fact that modifications are made to prediction models and data assimilation systems. While these changes improve the quality of the analyses and prognosis of the model, it does mean that the analyses produced are not homogeneous. For example, more recent modifications of the ECMWF model, after 1985, produce better enhancement of the Hadley circulation. The advantage is that this sort of analysis can generate information at a finer scale than a conventional observing system and it can generate data in data void area (Triegaardt and Landman 1992).

Note, due to the difficulty of pressure reduction to sea level over the continents isobars are confined to the oceans and for clarity the UAE appears as a black silhouette in the figures.

3.4 JANUARY CIRCULATION

The sea level and 850 hPa charts show that the circulation over the Asian continent is dominated by an anticyclone with a ridge, or separate cell, of the Asian anticyclone over Arabia (figures 3.1 and 3.2, respectively).

Latitudinal movement of this anticyclonic cell over Arabia and the passage of mid-latitude disturbances result in alternating southerly to south-easterly winds and Shamal winds. Rao, et al (2001) define the Shamal as a seasonal northerly to north-westerly wind with higher than normal strength (greater than 17 knots) blowing for three, or more, hours in a day. In winter they occur in the flow of colder air from the north in the wake of passing mid-latitude lows and the ensuing strong pressure rise ahead of the following anticyclone.

The southern part of the anticyclone is associated with an easterly flow over the Arabian Sea and northern Indian Ocean that forms the easterly trades, or the winter north-east monsoon, which brings rain to East Africa in the vicinity of the equator. The north-easterly flow over the Arabian Sea crosses the equator into the Indian Ocean, where it becomes westerly and converges with southern hemisphere air in the low pressure belt at the Inter-tropical Convergence Zone, or near-

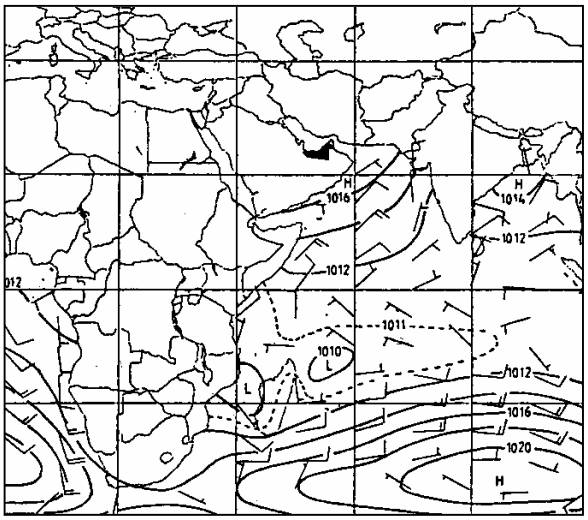

Figure 3.1. January mean sea level pressure (hPa) circulation. Mean wind velocity in knots (each full barb = ten knots = 5ms^{-1}).

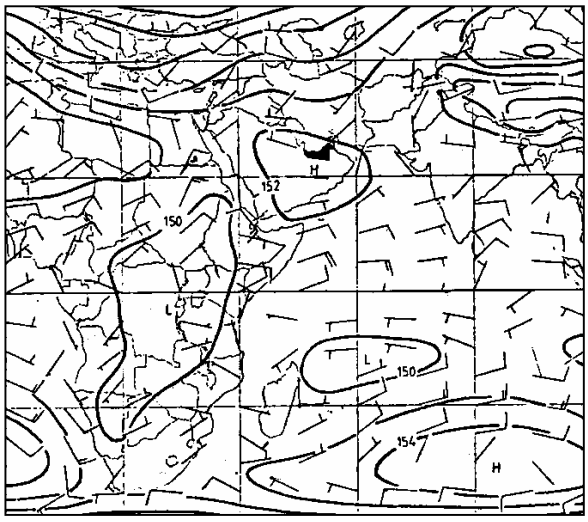

Figure 3.2. January mean 850 hPa circulation. Mean wind velocity in knots (each full barb = ten knots = 5ms^{-1}).

equatorial trough (figures 3.1 and 3.2).

At 700 and 500 hPa (figures 3.3 and 3.4) there is a change to a westerly flow and strengthening of the wind with height. A significant feature of the wind at 300 and 200 hPa (figures 3.5 and 3.6) is the sub-tropical westerly jet stream that reaches maximum strength at 200 hPa. It dominates the middle and lower latitudes in winter and is known for its steadiness of wind direction and geographical location. At times its steadiness and location is affected by the passing of westerly troughs from west to east when 5° to 10° meridian oscillations of the jet stream occur (Taha, et al 1981).

Notice the trans-equatorial flow of air over Africa and the Indian Ocean from the southern hemisphere to the northern hemisphere at 200 hPa (figure 3.6). This is the reverse flow of air seen at the surface and at 850 hPa in figures 3.1 and 3.2 and forms part of the Hadley circulation (Triegaardt and Landman 1992).

The tropospheric wind divergence at the sub-tropical jet stream in association with upper air troughs, along with the lower wind convergence associated with passing low pressure cells, are important winter weather producers. These marked synoptic systems are the main producers of cloudy weather and rain in the area. Precipitation is highest in the north and decreases from west to east, except where the topographic effect of the high mountains in the south-west again increases rainfall. The polar jet stream, in association with the passage of mid latitude depressions, frequently invades the area and amalgamates with the sub-tropical jet stream. Extensive middle layer clouds with embedded isolated thunderstorms often precede the trough (Taha, et al 1981). However, the often prevailing dry conditions and consequent high cloud base mean that not much rain reaches the surface, although strong wind gusts and sandstorms do occur (Tantawy 1961).

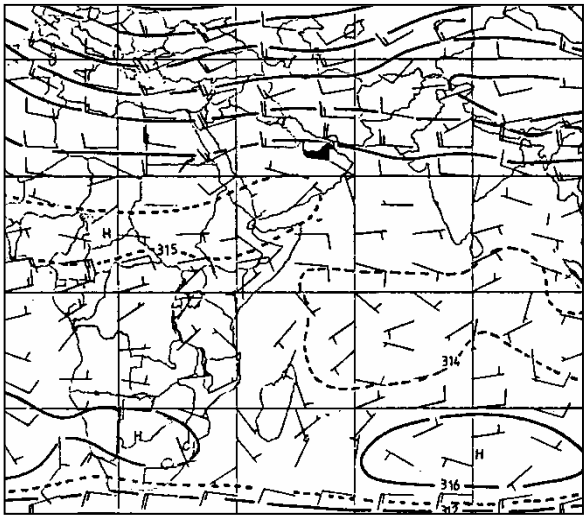

Figure 3.3. January mean 700 hPa circulation. Mean wind velocity in knots (each full barb = ten knots = 5ms^{-1}).

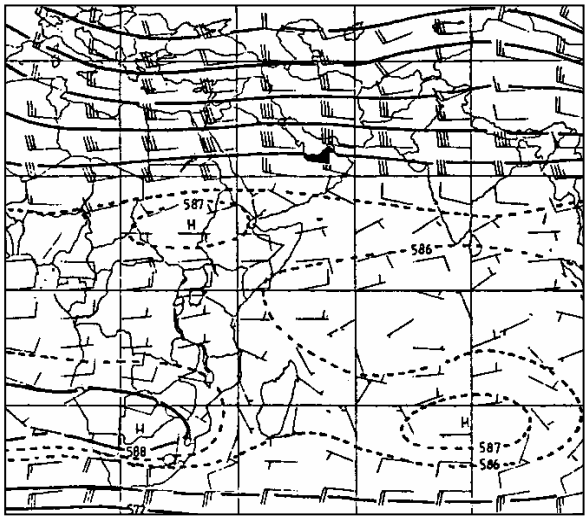

Figure 3.4. January mean 500 hPa circulation. Mean wind velocity in knots (each full barb = ten knots = 5ms^{-1}).

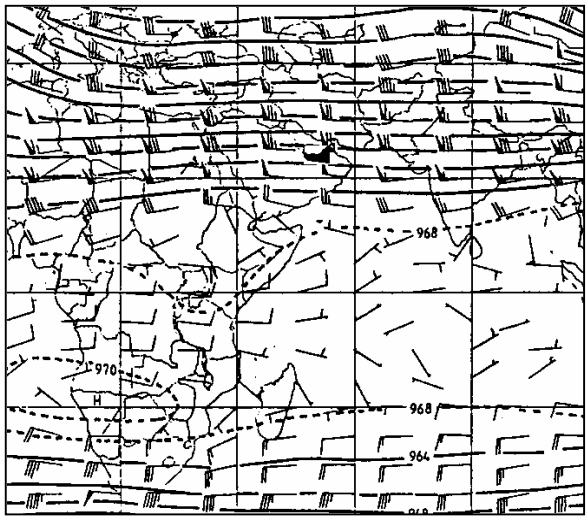

Figure 3.5. January mean 300 hPa circulation. Mean wind velocity in knots (each full barb = ten knots = 5ms^{-1}).

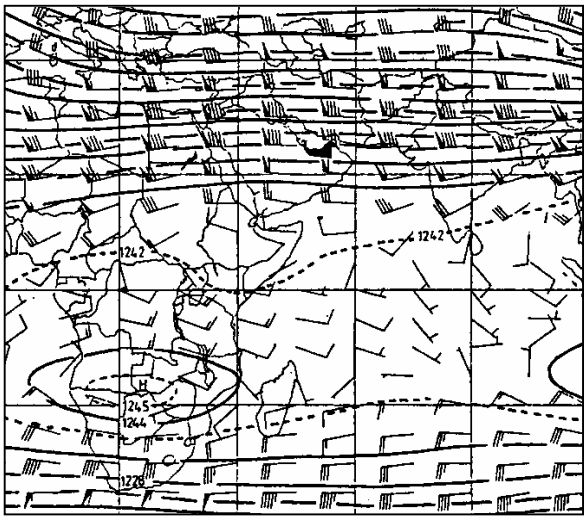

Figure 3.6. January mean 200 hPa circulation. Mean wind velocity in knot (each full barb = ten knots = 5ms^{-1}).

3.5 APRIL CIRCULATION

In this transition period from winter to summer circulation, the surface (figure 3.7) and 850 hPa (figure 3.8) anticyclone of January, over Arabia and the Arabian Sea, is already less intense. Mean sea level pressures show a fall from 1016 hPa and higher to about 1010 hPa in April. The north-east monsoon over the northern Indian Ocean becomes weaker and the flow more confused. The same applies to the westerly flow at 850 hPa to the north where low pressure cells migrate from the Mediterranean to the west.

At 700 hPa (figure 3.9), 500 hPa (figure 3.10) and 300 hPa (figure 3.11) the westerly wind, over predominately the northern part of Arabia, also weakens and shows a slight shift to the north. A similar process is evident at 200 hPa (figure 3.12), while the trans-equatorial flow from the southern hemisphere is very weak, or non-existent. Although the westerly flow moves further

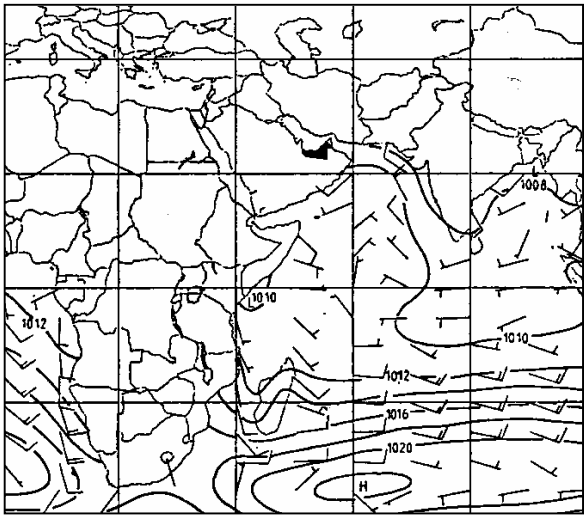

Figure 3.7. April mean sea level pressure (hPa) circulation. Mean wind velocity in knots (each full barb = ten knots = 5ms^{-1}).

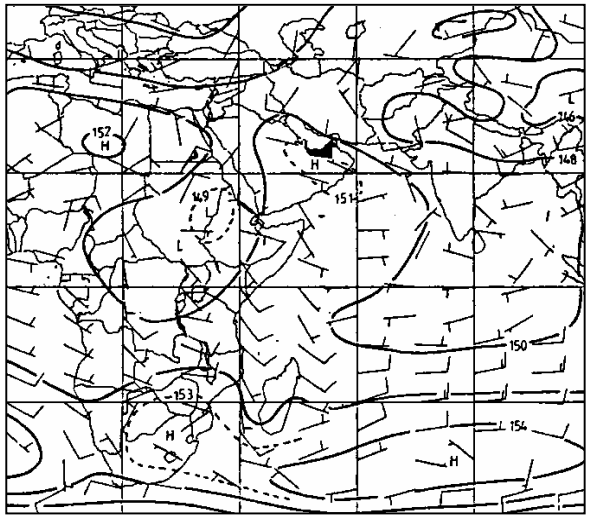

Figure 3.8. April mean 850 hPa circulation. Mean wind velocity in knots (each full barb = ten knots = 5ms^{-1}).

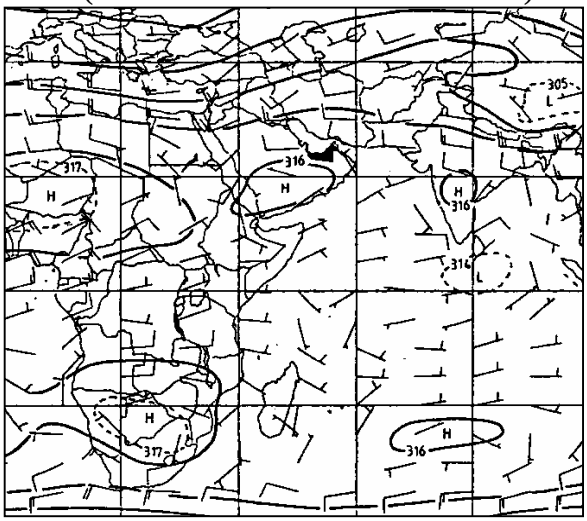

Figure 3.9. April mean 700 hPa circulation. Mean wind velocity in knots (each full barb = ten knots = 5ms^{-1}).

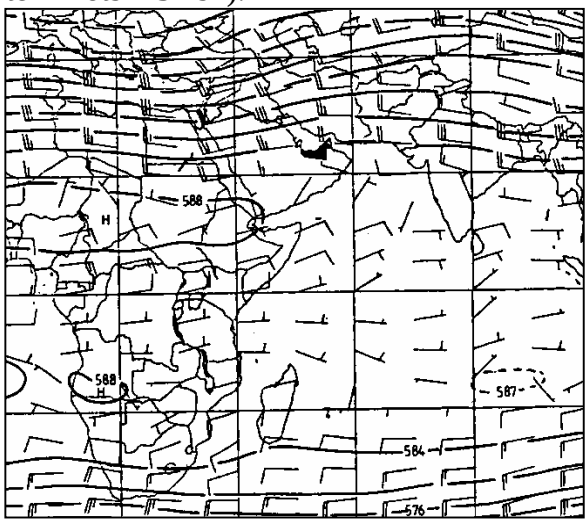

Figure 3.10 April mean 500 hPa circulation. Mean wind velocity in knots (each full barb = ten knots = 5ms^{-1}).

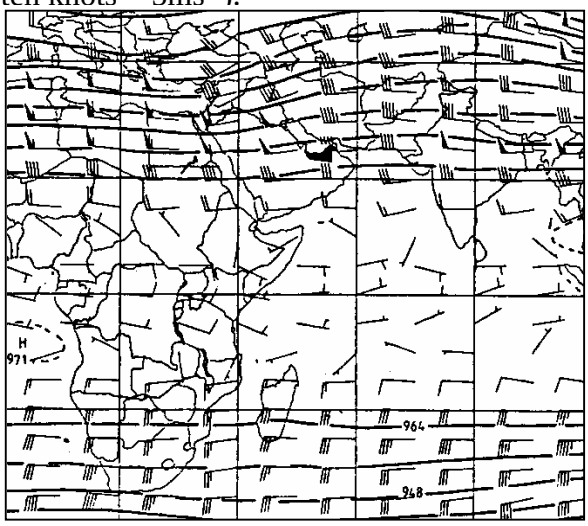

Figure 3.11. April mean 300 hPa circulation. Mean wind velocity in knots (each full barb = ten knots = 5ms^{-1}).

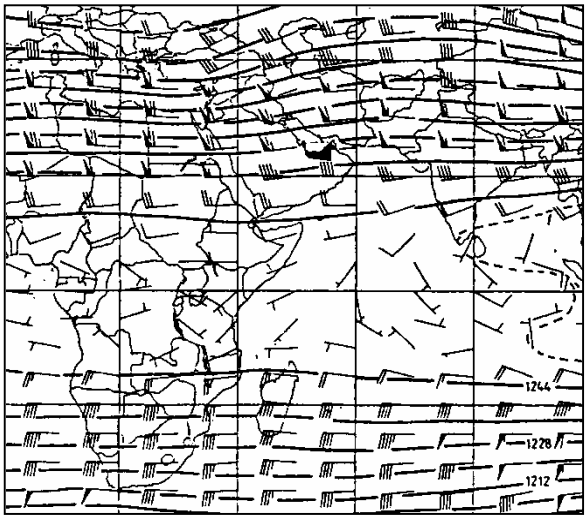

Figure 3.12. April mean 200 hPa circulation. Mean wind velocity in knots (each full barb = ten knots = 5ms^{-1}).

northward, upper air troughs in the westerly flow and topographic ascent over mountains remain conducive to spring rainfall.

Rao et al (2001) regard April as not being part of the winter season by virtue of the fact that mid-latitude frontal systems no longer occur over the Gulf Sea. However, Taha, et al (1981) state that winter to summer circulation change takes place in two, or three, weeks in May to June. Whatever the conclusion reached about this time of the year, an important factor is the change in low level atmospheric static stability. Rapid heating of the land increases the ambient temperature lapse rate in the lower layers and this decreases the stability (increased instability). At the same time the density of the air decreases, as does the air pressure and this has the effect of deepening desert depressions. The large day time temperature difference between the land and the still cool water surfaces results in increased local wind circulations such as land and sea breezes (Taha, et al 1981).

A characteristic of spring is the frequent passage of desert depressions that originate over north-west Africa and move eastward parallel to the coast to the northern part of the Arabian Peninsula. They are of sub-synoptic scale and usually disappear above the 700 hPa level. Ahead of these depressions southerly winds cause intense heat waves and sand storms. The sand storms can extend upward to a height of 3 kilometres (nearly 10 000 feet), while post-low moist advection from the Gulf Sea can provide enough moisture for infrequent thunderstorms (Taha, et al 1981).

3.6 JULY CIRCULATION

Comparison of the July surface circulation (figure 3.13) and at 850 hPa (figure 3.14) with the corresponding charts in January (figures 3.1 and 3.2) reveals significant differences. Over Arabia, the Arabian Sea and across to northern India, an area of low pressure has replaced the anticyclone of winter. Pressures are as low as 998 hPa occur in the vicinity of the Gulf of Oman. To the east, the low pressure area centred over the Asian continent, with a trough extension toward Arabia, is due to the summer continental heat low (Hastenrath 1985).

The near-equatorial trough is now situated much further north of its January position and there is a strong flow of air from the South Indian Ocean sub-tropical high pressure cell across the equator to the Asia low (Webster, 1983). This results in the strong south-west monsoon over the northern Indian Ocean and Arabian Sea and southern Arabia (figures 3.13 and 3.14). Over the rest of Arabia, the position of the summer low results in a consistent northerly to north-westerly wind over most of Arabia, particularly in the north. Locally this is often referred to as the forty day Shamal. The consistency of this summer wind is emphasised by Rao, et al (2001) who state that the 3 summer months of May to July account for 51% of the annual Shamal days, while only 21% the occurrences are in the 5 winter months of November to March.

At 700 hPa, 500 hPa and 300 hPa (figures 3.15, 3.16 and 3.17, respectively) the westerly wind has moved well to the north of Arabia and is considerably weaker than in January. Furthermore, although a cyclonic circulation extends up to about 700 hPa, from 500 hPa upward to 200 hPa (figures 3.16 to 3.18) a strong and well developed anticyclonic circulation replaces the westerly flow over most of northern Africa, Arabia and eastward to northern India. This anticyclonic belt results in middle troposphere subsidence and warming over northern Arabia in particular. Note the easterly flow, south of the anticyclone at 500 hPa and 300 hPa (figures 3.16 and 3.17, respectively) that drives thunderstorms from the eastern highlands of the Emirates, westward to

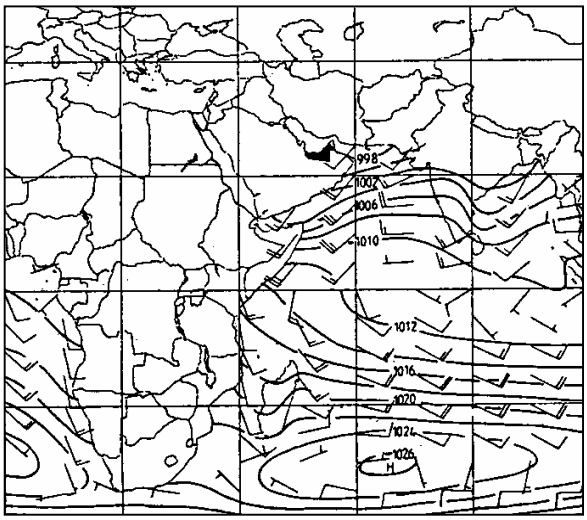

Figure 3.13. July mean sea level pressure (hPa) circulation. Mean wind velocity in knots (each full barb = ten knots = 5ms^{-1}).

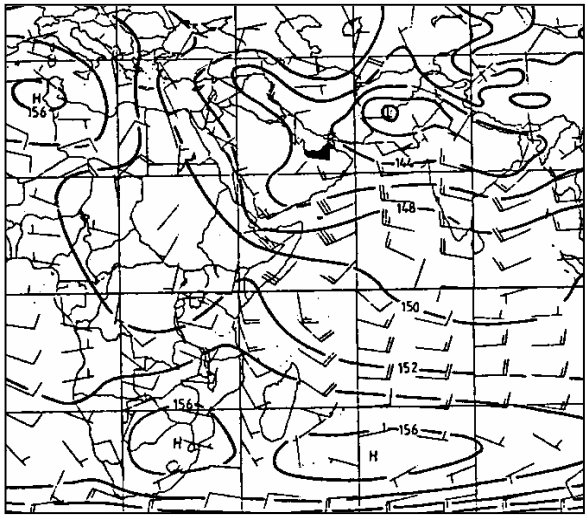

Figure 3.14. July mean 850 hPa circulation. Mean wind velocity in knots (each full barb = ten knots = 5ms^{-1}).

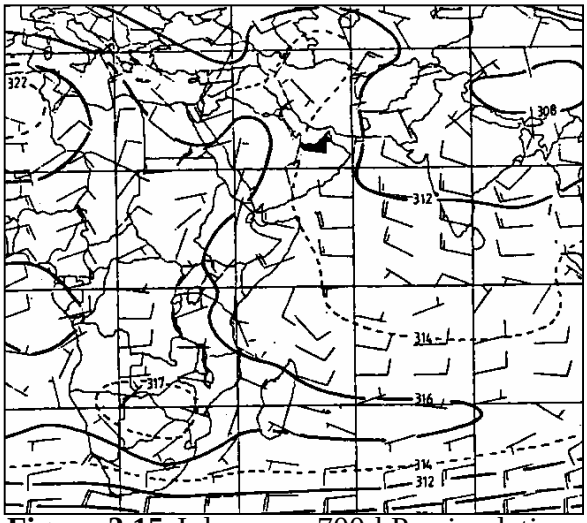

Figure 3.15 July mean 700 hPa circulation. Mean wind velocity in knots (each full barb = ten knots = 5ms^{-1}).

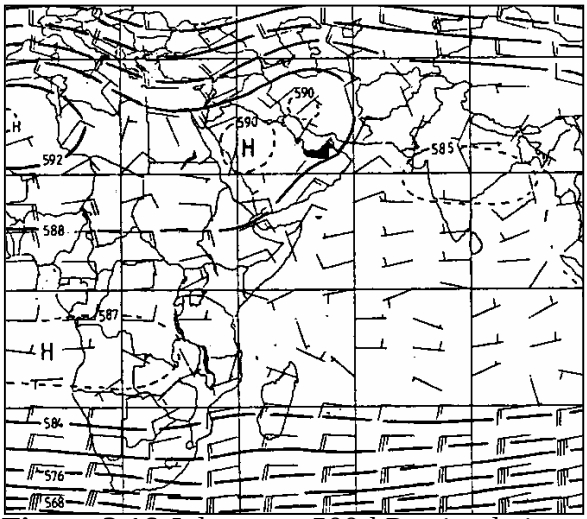

Figure 3.16 July mean 500 hPa circulation. Mean wind velocity in knots (each full barb = ten knots = 5ms^{-1}).

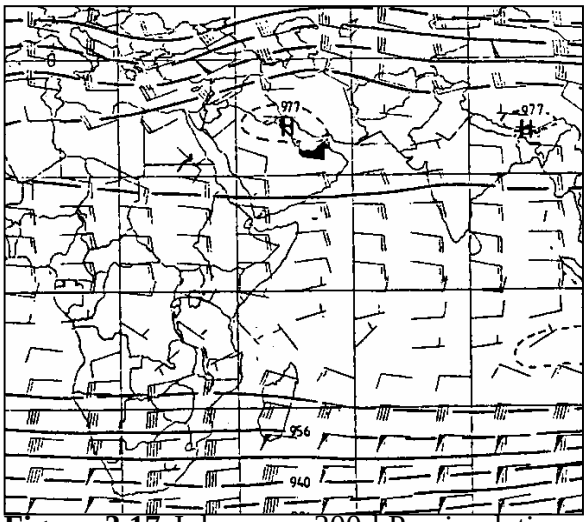

Figure 3.17 July mean 300 hPa circulation. Mean wind velocity in knots (each full barb = ten knots = 5ms^{-1}).

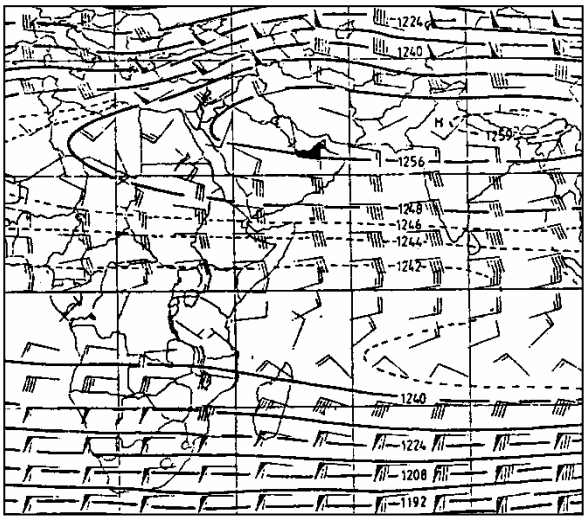

Figure 3.18 July mean 200 hPa circulation. Mean wind velocity in knots (each full barb = ten knots = 5ms^{-1}).

the Emirates coast in summer.

The anticyclonic circulation at 200 hPa (figure 3.18), centred over Tibet, is most prominent with a strong tropical easterly jet on the equator side of the anticyclone, which lasts from late June to early September (Hastenrath 1985). Another feature is the trans-equatorial flow from the northern hemisphere to the southern hemisphere. This is the converse of what happens in January and is a reversal of the Hadley circulation.

In summery, during January there is a surface north-east monsoon flow to the southern hemisphere with a compensating south to north air flow and westerly jet stream at 200 hPa. In July this is reversed to a surface south-west monsoon flow to the northern hemisphere with a compensating north to south flow and tropical easterly jet at 200 hPa.

3.7 OCTOBER CIRCULATION

By October continental radiation cooling causes a considerable rise in the surface pressure, which extends to the Arabian Sea and eastward to China (figure 3.19). This pressure rise is also evident in the 850 hPa geopotential heights over Arabia and Asia (figure 3.20) and it should be noted that the 850 hPa geopotential heights over Arabia are back to January values.

At 700 hPa and 500 hPa (figures 3.21 and 3.22, respectively), while the anticyclone is still prominent over Arabia, there is a distinct increase in the westerly flow to the north of Arabia when compared with the same levels in July (figures 3.15 and 3.16).

Comparing the 300 hPa and 200 hPa levels (figures 3.23 and 3.24, respectively) with those of July (figures 3.17 and 3.18) it will be noted that the westerly circulation has increased and extended southward as far as northern Arabia and the anticyclonic circulation has all but vanished.

In the same way that change in spring from a winter to summer circulation takes place over a few weeks (Rao el all 2001), the transition from summer to winter weather patterns also takes place in a short period of time, usually between October and November (Taha, et al 1981). Rapid cooling of the land in autumn causes much more stable air in the lower layer of the atmosphere and the frequency and intensity of sandstorms decreases considerably. However, the upper layer tends to become more unstable when cold air invades from the north behind westerly troughs. Occasionally the advancing trough is intense enough to cause thunderstorms and on occasion the trough may be deformed into an upper cut-off low through a process described as anticyclonic disruption (Taha, et al 1981).

3.8 WIND DIVERGENCE AT 200 HPA

Figures 3.25 to 3.28 show the mean January, April, July and October divergence fields at 200 hPa for the period 1980 to 1987. The divergence was calculated from the mean u and v components of the initialised ECMWF wind fields at the 200 hPa level (Triegaardt and Landman, 1992). A definition of divergence can be found in appendix A.

There is marked convergence (negative divergence) in January at 200 hPa (figure 3.25) between

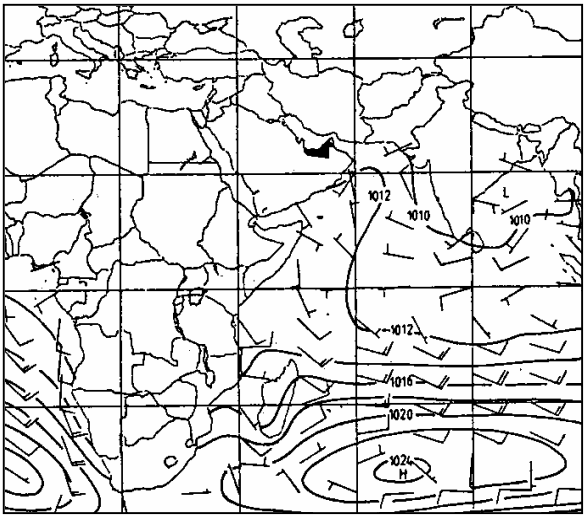

Figure 3.19. October mean sea level (hPa) circulation. Mean wind velocity in knots (each full barb = ten knots = 5ms^{-1}).

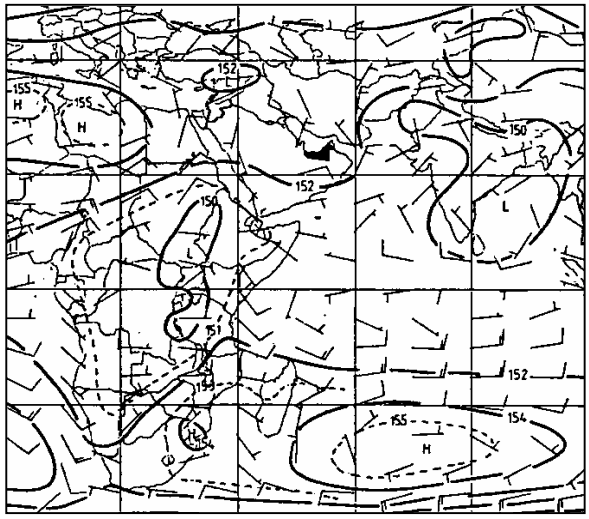

Figure 3.20. October mean 850 hPa circulation. Mean wind velocity in knots (each full barb = ten knots = 5ms^{-1}).

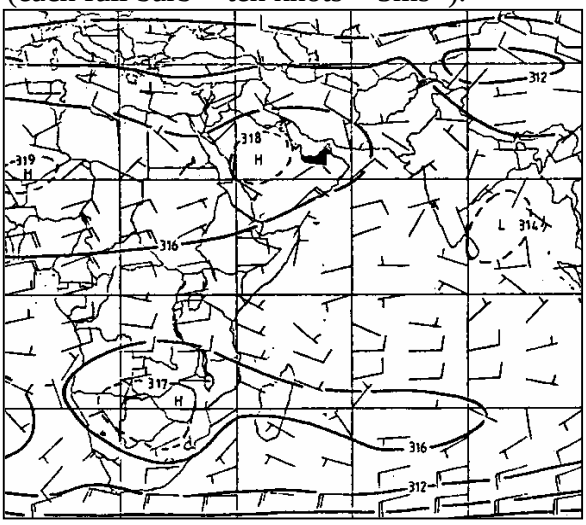

Figure 3.21. October mean 700 hPa circulation. Mean wind velocity in knots (each full barb = ten knots = 5ms^{-1}).

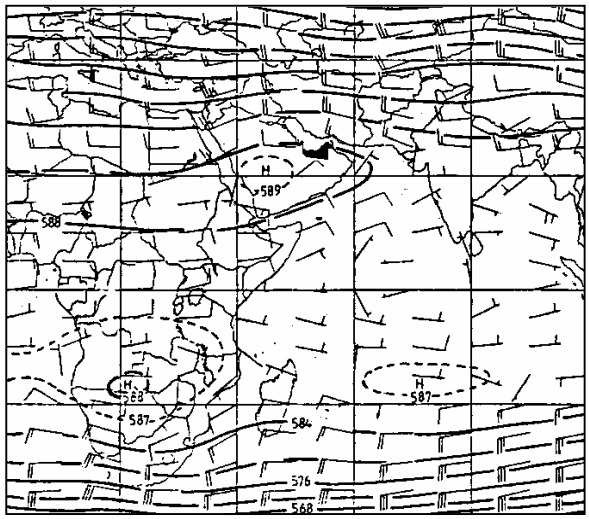

Figure 3.22. October mean 500 hPa circulation. Mean wind velocity in knots (each full barb = ten knots = 5ms^{-1}).

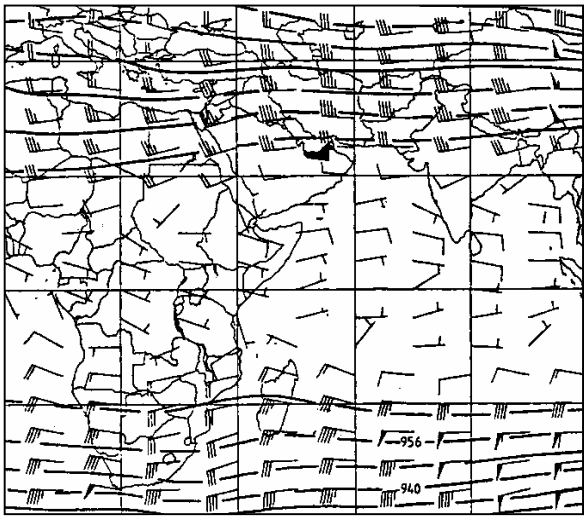

Figure 3.23. October mean 300 hPa circulation. Mean wind velocity in knots (each full barb = ten knots = 5ms^{-1}).

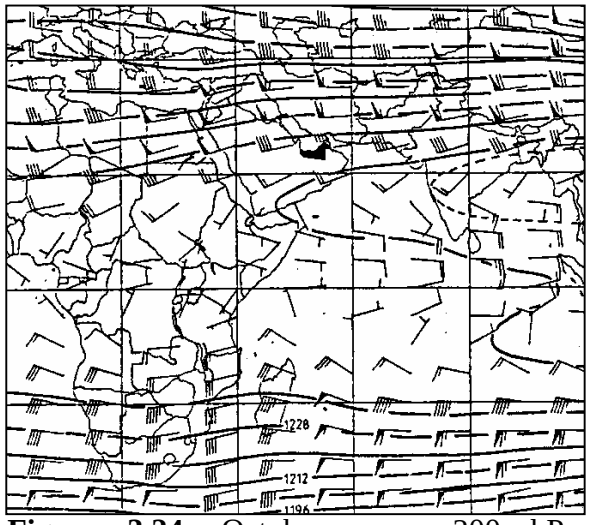

Figure 3.24. October mean 200 hPa circulation. Mean wind velocity in knots (each full barb = ten knots = 5ms^{-1}).

20° to 40° north, predominantly over the Asia continent. This implies subsidence below this level with divergence at the surface. Inspection of the surface and 850 hPa circulation in section 3.4 (figures 3.1 and 3.2) confirms the presence of high pressure at the surface and surface divergent trans-equatorial flow toward the near-equatorial surface trough in the southern hemisphere. This is indicated by the north-east monsoon over the Arabian Sea and northern Indian Ocean which becomes and easterly wind south of the equator. At 200 hPa (figure 3.6) there is a compensating northward flow.

In April the 200 hPa pattern is still very similar to January, but showing signs of weakening convergence over the Asian continent (figure 3.26). The divergence associated with the surface near-equatorial trough has also moved northward nearer to the equator.

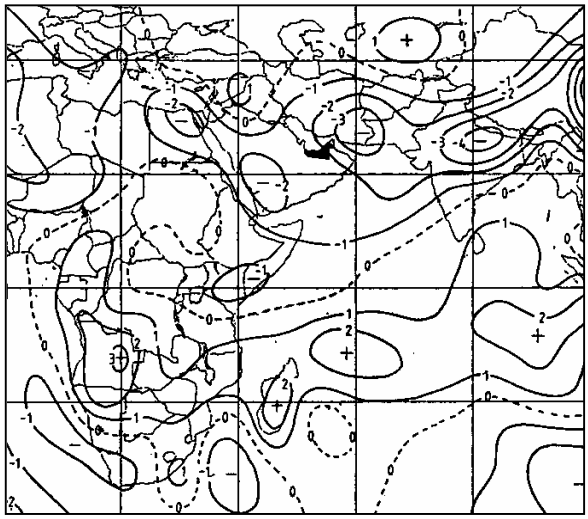

Figure 3.25. January mean 200 hPa divergence (x 10^{-6} sec^{-1}) from 1980 to 1987.

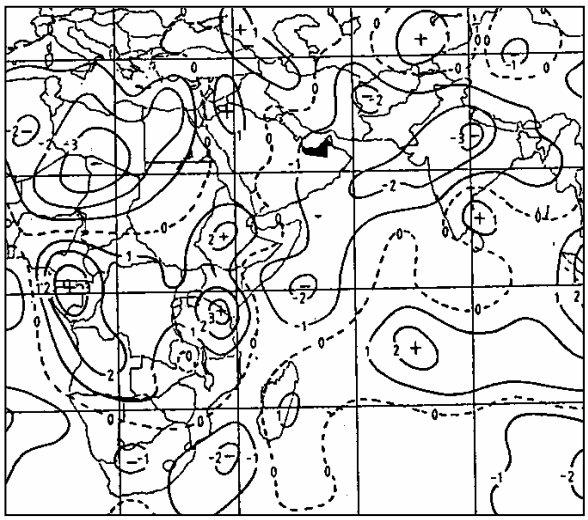

Figure 3.26. April mean 200 hPa divergence (x 10^{-6} sec^{-1}) from 1980 to 1987.

In July (figure 3.27) there is a complete reversal with positive divergence north of the equator to about 20°N, which corresponds with the steady 200 hPa easterly jet (figure 3.18). This compensates for the marked surface convergence in the belt of surface near-equatorial low pressure that now lies north of the equator (figures 3.13 and 3.14) and which is reinforced by summer surface radiation heating. By October there is already a return to marked winter convergence, similar to January, over the Asian continent and extending into Arabia (figure 3.28).

Triegaardt and Landman (1992) noted that marked positive divergence extends in an almost unbroken belt from Africa east across the Asian continent in July (figure 3.27). However, at about 40°E there is a break with neutral (and possibly negative divergence) while at about 70°E, immediately west of the India west coast, there is zone of enhanced positive divergence. The revised July 200 hPa analysis for 1985 to 1987 (not shown) indicated much stronger positive divergence in this zone. The strong divergence corresponds with a zone of heavy rainfall in excess of 500 mm in July along the Indian west coast where the surface and 850 hPa circulations in July (figures 3.13 and 3.14) show that this is an area of marked onshore flow from the south-west monsoon. This implies that the rainfall is the result of marked topographic forcing. The zone of enhanced 200 hPa divergence is therefore believed to be compensation for the marked surface convergence and strong upward vertical (positive) velocity (Triegaardt and Landman 1992). To take this one step further, it is postulated that the zone of neutral, or possibly

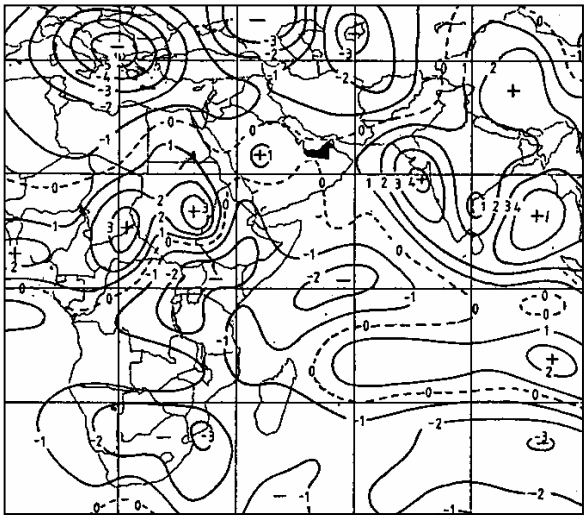

Figure 3.27. July mean 200 hPa divergence (x 10^{-6} sec^{-1}) from 1980 to 1987.

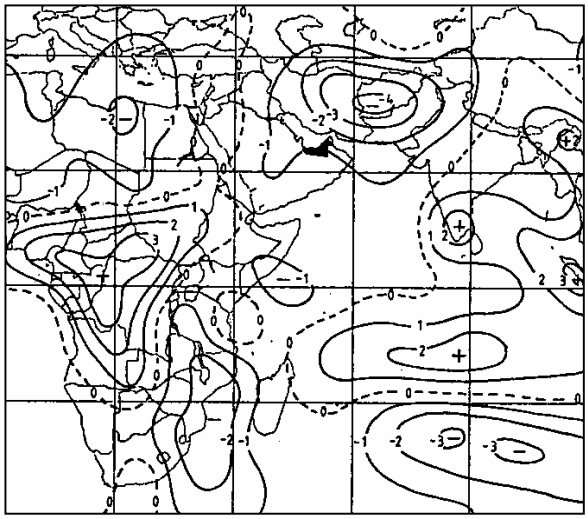

Figure 3.28. October mean 200 hPa divergence (x 10^{-6} sec^{-1}) from 1980 to 1987.

convergent air at about 40°E (figure 3.27) is a compensatory effect for the upward flow at 70°E and the subsiding air below this weak convergent zone at 40°E in turn contributes to the dry summer weather over Arabia.

3.9 WATER VAPOUR FLUX

The mean horizontal water vapour flux (transport) for the 850 hPa to 300 hPa layer (Triegaardt and Landman 1992) in January (figure 3.29) indicates weak winter moisture transport from the east over the Arabian Sea and northern Indian Ocean. This is consistent with the drier continental north-east monsoon shown in figures 3.1 and 3.2. However, over northern Arabia and the United Arab Emirates, there is stronger moisture transport from the west. As stated in section 3.2, this is consistent with the winter rainfall brought by low pressure systems, and their associated upper air troughs, that originate in the Mediterranean and sometimes as far west as the Atlantic (Kendrew 1961).

Comparing the July mean horizontal water vapour flux (figure 3.30) with that of January (figure 3.29), it will be seen that there is a total reversal of the circulation over the Arabian Sea and across India to the Bay of Bengal. In July this moisture, in association with the strong westerly to south-west monsoon, is transported from the ocean off east coast of Africa and to some extent from the southern hemisphere.

Over northern Arabia and the United Arab Emirates, the water vapour flux is somewhat less and is now from a northerly direction (figure 3.30), as opposed to westerly in winter (figure 3.29). The northerly direction can be attributed to the air which circulates southward to the east of the monsoon trough over Asia and often arrives as a modified very hot and dry air mass. Other, weak, water vapour flows present can be attributed to moisture from the Gulf of Oman to the east and the Gulf Sea to the north. Thunderstorms that develop in this moist air along the eastern mountains are then propagated westward to the coast by the prevailing easterly winds in the mid and upper levels (figures 3.16 and 3.17).

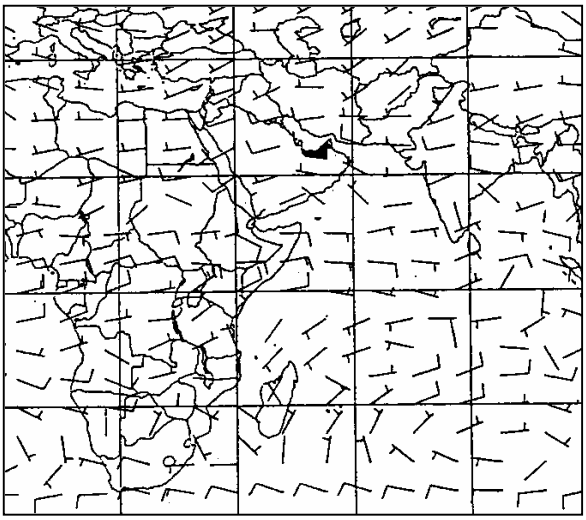

Figure 3.29. January mean horizontal water vapour flux vectors from 1980 to 1987. Each barb represents 10^2 gm cm^{-1} sec^{-1}.

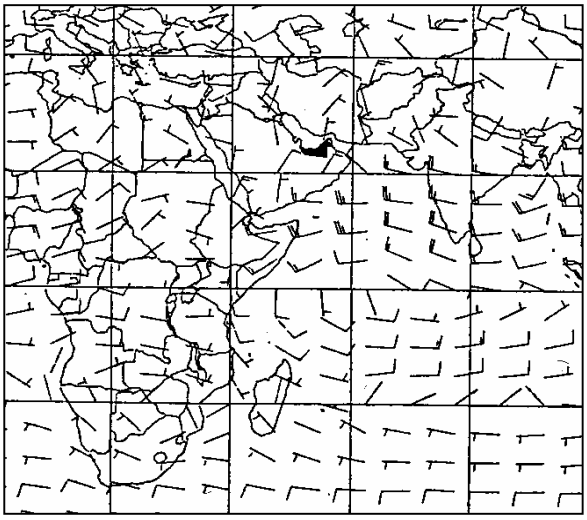

Figure 3.30. July mean horizontal water vapour flux vectors from 1980 to 1987. Each barb represents 10^2 gm cm^{-1} sec^{-1}.

3.10 SEA SURFACE TEMPERATURE

Annually the large heat capacity of the water in the Gulf Sea means that sea temperature changes tend to lag behind that of the land (Bradbury, 1989 and Griffiths, 1976). Consequently, the lowest sea temperatures tend to occur in February in winter and the highest temperatures in the summer month of August. That is, about a month later than the coldest and hottest times on land. In winter (February) the water around Arabia and in the Gulf Sea is about or slightly below 25°C (figure 3.31). In summer (August) it rises to about 27°C in the Gulf of Oman and above 30°C in the Gulf Sea (figure 3.32).

The differences in the diurnal heating and cooling over the land and sea (and resultant local pressure gradient differential) give rise to the well known mesoscale circulation known as the land and sea breeze (Riehl 1979). The seasonal temperature lag results in a stronger sea breeze effect at the beginning of summer when the land has already become considerably hotter and the sea surface is still closer to winter temperatures (Bradbury 1989).

Close proximity to the sea means that ADIA is prone to fog. High water vapour content sea air is brought over the land by the afternoon sea breeze. During the night the air is cooled to below its dew point temperature by the colder land surface, resulting in condensation in the form of dew, or fog (Hsu 1988).

The sea surface temperature reaches and exceeds 30°C in summer in the Gulf Sea. However, in the Arabian Sea, adjacent to the coast of Oman and toward the horn of Africa, it is about 5°C cooler (figure 3.31) with little change in winter (figure 3.30). The lack of warmer water in summer is due to up welling caused by the offshore component of the summer south-west monsoon wind, known locally as the Khareef. The upwelling of cooler water from below also brings plankton that attracts fish and gives rise to the fishing industry along the coast (Gill 1982). However, the stabilising cooling effect of the sea decreases the amount of rainfall along the southern coast (Taha, et al 1981).

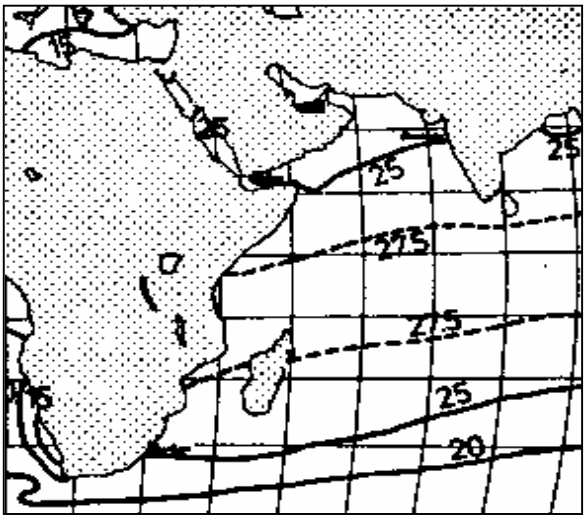

Figure 3.31. February mean sea surface temperature in ˚C (Rudloff 1981).

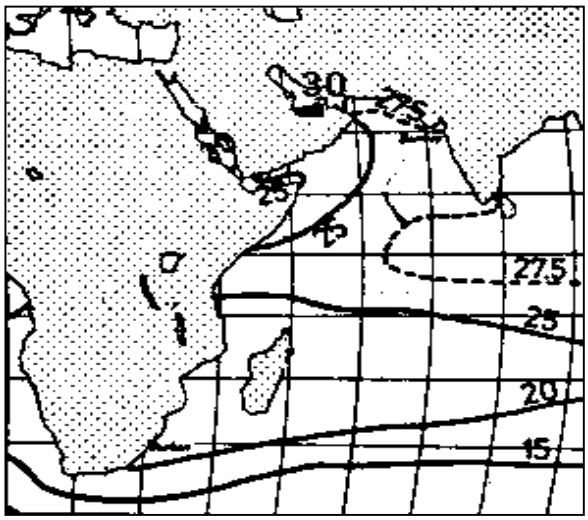

Figure 3.32. August mean sea surface temperature ˚C (Rudloff 1981).

3.11 SUMMARY

The atmospheric circulation and the weather experienced in the Arabian Peninsula, are strongly influenced by the summer and winter Monsoon over Asia and the annual reversal of trans-equatorial flow of air at the surface and the upper troposphere, as well as associated changes in divergence and convergence.

Primary effects are the surface transition from winter high pressure to summer low pressure, while in the upper troposphere, there is a change from a winter subtropical westerly jet stream to the summer tropical easterly jet. The circulation changes are reflected in a corresponding change in the water vapour flux.

Although Arabia is dominated by a high pressure cell in winter, the passage of mid-latitude low pressure cells, in association with upper air troughs, are important weather and rain producers. In conjunction with the passing lows, latitudinal movement of the surface anticyclonic cell over Arabia results in alternating southerly to south-easterly winds and northerly Shamal winds.

The summer circulation is dominated by the effect of the Asia low, the position of which results in a consistent northerly to north-westerly Shamal wind over most of Arabia, particularly in the north. Moist advection, into the low from the Arabian Gulf can provide enough moisture for frequent thunderstorms, which are driven to the UAE Gulf coast by the mid-level easterly circulation.

In spring rapid land surface heating causes increased instability, which accentuates shallow, near sub-synoptic depressions from north-west Africa. These shallow low pressure cells are preceded by southerly winds with intense heat waves and sandstorms.

Spring is also characterised by large day time temperature difference between the land and the still cool Gulf sea temperatures. This results in increased local wind circulations such as land and sea breezes and valley wind effects. The sea temperature is also influential in increased fog, particularly in autumn.

CHAPTER 4

FOG

4.1 INTRODUCTION

Fog is defined as occurring when water vapour in the atmosphere condenses into minute water droplets and the horizontal visibility falls below 1000 metres (UKMO 1991). Fog that reduces the visibility to the point where aircraft have to divert to another airport is not uncommon at ADIA. Over the period 1982 to 2003, the average annual frequency of fog at ADIA was 38 nights a year, the highest being 56 days in 2000 and the lowest, 23 days in 1992.

Until recently, the airport was equipped with a CAT IIIA Instrument Landing System (ADAC 2009a). This means that aircraft could land with a minimum runway visual range (RVR) of 200 m and 0 m decision height, or put another way 0 m cloud base or vertical visibility, provided the pilots are currently qualified and the aircraft is suitably equipped (table 4.1). However, from 2009 ADIA now has CAT IIIB capability, but, for technical reasons, is limited to 125m RVR (ADAC 2009a). RVR is the greatest distance that runway lights can be seen in the direction of landing, or take-off, along the runway as seen from the centreline at the point of touchdown at the average eye-level of the pilot (UKMO 1994). At ADIA RVR is electronically measured by equipment alongside the touchdown point at each end of the runway with another sensor at the centre point. This distance is usually further than the minimum non-directional distance that can be observed with the naked eye.

Table 4.1. Instrument landing system (ILS) criteria. Note, pilots must be suitably (and currently) qualified and the aircraft fitted with certified ILS equipment and autopilots operative.

ILS Category	CAT1	CAT2	CAT3A	CAT3B	CAT3C
Decision height in feet (metres)	200 (60)	100 (30)	0	0	0
Minimum runway visual range in metres	550	350	200	50	0
Or minimum visibility in metres	800				

Diverting flights to another airport due to below limit visibility results in considerable cost to airlines. The extra expense includes fuel used and hotel accommodation for the passengers. Flight and cabin crew can become duty time expired and by law may not fly again until they have been off duty for a specific period of time. Furthermore, passengers still have to get to their desired destination. When inclement weather is forecast by law civil aircraft must carry more fuel. This results in extra weight and therefore extra fuel consumption and lower profit for the flight. If cargo carried has to be decreased as a result, this will further decrease profit. Diverted and delayed flights also have a disruptive effect on the airport concerned. ADIA, the capital city's airport and Dubai International Airport, are important gateways to the United Arab Emirates. During 2008 there were over 93 163 aircraft movements at ADIA with 9 016 900 passengers and 353 820 tonnes of cargo processed (ADAC 2009b). Dubai airport in 2008, processed 37 441 440 passengers and 1 824 991 tonnes of cargo from more than 313 600 aircraft movements (Dubai International Airport, Department of Civil Aviation, 2009).

Many flights to ADIA originate from places up to ten hours flight time away. Added to this the flight dispatcher does the flight planning at least an hour before departure time. Fog is most common between 0300 to 0900 local time (2300 to 0500 UTC), so the best possible forecast, and fog warning, needs to be available by 1600 to 1800h. The latest available 24 hour terminal area forecast (TAF) would be the 1200 to 1200 UTC TAF, which is issued 6 hours before the valid time at 1000h or possibly the 1800 to 1800 UTC TAF issued by 1600h. This means that the latest available forecast could be 23 or more hours old by the time aircraft is due to land, or at best, at least 11 hours old for the later TAF. Aircraft such as the Airbus A340-500 have an endurance of up to 19 hours with Singapore Airlines making 18-hour non-stop flights between Singapore and New York (Airbus Industrie 2006). Since the 5th November 2008 the lead-time for forecasts issued at ADIA has been even longer, due to the introduction of 30 hour TAFs (ICAO 2007).

Better understanding of the conditions that cause, or accompany fog, or prevent it, will result in more accurate fog forecasts, less false alarms and earlier warning of the onset of fog. This will in turn result in improved flight planning by the airlines operating in and out of the airport, increased profit and improved preparedness on the part of the relevant airport authorities.

4.2 SCOPE OF THE STUDY

The weather conditions when fog occurred at ADIA during the 22 years from 1982 to 2003 are examined by means of a statistical analysis and case studies. This data set allowed the investigation of some local myths surrounding fog forecasting and at the end a proposed a methodology for forecasting fog at ADIA is presented.

A fog event, by meteorological definition, occurs when the horizontal visibility falls below 1000 metres (Roach 1994, UKMO 1991). Fogs observed in the close vicinity to the airport when the visibility remained ≥1000m have not been included in this study.

4.3 METHOD

The fog events were researched using surface observations at ADIA, as well as 1200 UTC and 0000 UTC atmospheric soundings at ADIA as well as Eta GFS NWP model data.

551 fog events at ADIA were used in the statistical analysis. 31 fog events during 2002 to 2003 were researched and includied 56 atmospheric soundings on most afternoons prior to the fog event and the early morning in question. During the two years of 2002 and 2003, 20 events, when fog was not expected and did not occur were also analysed for comparative purposes.

4.4 FOG PRODUCING PROCESSES

4.4.1 FOG TYPES

Most fog forms when the air in contact with the earth's surface cools and becomes saturated with respect to water. The two main types of fog being due to:

i Ground heat loss due to outgoing radiation (radiation fog).

ii Warmer air streaming over a colder surface (advection fog).

Other fog types are:

i Adiabatic cooling to saturation due to the expansion of air moving upslope under stable conditions, resulting in adiabatic cooling and saturation (upslope fog).

ii Frontal fog. This occurs when precipitation from warmer air falls into cold and stable air below and saturates the layer

iii A form of advection fog also occurs when cold, dry and stable air flows over a considerably warmer water surface (steaming fog).

iv The mixing of two slightly unsaturated air parcels at different temperatures, resulting in saturation (UKMO 1997, Roach 1994).

Most of the UAE is below 1500 feet, apart from at Al Hajar Mountains in the east, so upslope fog is not an important form of fog production. Due to its tropical position frontal fog is also, at most, a rare occurrence. The same applies to steaming fog.

In spite of the dominant fog forming mechanism, fog is rarely produced by a single process, but rather by any combination of the above, although one of them may be dominant (Petterssen 1956). Due to dry desert conditions next to the warm Gulf Sea, fog formation in the UAE is usually a combination of advection and radiation processes. Warm and moist Gulf Sea air is advected by the afternoon sea breeze and radiation cooling from the desert surface does the rest.

Radiation fog is most likely to occur when surface winds become calm, or light (below 7 knots at 10 m), with a clear sky (or limited to thin high cloud) and dry air above a moist boundary layer of about 350 feet (about 100 metres) and a weak pressure gradient. Anticyclones often cause weak pressure gradients suppressing the surface wind with stable atmospheric conditions due to subsidence and clear sky that promotes surface outgoing long wave radiation and cools the lower layers of air. A light wind enables the correct amount of turbulent mixing to take place, spreading the saturated layer through several metres, preventing all condensation to take place in the form of dew (UKMO 1994, UKMO 1997, Ricks 1981, Taylor 1917). Fog events are rarely associated with a cyclonic circulation.

Nocturnal radiation fog, over land with relatively windless air, is further encouraged to develop when the air has been previously moistened by rain or wet ground (Petterssen 1956, Xinmei, Lyons and Pitts, 1990).

The advection of warmer air over a colder surface, followed by nocturnal radiation cooling is a frequent combination resulting in the formation of fog (Petterssen, 1956). The formation of advection fog over land "is particularly likely in winter after a cold spell when a supply of milder air arrives from the sea" (UKMO 1997).

4.4.2 RADIATION FOG FORMATION PROCESS

After sunset incoming short wave solar radiation ceases but terrestrial outgoing long wave

radiation to space in the atmospheric radiation window (wavelength 10 micron) continues with the result that the ground surface cools rapidly. This in turn cools the air in contact with the ground and creates a shallow surface inversion. When the air in contact with the ground is cooled to below its dew point temperature (saturation point), the excess water vapour in the air condenses on the ground and is observed as dew. The condensation process releases latent heat into this near surface layer and slows down surface cooling (figure 4.1a). If the light wind continues to bring new moist air over the surface and just enough turbulent mixing results to dissipate the latent heat, dew will continue to form. This continual dew deposition, removing water vapour from the air, will prevent fog from forming. The dew point temperature will continue to fall and the air will have to be further cooled before fog forms (UKMO 1997, Brown and Roach 1976, Roach, Brown, Caughey, Garland and Radings 1976).

If the wind drops and water vapour advection ceases, so that the air dries out at the surface due to latent heat release and dew formation ceases, but there remains just enough turbulent mixing, radiation cooling can be carried upward and the air immediately above the ground becomes supersaturated (figure 4.1b). Then a deeper layer of air is cooled to below its dew point temperature, or fog point. Water droplets form in the air and fog begins to form about 20 cm above the ground. It has been noted that initial fog formation occurs when the wind at 2 metres above the ground temporarily drops to 1 knot or less (Galvin 2004, Findlater 1985, UKMO 1997). It is obvious that there is a delicate balance between dew, or fog formation exists.

At first the ambient temperature inversion base remains close to the ground and the density of the fog decreases with height with the colder air at the surface. However, further radiation cooling lifts the temperature inversion and, as the fog thickens, a point is reached where the fog is deep enough to obscure the sky (at about 20 to 50 metres) and prevent infrared radiation cooling at the surface. Instead, this takes place at the top of the fog layer (figure 4.1c). Consequently, the top of the fog layer becomes colder and denser than at the surface. Convection overturning occurs. Turbulent mixing caused by sinking cold thermals and rising warm thermals quickly creates a well-mixed fog with uniform liquid water content (UKMO 1997, Stull 2000, Cotton and Anthes 1989, Korb and Zdunkowski 1970).

Radiation cooling at the top of the fog layer causes further condensation and the fog deepens (Roach 1995). This process lifts the inversion away from the ground with a saturated adiabatic temperature lapse rate below (figure 4.1d). Marked wind shear occurs at the fog ceiling, which is usually about 25 metres above the base of the temperature inversion (UKMO 1997), or 50 metres according to Stull (2000).

Radiation heating from the sun is the main cause of the fog dispersion with clearing from the outer edges inward. Ground heating also warms the lower part of the fog. The relative humidity decreases and droplets begin to evaporate. Heating and turbulent mixing of warmer and drier air at the top of the fog causes the fog to dissolve, as does lowering of the inversion. An increased wind above the fog will entrain dry air into the fog top and the fog will thin. Advection of cloud over the top of the fog is another reason for dispersion. This stops, or reduces, radiation cooling from the top of the fog and droplet settling causes the fog to become thinner. Dry air advection obviously reduces moisture in the air and causes the fog to clear (UKMO 1997).

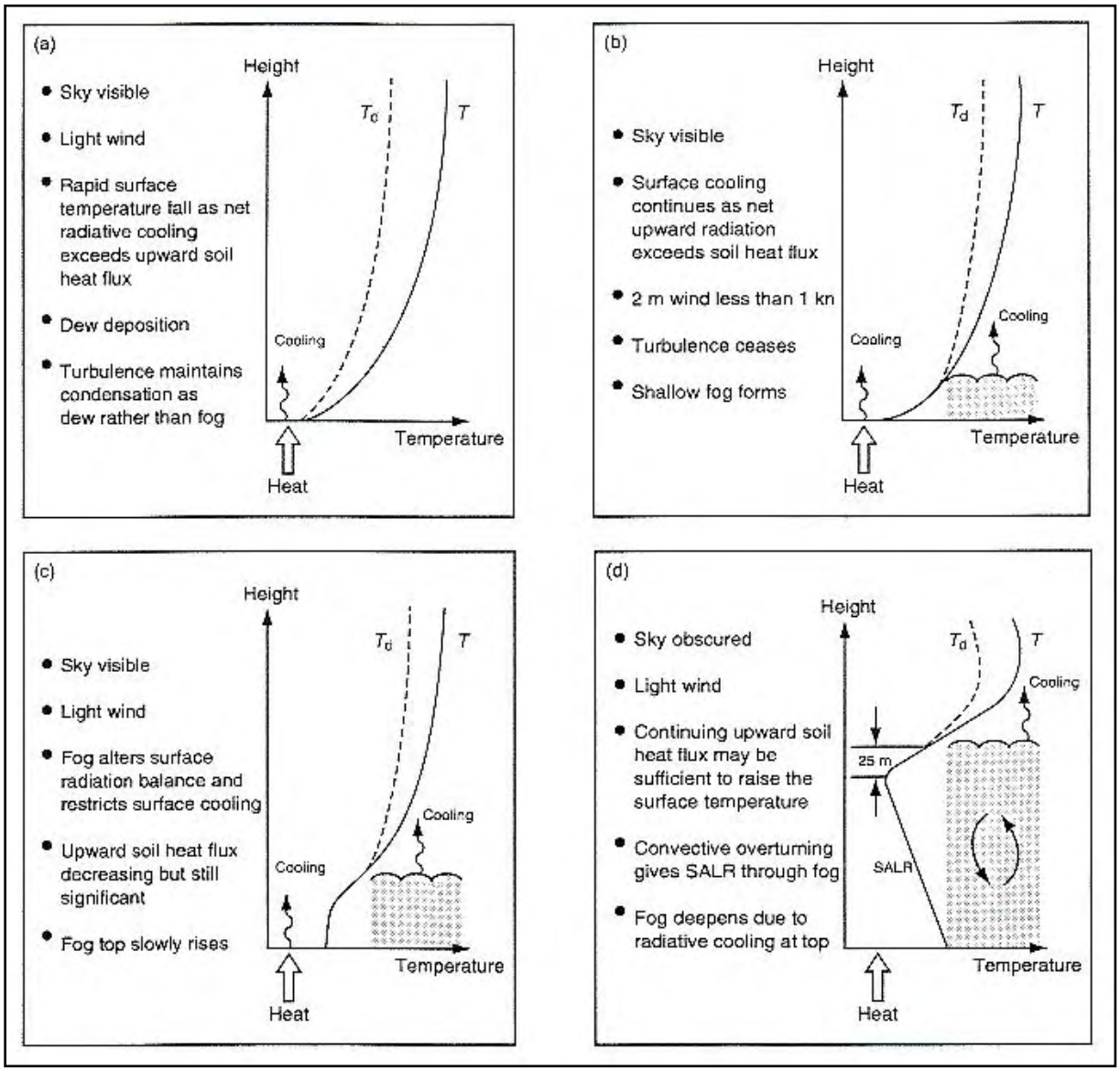

Figure 4.1. The sequence for fog formation taken from the UKMO Source book to the Forecaster's Reference Book (1997).

4.5 STATISTICS

Local rules of thumb for forecasting fog at ADIA abound. These include the relative humidity must be greater than 80% at 1800 UTC for fog to form later in the night; fog always occurs two nights in a row; fog does not form when certain wind directions occur and fog does not occur during full moon. Another is that very hazy conditions during the afternoon are often a precursor to fog later in the night, especially if low stratus cloud comes off the sea and passes inland of the airport. These factors confirm the abundance of hygroscopic particles, which promote condensation near the saturation level (Pruppacher and Klett 2003). Some rules of thumb can be shown to be statistically valid, others logically valid (as above) and others difficult to prove.

With respect to greater than 80% surface relative humidity at 1800 UTC being an indicator of fog, an analysis of all fog events during the 3 years from 2000 to 2002 was made. Results

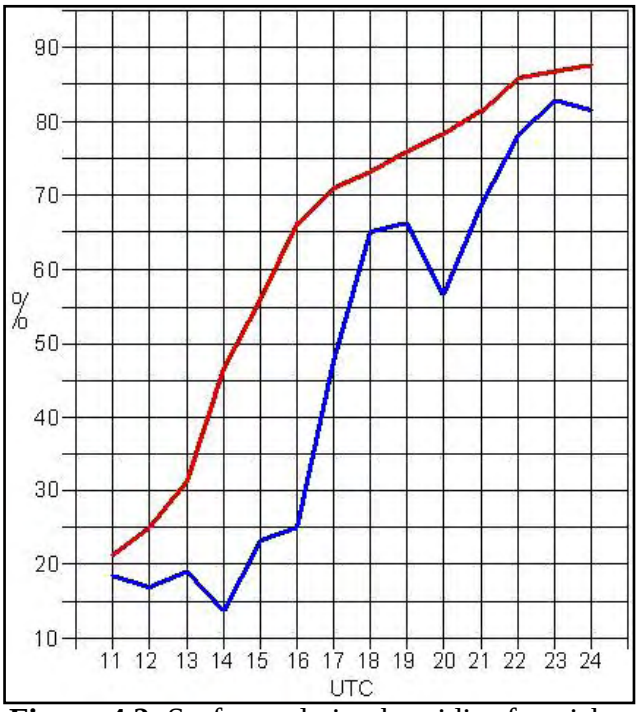

Figure 4.2. Surface relative humidity fog risk. The risk of fog later in the night is ≥90% if the relative humidity at a given time equals, or exceeds, the red line value. The blue line indicates the minimum value when fog has formed later in the night.

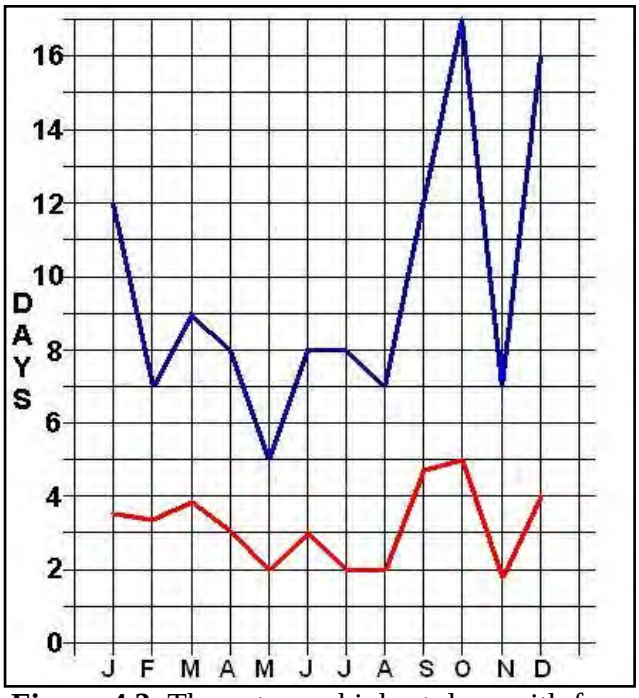

Figure 4.3. The extreme highest days with fog per month (blue line) and mean number of days with mean fog days per month (red line).

indicate that 90% of fog events occurred when the relative humidity was greater than 73% at this time (figure 4.2). Investigation of nights when fog did not occur showed that the relative humidity often exceeded 80% at this time as well. This was specially so during the hot and humid summer nights. Figure 4.2 shows the 90% and higher probability for other times in the night and late afternoon. The minimum relative humidity at a specific hour during a fog night is also shown. The conclusion is that this method can only be used as a short lead-time Nowcast tool.

During the ten-year period from 1993 to 2002 it was found that there was an 18% chance that fog will occur on two consecutive days, 6% that it will occur three days in a row, 2% and 1% for four and five days in succession, respectively. That is, persistence forecasting is practically useless.

The highest frequency of fog occurs in the autumn months of September and October and far exceeds the number of fog days at the end of winter and spring (figure 4.3). Ideally a minimum of 30 years data is needed to determine the climate of a place, but the airport has only been at its present location since 1982. Therefore, the figures may not be entirely climatologically representative. The monthly fog frequency distribution, both extreme and mean values, could possibly have a sinusoidal wave pattern, but they have been distorted by the anomalous October, November and December values, such as 17 days in October 1991, 16 days in December 1998 and 12 days in January 1985.

With longer nights in winter, fog occurs during more hours of the night and more frequently than in summer. During the winter months of January and February 1993 to 2002 (10 years) fog generally occurred between 1800 to 0700 UTC, but most frequently between 2200 to 0500 UTC

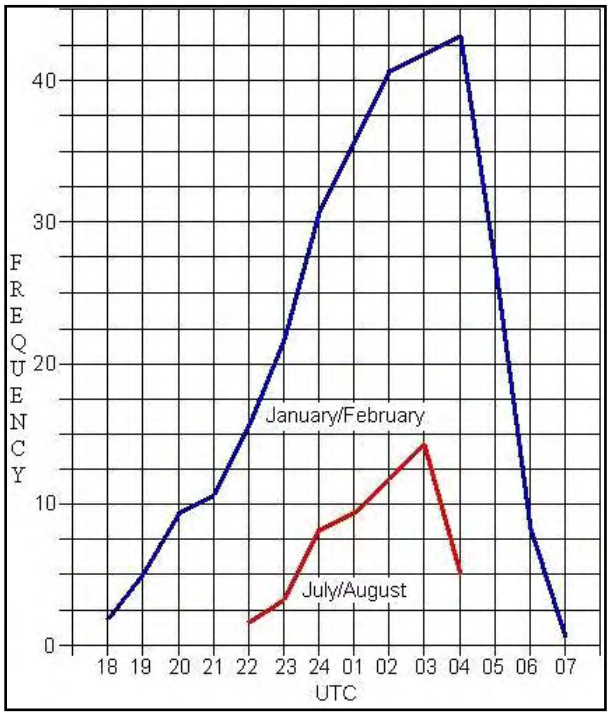

Figure 4.4. The hourly frequency of fog (visibility <1000) metres in winter (upper blue line) and summer (lower red line) for the period 1993-2002. The frequency is higher in winter, begins earlier in the evening and ends later in the morning than in summer.

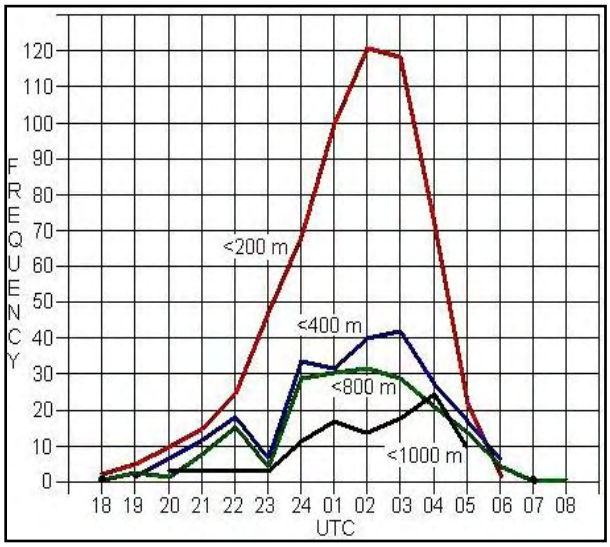

Figure 4.5. The hourly frequency of fog below different visibility levels for the period 1993-2002. 0200 – 0300 UTC) are most often the times of the worst visibility.

(figure 4.4). In summer (July and August) fog occurred between 2200 and 0400 UTC, but most frequently between 0000 and 0300 UTC. These two summer months and two winter months were selected because they are the two hottest and two coldest months respectively.

As soon as a fog event begins the horizontal visibility rapidly deteriorates, often to below the CAT3A ILS 200 m minimum (figure 4.5). This occurred on 54% of the 1166 fog hours in the ten year period 1993 to 2002, or 58% out of a total of 104 fog hours if one considers the visually observed CAT1 800 metres limit. The visibility reduction is particularly apparent between the hours of 2200 to 0500 UTC (figure 4.5). Taken into consideration with the graphs in figure 4.4, fog is a bigger aviation problem in winter than in summer. Airline flight schedule planners take the tendency for fog to occur from about 2200 UTC to 0500 UTC into consideration. Figure 4.6 shows that there is a distinct absence of, or drop in, passenger flight activity between these times. Those that operate later in the period are usually freighters. Unfortunately, some scheduled passenger flights arrive from Europe about 0200 to 0300 UTC. Fortunately, take-off, in poor conditions is less of a problem.

Local lore, with respect to wind change, is that fog forms when the north-westerly wind during the day veers through easterly to south-easterly overnight, becoming light, or calm in the process. Legend also has it that fog is likely to occur after the Shamal has been blowing for a few days and then drops. A Shamal is defined as a north-westerly, or northerly, wind with the hourly mean wind speed at, or greater than, 17 knots for at least three hours in a day (Rao *et al.* 2001).

On the other hand, if the wind backed from north-westerly to a light south-westerly, or a southerly desert track and perhaps south-easterly later, fog does not occur. A study of overnight hourly-observed wind changes during fog events from 2000 to 2003 revealed that the local lore is generally valid. Fog occurred 87% of the time when the wind veered through easterly, with the wind backing through westerly during the

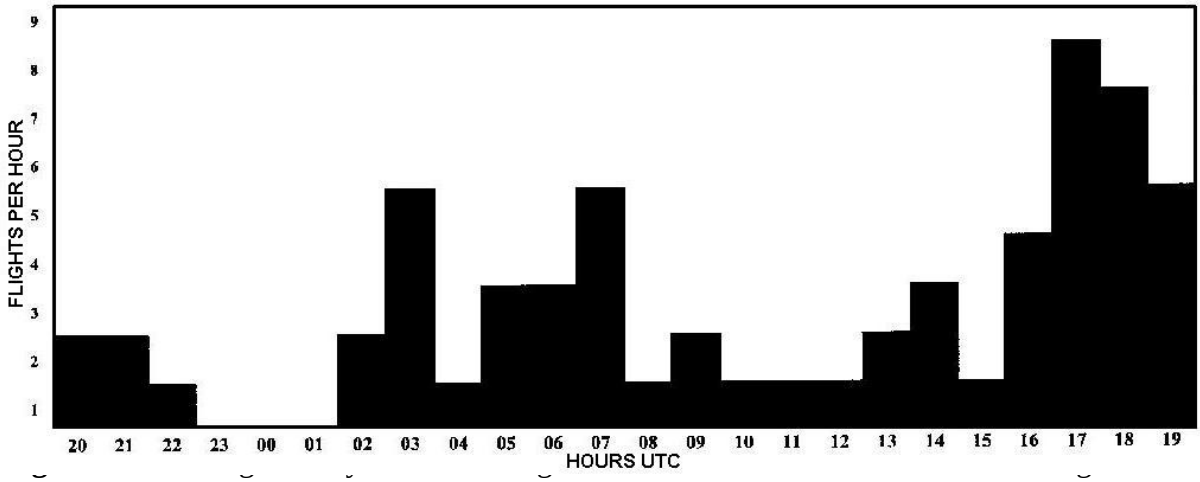

3 winter schedule.

remaining 13%. The propensity for the wind to veer rather than back is to be expected given the fact that the Coriolis force deflects the wind to the right in the Northern Hemisphere (Bradbury 1989, UKMO 1994). Note, there were no fog events when the wind persisted off the desert from a southerly direction throughout the night.

The wind generally becomes lighter at night, especially during fog events. Inspection of hourly wind observations on 20 nights when fog was expected and did not occur revealed that most often the surface wind blew consistently at about 3 to 6 knots and sometimes higher, irrespective whether it veered or backed. On one occasion when fog did occur, the wind veered from north-westerly to easterly and persisted blowing at 5 knots.

Fog did not occur when the wind persisted from the north-west to north-east. This is most likely during a Shamal when there is an increased pressure gradient between a surface low pressure cell or trough to the north-east, or east of the UAE and a ridge of high pressure situated over northern Saudi Arabia (Membury 1983). Under these conditions the wind is more likely to back to south-westerly over the Emirates at night due to the contribution of the land breeze. On rare occasions fog did occur when the wind backed through westerly (13%). This could happen when the Shamal drops and fog formation is likely. This happened when Abu Dhabi had been subjected to days of persistent moderate to fresh summer north-westerly Shamal wind, followed by 4 nights of fog from the 18 July 2002.

4.6 STUDY OF FOG EVENTS

4.6.1 INTRODUCTION

The conditions, under which fog forms and how its formation conforms to conditions established by research, is demonstrated in the following case study when fog occurred on four consecutive days. Other interesting and important aspects will be demonstrated by presenting more brief examples. The conditions when fog does not occur will also be discussed and examples presented.

4.6.2 FOUR CONSECUTIVE FOG DAYS IN SUMMER: 19TH TO 22ND JULY 2002

This summer fog event details, fog of varying intensity that occurred on 4 consecutive mornings from the 19th to the 22nd July 2002. The fog occurred after days of persistent north-westerly Shamal conditions that induced very humid air to flow southward onto the land from the Gulf, where surface sea temperatures were in the vicinity of 32°C.

4.6.2.1 NWP model data

Eta NWP model data analysis of the 0000 UTC (0400 local time) surface pressure fields indicated that, during the 4 day period, a col with a weak pressure gradient of about 1 hPa, persisted over the UAE. This col formed between a low pressure cell over the Gulf Sea and a semi-stationary low pressure cell over Saudi Arabia to the south of the UAE (figure 4.7a, b, c, d). The surface pressure over the Gulf slowly deepened from 999 hPa to 996 hPa, while inland it changed from about 1000 hPa to 997 hPa. At the 850 hPa and 700 hPa levels the circulation was persistently anti-cyclonic from the north to north-west with the centre of the anticyclone to the west of the UAE (not shown).

4.6.2.2 Surface observations

On all of the nights that fog occurred the onset of the 10 to 15 knots north-westerly sea breeze was between midday and 2 pm during the previous afternoon (0800 UTC to 1000 UTC). This gave ample time for the advection of surface moisture over the coast and adjacent interior (figures 4.8 to 4.11).

Every night fog formed after the wind at 10 metres became light variable, or light east-south-easterly, at 1 to 2 knots. Allowing for the effect of surface friction, it is feasible that the wind temporarily became calm at 2 metres above ground level prior to fog formation. An exception was the night of the 20th to the 21st when the wind blew consistently from the east-south-east to south-east at 3 to 5 knots, briefly dropping to 2 knots at 2300 UTC, over an hour after fog had already formed.

The fog naturally enough began to clear when the temperature began to rise after sunrise and the southerly to south-westerly land breeze picked up and had totally dissipated by 9 am (0500 UTC). Note the air temperature began to rise about two hours after the climate mean time of 0200 UTC indicated on the charts (figures 4.8 to 4.12). Sunrise at this time of the year is about 0145 UTC.

Local lore is that very hazy conditions the previous evening are often a forewarning of fog later in the night and especially so if low Stratus cloud comes off the sea and passes inland of the airport. The logic behind this is that hazy conditions confirm the abundance of hygroscopic particles favourable for condensation. On the first night, during the evening of the 18th (figures 4.8 and 4.9), hazy weather began about six hours before fog formed and the surge of shallow surface moist air was indeed sufficient to generate low Stratus cloud in the late evening between 10 pm and 1 am (1800 to 2100 UTC). On the other evenings the weather became hazy two to four hours before fog formed, except the 20th, which was hazy most of the preceding afternoon as

well. These results appear to confirm the local lore, but by the time these factors are confirmed it is too late to be of much use in the preparation of landing forecasts, except in the very short term

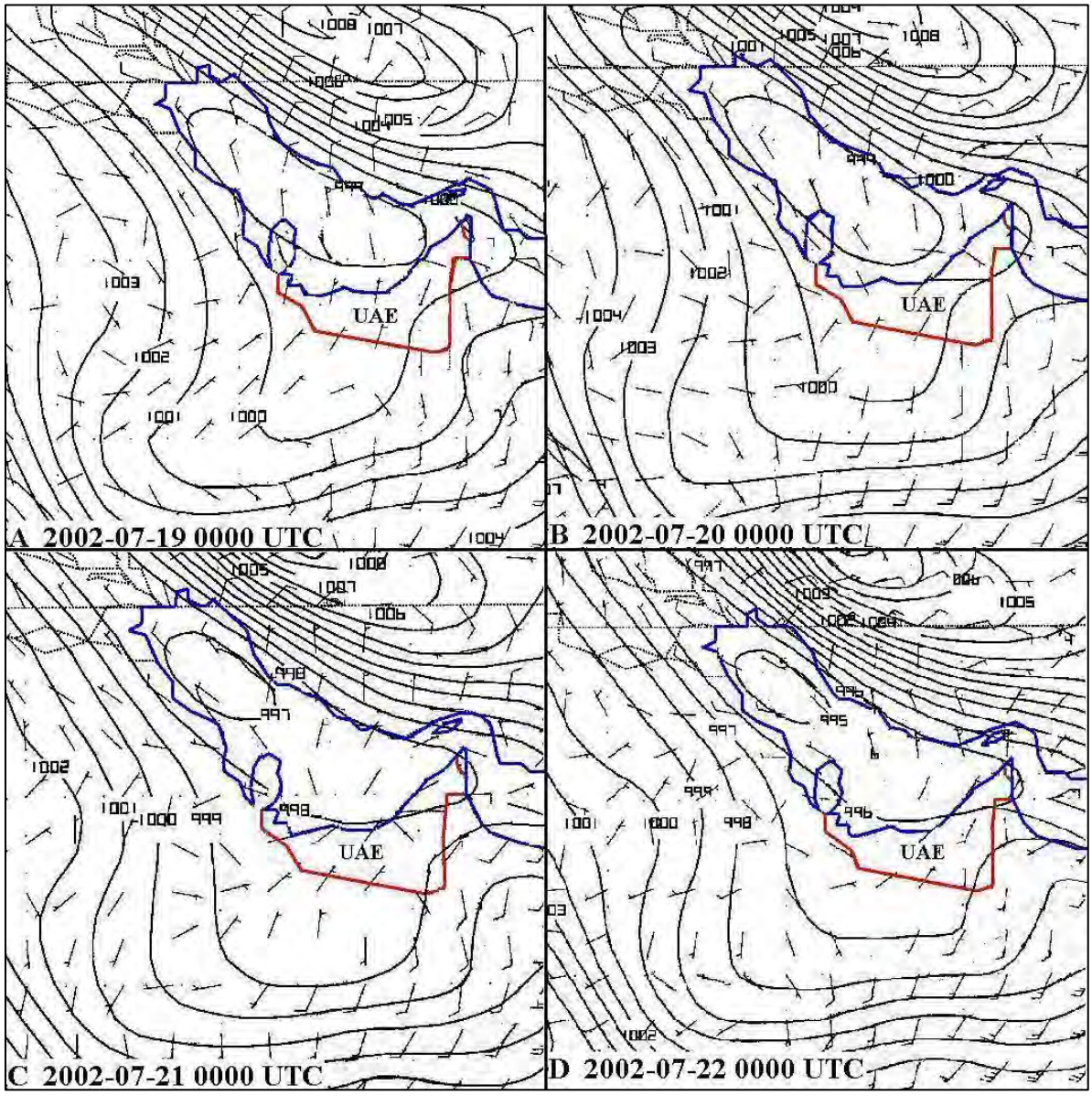

Figure 4.7. Eta GFS T+0 surface pressure and 10 metre wind analysis at 0000 UTC from the 19th to 22nd July 2002. Note a persistent low pressure cell over the Gulf Sea and the typical summer low pressure south of the UAE over the Empty Quarter.

Although fog was in and around the airport from 0000 UTC to about 0430 UTC on the 20th, it was only fully developed at the airport for about an hour around sunrise when the minimum temperature occurred (figure 4.10). This is probably due to the random nature of radiation fog, because the wind was certainly light enough at 3 knots from the east and the air over 95% moist from the surface up to 963 hPa (figure 4.11).

All of the hourly surface relative humidity observations on all four days exceeded the optimum values specified in figure 4.2 and in section 3 and the fog formed when the Stevenson screen relative humidity reached about 95%.

It is also worth noting that fog formed when the air temperature fell to below the maximum dew-

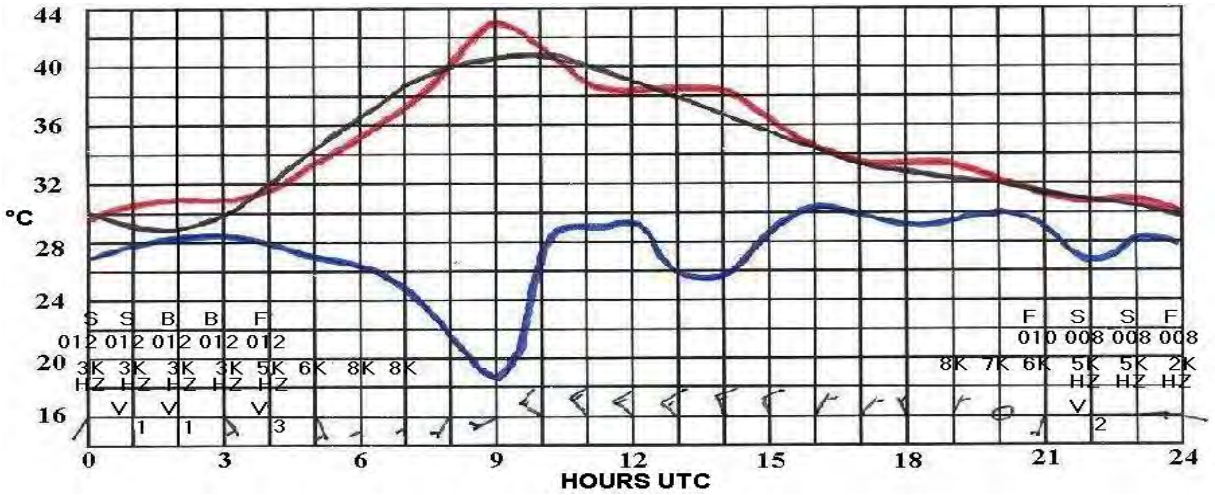

Figure 4.8. Surface observations on 2002-07-18. Air temperature (°C), red line; dew point temperature, blue. The black line is the long term mean derived from hourly observations from 1983 to 2002. Wind in knots. Few (F) scattered (S) and broken (B) cloud at 240 m 370 m (800 - 1200 ft) AGL. Visibility in metres and km. FG = fog, BCFG = broken (patches) fog. VCFG = fog in vicinity, BR = mist, and HZ = haze.

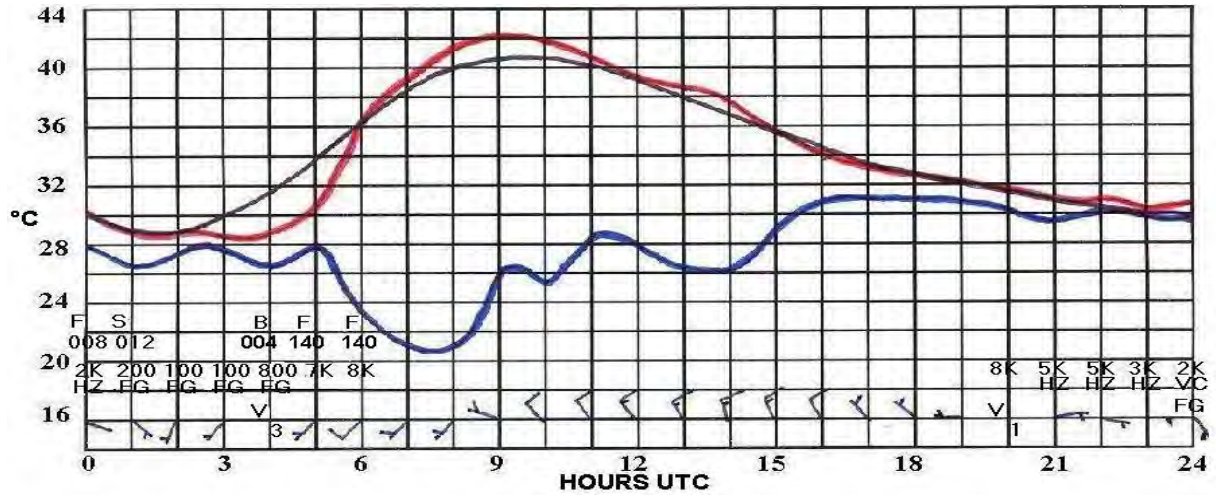

Figure 4.9. As in figure 4.8, but for 2002-07-19. The cloud is at 130 – 430 m (400 - 1400 ft) AGL

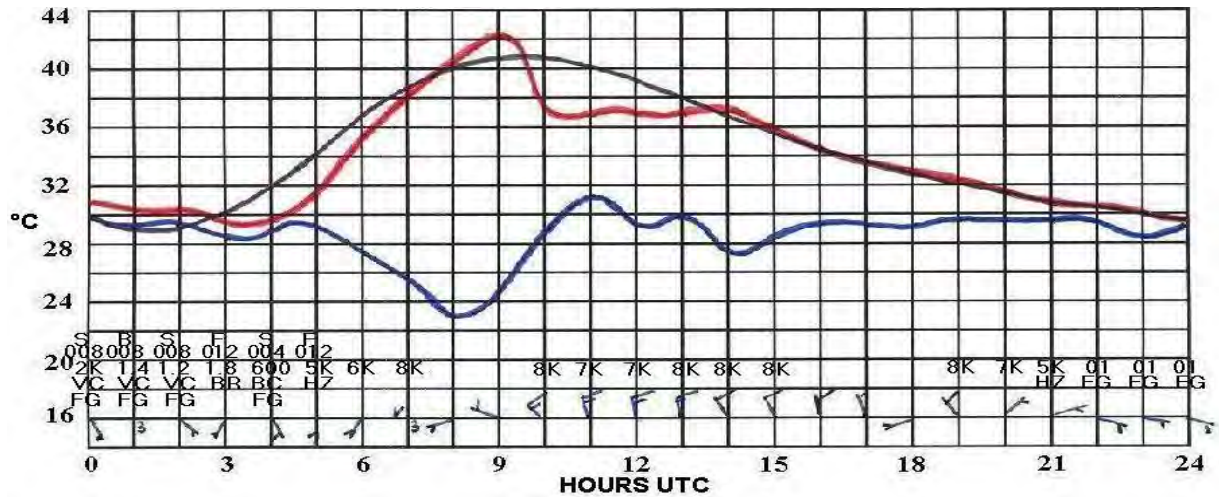

Figure 4.10. As in figure 4.8, but for 2002-07-20. The cloud is at 120 – 430 m (400 - 1400 ft) AGL.

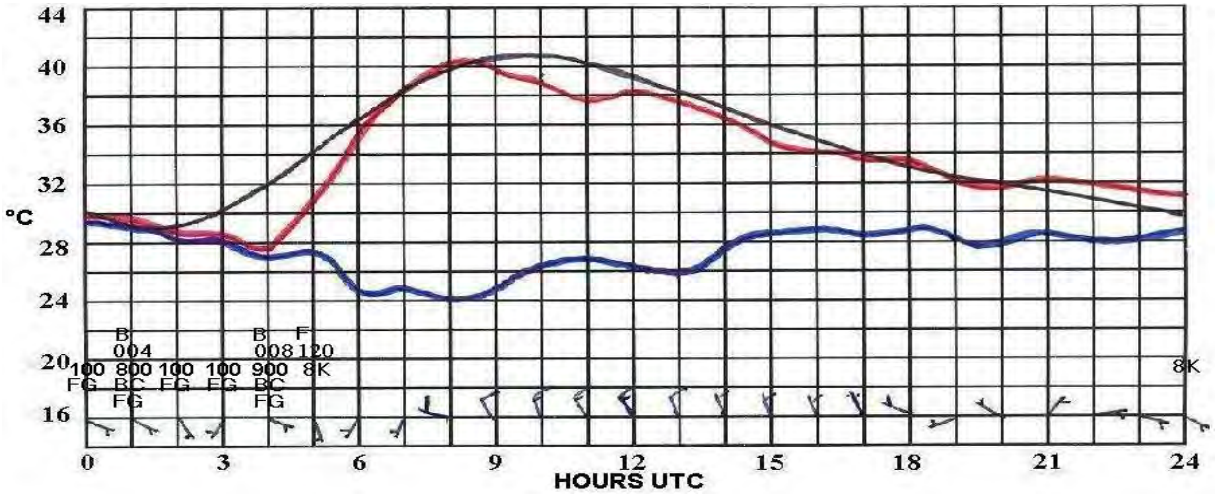

Figure 4.11. As in figure 4.8, but for 2002-07-21. The cloud is at 120 – 370 m (400 - 1200 ft) AGL.

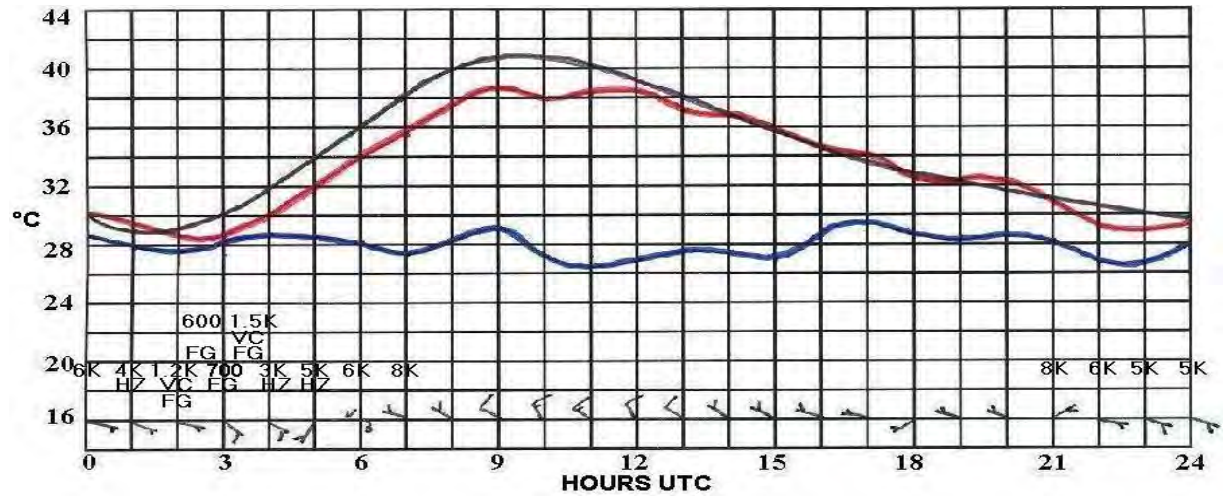

Figure 4.12. As in figure 4.8, but for 2002-07-22.

point temperature that prevailed the previous evening. For example, on the night of the 18th/19th, fog occurred at the airport from 0000 UTC when the air temperature fell to 30°C, which was the maximum dew-point temperature between 1600 UTC to 2000 UTC the previous day. Similar characteristics can be seen on the following nights (figures 4.8 to 4.12).

4.6.2.3 Atmospheric soundings

All of the soundings at 1200 UTC, prior to the fog later in the night, had near surface temperature inversions, indicating the invasion of cooler sea breeze air into an otherwise dry adiabatic temperature lapse rate (figures 4.13 to 4.17). Note; for convenience the soundings have been grouped 5 pages further on at the end of the discussion. Attention is also drawn to the fact that the Eta model vertical resolution is rather course and therefore inhibits the model's ability to reflect boundary layer inversions. As seen in table 4.2, the bases of the temperature inversions varied from 972 hPa to 960 hPa (213 metres to 316 metres AGL).

The afternoon soundings had relative humidity values >50% in the layer below the low-level temperature inversion, with markedly dry air above the inversion. The exception was on the afternoon of the 19th, when the humidity was marginally lower at 44% to 48% (figure 4.14).

North-westerly to west-north-westerly winds of 10 to 15 knots occurred below the temperature inversion, the wind becoming light easterly to north-easterly below the inversion by the time of the 0000 UTC sounding. Wind shear was noted at the inversion level on the mornings of the 19th and the 20th (figures 4.13 and 4.14), but it was absent on the other mornings.

The morning soundings had profiles very similar to the model in figure 4.1c with marked surface radiation cooling induced temperature inversions. The exception being the sounding on the morning of the 20th (figure 4.14), which had a close to saturated adiabatic lapse rate below the temperature inversion that is reminiscent of the profile in 4.1d.

The base of the temperature inversions at 0000 UTC varied from 974 to 958 hPa (201 metres to 323 metres AGL). Bearing in mind that research has shown that the fog top is 25 metres to 50 metres above the base of the inversion (UKMO1997 and Stull, 2000), the fog top probably varied between 251 gpm to 373 gpm (251 metres to 373 metres). Table 4.2 below shows the inversion bases in detail. Is it coincidence that the days with the shortest lived fog at ADIA were also the days with the highest inversion, namely, the mornings of the 20th and 22nd (figures 4.14 and 4.16)?

Table 4.2. Temperature inversion base height from the afternoon of the 18th to the morning of the 23rd.

	0000 UTC				**1200 UTC**			
		MSL	**AGL**			**MSL**	**AGL**	
	HPa	**M**	**m**	**Ft**	**HPa**	**m**	**M**	**Ft**
18					972	240	213	699
19	974	228	201	659	965	317	290	951
20	963	331	304	1000	961	343	316	1037
21	965	300	273	896	960	344	317	1040
22	958	350	323	1060	965	288	261	856
23	992	36	9	30				

During 2002 and 2003 the average base of the near surface temperature inversion on fog mornings was 19 hPa lower than the surface pressure at 987 hPa (171 metres AGL). Atmospheric pressure at the highest inversion base was at 958 hPa (400 metres AGL).

On the 19th, considering that the morning sounding was done about 1½ hours before fog formed it already showed a typical fog profile (4.13). The inversion base was at 213 metres AGL and 201 metres at 0000 UTC. Earlier in the evening and at the time of the 0000 UTC sounding, broken to scattered Stratus cloud was estimated at 430 metres and later at 240 metres AGL. In view of the inversion base, it is doubtful if this observed cloud base was correct. The presence of this cloud drifting in from the sea, prior to fog formation, also suggests that advection played a role in the fog formation at 0030 UTC. It is also worth noting that the 10m wind became easterly to east-south-easterly at 2 knots to 1 knot from 2200 UTC to 0000 UTC. Allowing for ground friction, the wind was most likely dead calm at the surface at these times.

According to Erikson (2001) radiation fog forms with a temperature inversion below 100 metres

and the visibility rarely falls below 135 metres. By his definition the fog that occurred on these four days, was predominantly advection fog, because the height of the lowest temperature inversion was above 100 metres and the visibility fell below 135 metres. Except on the 20th and 22nd, days when, although the inversions were at their highest, the visibility was greater than 135 metres at 600 and 700 metres, respectively (table 4.3 and figures 4.13 to 4.17).

Table 4.3. Sounding data up to the temperature inversion level on the fog days 19th to 23rd July 2002. Atmospheric variables are: Pressure, gpm height, temperature, dew point, relative humidity and wind velocity.

PRES hPa	HGHT gpm	TEMP °C	DWPT °C	RELH %	DIRC deg	SPED knot
00Z 19 Jul 2002						
996.0	27	31.0	28.8	88	90	0
995.0	36	29.8	28.2	91	86	0
982.0	155	29.8	28.2	91	29	6
974.0	228	30.0	28.6	92	354	9
972.0	247	31.5	21.3	55	345	10
970.0	266	33.0	14.0	32	341	10
00Z 20 Jul 2002						
996.0	27	30.6	29.9	96	90	3
963.0	331	28.6	28.1	97	21	6
956.0	396	32.8	5.8	19	6	7
950.0	453	36.2	2.2	12	353	7
00Z 21 Jul 2002						
995.0	27	29.8	28.5	93	100	2
969.0	263	29.4	28.7	96	53	4
966.0	291	29.6	24.9	76	47	5
965.0	300	29.4	21.4	62	45	5
963.0	319	30.4	13.4	35	42	5
956.0	384	35.0	12.0	25	29	6
00Z 22 Jul 2002						
993.0	27	30.4	28.2	88	110	3
961.0	322	29.6	27.6	89	94	3
958.0	350	29.6	25.2	77	92	3
944.0	483	37.4	8.4	17	85	3
00Z 23 Jul 2002						
993.0	27	28.8	26.6	88	110	6
992.0	36	28.2	25.8	87	107	6
988.0	72	30.0	28.9	94	97	6
973.0	211	36.4	3.4	13	58	6
968.0	258	37.0	3.0	12	45	6
944.0	487	37.4	0.4	10	340	7

Erikson (2001) also makes a distinction between marine and advection fog, but admits that marine fog is really "another type of advection fog." From this point of view it can be argued that the fog on the mornings of the 19th, 20th and 21st (figures 4.13 to 4.15) was marine advection fog, because the winds below the temperature inversion were from the north-east to north-north-east.

That is, parallel, or onshore, to the coast. In similar vein, the fog on the 22nd (figure 4.16) must have been land advection fog, because the wind was light east-south-easterly to easterly (table 4.3). In any event, the author believes that there was moist air advection from the Gulf during the afternoon and evening and nocturnal radiation cooling did the rest. The author has also noted that fog tends to form inland of the airport and drift, or expand coastward on the light morning south-easterly wind.

Although fog did not occur on the morning of the 23rd, the soundings at 1200 UTC on the 22nd and 0000 UTC on the 23rd have been included (figure 4.17). The reason is that the temperature and dew-point profile was very similar to those of the preceding four afternoons. It was over 50% moist with 10 to 15 knots north-westerly winds below a temperature inversion at 965 hPa (288 gpm MSL). What changed seems to be that the surface wind remained consistently stronger throughout the night. Although the surface wind veered to east-south-easterly in the evening, it generally blew at 5 to 9 knots from the east-south-east and only momentarily dropped to 2 knots at 2100 UTC. Radiation cooling of the air was, therefore, limited to a very shallow near surface inversion at 992 hPa (9 gpm AGL, or 30 feet) (table 4.3). The wind maintained turbulent mixing and the visibility fell no lower than 5000 metres in haze.

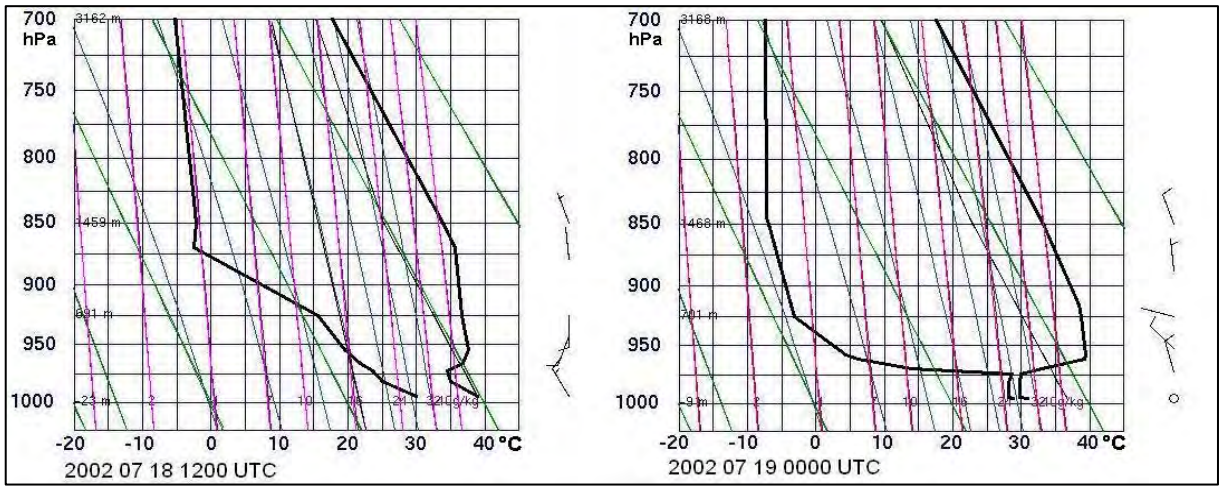

Figure 4.13.Atmospheric soundings at ADIA on 2002-07-18 1200 UTC and 2002-07-19 0000 UTC. The dry adiabatic lapse rate lines re in green and the mixing ratio lines in pink. (Courtesy

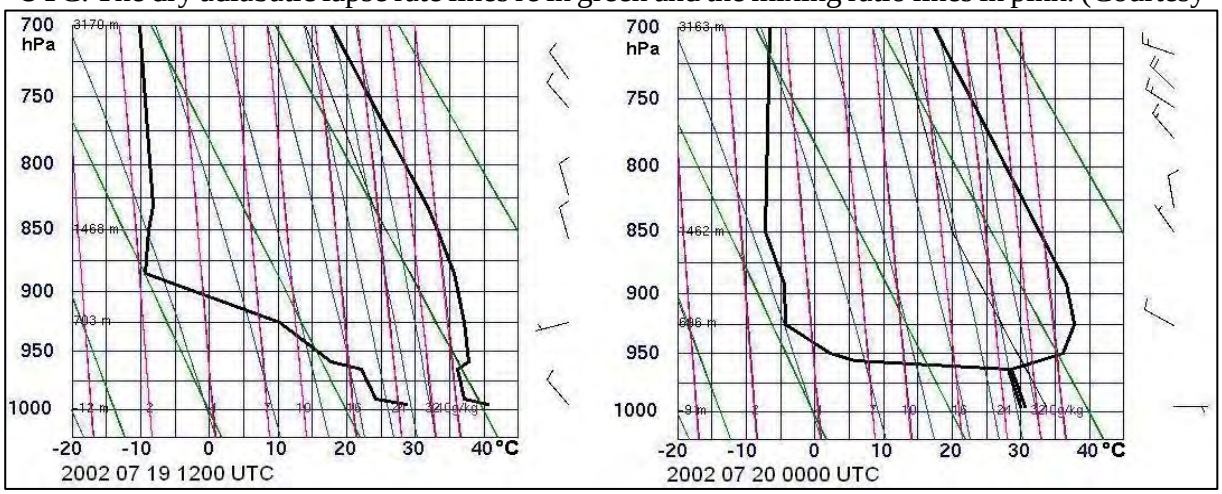

Figure 4.14. As in figure 4.13, but for 2002-07-19 1200 UTC and 2002-07-20 0000 UTC. (Courtesy of the University of Wyoming).

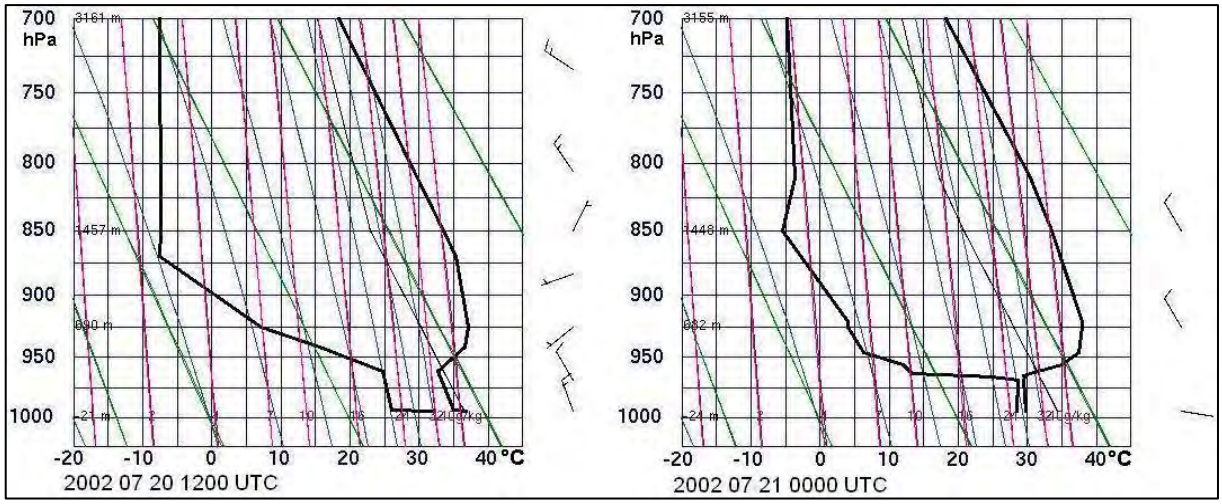

Figure 4.15. As in figure 4.13, but for 2002-07-20 1200 UTC and 2002-07-21 0000 UTC. (Courtesy of the University of Wyoming).

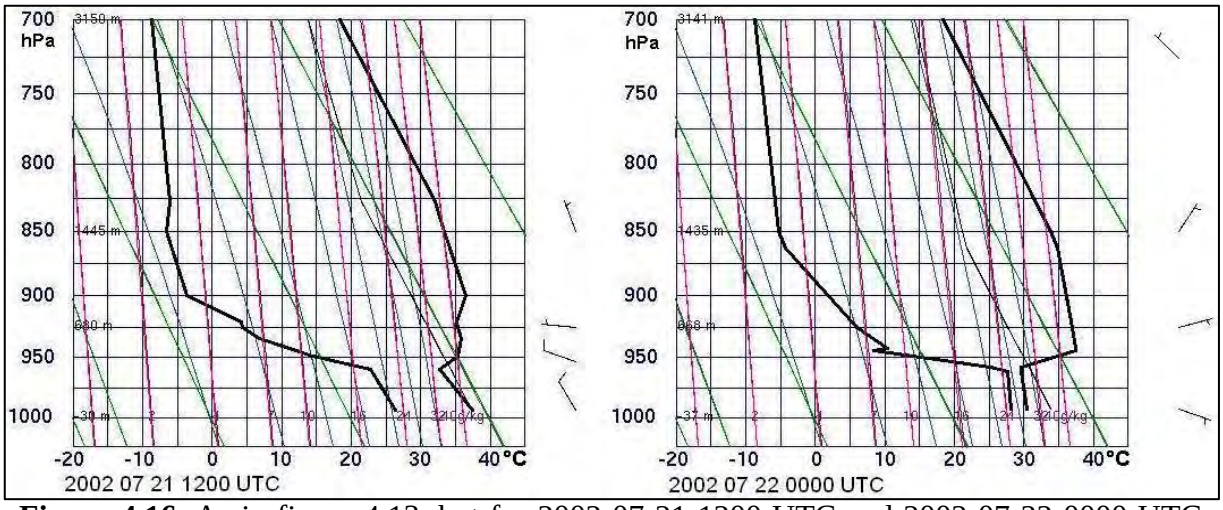

Figure 4.16. As in figure 4.13, but for 2002-07-21 1200 UTC and 2002-07-22 0000 UTC. (Courtesy of the University of Wyoming).

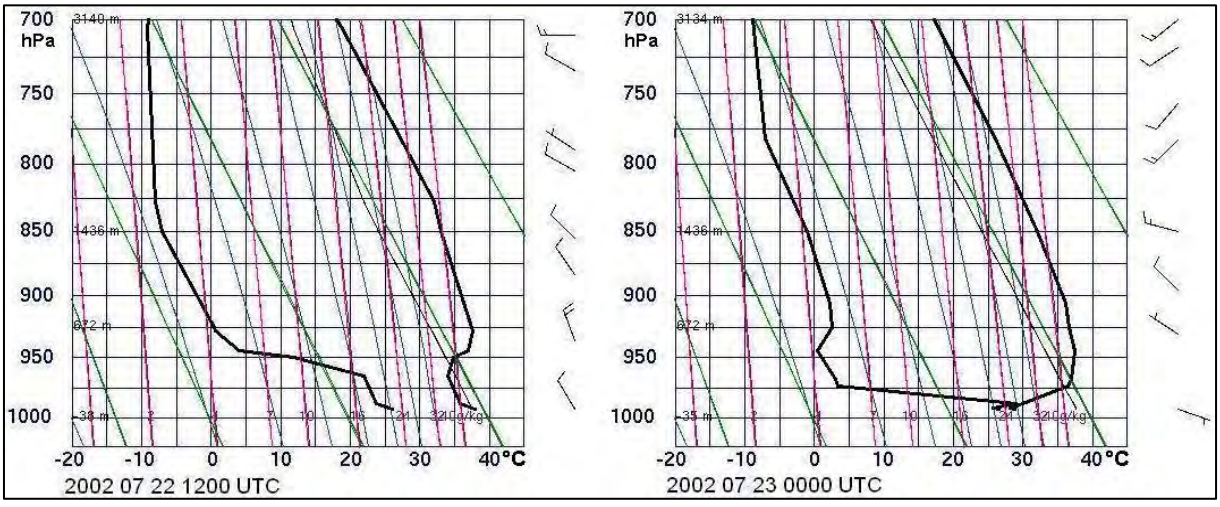

Figure 4.17. As in figure 4.13, but for 2002-07-22 1200 UTC and 2002-07-23 0000 UTC. (Courtesy of the University of Wyoming).

A feature of these soundings (figures 4.13 to 4.17), as well as other soundings detailed in this chapter is the extreme dryness of the air above a temperature inversion. This indicates the presence of a continental anticyclone, strong subsidence (superior air). During summer intense surface heating causes widespread thermal convection and a shallow warm cyclone (or heat low) develops below the subsiding air (Garbell 1947).

4.6.2.4 Summary

The fog formed in a weak pressure gradient after Shamal wind conditions.

A weak surface pressure gradient persisted over the UAE during the four days with the moderate afternoon sea breezes, which brought moist air from the Gulf Sea, and the surface wind veering to become a light south-easterly wind during the night. Although the weather conditions appeared favourable for fog formation on the 5th morning, this did not happen probably due to the wind at the surface, and the first 1000 feet, blowing consistently at 5 to 9 knots.

From the ground up to the temperature inversion the wind tended to back to north-north-easterly, but on the 23rd, when there was no fog, it remained east-south-easterly and stronger.

Evidence of moist air could be seen in the hazy conditions that developed in the evening prior to the fog forming. It was also apparent in the above 50% humidity below the near surface temperature inversions recorded by the afternoon atmospheric soundings.

Fog formed when the surface air temperature cooled to, and below, the maximum surface dew-point temperature that occurred in the late afternoon, or early evening.

The fog formed below temperature inversion bases that varied from about 200 metres (650 ft) AGL to just over 300 metres (1000 ft) AGL. A limited survey of fog events during 2002 and 2003 revealed that the inversion is on average 170 metres (560 ft) AGL. Wind shear was not always present at the temperature inversion. The marked dryness of the air above a temperature inversion is indicative of strong subsidence and superior air.

There is evidence that the fog formed as a result of a combination of radiation and advection processes.

The fog cleared about 2 hours after sunrise when the ground warmed due to insolation and the effect of insolation on the fog cloud top.

4.6.3 THREE CONSECUTIVE FOG DAYS IN WINTER: 9TH TO 11TH JANUARY 2003

Fog of varying intensity, occurred on three consecutive mornings from the 9th to the 11th January 2003.

The fog occurred after three days of north-westerly Shamal winds. These were fresh to strong at first due to the pressure gradient between an anticyclone of about 1025 hPa over Saudi Arabia and a low pressure cell over southern Iran. However, by the time the fog days occurred, the winds had moderated considerably as the weakened anticyclone moved over the area. The fog

happened when the anticyclone was overhead and, characteristically of an anticyclonic circulation, the winds became light at the surface and aloft in the boundary layer up to 900 metres (±3000 ft).

4.6.3.1 NWP model data

Model data was not available for all the days on which fog occurred. However, there is enough to demonstrate the dilemma faced as a result of conflicting information when forecasting fog.

During the night of the 8th/9th the ETA NWP model indicated sufficient 500 hPa to 350 hPa moisture that is indicative of extensive middle and high layer cloud. It was thought that with this cloud, radiation cooling would have been inhibited and fog would not form. However, all that transpired was very patchy and thin Cirrus cloud, which therefore did not have the expected effect.

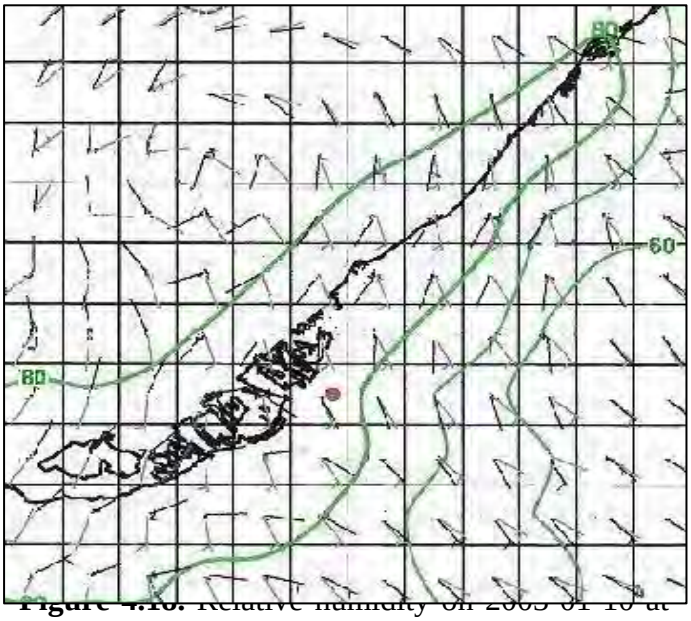

Figure 4.18. Relative humidity on 2003-01-10 at 0300 UTC (T+15). Winds (knots) at 10 metre (black) and 950 hPa (grey) with downward vertical velocity (blue lines).

The T+12 and T+15 humidity fields at 0000 UTC and 0300 UTC on the 10th gave conflicting evidence. Only about 80% humidity was indicated along the coast and adjacent interior, but the winds at the surface and at 950 hPa were light with little directional shear (figure 4.18).

The prognostic atmospheric profiles at the same times confirmed the very light low level winds, but showed a temperature inversion at about 950 hPa with a lifted condensation level close to 900 metres (figure 4.19). The latter is not really significant except that it means that the surface temperature and dew point temperature cannot be close to saturation and therefore there should not be a lot of surface moisture. But one has to bear in mind that the coarseness of the model resolution, available at this point, is too large for reliable profiles.

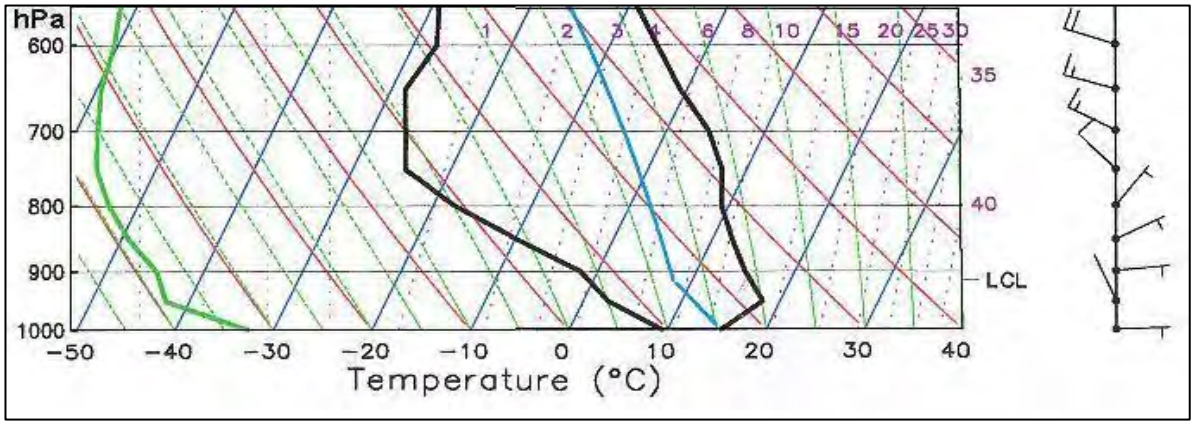

Figure 4.19. Eta WAFS prognostic profile at ADIA on 2003-01-10 at 0300 UTC (T+21).

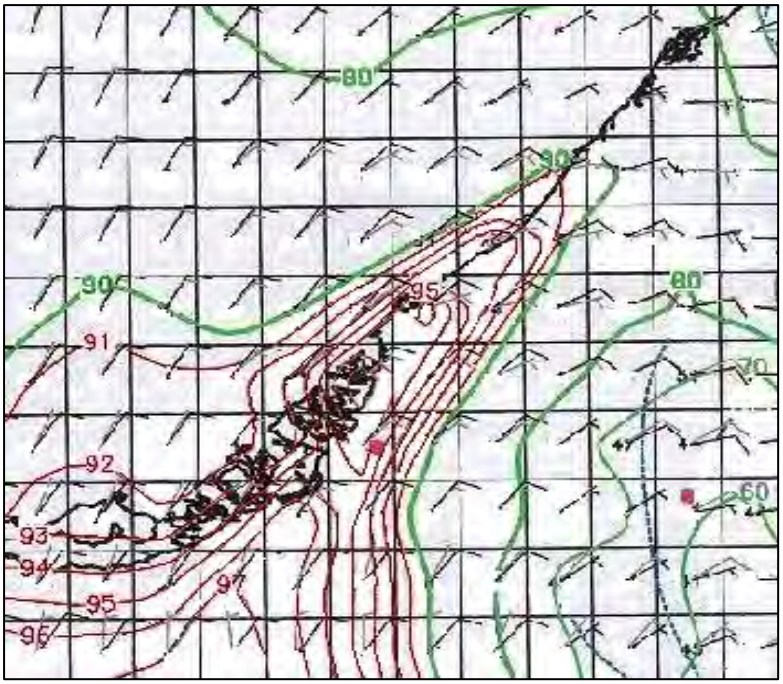

Figure 4.20. Relative humidity on 2003-01-11 at 0300 UTC (T+39). Winds (knots) at 10 metre (black) and 950 hPa (grey) with downward vertical velocity (blue lines).

The surface humidity and wind prognostic fields at 0000 UTC (T+36) and 0300 UTC (T+39, figure 4.20) for the following day the 11th, showed much higher humidity values than those of the 10th with light north-easterly surface winds, but stronger at 950 hPa. In other words there was again conflicting evidence, especially when experience with the model is that the humidity is always higher with a longer lead time. According to local belief, a north-easterly surface wind is also not a favourable wind direction for fog.

The conflicting information is clearly visible in the time cross section for Abu Dhabi which shows ideal light south-easterly surface winds around 0000 UTC on the 10th and moderate humidity, but less favourable stronger north-easterly winds with higher humidity around 0000 UTC on the 11th (figure 4.21).

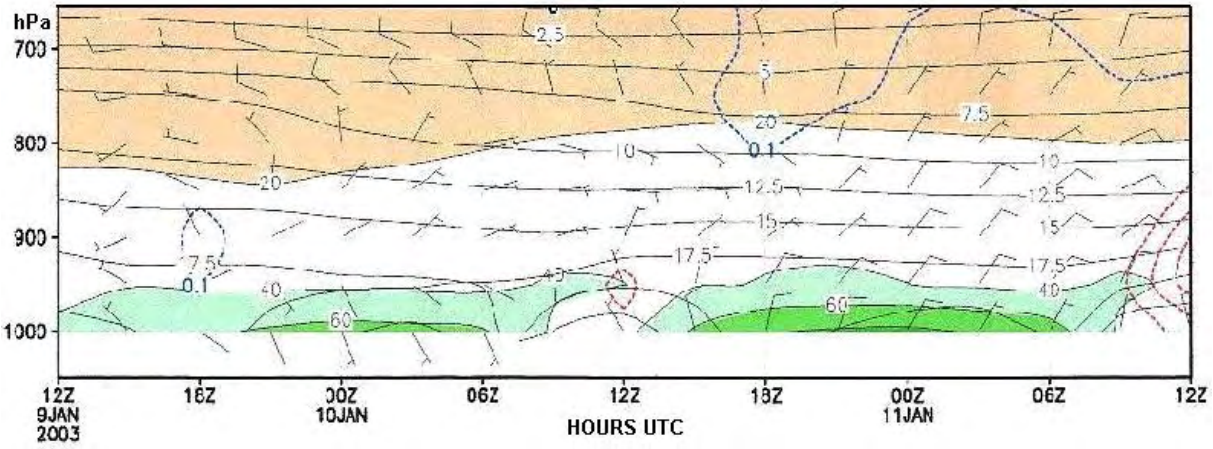

Figure 4.21. Time cross-section at ADIA from 2003-01-09 1200 UTC (T+0) to 2003-01-11 1200 UTC (T+48). The sequence reflects the higher humidity on the morning of the 11th around 0000 UTC, with less favourable 1000 hPa winds.

4.6.3.2 Surface observations

As in the previous study, a north-westerly sea breeze preceded the fog events, but the sea breezes were about 5 to 10 knots lighter (figures 4.22 to 4.25). Onset of the sea breeze wind was about 1 pm (0900 UTC), but it was as late as 5 pm (1300 UTC) on the 9th (figure 4.23). Veering of the wind to the east and its becoming light usually began about 1800 UTC, but was stronger and from the east at 4 to 6 knots until 2200 UTC on the 10th (figure 4.24).

Fog formed once the wind at 10 metres had become almost calm, but once again the exception was on the morning of the 10th (figure 4.24) when it formed with an easterly wind of 5 knots.

All of the hourly surface relative humidity observations on all days exceeded the optimum values specified in figure 4.2 in section 3 and the fog formed when the Stevenson screen relative humidity reached about 95%. The fog also formed earlier in the night than in the previous summer situation.

An intriguing and unexplained contrast with the summer study above was that fog formed three to six hours after the ambient temperature fell below the maximum dew-point temperature earlier in afternoon and evening. For example, on the night of the 10th/11th, the maximum dew-point temperature the previous evening was about 17°C, but the fog did not develop until 2200 UTC when the air temperature had fallen to about 14°C (figure 4.24). On the night of 8th/9th the air temperature was 6°C cooler before fog formed (figures 4.22 and 4.23).

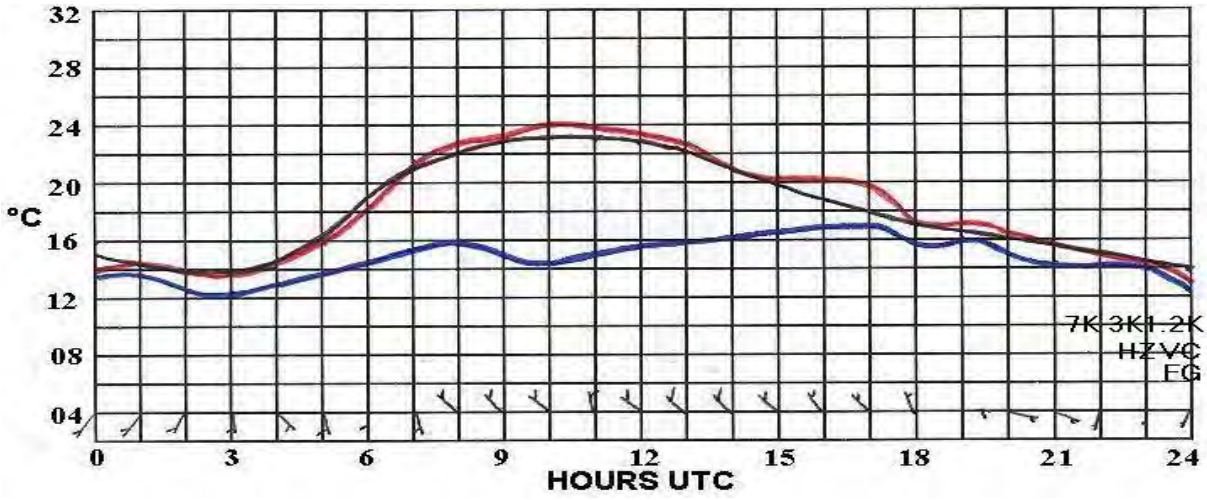

Figure 4.22. As in figure 4.8, but for 2003-01-08.

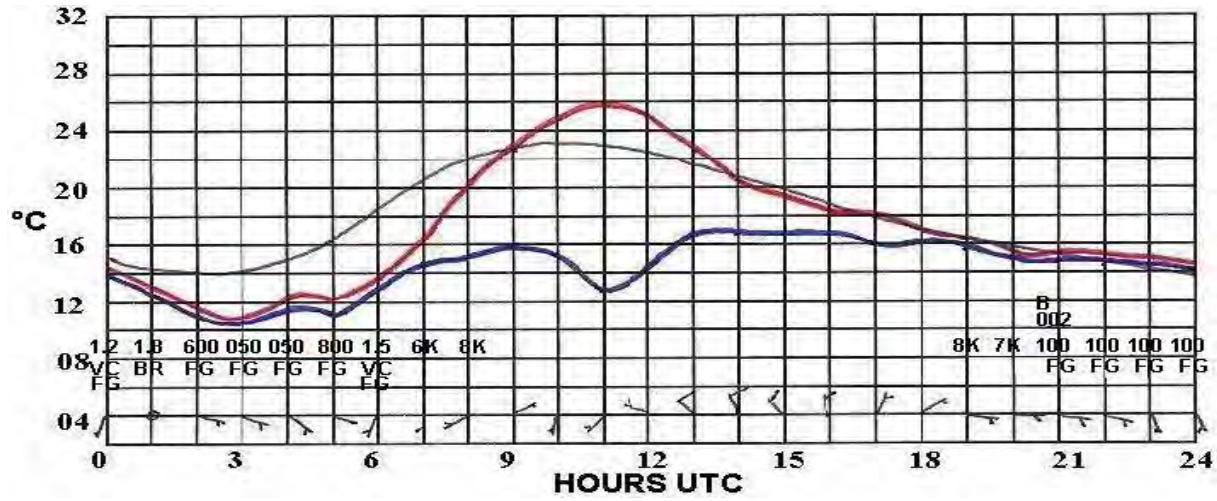

Figure 4.23. As in figure 4.8, but for 2003-01-09. The cloud is at 60 metres (200 ft) AGL

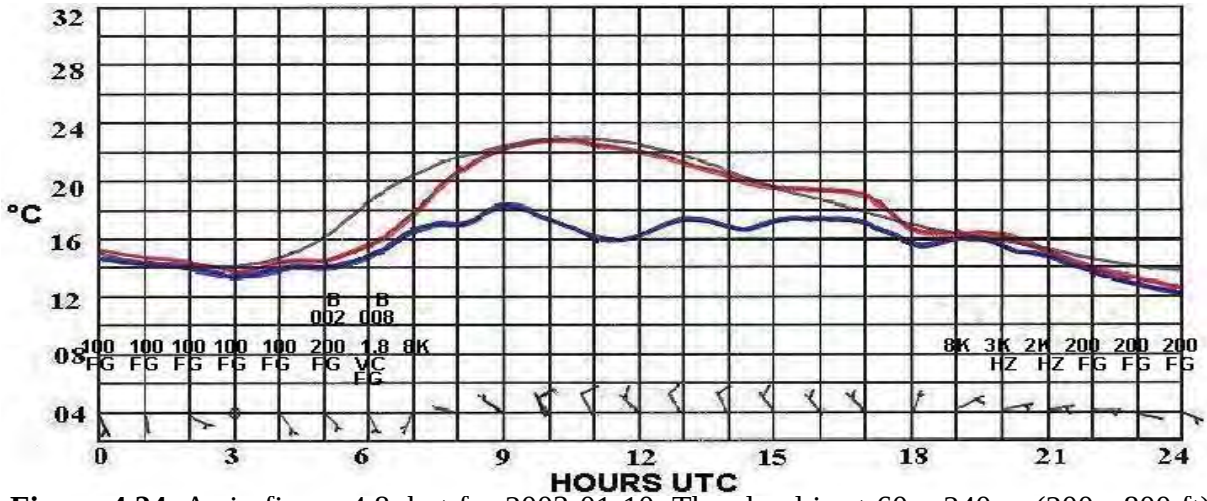

Figure 4.24. As in figure 4.8, but for 2003-01-10. The cloud is at 60 – 240 m (200 - 800 ft) AGL.

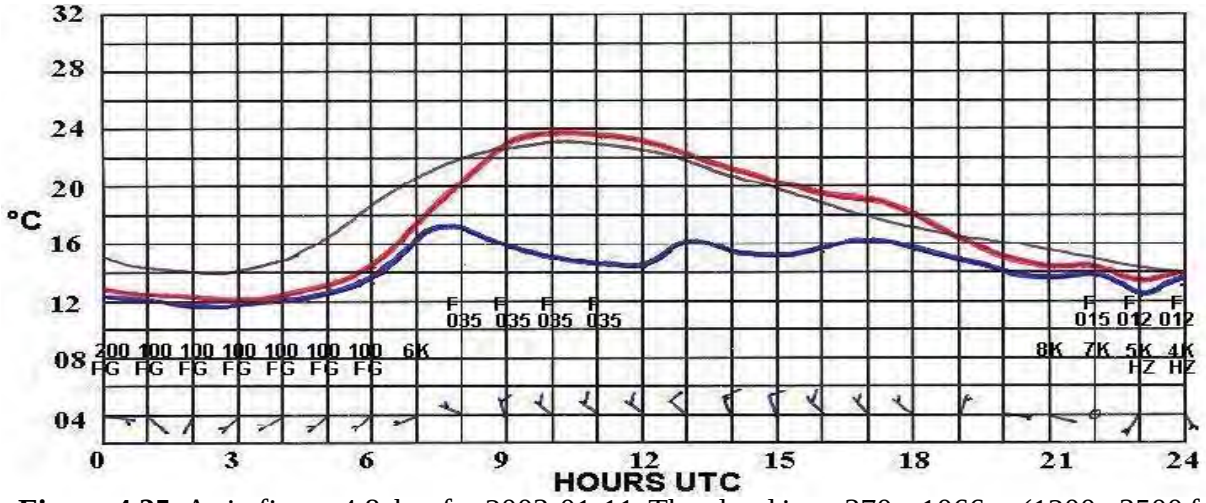

Figure 4.25. As in figure 4.8, but for 2003-01-11. The cloud is at 370 – 1066 m (1200 - 3500 ft) AGL.

4.6.3.3 Atmospheric soundings

What is clearly evident in this study is that the atmospheric sounding profiles (figures 4.26 to 4.28) differ from those in the previous study (figures 4.13 to 4.17). Due to the lower winter land temperatures, the wedge of cooler maritime air, brought by the sea breeze, is less pronounced on the afternoon soundings. Meanwhile, the morning ascents had shallow surface inversions, or difficult to discern near surface inversions surmounted by an isothermal layer as opposed to a marked temperature inversion that was evident in the previous summer event.

The sounding at 1200 UTC, on the afternoon of the 8th (figure 4.26), did have had a near surface temperature inversion, but, at 907 hPa (966 gpm MSL, or 961 metres AGL) this is usually considered to be far too high for later fog development, with the dry adiabatic lapse rate and near constant humidity mixing ratio below the inversion being indicative of turbulent mixing of the air and more likely to produce Stratocumulus cloud beneath the inversion.

Pre-fog afternoon soundings were moist near the surface. Near to 60% relative humidity existed

up to 966 metres MSL on the 8th (figure 4.26) and up to 167 metres on the 10th (figure 4.28), with near 50% relative humidity up to 608 metres on the 9th (figure 4.27) and marked drying of the air was present in a roughly isothermal layer above the moist air.

The afternoon ascents of the 8th and 10th (figures 4.26 and 4.28) were accompanied by north-north-westerly winds of 5 to 10 knots in the moist surface layer, veering to north-easterly higher up on the 8th (figure 4.26). The sounding on the afternoon of the 9th (figure 4.27) differed in that the low level winds were still light south-south-westerly. Inspection of the surface observations on the day show that at the time of the sounding the wind was still in the process of changing from a light southerly land breeze to a north-westerly sea breeze. The late persistence of the drier land breeze accounts for lower near surface relative humidity on this sounding as opposed to the other two days.

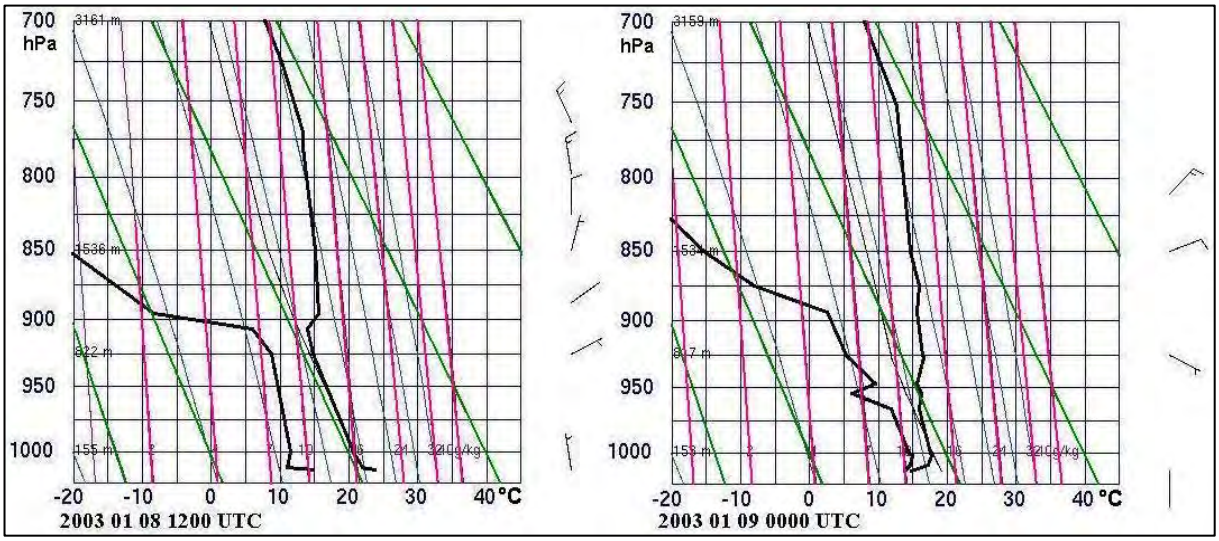

Figure 4.26. As in figure 4.13, but for 2003-01-08 1200 UTC and 2003-01-09 0000 UTC. (Courtesy of the University of Wyoming).

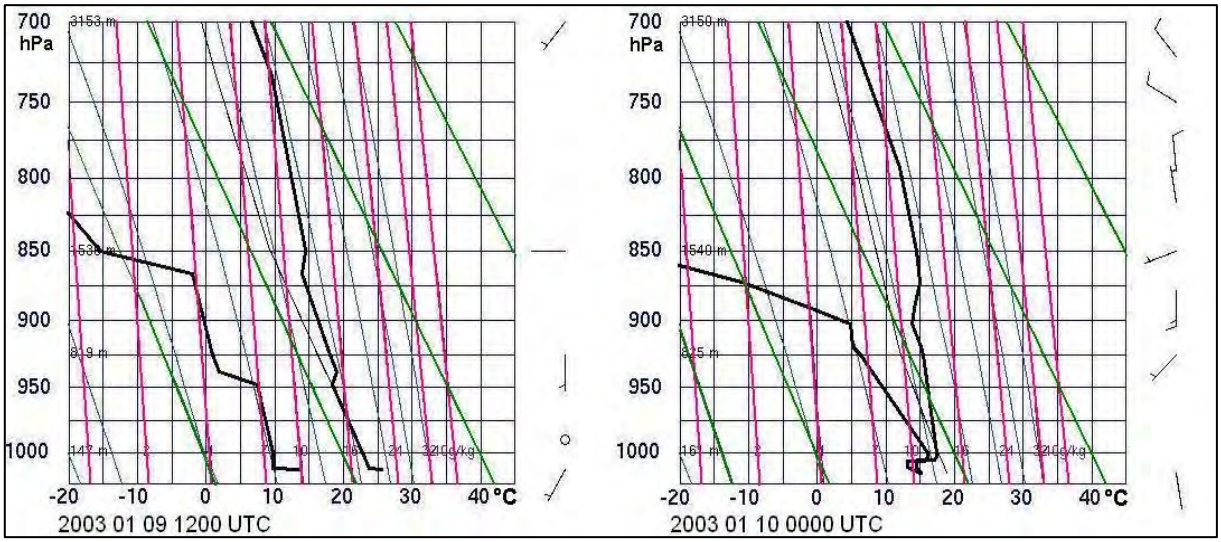

Figure 4.27. As in figure 4.13, but for 2003-01-09 1200 UTC and 2003-01-10 0000 UTC. (Courtesy of the University of Wyoming).

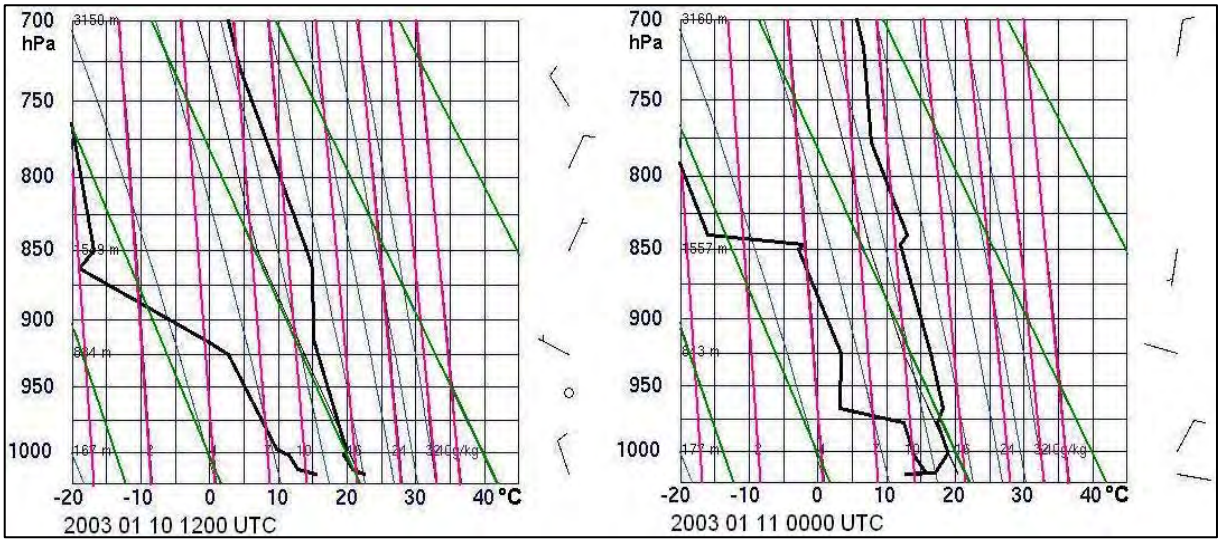

Figure 4.28. As in figure 4.13, but for 2003-01-10 1200 UTC and 2003-01-11 0000 UTC. (Courtesy of the University of Wyoming).

In contrast to the pronounced and usually elevated summer morning inversions, the base of the temperature inversion at 0000 UTC on the 9th and 11th lay at the surface, while on the 10th it was slightly elevated to 102 metres MSL (75 metres AGL). The low level winds were light south-easterly to easterly, with little in the way of wind shear, apart from the morning of the 11th when the wind changed to north-easterly 9 knots at the top of the inversion (table 4.4).

Table 4.4. Sounding data at ADIA for 09th to 11th January 2003. Pressure, gpm height, temperature, dew-point, relative humidity and wind velocity sounding data up to temperature inversion level on fog days.

PRES hPa	HGHT gpm	TEMP °C	DWPT °C	RELH %	DIRC deg	SPED knot
00Z 09 Jan 2003						
1015.0	27	14.8	13.8	94	180	1
1010.0	69	17.2	14.7	85	120	2
1002.0	136	17.8	14.9	83	24	3
00Z 10 Jan 2003						
1016.0	27	15.2	14.9	98	170	2
1012.0	60	14.4	13.1	92	144	3
1007.0	102	14.4	13.1	92	111	5
1006.0	110	17.0	15.7	92	105	6
1003.0	136	17.4	16.1	92	85	7
00Z 11 Jan 2003						
1018.0	27	13.2	12.9	98	100	1
1017.0	35	17.0	15.7	92	96	1
1002.0	160	18.8	13.8	73	38	9

4.6.3.4 Fog indices

The two previous case studies were used to investigate the use of fog indices to forecast fog. The three indices selected for trials were those given in the Source Book to the Forecaster's Reference Book (UKMO 1997), namely, the Saunders and the Craddock and Pritchard methods of fog-point calculation and the fog point in relation to the 850 hPa wet-bulb potential temperature (WBPT).

The Saunders method uses the condensation level calculated from the temperature and dew point temperature at the time of the midday sounding. The humidity mixing ratio where the condensation level cuts the dew point line is then traced back to the surface. The temperature at this level is the expected fog temperature. Certain provisos, such as excluding a surface superadiabatic temperature lapse rate and increased dew point lapse rate aloft are applied (appendix C). Invariably dry air present aloft at ADIA always rendered a far too low fog temperature. The Craddock and Pritchard method is an empirical formula that utilises the 1200 UTC screen temperature and dew point temperature along with wind and cloud tables to calculate a fog temperature in relation to the minimum temperature expected the following morning, values of 1°C or more above being an indication of fog (appendix C). It usually rendered values 2°C to 4°C below the expected minimum temperature, or about the same, thereby indicating no fog, or a risk of fog, respectively. The 850 hPa WBPT generally produced values below the fog temperature. The Saunders and 850 WBPT being closer to the mark in the winter event when there is a greater depth of higher humidity (appendix C, table 1)

Two locally suggested methods to calculate a WBPT fog point were tested. The first uses the surface 1200 UTC WBPT (excluding a surface superadiabatic temperature lapse rate), while the second uses the earlier 0000 UTC surface temperature and the 1200 UTC surface dew point temperature to calculate a forecast surface WBPT, or fog temperature for the following night. The two methods, tested on numerous fog days in addition to those shown in table 1, appendix C, yielded mixed results. The methods were just as likely to indicate values favourable for fog, or unfavourable values, the results being more reliable during persistent fog, that is, no air mass change, but unreliable at the onset and clearing phases.

The opinion of the author is that the indices are more suited to the wetter and more temperate climate of England where they were developed, than much drier UAE. The surface WBPT method using a 0000 UTC maximum temperature and 1200 UTC dew point gave favourable results often enough to be promising, but it must be more fully investigated and it is believed that numerous exception stipulations will have to be applied and their further use at ADIA is not advised.

4.6.3.5 Summary

The model data gave conflicting clues as to whether fog would form or not. First of all, middle and high layer moisture suggested cloud development at these levels, which did not materialise. Then on another night favourable light south-easterly to southerly winds were indicated with less than favourable surface humidity. Finally, on another night a light surface wind was indicated with high humidity, but it was from the north-east, a direction not locally considered conducive to formation. The stronger north-easterly wind at 950 hPa also did not help.

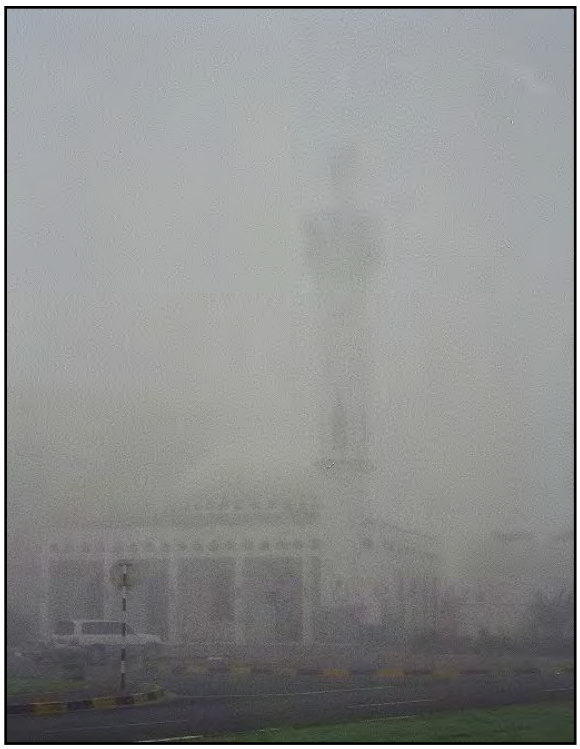

Figure 4.29. A photograph of winter fog at Abu Dhabi at 8 am on the 7th March 2004. The fog drifted, or expanded, to the island city from the interior via the airport.

As in the previous study, the fog is likely to form after the north-westerly Shamal wind has been blowing for a few days and then drops.

Also in common with the previous study, the fog formation on the three nights occurred with a weak surface pressure gradient and light surface wind, but with more moist surface conditions.

The event also differed from the previous study in that the fog was associated with an anticyclone, as opposed to a col area. The north-westerly wind was a precursor to an anticyclone, with a weak pressure gradient, arriving over the area where the stable and subsiding conditions, as well as clear sky aloft, fostered radiation cooling and fog formation immediately inland of the coast. Fog development was aided by the availability of hygroscopic particles in the form of sea salt in suspension, which the light morning south-easterly land breeze then carries back to the coast (figure 4.29).

The fog began earlier in the night than the previous summer event, probably due to the longer winter night and cooler temperatures. The air temperature also fell to well below the maximum dew point temperature earlier in the evening before fog formed.

The atmospheric soundings differed in that, due to the cooler winter land temperatures, the wedge of sea breeze air was less pronounced on the afternoon soundings. Meanwhile, the morning ascents had shallow surface inversions, or difficult to discern near surface inversions. These were surmounted by an isothermal layer as opposed to a marked temperature inversion seen in summer.

Pre-fog afternoon soundings relative humidity was 50% to 60% moist near the surface, with markedly dry air above. This is in common with the previous event, as were the light low level south-easterly to easterly winds.

4.7 STUDY OF NON-FOG PRODUCING EVENTS

4.7.1 INTRODUCTION

There are a few basic synoptic patterns that prevent fog formation. Essentially they involve a surface low pressure cell and its position in relation to the UAE. These are a low pressure cell to the west of the UAE (including north-west and south-west), or to the east (including south-east and north-east) of the UAE. Having said this there is another typical winter circulation that also

does not result in fog and this involves an anticyclone over southern Iran, of which a brief example will be given.

The key to all of them is a wind strong and/or dry enough to maintain turbulent mixing of the boundary layer air and prevent condensation in the air near the ground.

These situations are often not as obvious as one would like and can lead to mental agonising by the forecaster whether the wind is going to drop sufficiently for fog to form and then a nail biting night wondering whether the correct decision has been made.

4.7.2 SURFACE LOW PRESSURE CELL TO THE WEST: 13TH JUNE 2003

Irrespective of the position of the low pressure cell to the west, the cyclonic circulation brings dry air from the desert to the UAE from the south, or south-west.

4.7.2.1 NWP model data

A surface low developed over the western UAE and, according to NWP model data, it was expected to remain centred more or less in this position until the 14th, before moving to the eastern UAE on the 15th. This is not uncommon in the summer months. Intense surface heating, results in an almost permanent heat low over the Arabian Peninsula with fluctuations in the position of the centre of the low dependent upon surrounding synoptic scale changes.

Figure 4.30 shows the Eta NWP analyses and T+24 prognostic positions of the low pressure cell west of Abu Dhabi on the 12th and 13th, with a 1000 hPa high over Oman. In spite of the fact that there is normally a late afternoon north-westerly sea breeze, the cyclonic circulation is producing a southerly flow over the eastern UAE, particularly in the vicinity of Abu Dhabi. That is, dry air from the desert.

In addition to the indicated light southerly wind, the surface relative humidity prognostic field with low level winds at 0000 UTC on the 13th confirmed that dry air would be carried to the coast from the desert (figure 4.31).

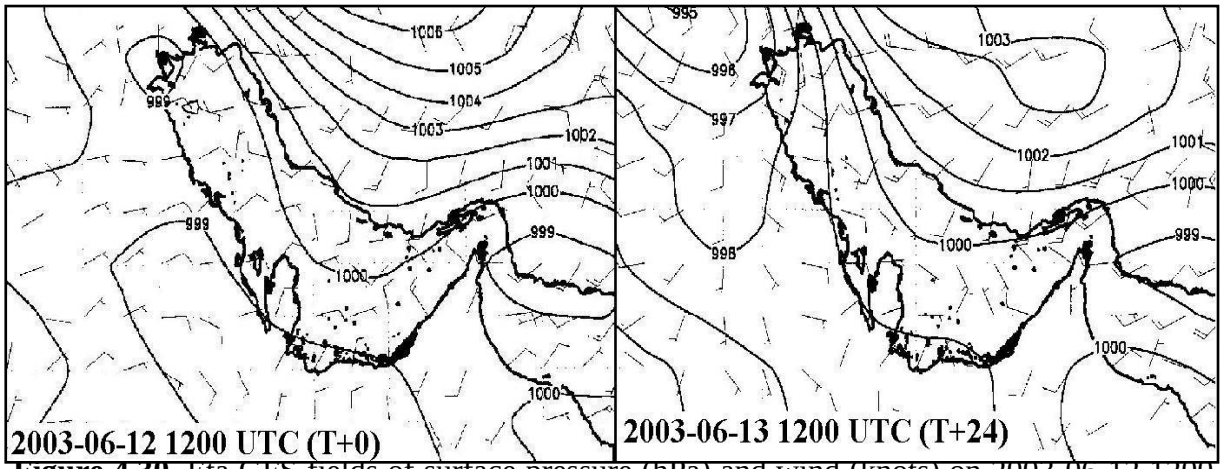

Figure 4.30. Eta GFS fields of surface pressure (hPa) and wind (knots) on 2003-06-12 1200 UTC (T+0) and 2003-06-13 1200 UTC (T+24).

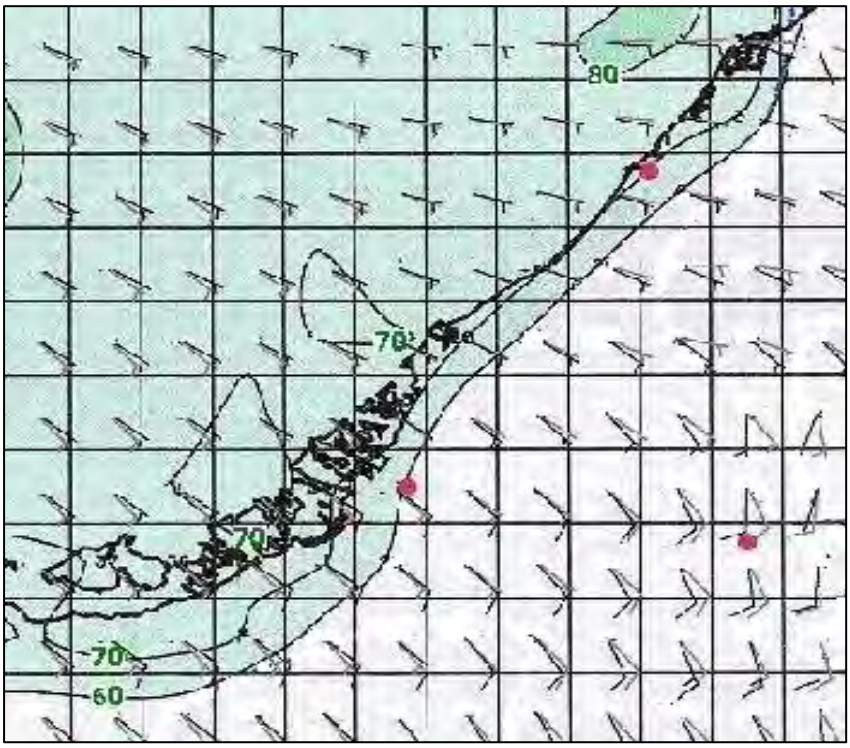

Figure 4.31. Eta relative humidity on 2003-06-13 at 0000 UTC (T+24). Winds (knots) at 10 metre (black) and 950 hPa (grey) with downward vertical velocity (blue lines).

The surface time cross sections at Abu Dhabi and Al Ain also indicated very dry surface conditions with delayed onset of the north-westerly sea breeze to after 1200 UTC. But, more important, they also show early onset of the morning southerly land breeze on the 13th (figure 4.32). The fact that this is more than a common land breeze is evident by the depth and strength of the southerly wind from about 0000 UTC to 0800 UTC at Abu Dhabi and Al Ain. Notice the lighter (and dry) southerly wind the previous morning of the 12th. Furthermore, on both days the model indicated a stronger wind at Abu Dhabi than further inland at Al Ain. This invariably results in worse visibility at Abu Dhabi than at Al Ain, but no fog.

4.7.2.2 Surface observations

Under these circumstances the southerly circulation east of the low pressure cell strengthens the morning land breeze and delays the start of the sea breeze until later during the afternoon. On the 12th the low was still developing and the land breeze was light. Never the less it was strong enough to raise the maximum temperature to about 4°C above the normal and delay the sea breeze until 1100 UTC, or 1500 local time (figure 4.33). Overnight the wind became light and variable enough to probably be of some concern to the forecaster, but the surface moisture remained reassuringly low enough to allay any last minute fears of fog forming.

On the 13th, a stronger pressure gradient produced an earlier and stronger southerly land breeze with higher temperatures throughout the day after the wind started and a later start of the sea breeze at 1200 UTC (1600 local time)(figure 4.34). Even so, there was enough surface moisture brought from the Gulf Sea by the sea breeze to cause much moister conditions overnight and result in early morning haze and mist patches. In this instance the pressure gradient effect was such that the sea breeze barely reached Al Ain and when it did it was a temporary affair in the early evening.

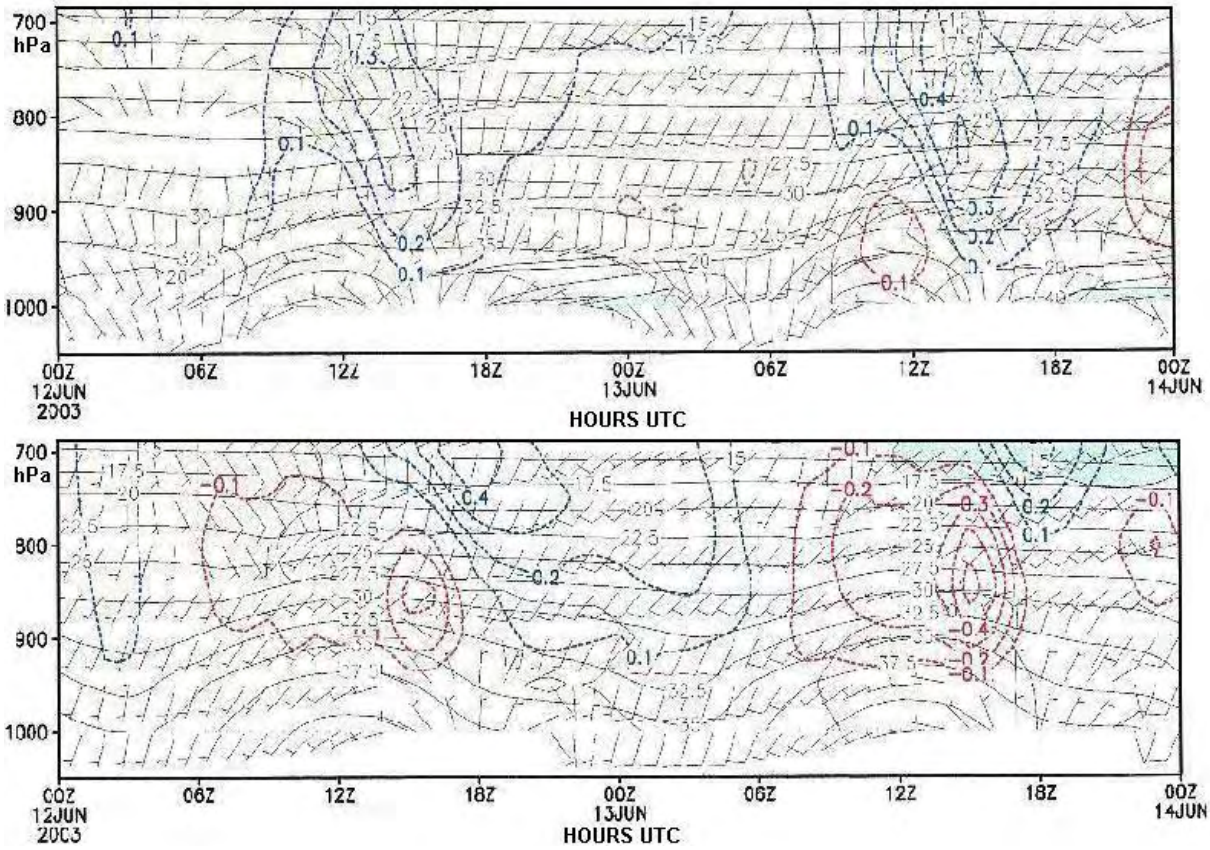

Figure 4.32. Time cross-sections at ADIA (top) and Al Ain (bottom) from 2003-06-12 0000 UTC (T+0) to 2003-06-14 0000 UTC (T+48). Note the very dry conditions, compared with figure 4.21. They also indicate early onset of the land breeze on the morning of the 13th.

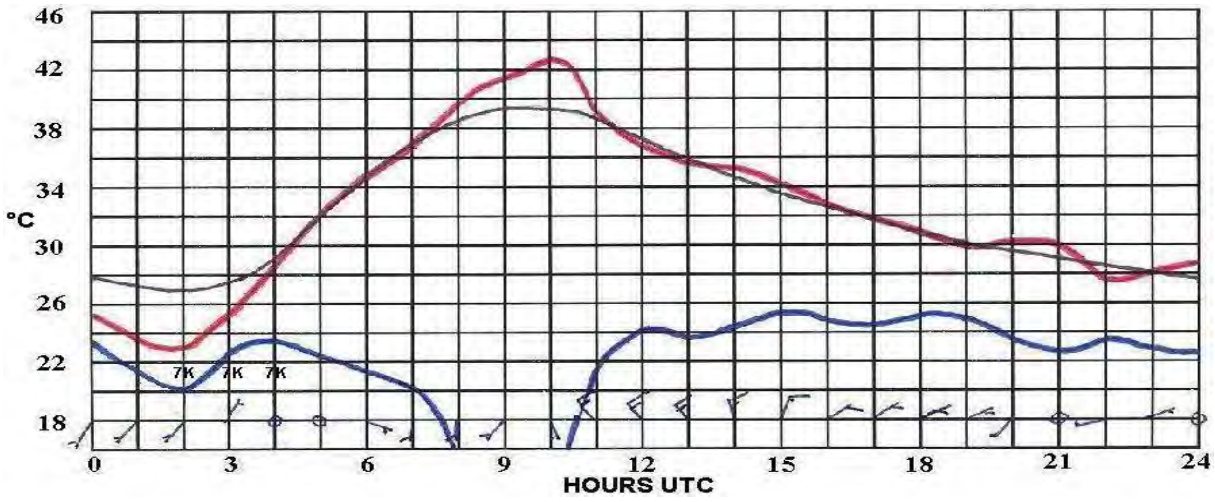

Figure 4.33. As in figure 4.8, but for 2003-06-12.

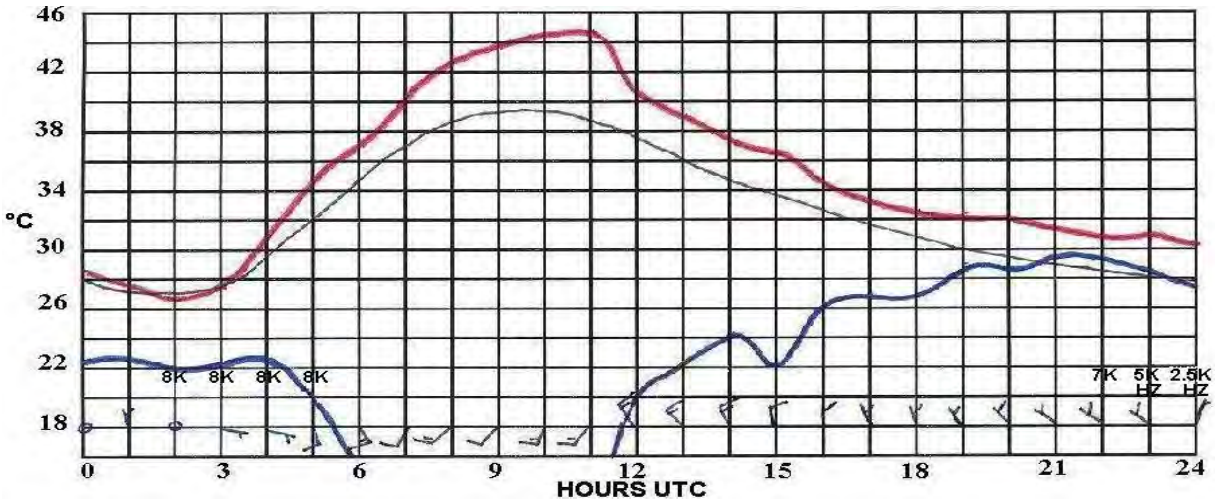

Figure 4.34. As in figure 4.8, but for 2003-06-13.

4.7.2.3 Atmospheric soundings

Unfortunately, no sounding data for the afternoon of the 12th is available, apart from wind velocity, which was north-westerly at 8 to 12 knots before backing to southerly higher up at 911 hPa.

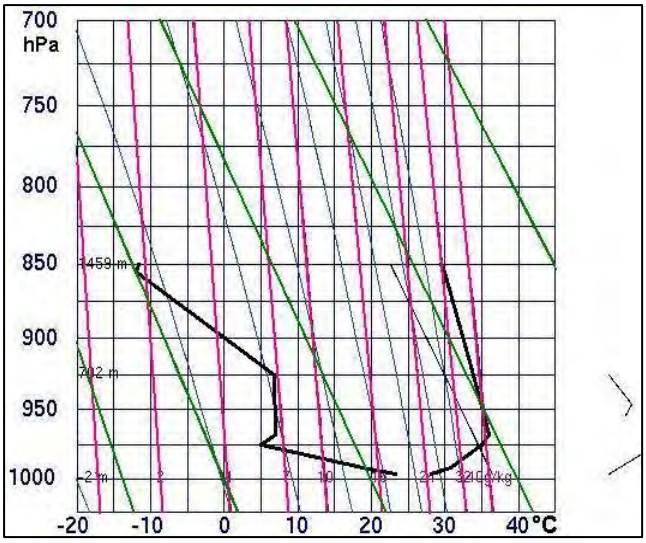

Figure 4.35. As in figure 4.13, but for 2003-06-13 0000 UTC. (Courtesy of the University of Wyoming).

On the morning of the 13th at 0000 UTC (0400 local time) the low level winds were light east-north-easterly to easterly at 3 to 6 knots up to 960 hPa with a 12 knot south-easterly wind at 925 hPa. Comparison with the surface observations reveals that the upper air sounding was made well before the southerly winds began, hence the low level east-north-easterly wind, which was probably still in the process of veering from the north-westerly of the previous afternoon and the very shallow surface moisture layer below a surface inversion (induced by nocturnal ground radiation cooling), with dry conditions above 992 hPa (±47 metres AGL) (figure 4.35).

4.7.2.4 Summary

A surface low pressure cell to the west of the UAE, or over the western part of the UAE, produced a dry offshore southerly flow that strengthens the early morning land breeze and prevents fog formation.

The synoptic circulation delays the onset of the sea breeze until late in the afternoon and can

prevent it from extending too far inland. This limits the amount of moisture carried inland. Along with the very dry air already in circulation there is not enough moisture for nocturnal radiation cooling to cause fog to form. Although, there can be enough present for early morning haze.

The stronger and earlier beginning of the land breeze also causes turbulent mixing of the surface air with drier air aloft, thereby prematurely curtailing the radiation cooling effect and prevents fog formation.

4.7.3 SURFACE ANTICYCLONE OVER SOUTHERN IRAN: 9TH NOVEMBER 2003

The surface fields, from model runs on the 6th, clearly indicated the development of the anticyclone over southern Iran from the afternoon of the 8th to the afternoon of the 9th and a strengthening southerly wind (figure 4.36).

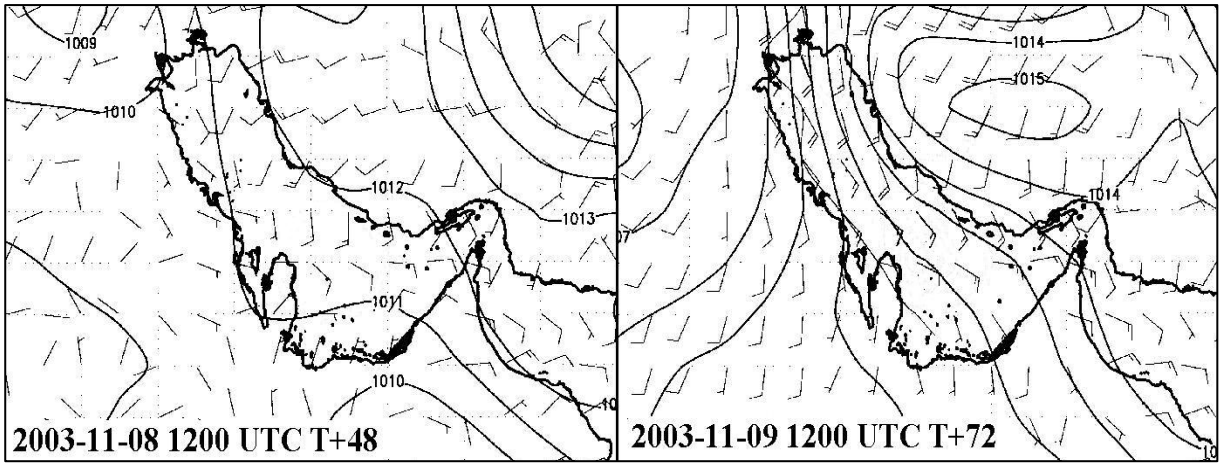

Figure 4.36. Eta GFS fields of surface pressure (hPa) and wind (knots) on 2003-11-08 at 1200 UTC (T+48) and 2003-11-09 at 1200 UTC (T+72)

The time cross section at Abu Dhabi (figure 4.37) reflects the change in the wind from a northerly to north-westerly flow into the low to the south on the 8th (figure 4.36), to a much deeper southerly flow early on the 9th.

What is interesting is the increase in moisture aloft and even, to some extent, near the surface. This is unusual in a wind from the south off the desert. What transpired was that the southerly circulation to the east of the high pressure cell over Iran brought moist air from the Arabian Sea and over Oman to the UAE.

The moisture was sufficient to produce high Stratocumulus cloud during the day under a temperature inversion at about 2400 metres AGL (figures 4.38), but not moist enough beneath the inversion, nor the wind light enough, to produce early morning fog.

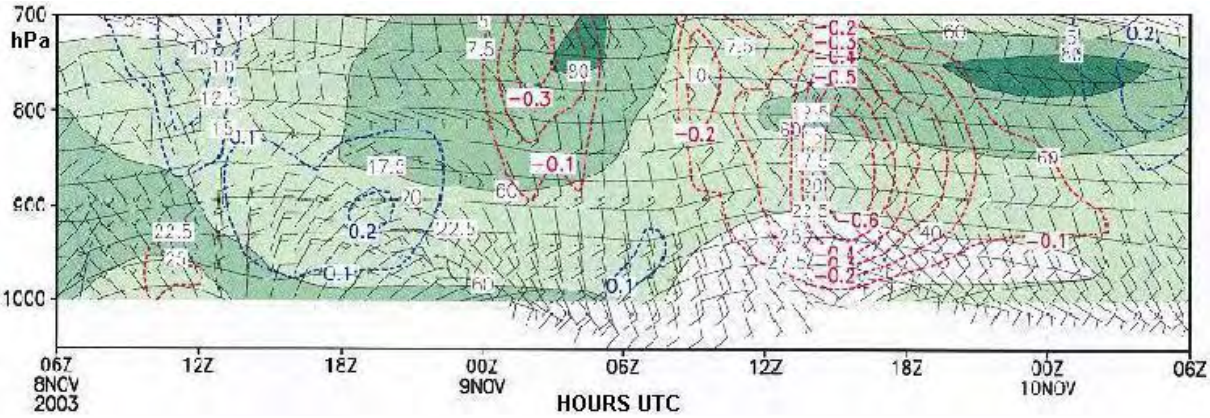

Figure 4.37. Time cross-section at ADIA showing the change from a northerly flow to a deep southerly flow from 2003-11-08 0600 UTC (T+0) to 2003-11-10 0600 UTC (T+48)

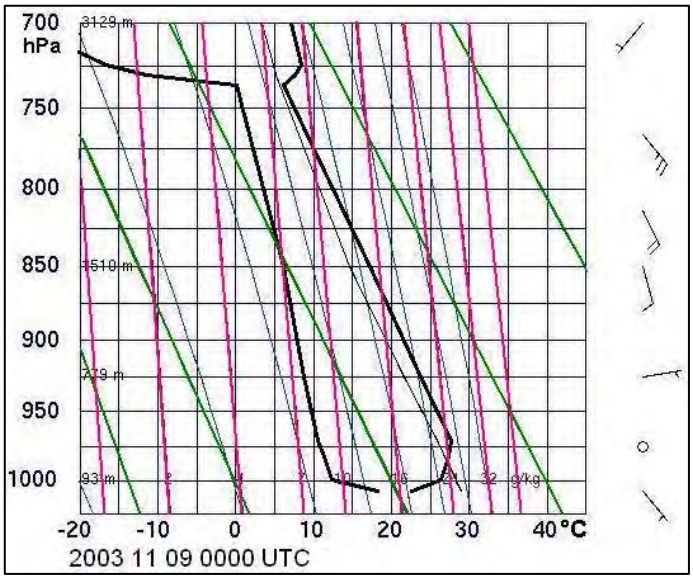

Figure 4.38. As in figure 4.13, but for 2003-11-09 0000 UTC. (Courtesy of the University of Wyoming).

4.7.4 SURFACE LOW PRESSURE CELL TO THE EAST: 31ST AUGUST 2003

4.7.4.1 NWP model data

The surface low was situated to the south–south-east of the UAE on both days and deepened by 1 hPa during the 24 hour period from 1200 UTC on the 30th to the same time the following day. However, the pressure gradient over the Gulf and the UAE weakened (figure 4.39).

Fog did not occur, even though very moist conditions were indicated by the surface relative humidity fields around Abu Dhabi at 0000 UTC and 0300 UTC on the 31st (figure 4.40) in a clearly evident cyclonic circulation with maximum moist air advection in the onshore northerly

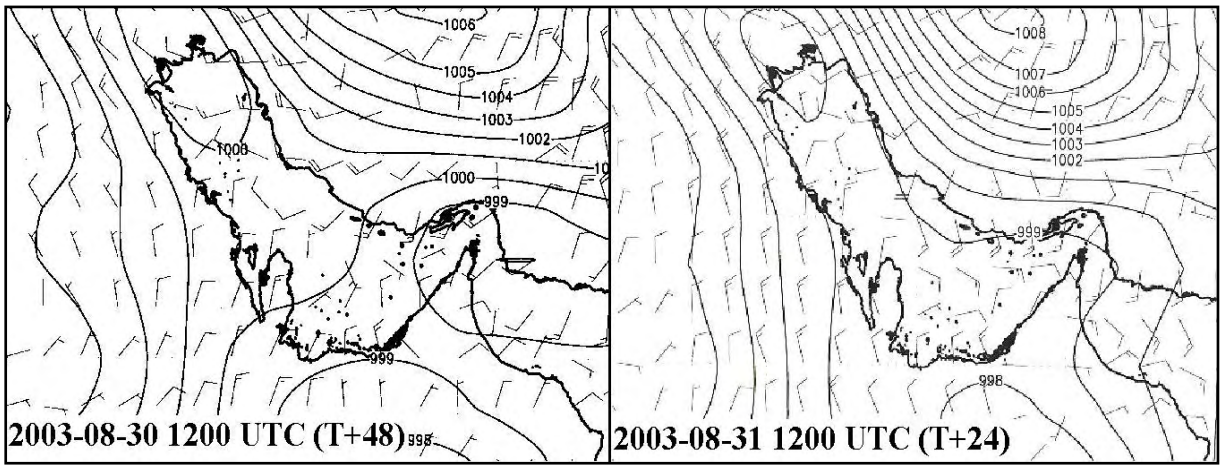

Figure 4.39. Eta GFS fields of surface pressure (hPa) and wind (knots) 2003-08-30 1200 UTC (T+48) and 2003-08-31 1200 UTC (T+24). Even 48 hours ahead the model gave a clear indication of a low pressure cell to the east, which, it transpired, weakened the following day.

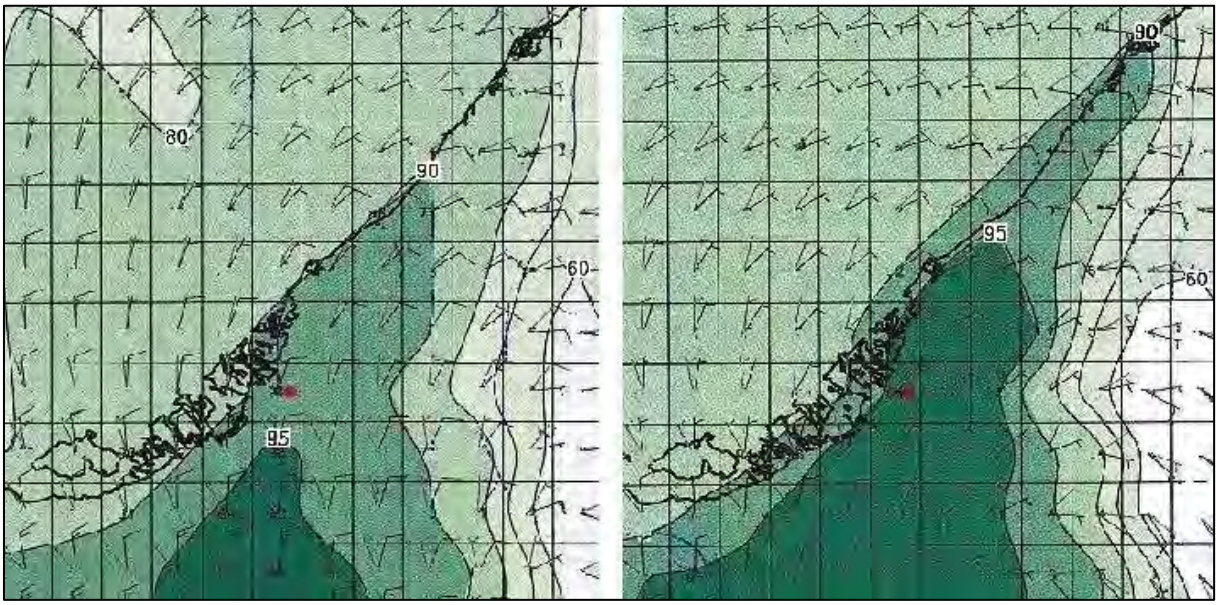

Figure 4.40. Eta relative humidity on 2003-08-31 at 0000 UTC (T+24) and 0300 UTC (T+27). Winds (knots) at 10 metre (black) and 950 hPa (grey) with downward vertical velocity (blue lines).

flow in the vicinity of Abu Dhabi.

The 950 hPa northerly wind, at about 10 knots in the vicinity of Abu Dhabi, is also a fair reflection of the wind that occurred at this level, although the light northerly surface wind indicated by the model was really out of the north-east.

The time cross section for Abu Dhabi (figure 4.41) shows that the model predicted a northerly flow throughout the night, even when very light to calm wind conditions were expected between 0200 UTC to 0500 UTC. Given that these are instantaneous values and not representative of the hour, the author's experience is that the model can be misleading about the wind direction when the speed is low. The prognoses must be treated with caution and the reality is that the wind tends to become light south-easterly to southerly.

Figure 4.41. Eta GRADS surface wind time section at ADIA showing the predicted light winds on the morning of the 31st.

The prognostic atmospheric profiles at 0000 UTC and 0300 UTC (figure 4.42) indicated the near surface wind would still be north-easterly and too strong at about 10 knots at 0000 UTC and only veer to the north-east and become light toward 0300 UTC. This is usually too late to allow fog formation. However, the soundings are not a reliable indicator due to the fact that the first wind presented above the surface is about 950 hPa. Furthermore, at about 950 hPa (±460 metres/1500 ft AGL) the temperature inversion would be rather high for the formation of fog.

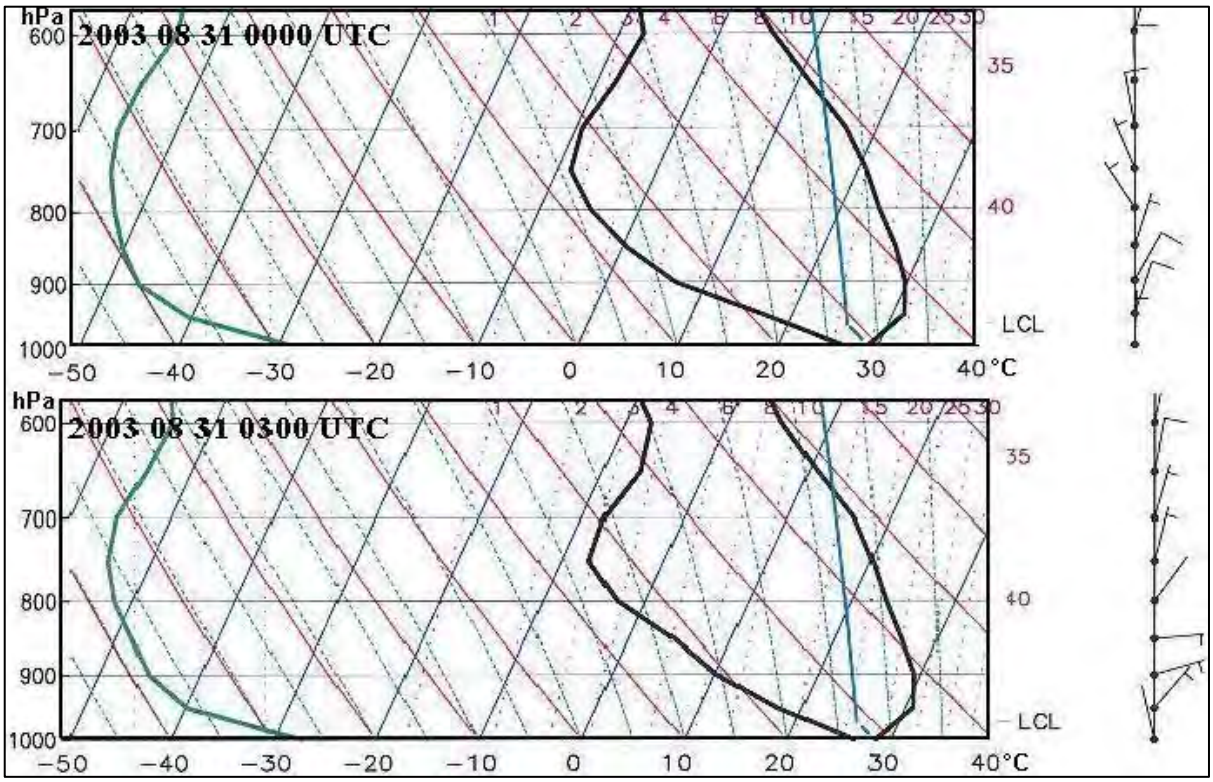

Figure 4.42. Eta GRADS prognostic atmospheric profiles at ADIA at times that are most critical for fog on 2003-08-31 at 0000 UTC (T+24) (top) and at 0300 UTC (T+27) (bottom).

4.7.4.2 Surface observations

As opposed to the previous example, the cyclonic circulation about the low results in an onshore north-easterly to north-westerly flow off the Gulf Sea. It also produces an earlier beginning of the sea breeze, which tends to be more from the north-north-west (figures 4.43 and 4.44).

In the evening, the wind veers to north-east and, if the pressure gradient is strong enough, the land breeze does not appear at all, as was the case later on the 31st (figure 4.44). Under a weaker pressure gradient conditions the wind turns to easterly during the night and it is sunrise before it

turns to a south-easterly land breeze. During the later part of the 30th (figure 4.43) the wind did indeed become easterly and it was about an hour before sunrise on the 31st at 0100 UTC before it turned to south-easterly (figures 4.44).

Obviously, the overnight land breeze, being in opposition to the synoptic circulation, is much lighter than when the low pressure cell is to the west, as in the previous case study. On the night of the 30th/31st the opposing pressure gradient was weak enough to allow a 5 to 8 knots southerly surface wind during the early hours of the 31st (figure 4.44).

The earlier sea breeze also brings cooler weather. In this instance the daytime temperatures were slightly lower than normal (figures 4.43 and 4.44).

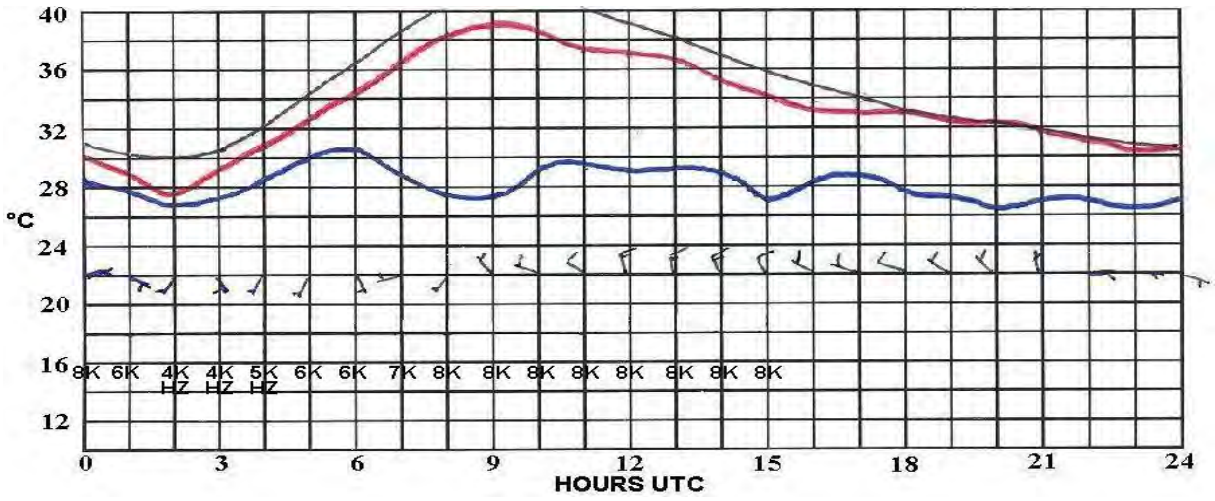

Figure 4.43. As in figure 4.8, but for 2003-08-30.

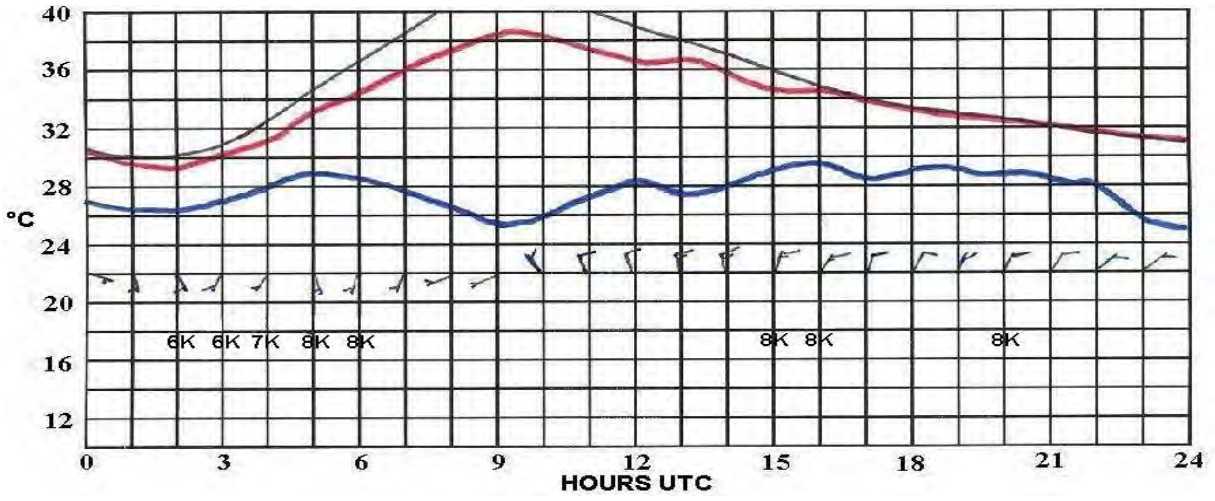

Figure 4.44. As in figure 4.8, but for 2003-08-31.

4.7.4.3 Atmospheric soundings

The sounding profile on the afternoon of the 30th shows the familiar wedge of cooler sea breeze air (figure 4.45, left). The wind near the surface was northerly at about 10 knots, but above this, up to the rather high temperature inversion base at 920 hPa, the wind was light variable. The relative humidity beneath the inversion was between 52% and 63%.

The following morning, a near surface temperature inversion had formed at 980 hPa with an offshore wind below it at 090° 5 knots to 070° 6 knots at the inversion top. The main inversion remained at nearly the same level as the previous afternoon (914 hPa) with a steady northerly wind off the sea at 8 knots (figure 4.45, right).

The wind above the near surface inversion to the main inversion was strong enough to maintain turbulent mixing. Evidence of this can be seen on the morning sounding in the form of the dry adiabatic air temperature lapse rate and the close to constant humidity mixing ratio dew point temperature trace.

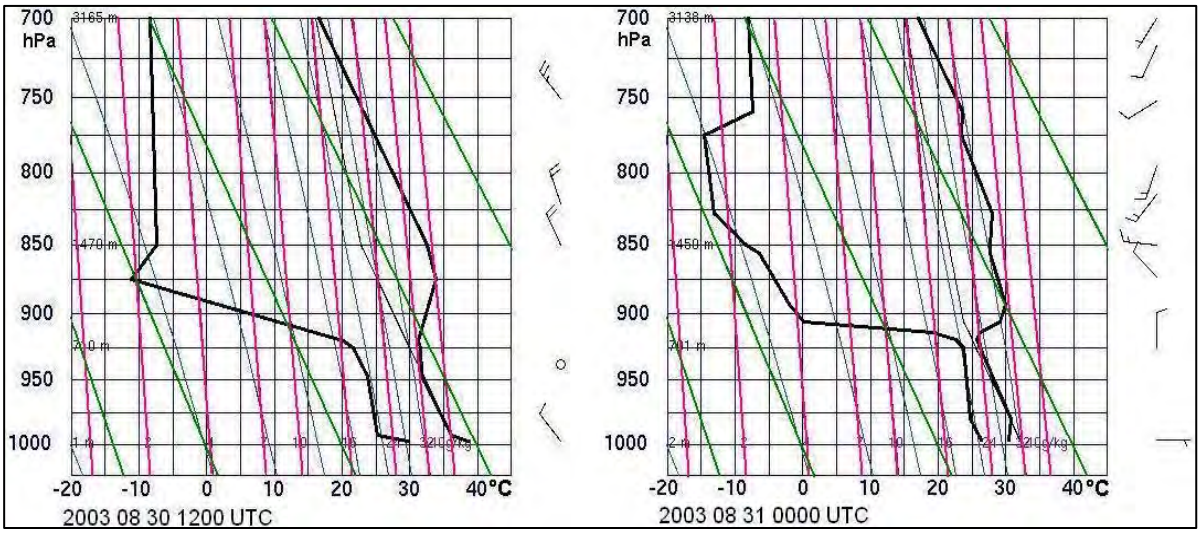

Figure 4.45. As in figure 4.13, but for 2003-08-30 1200 UTC and 2003-08-31 0000 UTC. (Courtesy of the University of Wyoming).

4.7.4.4 Summary

A source of concern for the forecaster would have been that up until 1800 UTC on the evening of the 30th, the relative humidity was well above the values one can expect with fog formation later in the night as indicated in figure 4.2 in section 3. However, the surface temperature, which had been cooler than the normal, began to cool less rapidly at this time and the air remained about 75% to 80% moist. This is normal under these conditions. Air off the sea, being less influenced by nocturnal surface radiation cooling maintains warmer conditions than when it arrives from the cooler desert. The later swing in wind direction to the south-east, due to the synoptic circulation, and increased radiation cooling over the land, was too late to enable the air to cool to below the dew-point temperature, or fog point.

The steady 6 to 8 knots north-easterly to northerly from the surface up to the main inversion, was also strong enough to maintain turbulent mixing, thereby preventing fog formation.

When the wind remains from the north-west to north-easterly throughout the night, due to a surface low pressure cell to the south, or south-east, fog does not occur.

4.7.5 SURFACE LOW PRESSURE CELL TO THE NORTH-EAST: 23RD OCTOBER 2003

This event demonstrates that fog does not occur when there is a low pressure cell to the north-east of the UAE in the Gulf. This situation is also normally associated with Shamal wind conditions, because there is invariably an anticyclone to the west over Saudi Arabia and if there is sufficient pressure gradient between the two systems, the Shamal can become strong.

4.7.5.1 NWP model data

The prognosis of the 0000 UTC run of AVN model on the 22nd October 2002 was that, by 1200 UTC, a moderate to fresh (15 to 20 knots) north-westerly Shamal would develop. This would be due to a 3 hPa pressure gradient in the Gulf between an anticyclone to the west over Saudi Arabia and a low pressure centre located in the vicinity of southern Iran and the Straits of Hormuz (figure 4.46, left). The situation would persist on the 23rd, but with a weakened pressure gradient and a moderated wind (figure 4.46, right).

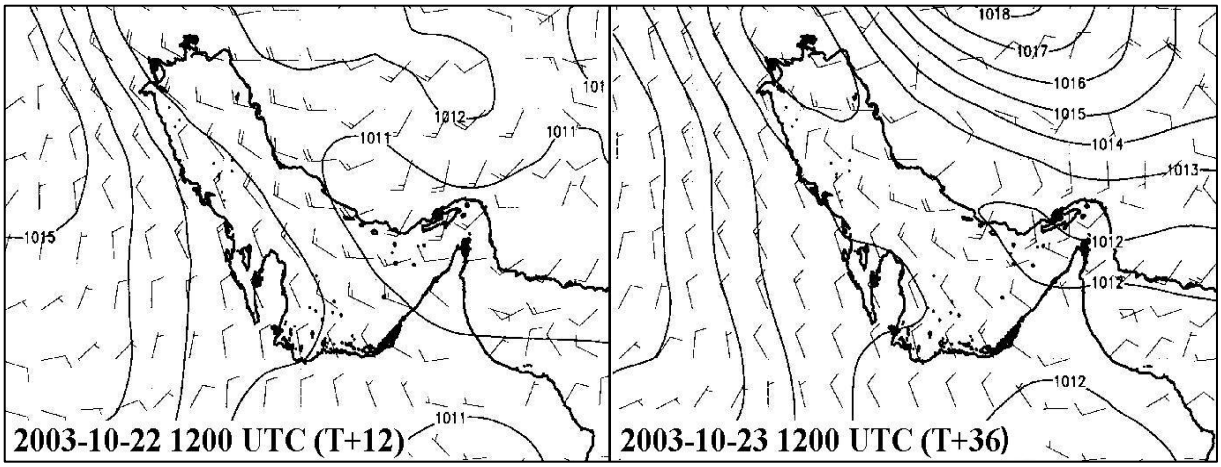

Figure 4.46. Eta GFS fields of surface pressure (hPa) and wind (knots) on 2003-10-22 at 1200 UTC (T+12) and 2003-10-23 at 1200 UTC (T+36).

The surface wind and pressure fields at 0000 UTC on the 23rd (figure 4.47) placed the low in the Gulf near to the Iranian coast, with the surface wind in the Gulf Sea from the north-west in the west backing to south-westerly in the east. Light westerly to southerly winds were indicated immediately inland of the coast from Abu Dhabi to Dubai with a pressure gradient of 1 hPa, or less, over the UAE. Both the light wind and the weak pressure gradient being favourable for radiation fog development.

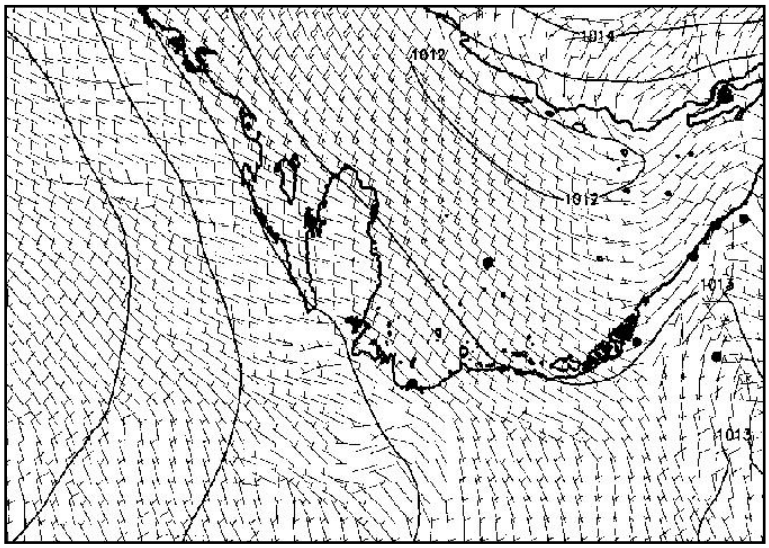

Figure 4.47. Eta GRADS surface pressure (hPa) and winds in knots) on 2003-10-23 at 0000 UTC (T+24).

Figure 4.48. Eta relative humidity on 2003-10-23 at 0300 UTC (T+27). Winds (knots) at 10 metre (black) and 950 hPa (grey) with downward vertical velocity (blue lines).

In addition to light winds and a weak pressure gradient, the model indicated that a zone of surface relative humidity of 90% and higher would increase over the eastern part of the UAE and extend southward into the Empty Quarter at 0000 UTC and 0300 UTC on the 23rd (figure 4.48). The surface wind would be light north-westerly backing to southerly. At 950 hPa (±460 metres MSL) the wind was also indicated as becoming light north-westerly, but remaining about 10 knots over the sea to the west of Abu Dhabi.

The prognostic atmospheric profiles at 0000 UTC (figure 4.49, top) and 0300 UTC (figure 4.49, bottom) indicated a temperature inversion at about 950 hPa (±460 metres MSL) with light north-westerly winds below it, becoming light south-westerly at the surface. At the inversion level a north-westerly wind of 10 knots was predicted. The temperature inversion usually forms in the afternoon when cooler maritime air, brought by the sea breeze, undercuts the normally dry air with a near dry adiabatic environmental lapse rate. The prognostic soundings looked very similar to the atmospheric sounding carried out the previous morning at 0000 UTC on the 22nd (figure 4.54) when fog very nearly formed at Abu Dhabi. Note, as opposed to earlier prognostic soundings these later soundings, from a newer and finer model grid, now had more levels between the surface and 900 hPa and, therefore, more detail.

The time section at Abu Dhabi (figure 4.50) indicated a marked north-westerly flow developing in an approximately 3000 feet boundary layer from the surface to 900 hPa from 0900 UTC on the 22nd. Increased moisture was indicated within this layer up to about 460 metres altitude (±1500 feet) from about 2100 UTC to 0900 UTC. Usually a very shallow surface layer is presented.

The later model run at 0600 UTC did not help matters. Apart form presenting very similar aspects as the previous run, it most disconcertingly indicated an even bigger area of higher relative humidity at 0300 UTC (figure 4.51) on the 23rd than the previous run (figures 4.48).

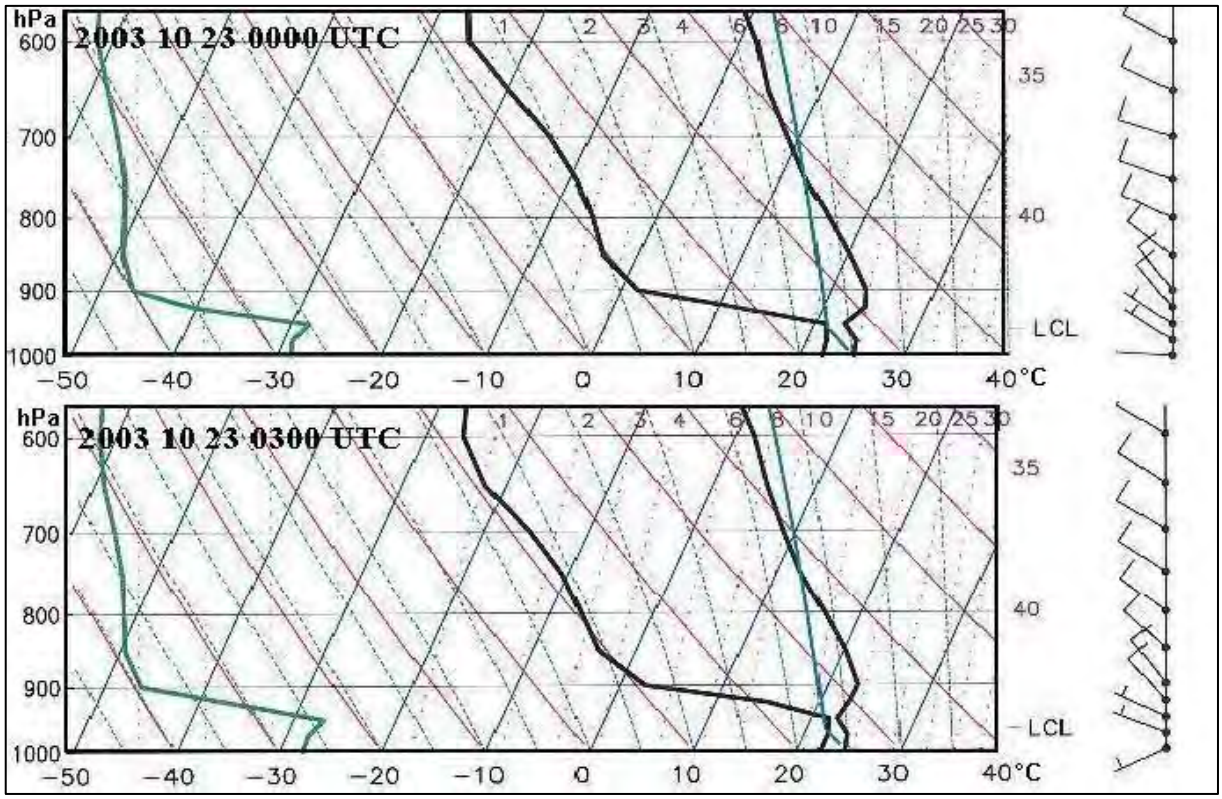

Figure 4.49. Eta GRADS prognostic atmospheric profiles at ADIA at times that are most critical for fog on 2003-10-23 at 0000 UTC (T+24) (top) and at 0300 UTC (T+27) (bottom).

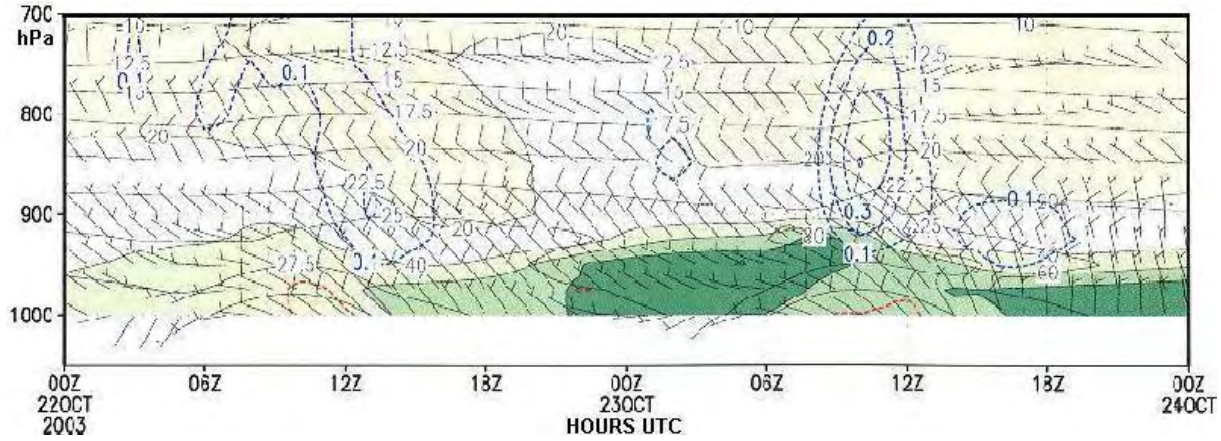

Figure 4.50. Eta time cross-section at ADIA showing the predicted north-westerly flow and increased surface moisture on 2003-10-22 at 0000 UTC (T+0) to 2003-10-24 at 0000 UTC (T+48).

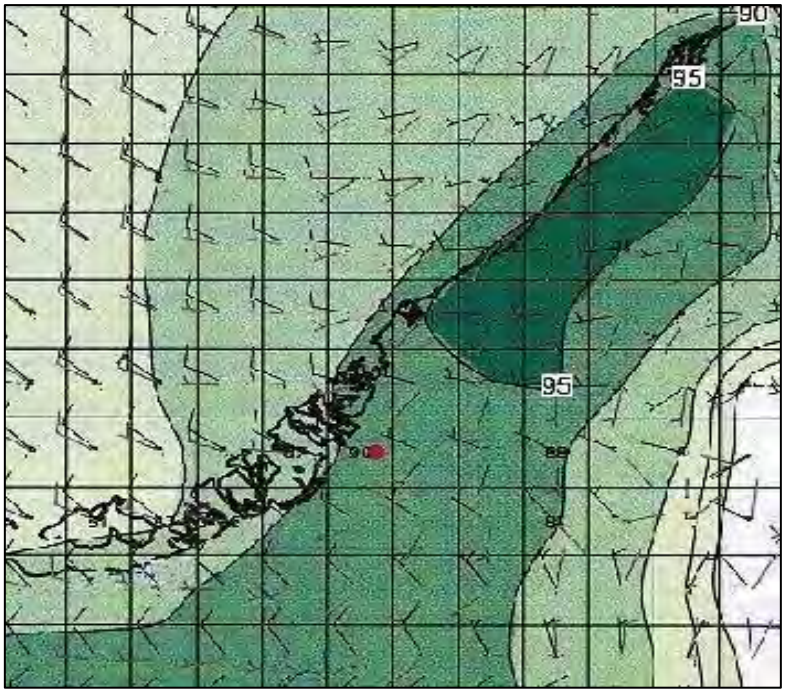

Figure 4.51. Eta relative humidity on 2003-10-23 at 0300 UTC (T+27). Winds (knots) at 10 metre (black) and 950 hPa (grey) with downward vertical velocity (blue lines).

4.7.5.2 Surface observations

Very moist surface conditions prevailed on the morning of the 22nd with the observed surface relative humidity 92% to 96% at ADIA. The visibility came down to 1.4 kilometres due to fog in the vicinity and a cool light southerly wind blew (figure 4.52). The air remained moist during the day and one could be forgiven for believing that it would remain very moist the next morning and with light winds forecast, fog was highly likely.

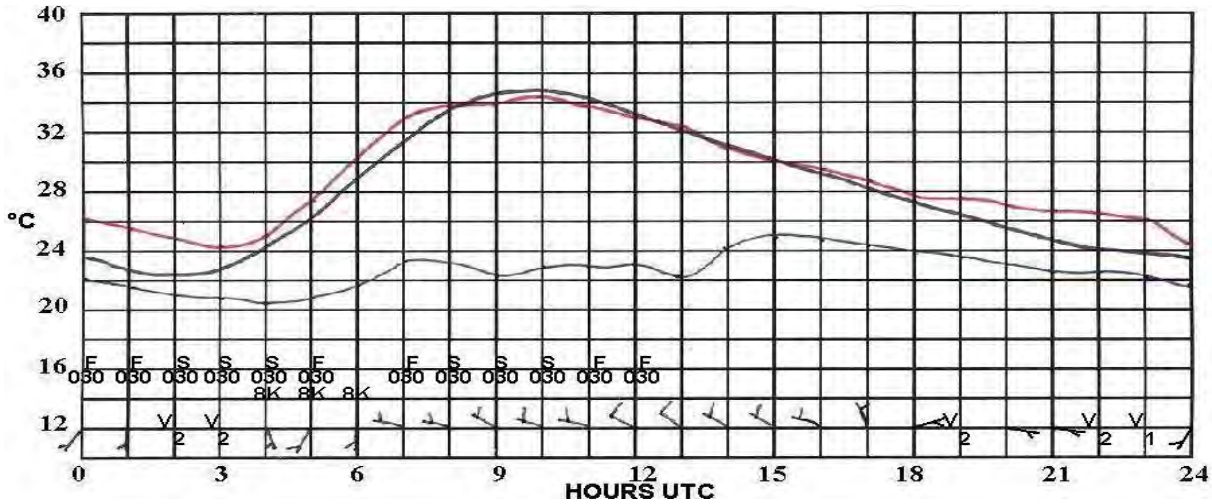

Figure 4.52. As in figure 4.8, but for 2003-10-22. The cloud is at 900 metres (3000 ft) AGL.

However, on the morning of the 23rd (figure 4.53), although the dew-point temperature was still about the same as the previous morning, the low level onshore westerly to south-westerly wind maintained warmer maritime air in circulation than the previous night and the relative humidity did not exceed 82% at ADIA. This was lower than the 90% and above indicated by the NWP model (figures 4.48 and 4.51). When the wind did become light variable it was too late in the night and the air was still too warm for sufficient radiation cooling and condensation.

There is also evidence of turbulent mixing as seen by the low cloud patches observed at about 900 metres and by the visibility that did not deteriorate to worse than 8000 metres (figure 4.53).

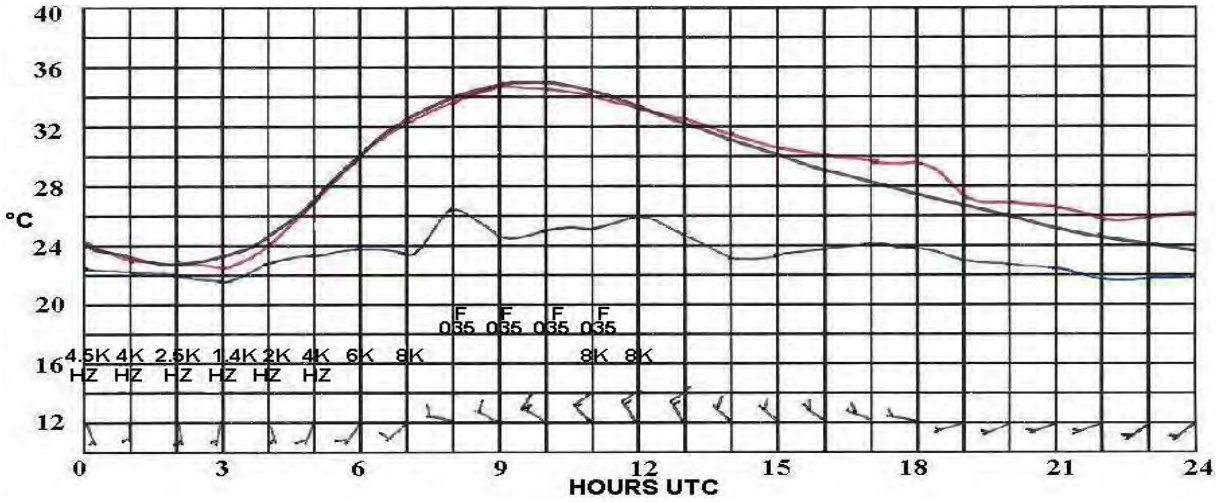

Figure 4.53. As in figure 4.8, but for 2003-10-23. The cloud is at 1067 m (3500 ft) AGL.

4.7.5.3 Atmospheric soundings

The sounding on the morning of the 22nd (figure 4.54, left), when fog very nearly formed, has a marked temperature inversion at 952 hPa (±516 metres AGL), with another near surface inversion below it. The lower inversion probably developed due to nocturnal radiation cooling of the ground and conduction to the air in contact with it. The wind below the higher inversion was southerly to south-south-westerly at 2 to 3 knots (table 4.5).

At 1200 UTC on the 22nd (figure 4.54, right) a surface superadiabatic lapse rate was evident with a weak temperature inversion at about 930 hPa (±728 metres AGL). The wind below the inversion being west-north-westerly at 8 to 11 knots (table 4.5). As the soundings are actually carried out at 1100 UTC and the sea breeze only began to blow about an hour to an hour and a half earlier, it is assumed that the full effect of the cooler maritime air brought by the sea breeze is still not evident on the environmental lapse rate. The wedge of cooler air above the ground could therefore be expected to increase and the surface superadiabatic lapse rate would disappear.

On the morning of the 23rd (figure 4.55) the inversion had lifted up to 894 hPa (±1069 metres AGL). This is more than double the altitude indicated by the model (figure 4.49). Near the surface, radiation cooling resulted in a shallow temperature inversion at 1000 hPa (±86 metres

AGL). Although the air is moist at the surface (80%) and immediately below the upper inversion (87%), the air in between has relative humidity of about 60% to 75% (table 4.5). It is worth noting that the wind between the two inversions was still off the sea, namely, a south-westerly to west-north-westerly wind at 6 to 10 knots (table 4.5).

As mentioned at the end of the previous section, the observations showed evidence of turbulent mixing of the air. The sounding supports this in that the temperature lapse rate has been reduced to the dry adiabatic lapse rate and the dew-point trace to a constant humidity mixing ratio lapse rate (figure 4.55) (Handbook of Aviation Meteorology, 1997).

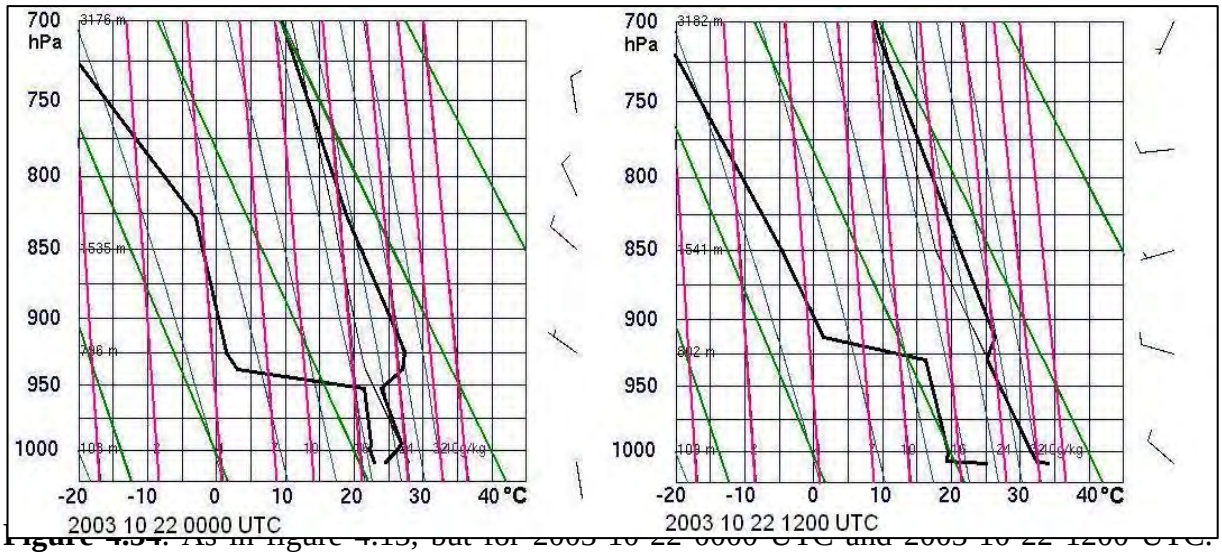

Figure 4.54: As in figure 4.13, but for 2003-10-22 0000 UTC and 2003-10-22 1200 UTC. (Courtesy of the University of Wyoming).

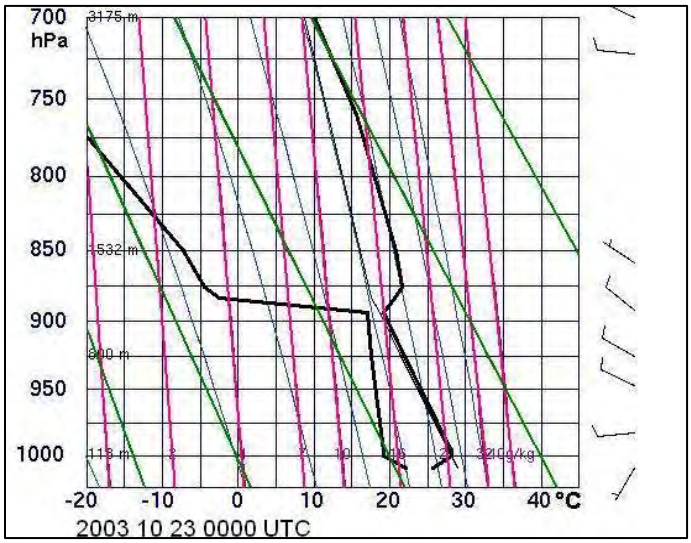

Figure 4.55. As in figure 4.13, but for 2003-10-23 0000 UTC. (Courtesy of the University of Wyoming).

.

Table 4.5. Details of pressure, gpm height, air temperature, dew-point temperature, relative humidity and wind velocity up to temperature inversion level on the 22nd and 23rd October 2003.

PRES hPa	HGHT gpm	TEMP °C	DWPT °C	RELH %	DIRC deg	SPED knot
0000 UTC 22 October 2003						
1010.0	27	24.6	22.9	90	170	2
1000.0	108	26.2	22.3	79	195	2
995.0	152	26.8	22.4	77	202	2
952.0	543	24.0	21.5	86	264	3
938.0	673	27.0	3.0	21	285	3
1200 UTC 22 October 2003						
1010.0	27	34.0	25.0	59	310	11
1008.0	43	32.4	19.4	46	309	11
1000.0	109	31.6	19.6	49	305	10
930.0	755	25.2	16.2	57	286	8
913.0	917	26.4	1.4	20	280	7
0000 UTC 23 October 2003						
1010.0	27	25.8	22.1	80	210	3
997.0	140	28.2	19.2	58	240	7
947.0	593	23.9	18.1	70	295	9
894.0	1096	19.2	17.0	87	309	10
876.0	1272	21.6	-4.4	17	308	8

4.7.5.4 Summary

The model correctly presented the low level circulation in the region, but the surface relative humidity was misleading.

The prognostic atmospheric soundings at ADIA gave a good indication of the environmental lapse rate that could be expected and the presence of a boundary layer temperature inversion, although the observed inversion was over double the altitude indicated by the model.

The winds and moisture layer below the inversion were accurately presented and gave a clear indication of low cloud development, but the forecaster would have been misled into forecasting a cloud base of about 300 metres AGL as opposed to the observed base of 900 metres AGL.

In spite of the weak surface pressure gradient, high relative humidity and light low level winds predicted by the NWP model, which duly occurred, fog did not form.

The low pressure cell to the north-east of the UAE, over the Gulf Sea, caused moderate to fresh north-westerly to westerly winds to blow during the day to the south of the low over the southern Gulf Sea and the UAE. The so-called Shamal winds.

During the Shamal conditions fog does not form. Turbulent mixing of the warm and moist air from the Gulf Sea tends to form thin Stratocumulus, or Stratus, cloud under the inversion with sea haze moderately reducing the visibility.

4.7.6 SURFACE LOW PRESSURE CELL TO THE NORTH-EAST: 6TH OCTOBER 2003

This episode is similar to the previous study in that it demonstrates that fog does not occur when there is a low pressure cell to the north-east in the Gulf. What sets is apart and makes it particularly interesting, is that it disproves the local traditional belief that if fog occurs on one morning, more likely than not, it will occur on the second morning. In this instance fog occurred on the morning of the 5th, but not on the 6th.

4.7.6.1 NWP model data

The fog on the morning of the 5th formed in a weak surface pressure gradient that existed over the UAE (figure 4.56, left). However, the Eta model indicated that the low pressure cell, to the east of the Straits of Hormuz would move westward into the Gulf and the pressure gradient in the Gulf would intensify by the following day (figure 4.56, right). By 0000 UTC on the 6th the pressure gradient in the Gulf would be about 3 hPa (figure 4.57).

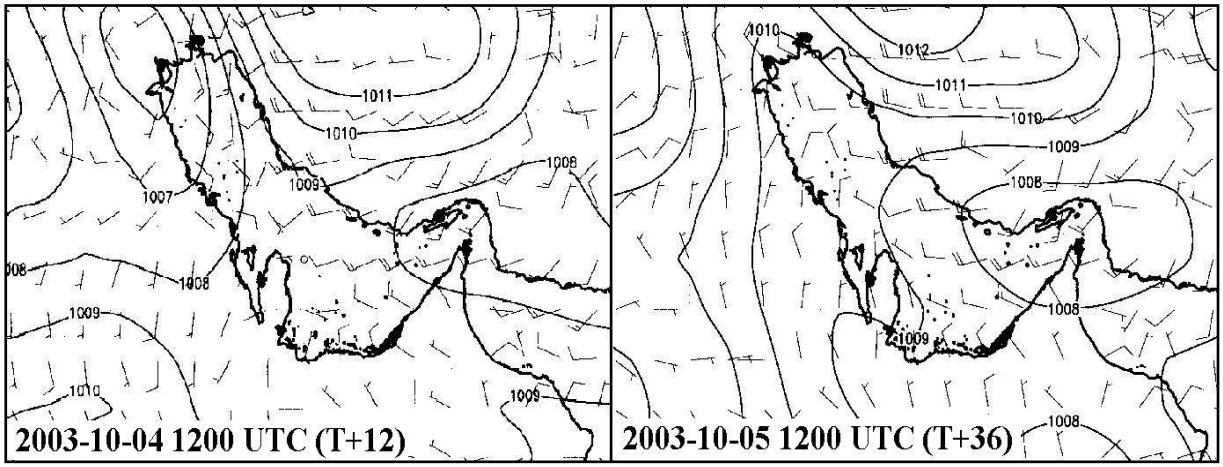

Figure 4.56. Eta GFS fields of surface pressure (hPa) and wind (knots) on 2003-10-04 at 1200 UTC (T+12) and 2003-10-05 at 1200 UTC (T+36).

Considering the surface relative humidity indicated by the model data, fog formation seems probable. More than 95% relative humidity was indicated for the region at 0300 UTC on the 6th in the prognostic field at T+33 for the region (figure 4.58). This is considerably moister than the model predicted for the previous morning when fog actually occurred. A light surface wind was indicted from the south-west, but stronger from the north-west at 950 hPa in the vicinity of ADIA. Both these winds are indicative of fog not occurring. However, a later model run reduced relative humidity at 0300 UTC. This prognosis was reassuring for a “no fog” forecast.

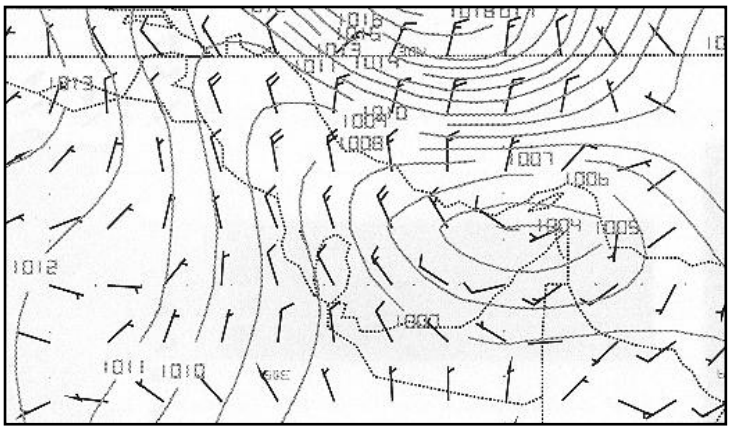

Figure 4.57. Eta WAFS fields of surface pressure (hPa) and wind (knots) on 2003-10-06 at 0000 UTC (T+24).

The surface wind time section for ADIA (figure 4.59) supported the conviction that there would be no fog in that it indicated a light south-westerly wind in the early hours of the 6th. This is the opposite of the very light south-easterly to light southerly winds of the previous morning when the fog occurred.

The resolution of Eta model prognostic atmospheric profile is usually not good enough to be trusted. However, it indicated that the 950 hPa wind at 0000 UTC (T+30) on the 6th, would be stronger from the north-west than the previous morning (figure 4.60). On the other hand more surface moisture was indicated with a more pronounced surface temperature inversion.

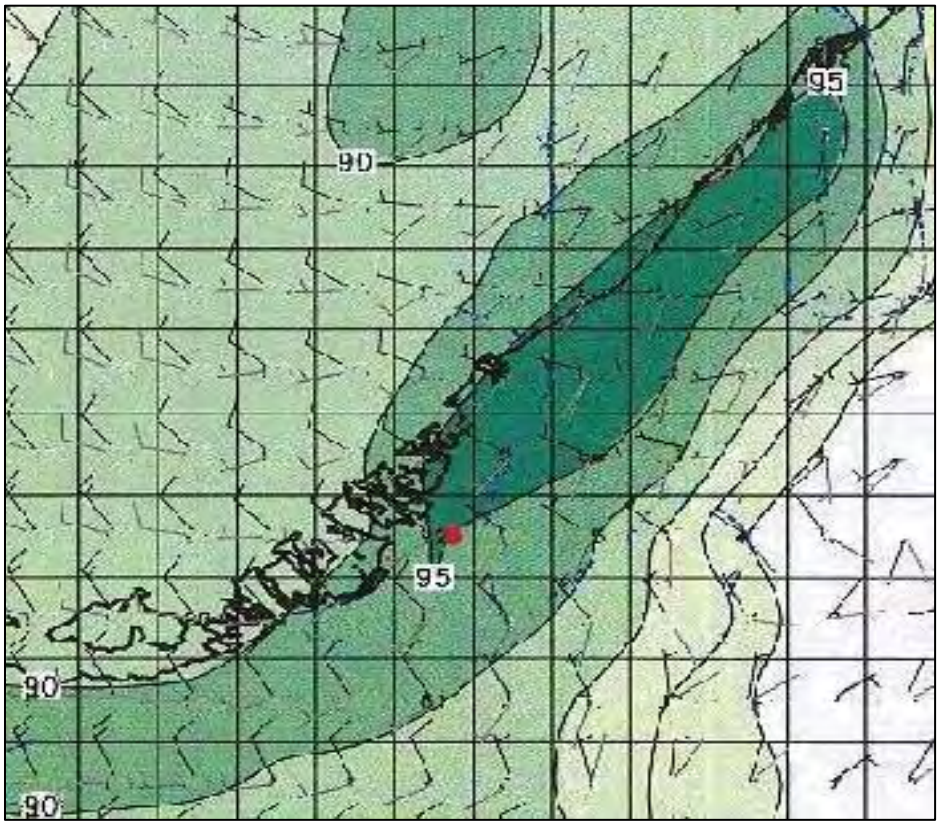

Figure 4.58. Eta relative humidity on 2003-10-06 at 0300 UTC (T+33). Winds (knots) at 10 metre (black) and 950 hPa (grey) with downward vertical velocity (blue lines).

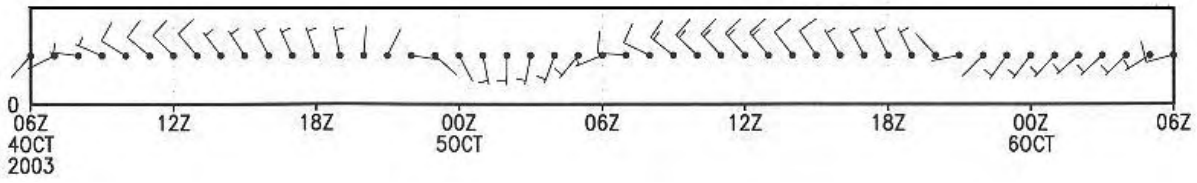

Figure 4.59. Eta GRADS surface wind time section at ADIA from 2003-10-04 to 2003-10-06. A light south-westerly wind is indicated for the morning of the 6th, as opposed to the slight south-easterly to southerly wind on the morning of the 5th.

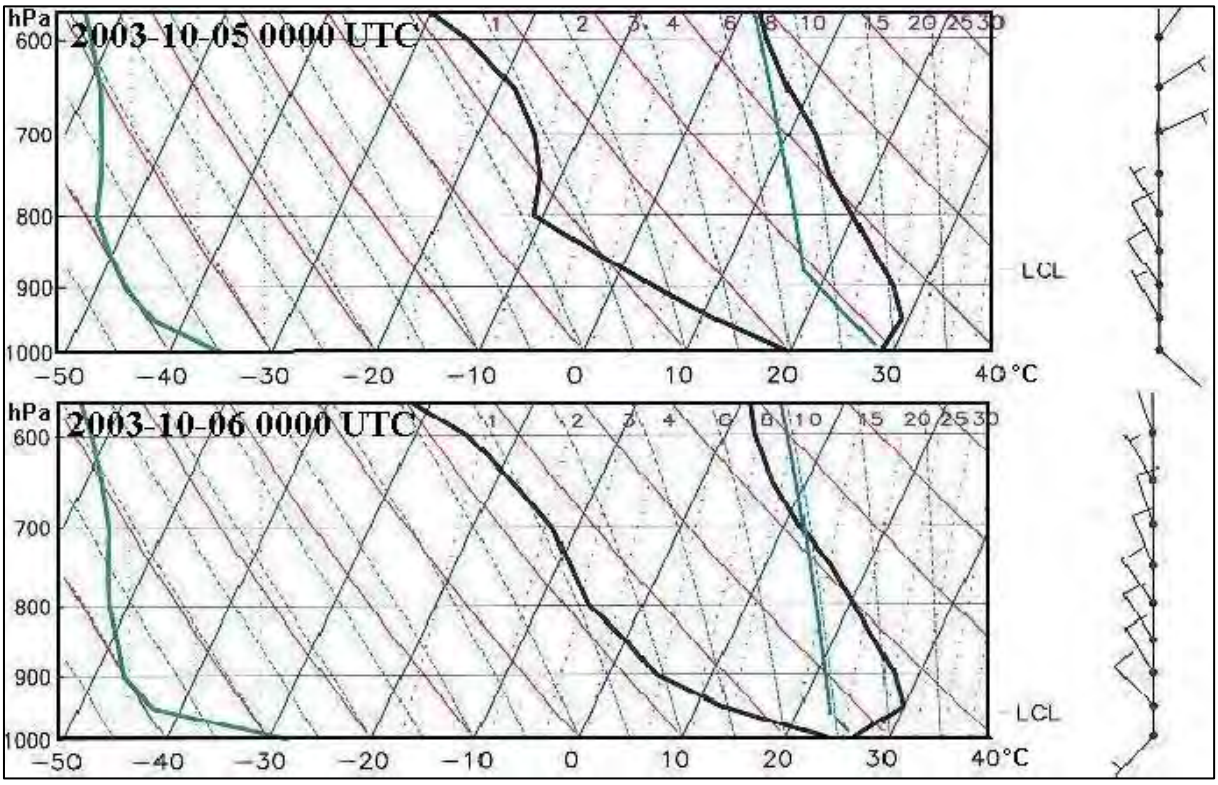

Figure 4.60. Eta GRADS prognostic atmospheric profiles at ADIA on 2003-10-05 at 0000 UTC (T+12) (top) and 2003-10-06 at 0000 UTC (T+30) (bottom).

4.7.6.2 Surface observations

The surface observation graphs at ADIA show the moist conditions on the 4th and 5th (figures 4.61 and 4.62). Fog formed on the morning of the 5th (figure 4.62) when the surface wind became light east-south-easterly and when ambient temperature fell below the dew-point temperature experienced earlier in the evening.

During the 5th, the increasing pressure gradient resulted in a stronger north-westerly sea breeze than the previous day and caused a persistent south-westerly wind during the night. The effect of this wind was that, although the ambient temperature fell to below the dew-point temperature experienced earlier in the afternoon and evening, it kept warmer maritime air in circulation and maintained turbulent mixing with drier air aloft. The result was no saturation of the air and no fog (figure 4.62).
The moderating effect of the maritime air overnight, becomes apparent when comparing the

much higher evening temperatures on the 6th (figure 4.63), after the north-westerly circulation about the low became properly established, with the cooler east-south-easterly wind off the desert on the evening of the 4th prior to the fog forming (figure 6.61).

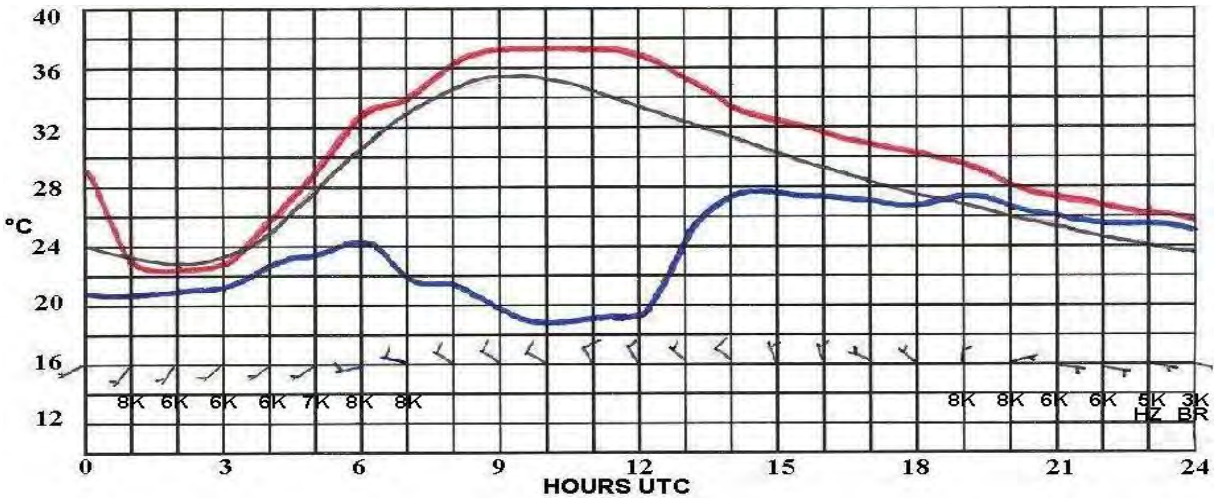

Figure 4.61. As in figure 4.8, but for 2003-10-04.

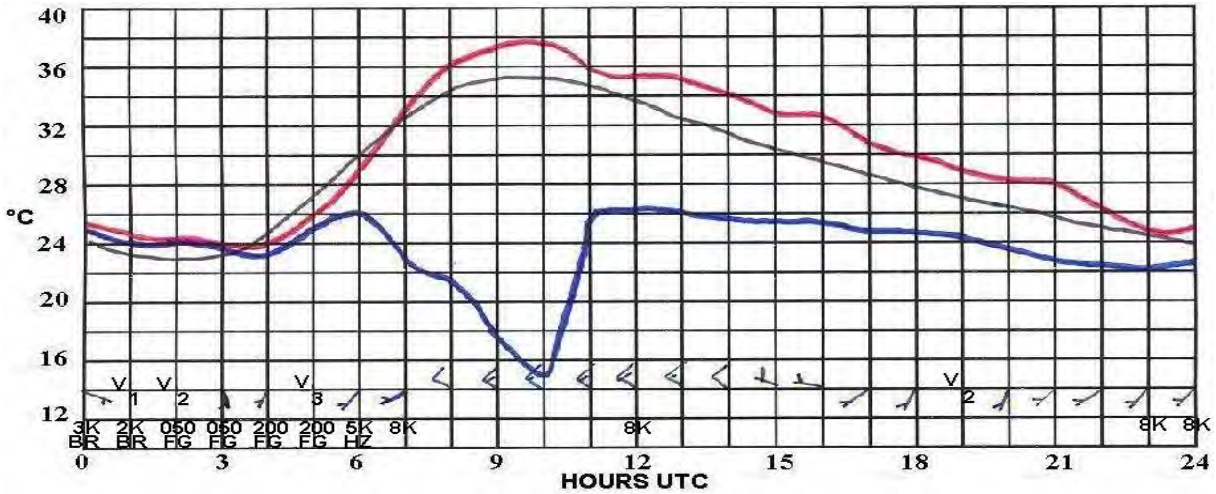

Figure 4.62. As in figure 4.8, but for 2003-10-05.

4.7.6.3 Atmospheric soundings

Fog formed under a rather marked temperature inversion with its base at about 986 hPa (±188

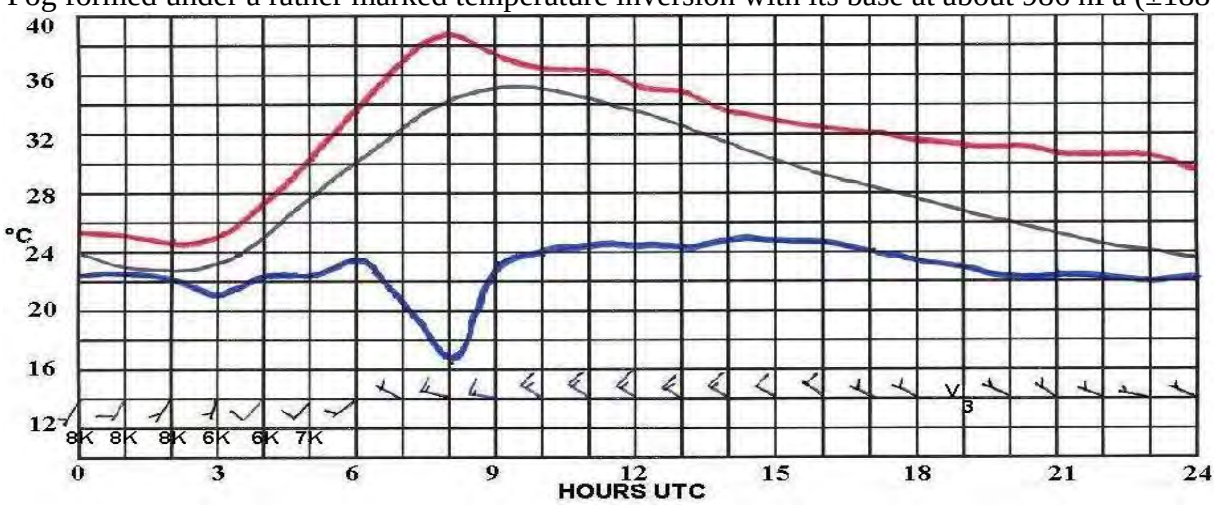

although the inversion was higher than normal at 937 hPa (±637 metres AGL). An inversion at this height being more likely to cause Stratocumulus clouds to collect under it.

On the morning of the 6th, a temperature inversion had formed at 995 hPa (±78 metres AGL) with the wind below it having backed from north-westerly to south-westerly at 5 to 7 knots (figure 4.65). That is, increased thermal stability at night causes the wind under the inversion to become uncoupled from the circulation around the low above the boundary layer and then backs from north-west to blow from the south-west toward the low pressure cell. Conversely, one can say the wind veers with height from the surface upward (Pal Arya 1988, Riehl 1954).

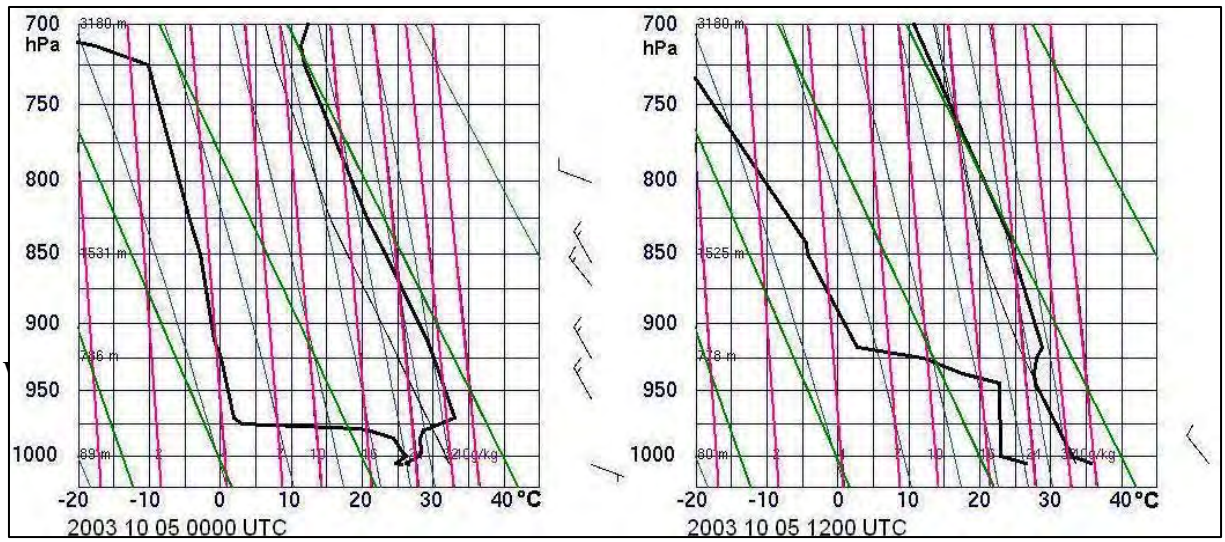

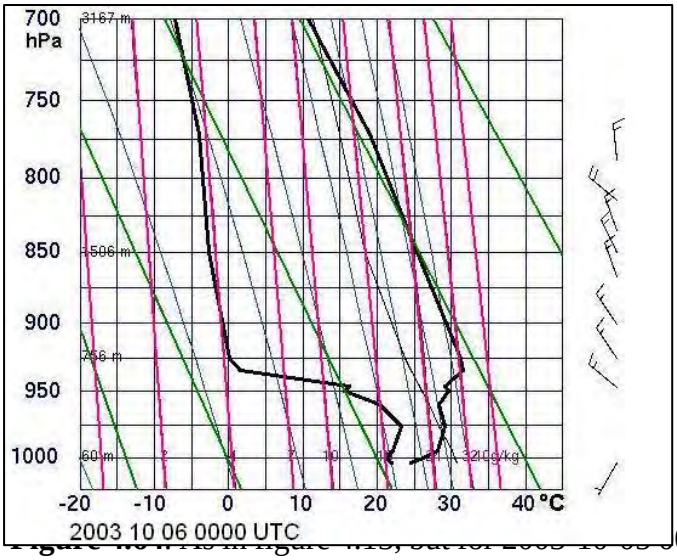

Although moist below the inversion at 70% to 85% relative humidity, this is not much moister than the previous afternoon ascent and not sufficiently moist for fog to form. A higher temperature inversion was at 945 hPa (±400 metres AGL) with the wind between the two inversions off the sea from the west to west-north-west at 10 to 12 knots.

In view of the change from a weak pressure gradient with fog to Shamal

Figure 4.64 As in figure 4.63, but for 2003 10 05 0000 UTC and 1200 UTC. (Courtesy of the University of Wyoming).

conditions and air transported from the north over the UAE, it was thought that there might have been a change of air mass. In order to determine this, the wet bulb potential temperature (WBPT) at 850 hPa was calculated from the Abu Dhabi soundings at the time of the fog and afterwards. The WBPT was chosen because it is conservative with respect to dry and moist adiabatic processes (Hess 1959) and the 850 hPa level was selected, because it is high enough to eliminate boundary layer influences such as surface heating and cooling (Galvin 2003). It was found that there was very little change in value from the 8th to the 9th, with the temperature varying between

289°K and 290°K.

With this in mind the WBPT was determined at the time of the previous case studies. Once again the variation was found to be very small in every episode, being less than 3°K, apart from 4°K during the case study of the 8th to 11th January 2003. Therefore the conclusion is that there is no marked change in air mass during fog events and that fog formation is rather due to smaller scale boundary layer influences.

4.7.6.4 Summary

One must not fall into the trap of simply forecasting fog because it occurred the previous morning. Persistence forecasting of fog will fail.

Although inspection of the 850 hPa wet bulb potential temperature leads one to believe that there is no change of air mass during fog events, developing synoptic processes and smaller scale boundary layer influences must be taken into consideration.

The model data clearly show a change in synoptic circulation, therefore fog was not to be expected. Although the moisture fields were at times misleading, the main considerations were the increased pressure gradient and stronger north-westerly to south-westerly wind due to the development of a low pressure to the north-east.

Fog is highly unlikely when the wind backs from north-westerly to south-westerly. This situation arises when there is a low pressure cell to the north-east, particularly a developing low pressure cell. The reason is that the resulting pressure gradient over the UAE generates a wind that is strong enough to maintain turbulent mixing. In this situation the surface wind at night becomes uncoupled from the circulation around the low above the boundary layer and backs from north-west to south-west.

The moderating influence of the Gulf Sea, brought by the wind from the north-west and possibly curving to south-west along the coast, maintains warmer overnight surface temperatures. This, combined with turbulent mixing, prevents, or inhibits, nocturnal radiation cooling of the air.

4.8 RESULTS

4.8.1 GENERAL

Typically, fog at Abu Dhabi forms at night in a clear sky with a weak pressure gradient, light winds and sufficient moisture, that is, radiation fog, although a preceding advection process plays a supporting role by bringing moisture from the sea. A secondary observed form of advection is that the fog often appears to form over the southern inland part of the airport and drift, or expand, coastward on a light southerly wind off the desert.

Seasonally, the highest frequency of fog is in the autumn months of September and October and the least in summer. It tends to form earlier in the evening during the winter months and last longer after sunrise than in the summer. The 10 year study of the winter months of January and

February revealed that fog occurred between 1800 to 0700 UTC and most frequently between 2200 to 0500 UTC. In summer (July and August) fog occurred between 2200 and 0400 UTC and most of it between 0000 and 0300 UTC. More often than not the fog clears within about 2 hours after sunrise. The earliest fog occurred during the study period from 1983 to 2002 was 1800 UTC and the latest was 0700 UTC.

Inspection of the fog events for the ten-year period from 1993 to 2002 revealed that there is only an 18% chance of fog on two consecutive days, while the risk of fog three days in a row is 6% and 2% and 1% for four and five days, respectively. These figures emphasise that one must not go the persistent forecasting fog. Consideration must be given to changing circumstances and conditins. A case in point is the non-occurrence of fog on the 6th October 2003.

Although inspection of the 850 hPa wet bulb potential temperature leads one to believe that there is no change of air mass during fog and no fog events, developing synoptic processes and smaller scale boundary layer influences must be taken into consideration.

4.8.2 PRESSURE AND PRESSURE PATTERNS

Fog forms in a weak pressure gradient across the UAE, usually 1 hPa, or less, particularly after persistent Shamal winds, or sea breezes, with attendant high humidity.

Fog does not occur when a surface low pressure cell is situated to the west of the UAE, or over the western part of the UAE. It produces a dry offshore southerly flow that strengthens the early morning land breeze and delays the onset of the sea breeze until late in the afternoon and can prevent it from extending too far inland. The stronger and earlier beginning of the land breeze causes turbulent mixing of the surface air with drier air aloft, thereby prematurely curtailing the radiation cooling effect and prevents fog formation.

The presence of an anticyclone over southern Iran and the Strait of Hormuz also produces a southerly flow over the UAE and produces the same effect.

When the wind remains from the north-west to north-easterly throughout the night, due to a surface low pressure cell to the south, or south-east, fog does not occur. The steady wind off the sea is also usually strong enough to maintain turbulent mixing, thereby preventing fog formation. Air off the sea, being less influenced by nocturnal surface radiation cooling maintains warmer conditions than when it arrives from the cooler desert, with less likelihood of the air cooling to its condensation level. If the wind does swing to the south-east, due to the synoptic circulation, and increased radiation cooling over the land, it is usually too late to enable the air to cool to below the dew-point temperature.

Under Shamal conditions, such as when a surface low pressure cell is to the north-east of the UAE, fog does not form. The low level winds at night, which become light south-westerly to westerly and may even remain north-westerly, maintain warm Gulf air in circulation relative to the cooler overnight land air. Turbulent mixing of the warm and moist air from the Gulf Sea may cause a thin layer of stratocumulus, or stratus cloud, to form under a temperature inversion in the approximately 900 metres (3000 feet) atmospheric boundary layer, with sea haze moderately reducing the visibility.

4.8.3 TEMPERATURE

It was noted that fog forms when the air temperature falls to, or below, the maximum dew-point temperature that occurred in the previous late afternoon, or early evening. This is significant enough to be taken into consideration when determining the overnight minimum temperature. Fog does not always form immediately the air temperature has fallen to, or below, the maximum dew-point temperature earlier in the day. It can form up to a few hours later. This is not an absolutely reliable indicator, as the air temperature can fall below this level with no fog formation.

4.8.4 HUMIDITY

As a rule the chance of fog later in the night is very good if the surface humidity exceeds the specific hourly values during the preceding evening, as indicated in figure 4.1. However, it is by no means a rigid rule, as it can be lower, particularly during the early evening. Certainly if the surface relative humidity is expected to reach, or exceed, 95%, fog must be considered.

4.8.5 WIND

The 10 m wind often falls to 2 knots, or less, about an hour prior to the fog forming. Allowing for surface friction effect, it can be assumed that the wind at about 2 m decreases to less than this and possibly calm at this time, which is favourable for initial fog development.

Fog is most likely (87% of the time) when the wind veers during the night from north-westerly through easterly to a calm or light east-south-easterly or south-easterly wind. It is most unlikely, but not impossible, when the wind backs to south-westerly to southerly.

Fog does not occur when Shamal conditions exist and the surface wind persists from the west through north-west to north-east during the night, or most of the night before possibly becoming a temporary light south-easterly land breeze around sunrise.

From the ground up to the temperature inversion the wind tends to back from south-easterly to north-north-easterly in fog conditions, but this is not always true. As the case study for the 9th to the 11 January showed, the wind can remain easterly. A southerly wind brings dry desert air and no fog. The critical factor remains the strength of the wind, a wind of around 5 knots, or less, being the most productive.

4.8.6 VISIBILITY

The visibility during fog events normally rapidly deteriorates to less than 200 metres, on some occasions as low as 50 metres. Visibility less than 200 metres is most prevalent between 2200 UTC and 0500 UTC. 200 metres is a critical visibility level at ADIA and determines whether the airport remains operational, or not.

Misty conditions and/or low stratus cloud in the afternoon or evening, are a useful visual

indicator of fog later, but are not infallible.

4.8.7 ATMOSPHERIC SOUNDINGS

The extreme dryness of the air above a temperature inversion, in the atmospheric soundings, epitomise the prevailing presence of a continental anticyclone with strong subsidence and creating so called superior air.

The soundings reveal profiles around the time of fog formation at 0000 UTC that conform closely to those suggested by Stull and the UK Met Office in figure 4.1.

An ideal fog profile at 12 UTC that is indicative of fog later in the night is more difficult to categorise. However, the ambient air temperature profile most likely to be a precursor to fog formation later in the night, is one that indicates the base of a temperature inversion somewhere in the layer between the surface and 960 hPa. This pressure level is approximately 270 metres (900 feet) AGL in summer to about 490 metres (1600 feet) AGL in winter.

Morning soundings show that fog most often forms when the temperature inversion base is about 171 metres (560 feet) AGL, or lower, but can be up to about 1000 feet AGL. This implies that sinking of the inversion toward the ground occurs in the evening, or a new ground inversion develops in conjunction with nocturnal surface radiation cooling. Wind shear is not always present at the temperature inversion.

Preferably, the pre-fog afternoon dew-point temperature profile will reflect moist air with markedly dry air above. Greater than 50% relative humidity, from the surface to the base of the temperature inversion, or at least up to 100 metres above the ground is a good indicator, but it is not an infallible indicator. On occasion relative humidity, at the time of the sounding, has been as low as 30%.

On summer afternoons the cooler sea breeze tends to carve a very prominent wedge into the very hot dry adiabatic lapse rate temperature profile, with a near surface superadiabatic lapse rate. In winter the afternoon soundings differ in that, due to the lower winter land temperatures, the wedge of sea breeze air is less pronounced. The morning winter upper air profiles generally had shallow surface inversions The winter upper air profiles also often had difficult to discern near surface inversions topped by an isothermal layer. This is in complete contrast to the marked summer temperature inversion. Winds below the inversion tend to back from south-easterly to north-easterly irrespective of the season.

4.8.8 FOG INDICES

Generally, fog indices, developed elsewhere, yielded erratic results when applied at ADIA. The Saunders and Craddock and Pritchard methods were derived in the United Kingdom for a wetter and milder climate and did not fare well in the much drier conditions immediately above the surface layer at ADIA. The same applies to using the 850 hPa wet-bulb potential temperature (WBTP). The fact that these indices gave more realistic values in the cooler and moister winter conditions at ADIA supports this assumption.

The two locally developed WBPT methods fared better. One method uses the 1200 UTC surface WBPT as the forecast the fog temperature. The second method uses the 0000 UTC surface temperature and the 1200 UTC surface dew point temperature to calculate a forecast surface WBPT, or fog temperature for the following night. The second method has promise with the application of exception stipulations, but it requires further investigation.

4.8.9 NWP MODEL DATA

Larger scale synoptic patterns that do not produce fog are easy to identify. These include; Shamal conditions with a low pressure cell to the east, or north-east, a southerly wind off the desert in association with a low pressure cell to the west and south, or an anticyclone to the north and east of ADIA. The problem arises when the pressure gradient is weak, such as when an anticyclone or col is over the UAE. Whether condensation will be in the form of dew or fog then depends on the delicate balance between moisture available and the wind, a condition that is still beyond the ability of current NWP models.

Model data can give misleading clues as to whether fog would form or not. Model conflicts include indicating fog favourable light south-easterly to southerly winds, but with insufficient moisture, or on the other hand, high moisture content, but with a light wind from the wrong direction. Another problem with model data is predicting high moisture content at longer lead times and then scaling it down closer to the target time. The conclusion is that model prognoses relative humidity and wind fields must not be used in isolation and other fog indicators must also be taken into consideration.

Prognostic atmospheric profiles, particularly those from finer resolution NWP models, can give a good indication the environmental lapse rate that is expected and the presence of a boundary layer temperature inversion as well as low level winds.

In spite of NWP models correctly predicting a weak surface pressure gradient, high relative humidity and light low level wind, fog may still not occur. Under these circumstances consideration must be given to the predicted pressure pattern.

4.9 FORECAST CHECKLIST

A fog forecast checklist has been established to help the forecaster decide whether fog will occur. Taking into consideration that forecasts can be required up to eleven to thirteen hours before the flight arrives at ADIA, the checklist has been divided into separate short (<12 hours) and long term (>12 hours) checks.

Long term (>12 hours)

Favourable for fog

- Clear sky expected.
- A weak pressure gradient of 1 hPa, or less.
- Surface col, or anticyclone, over the UAE.
- Shamal ceases during the afternoon, or evening.
- ≥ 90% surface relative humidity indicated in the night at 0000 UTC and 0300 UTC.

- ≤ 5 knots surface winds and in the atmospheric boundary layer expected.
- Surface wind expected to veer from north-west to south-easterly.
- A surface, or near surface temperature inversion expected overnight, preferably ≤ 168 metres (± 550 feet) above MSL.

Unfavourable for fog

- Wind ≥ 5 knots.
- A southerly offshore surface wind.
- Low level southerly to south-easterly wind (≥ 5 knots).
- Early surface land breeze expected.
- Pressure gradient > 1 hPa.
  The above conditions occur with:
  a) A low pressure cell to the west.
  b) An anticyclone over southern Iran and/or the Strait of Hormuz.
- Shamal wind.
- Low pressure cell to the south, south-east, or east with a ≥ 5 knots easterly to north-easterly wind.
- Surface winds expected to back from north-west to south-west, or southerly.

Short term (< 12 hours)

Favourable

- Afternoon sounding has;
  a) A near surface temperature inversion ±270 m, 885 ft (summer) ±490 m, 1607 ft (winter).
  b) ≥ 50% relative humidity within ± 100 metres of the surface.
- Forecast minimum temperature lower than, the maximum dew point temperature the previous late afternoon or evening.
- Hazy visibility late afternoon and/or evening.
- Early evening low stratus cloud.
- Relative humidity ≥ 73% by 1800 UTC.

Unfavourable

- The afternoon sounding has;
  a) A surface temperature inversion higher than 960 hPa.
  b) ≤ 50% relative humidity within a few hundred feet of, the surface.
- The forecast minimum temperature is higher than, the maximum dew point temperature the previous late afternoon and evening.
- Clear and crisp late afternoon and evening visibility conditions.
- ≥ 5 knots southerly surface desert wind begins early in the night.
- Surface wind backs to south-westerly instead of south-easterly.

Imminent

- The 10 m wind is light variable and approaches calm.
- The 2 metres wind falls below 2 knots, or calm (and increases again).
- The observed surface relative humidity ≥ 95%.

CHAPTER 5

SHAMAL

5.1 INTRODUCTION

Shamal is an Arabic word that means north and is the name given by the local inhabitants to the above normal northerly to north-westerly wind that blows in the Gulf region. There is no universally accepted definition of a Shamal. The UK Meteorological Office Glossary (1991) defines it as "a hot, dry north-westerly wind which blows with special persistence in summer over Iraq and the Persian Gulf", adding that "it is often strong during the daytime but decreases at night." However, Rao, et al (2001) simply define it as a northerly to north-westerly wind with a mean hourly speed of 17 knots, or more, that blows for at least three hours in a day.

The Shamal is the only persistently strong wind in the region that can last for several days with winds that can reach strong to gale force over the open sea and routinely produces 3m to 4m (10 ft to 12 ft) wind waves. Given the numerous oilrigs in the Gulf it is clear that the wind and sea waves can be at least a nuisance and, at worst, a threat to oil production. Marine warnings for the offshore areas are issued by the ADIA weather office when the wind reaches, or is expected to reach, force 6 (22 to 27 knots) on the Beaufort wind scale.

5.2 SCOPE OF THE STUDY

This chapter examines the winter and summer synoptic conditions under which Shamal winds occur at ADIA by way of a statistical analysis as well as case studies and proposes a methodology for forecasting the Shamal. Shamal events researched were from 1992 to 2003 in the ADIA data base.

5.3 METHOD

Shamal events are researched using surface observations at ADIA, the 1200 UTC and 0000 UTC atmospheric soundings at ADIA, as well as Eta GFS NWP. Case studies of a winter and a summer Shamal are presented and discussed, along with statistical data and the wind's effect on the sea state in the Gulf Sea.

5.4 THE WINTER AND SUMMER SHAMAL

The Shamal can be divided into the long and persistent Shamal of summer and the more intermittent winter Shamal. Membery (1983) refers to the wind as being particularly persistent over Iraq and the Gulf in summer from May to early July. This is when there is a quasi-permanent high pressure cell over northern Saudi Arabia and the summer Asian low to the north-west. The enhanced gradient between these two pressure system results in an intensified and persistent north-westerly wind over the Gulf Sea. The Shamal is enhanced by

a lee low effect west of the Zagros Mountains, immediately inland over south-western Iran. However, during the summer months, an approximately north-south trough from the Iran/Asian low to the southern Arabian Peninsula heat low often lies across the UAE so that the Shamal is often restricted to the western Gulf Sea and western UAE (Rao, et al 2003).

In winter Shamal conditions develop in association with mid-latitude upper air troughs that pass from west to east through the region, mainly during the months of November to March. In character with these baroclinic systems, a surface low pressure cell exists below the south-westerly flow ahead of the trough and a surface high pressure cell follows to the west of the low pressure cell. This surface low usually passes to the north across Syria, Iraq and northern Iran, while a secondary low usually develops and moves from the Red Sea across Saudi Arabia to southern Iran (Rao, et al 2001).

The greater persistence of the summer Shamal is borne out by Rao, et al (2001) in a study at Doha, in neighbouring Qatar, where they found that 51% of Shamal days occurred in the summer months of May to July compared with 26% during the winter months of November to March. They also found that the Shamal is strongest between 0600 to 1100 UTC, that is, 1000 to 1500 local UAE time.

No statistics of Shamal days over the UAE could be found. Using Rao, et al's (2001) definition, an inspection was made of all days from 1992 to 2003 (inclusive) when the wind reached, or exceeded, 17 knots for three hours or more. As ADIA is some distance inland from the open sea, a lower wind limit of 15 knots was also considered so as to compensate for the increased friction on the wind overland. The selection of this lower limit resulted in nearly double the average monthly Shamal events at ADIA (figure 5.1). It was discovered that the Shamal at ADIA is more prevalent during the spring and summer months from March to August with a distinct drop during the autumn and winter months. The 15 knot limit events also revealed a peak during May to July, which is in accord with findings of Membery (1983) and Rao, et al (2001). The Shamal is also strongest and most frequent during the later part of the afternoon and early evening (figure 5.2), being most prevalent from about 0900 UTC to 1500 UTC (1300 to 1900 local time) and least frequent overnight. It was also noted that low cloud most often accompanied the Shamal in winter, but there was virtually no low cloud associated with the summer Shamal (figure 5.1).

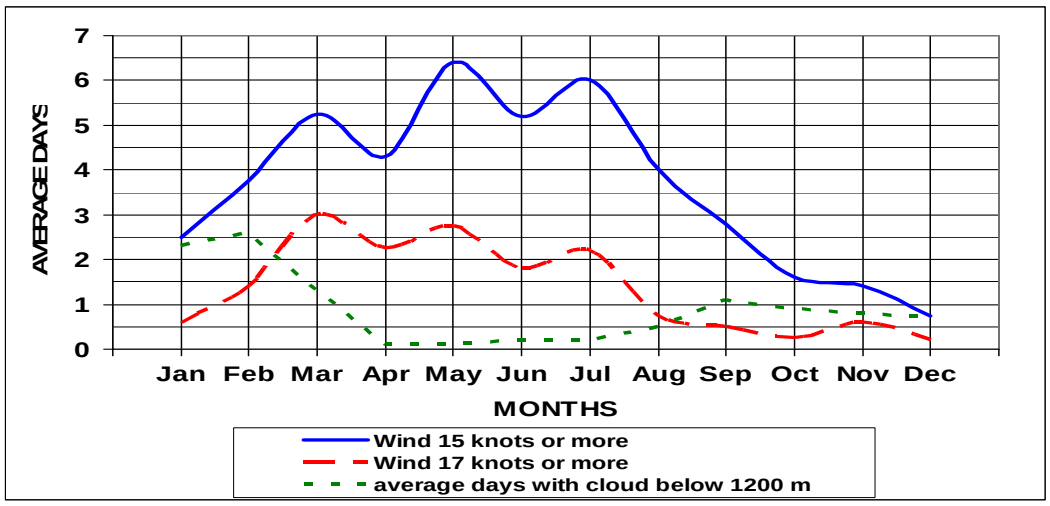

Figure 5.1. The average number of Shamal days per month, daily duration 3 hours, or more, at ADIA for the years 1992 to 2003.

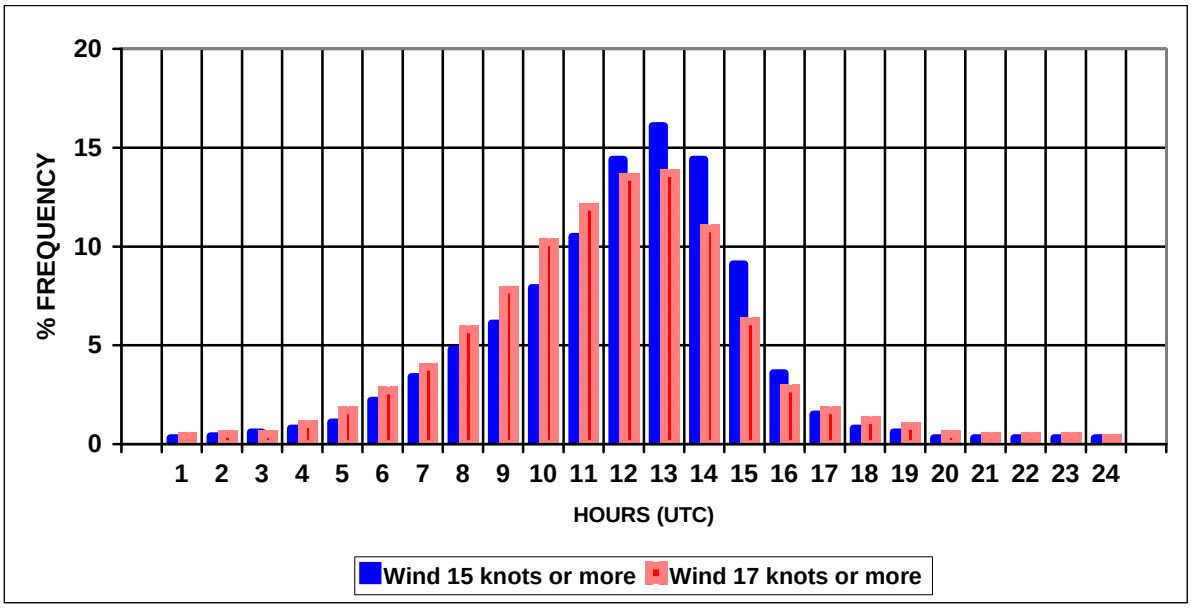

Figure 5.2. The daily hourly frequency of the Shamal at ADIA from 1992 to 2003, inclusive. Wind speed ≥ 15 knots in blue and ≥17 knots in red.

5.5 WINTER SHAMAL: 13TH TO 19TH NOVEMBER 2003

5.5.1 INTRODUCTION

A south-easterly to southerly wind blows off the desert ahead of a surface low approaching from the west and when the upper air trough is about a ¼ wavelength away, west of the surface low, cloudy weather occurs, sometimes attended by light rain and/or a brief thunderstorm line squall. A following surface anticyclone can cause a marked pressure rise and a fresh to strong Shamal wind blows. The flow of air from the north, off southern Iran, facilitates the development of a lee low, which strengthens the pressure gradient. Occasionally these systems will produce more persistent cloudy weather and heavier rain. For example, on the night of the 26th/27th December 2004 16 mm of rain fell at ADIA and for the first time in recorded history light snow fell on the Musandam part of the Hajar Mountains in the vicinity of Ras Al Khaimah.

However, as will be seen in this November 2003 case study, although an upper air trough was present it was too far north to have much effect other than to produce middle and high cloud over the rest of the Gulf with no secondary lee low developed.

5.5.2 NWP MODEL DATA

The NWP model gave adequate advance warning of the beginning of Shamal winds and predicted that it would last for several days due to the semi-stationary nature of an anticyclone. The model indicated that the winter anticyclone over Iran would cause a dry south-easterly to southerly wind to blow over the UAE from the Arabian Peninsula desert. By the 11th the gradient collapsed. On the 12th a low pressure cell of about 1012 hPa was predicted over the Strait of Hormuz with a weak trough extending north-westward along the Gulf and a high pressure ridge would develop over northern Saudi Arabia (figure 5.3a).

The following day, the 13th, a 5 hPa pressure gradient was expected across the southern Gulf Sea between the now established ridge over Saudi Arabia and the low pressure cell that was now east of the Strait of Hormuz. The Shamal was expected to reaching 15 to 25 knots over the sea (figure 5.3b). The strongest gradient (7 hPa) and maximum wind (20 to 30 knots), was predicted on the 14th (figure 5.3c), with wind speed moderation predicted on the 15th and 16th.

By the 18th (figure 5.3d), a weakened pressure gradient meant that the wind experienced at ADIA was more likely to be in the form of a moderate sea breeze, while the north/south pressure gradient meant that there should still be little, or no, early morning land breeze. However, later model runs indicated a delay in the reduction of the pressure gradient by a day to the 19th (figures 5.3d and 5.3e).

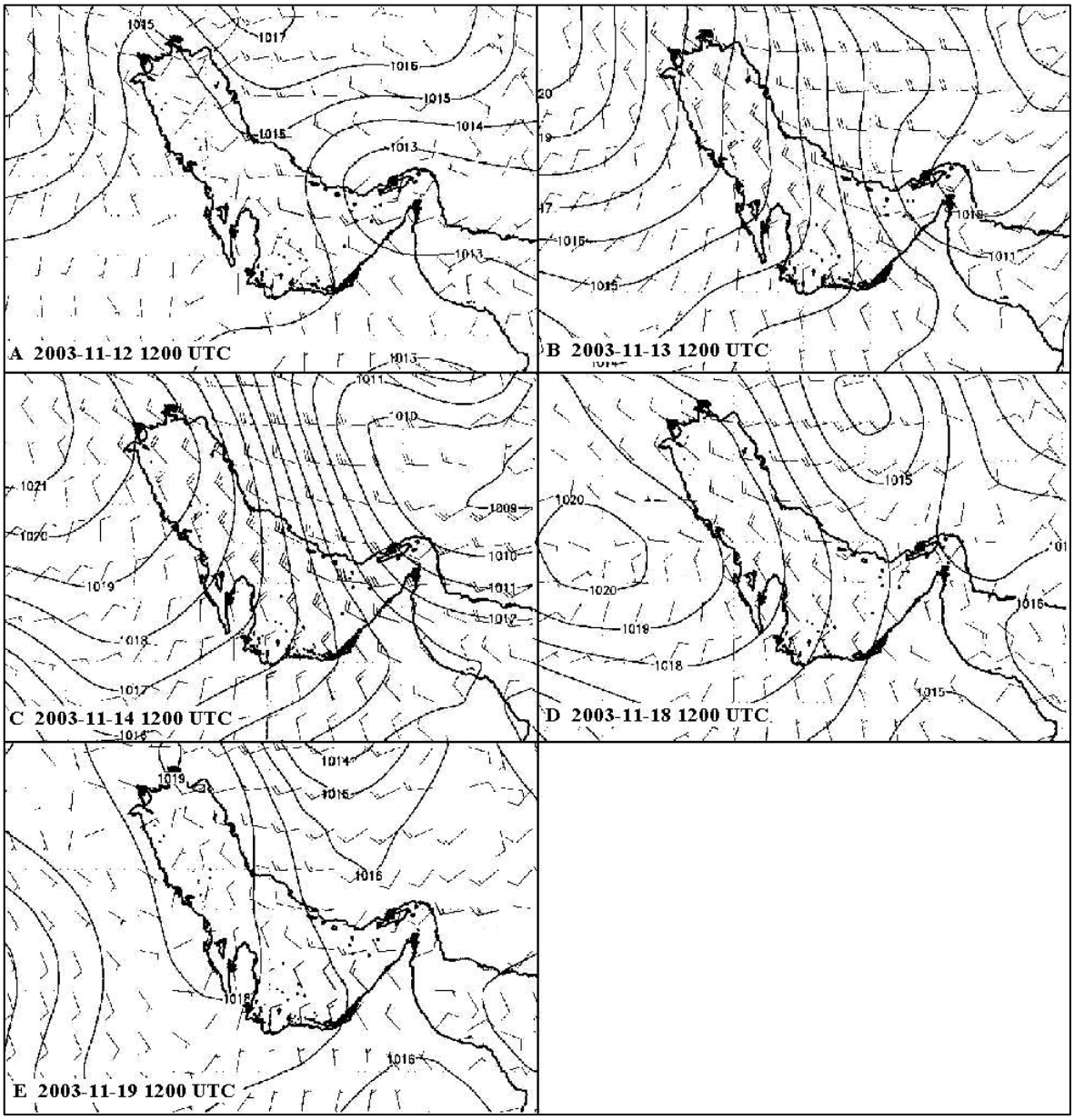

Figure 5.3. Eta GFS prognostic fields of surface pressure (hPa) and wind (knots) 2003-11-12 to 2003-11-19 at 1200 UTC. The fields for the 12th to the 14th are from the 2003-11-11 0000 UTC model run. The 18th and 19th are from the 2003-11-17 1200 UTC model run.

Apart from showing the persistence and depth of the Shamal, the sequence of time cross sections at Abu Dhabi reflect the change from a dry environment on the 11th, with south-easterly winds in the lower levels, to more moist boundary layer conditions associated with the Shamal below 900 hPa (figures 5.4a and 5.4b). The surface pressure averaged about 1015 hPa, which means that the 900 hPa pressure level in the time sections is about 1050 metres MSL (±3450 feet). Note the lack of an early morning south-easterly land breeze from the 13th onward. At best the wind near the surface becomes lighter, backs to westerly and on one occasion to south-westerly. The 10 metre winds in figure 5.5, unfortunately with a six hour break early on the 18th, show no such inclination for the wind to back in the early hours of the morning.

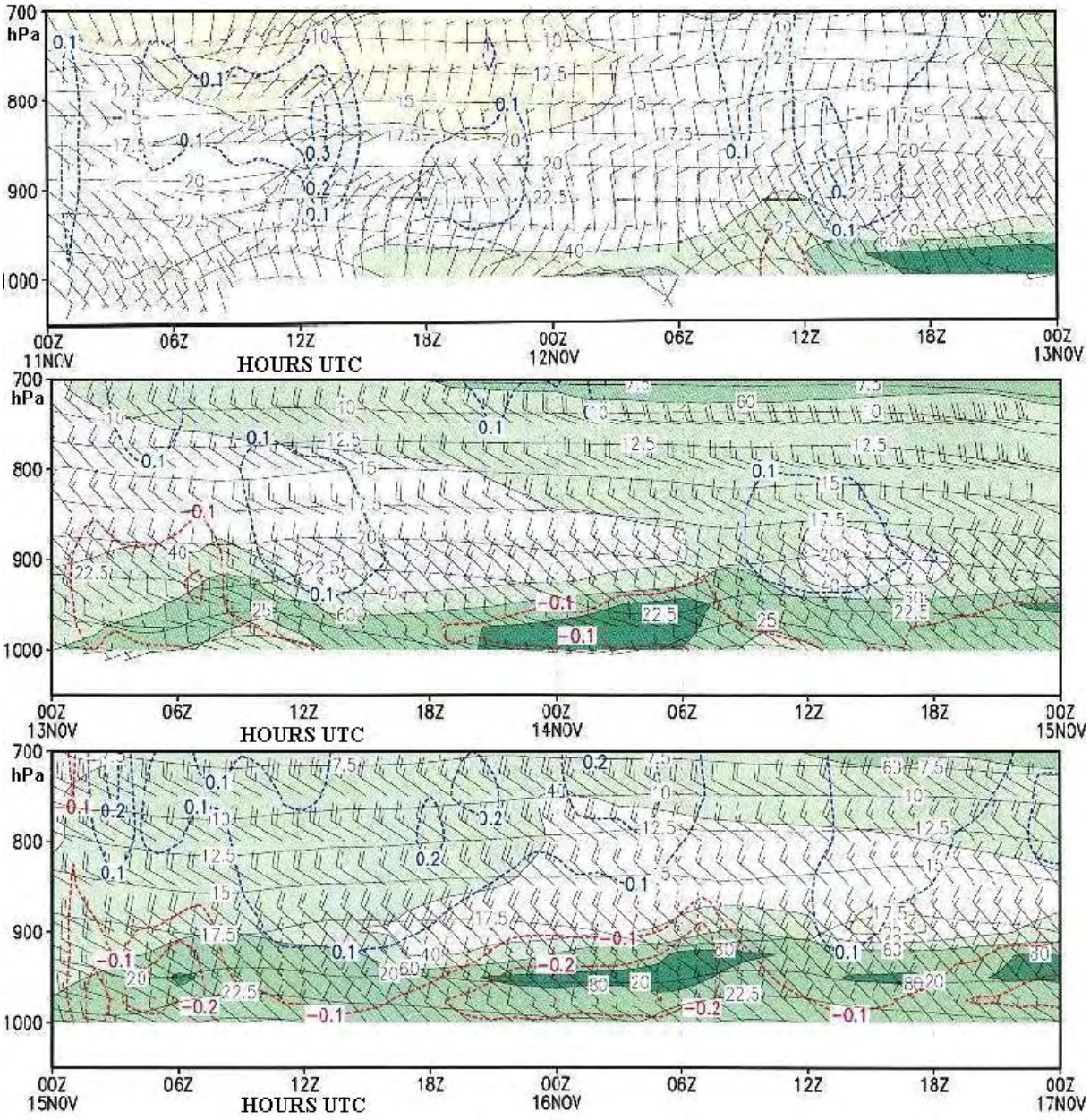

Figure 5.4a. Time cross-sections of wind, dew point and vertical motion at ADIA from 2003-11-11 to 2003-11-17, extracted from Eta model runs. The sequence reflects the change from a dry environment on the 11th, with south-easterly winds in the lower levels, to moister boundary layer conditions associated with the Shamal.

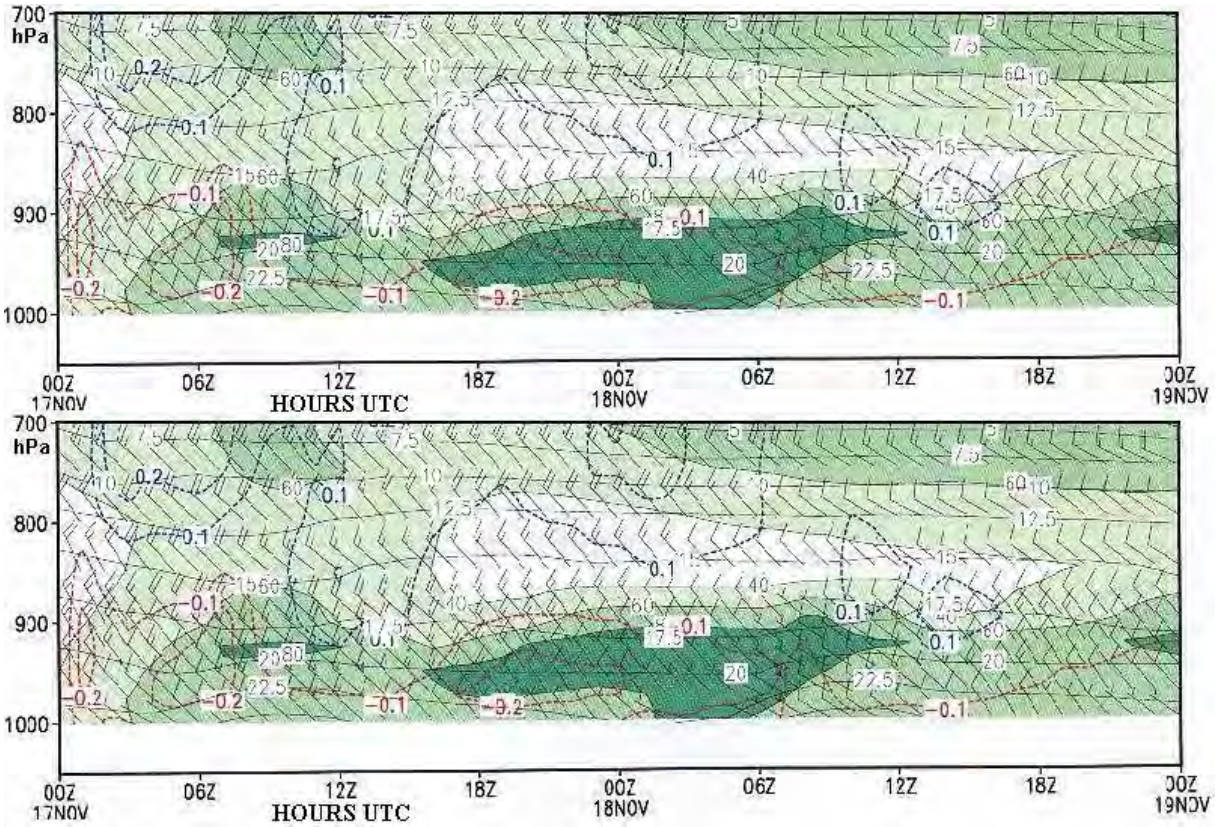

Figure 5.4b. As figure 5.4a, but for 2003-11-17 to 2003-11-19.

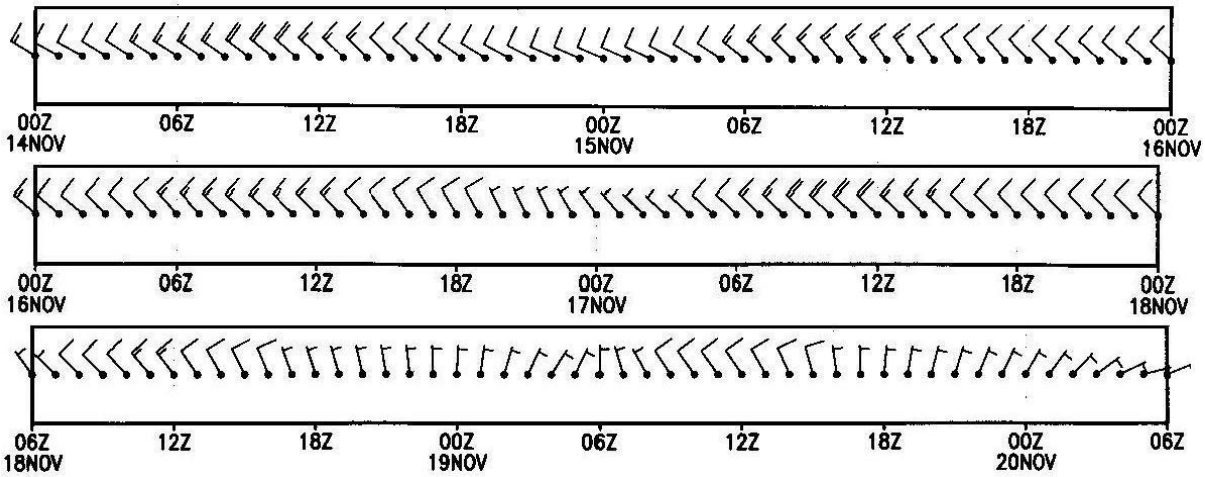

Figure 5.5. Eta model 10 metre prognostic winds (in knots) for the period 2003-11-14 to 2003-11-20. Data for 2003-11-18 0000Z to 0600Z is missing.

The accumulation of moisture inland of the coast, due to the Shamal, is indicated in the surface fields at 0300 UTC on the 15th and 16th (figure 5.6). Although there is an accumulation of low level moisture over the land during Shamal conditions, fog does not occur along the coast. This is not always valid inland and will be discussed in the section 5.7.

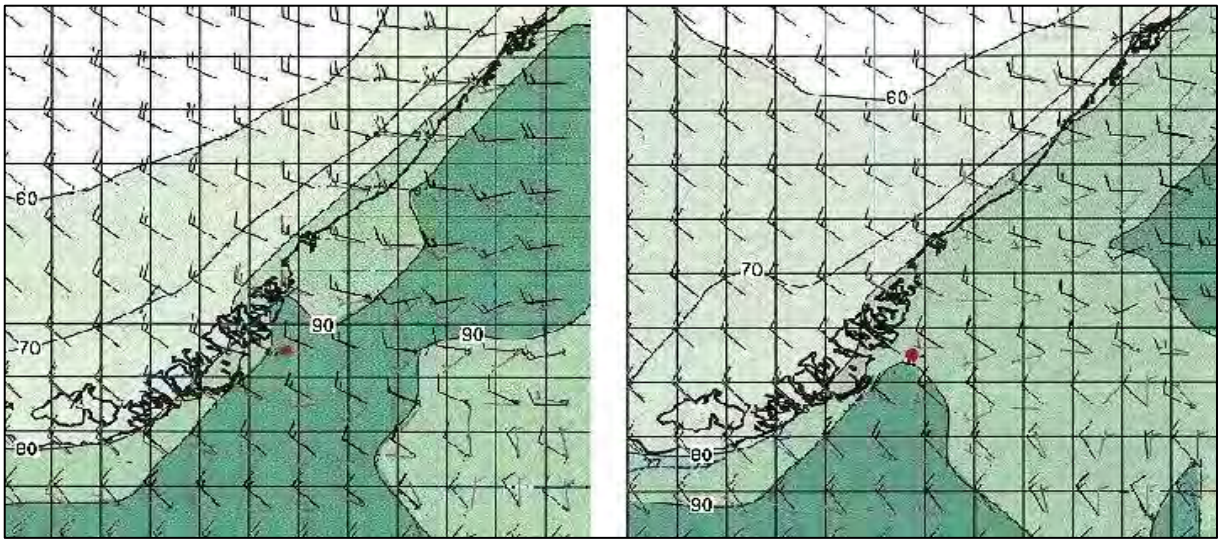

Figure 5.6. Eta model prognoses of surface relative humidity, wind (knots) at 10 metre (black), 950 hPa (grey) and downward vertical motion (blue lines) for 2003-11-15 0300 UTC (T+27) and 2003-11-16 0300 UTC (T+27).

5.5.3 OFFSHORE WIND AND SEA STATE

The feathers on the winds plotted on the marine charts (figures 5.7a to 5.7d) are rounded to the nearest 5 knots, so it is not possible to accurately identify Shamal conditions using Rao's 17 knot minimum limit (Rao, et al 2001). Nevertheless, 20 knot winds from the north-west qualify and are clearly evident over the southern Gulf Sea from the 12th and continued until the 18th.

Wind waves in the Gulf Sea increased from 0.5 m to 1 m on the 11th (figure 5.7a) to 1.5 to 2.5 m later on the 12th. From the 14th to the 18th wind waves reported were generally 2 to 3 m. At Sir Abu Nu'ayr island (±25¼°N 54¼°E) to the north-north-west of Abu Dhabi the wind waves increased from 0.5 m prior to the Shamal to 4 m on the 14th (figure 5.7c) decreasing to 2 to 3 m from the 15th and became approximately 1 m on the 19th. The Pearson product-moment coefficient of correlation (Harper 1977) between the wind speed and visually observed wind wave height at Sir Abu Nu'ayr was +0.67 (figure 5.8). In general 2.5 m wind waves result from a wind of 15 knots reaching 3 to 4 m when the wind exceeded 20 knots. These wind and sea wave conditions, during this period, caused helicopter flights to the oil rigs to be cancelled.

Overall the observed winds were about 5 to 10 knots stronger over the western Gulf. Due to the "L" shape of the Gulf, the western part of the Gulf, toward Qatar, is exposed to a longer uninterrupted flow of air from the north. The wind here tends to be stronger and the sea rougher than the eastern part, toward Dubai and the Strait of Hormuz, which are sheltered from the Shamal by the land area of Iran to the north. Local sailors have long known of the shorter fetch and the shelter to be found from the brunt of the wind in the lee of the land to the north. Thesiger (1994), during his trip in a Dhow from Dubai to Bahrain in 1948 mentions how they sheltered for days in the lee of southern Iran to avoid a gale and a very rough sea that broke over the ship. The normally four day trip eventually took 11 days. Friction over land rapidly reduced the wind speed to mere 5 to 15 knots inland.

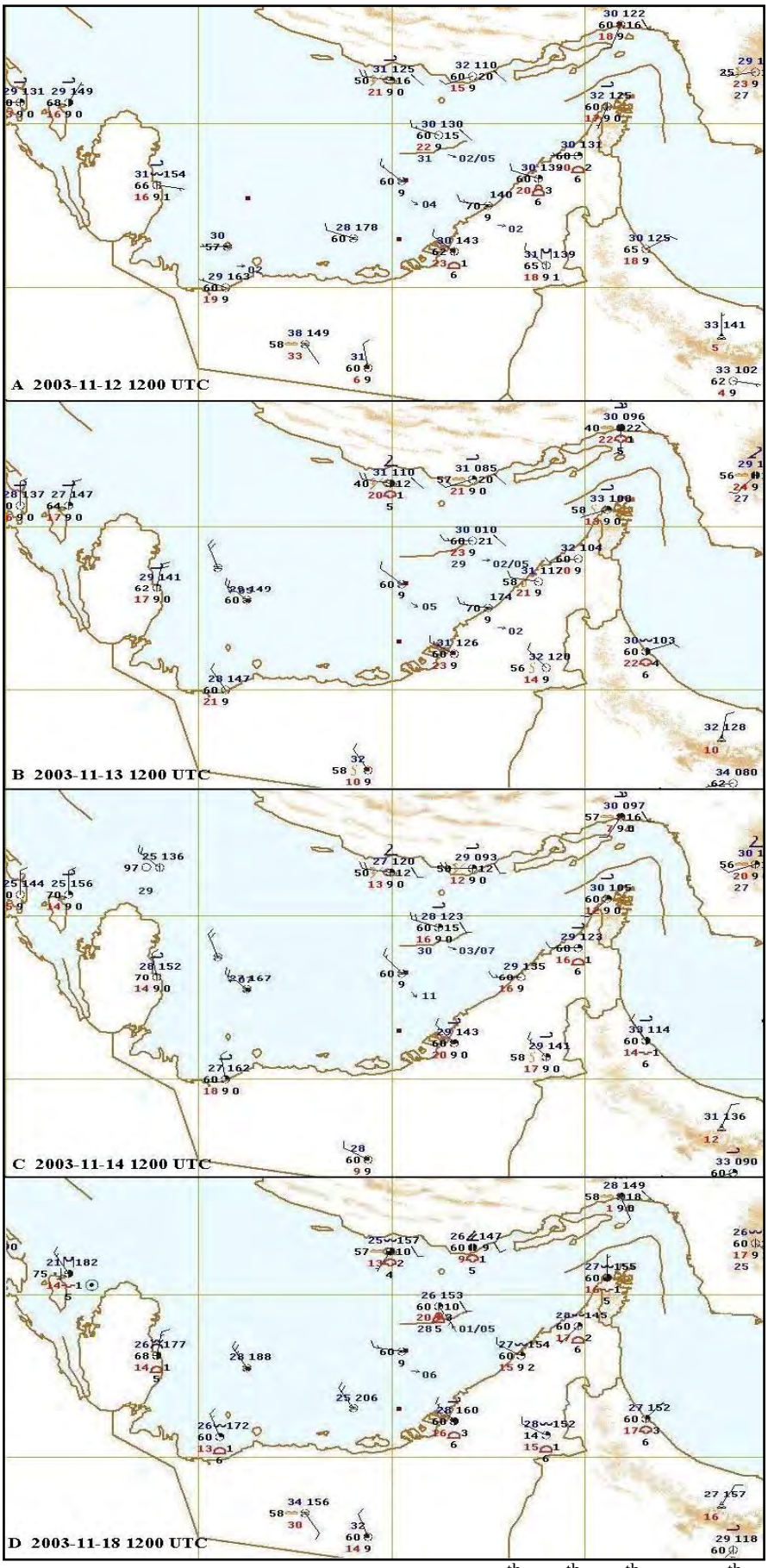

Figure 5.7. Surface observations for the 12th, 13th, 14th and 18th November 2003. Note, the wind direction at Bu Hasa inland in the south-west of the UAE is often erroneous.

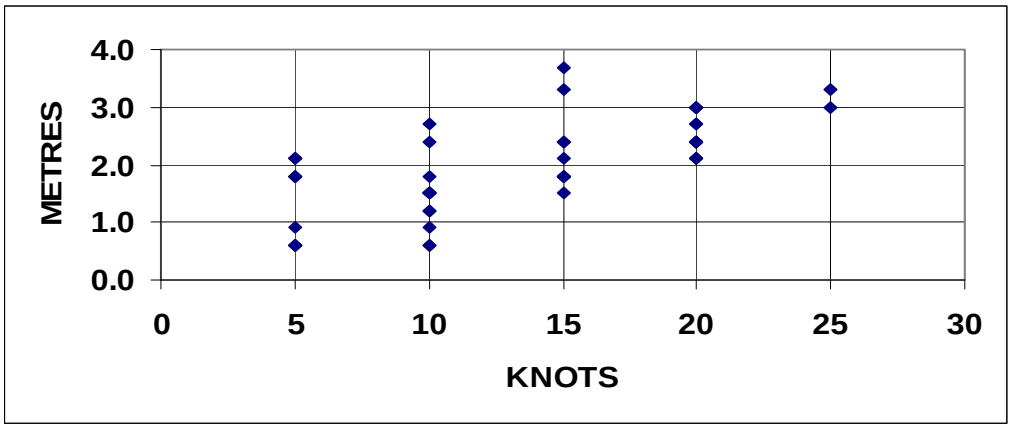

Figure 5.8. Wind speed (to nearest 5 knots) and wind wave height (metres) scatter graph of 3 hourly observations from 0000 UTC on the 11th to 1500 UTC on the 19th. The graph does not show all 51 scatter points due to superimposing of similar observations.

5.5.4 SURFACE OBSERVATIONS

Characteristically, the Shamal brings cold air from the north over the UAE and there is a noticeable drop in temperature. The maximum temperature at Abu Dhabi decreased from 35°C on the 10th and 11th to 32°C on the 12th (figure 5.9), 30°C on the 14th (figure 5.11) and 28°C on the 16th (figure 5.13). While the dew point temperature during the day fell from about 23°C to 16°C, the relative humidity during the day remained about 60% to 50%.

As predicted by the NWP model, the surface observation graphs (figures 5.9 to 5.15) reflect the lack of a south-easterly land breeze with the wind on most mornings, either blowing from the north-west, or at the most being deflected to the south-west, due to a weak land breeze effect. Notice the higher temperatures on the nights of the 13th/14th (figure 5.10) and the 15th/16th (figure 5.12) when the wind remained onshore overnight and the nocturnal land thermally induced pressure gradient, forced by radiation cooling, was unable to overcome the synoptic scale pressure gradient. The colder continental and warmer maritime air effect is particularly noticeable late on the 16th and the 18th when the wind became light from the south-south-west at 1900 UTC and then again became an onshore north-westerly at 2000 UTC (figures 5.13 and 5.15).Eventually, an approaching surface low pressure cell to the south-east of the UAE caused the surface wind to veer to a south-easterly land breeze during the nights of the 19th and 20th (figure 5.16).

The NWP model can fail to correctly predict these early morning changes in wind direction, as is revealed in a comparison of the surface observations (figures 5.8 to 5.14) with the forecast winds in figure 5.5. The model incorrectly maintained northerly to north-westerly winds on all nights. This is a dilemma for the forecaster who has to decide whether the wind will remain north-westerly, or back to south-westerly. If it is any consolation, the observations show that on most occasions the wind will back to south-westerly and it will decrease and if it does not turn to south-westerly, it will at least back as far as west-north-westerly.

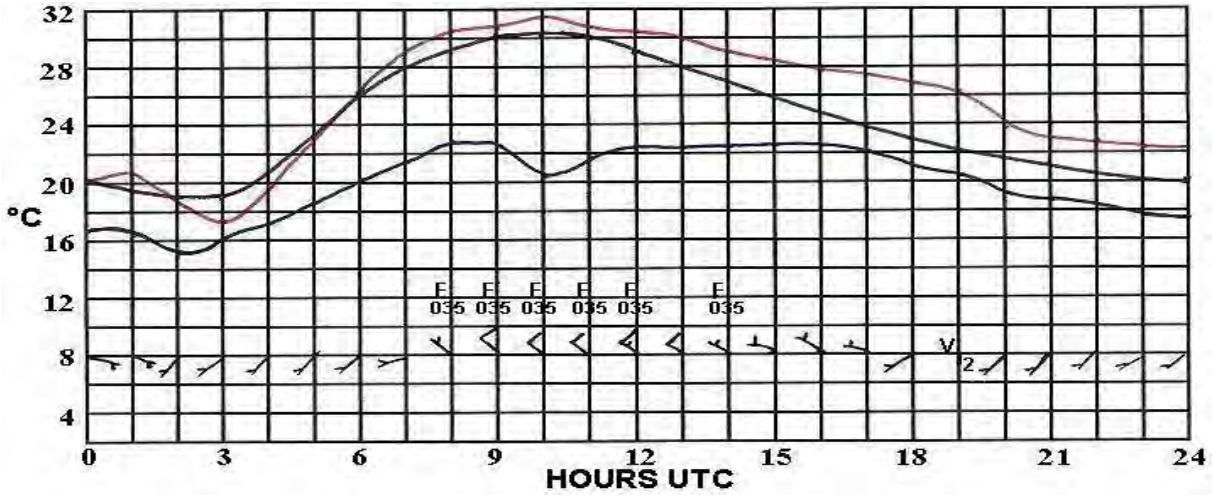

Figure 5.9. Surface observations on 2003-11-12. Air temperature (°C); red line; dew point temperature (°C), blue line; mean monthly temperature, black line. and wind flags (full feather = 10knots). F = few oktas. S = scattered, B = broken and O = overcast. The cloud is at 3500 feet AGL.

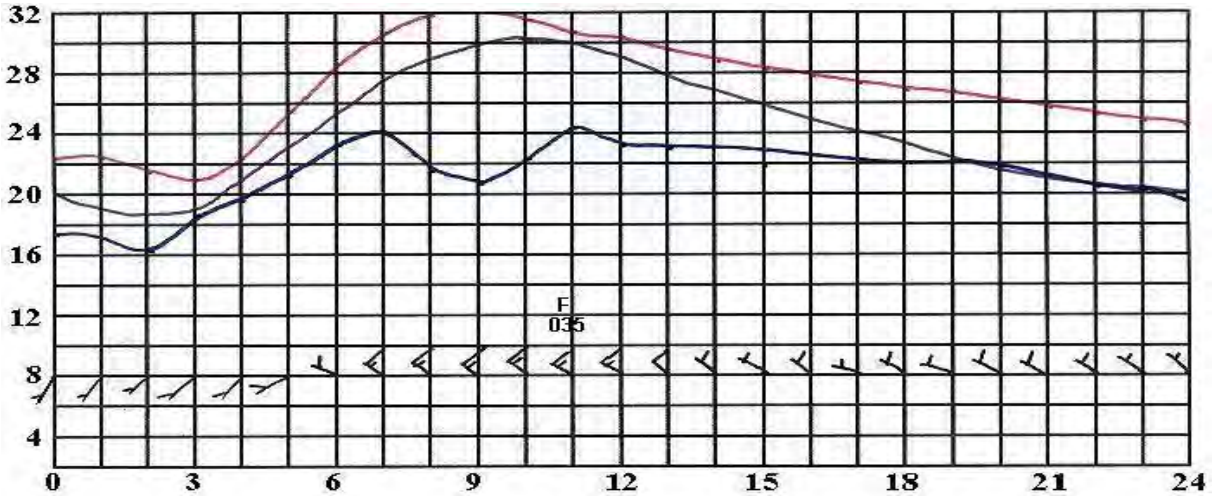

Figure 5.10. As figure 5.9, but for 2003-11-13. The cloud is at 1100 m (3500 ft) AGL.

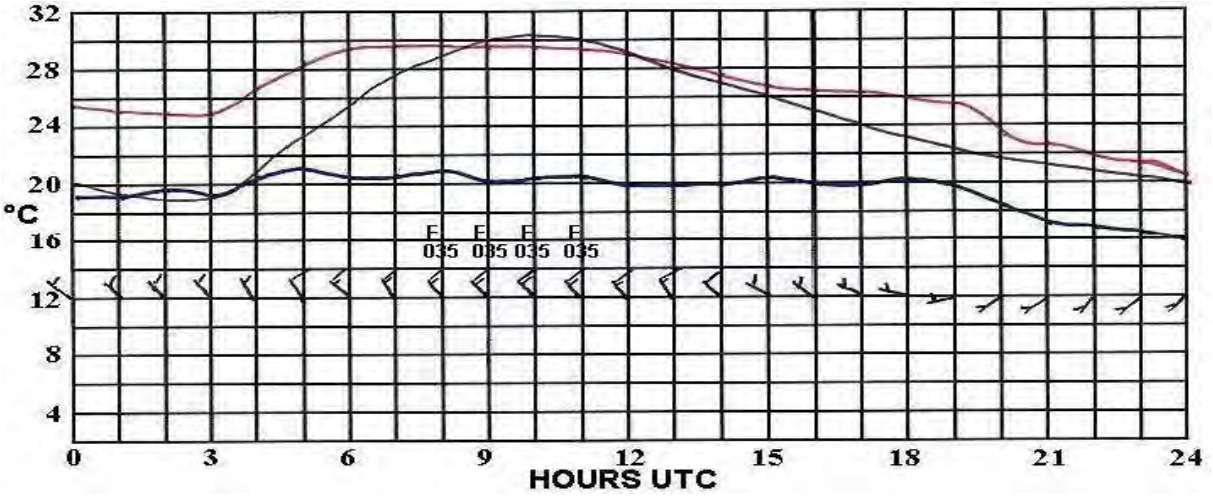

Figure 5.11. As figure 5.9, but for 2003-11-14. The cloud is at 900 m (3000 ft) AGL.

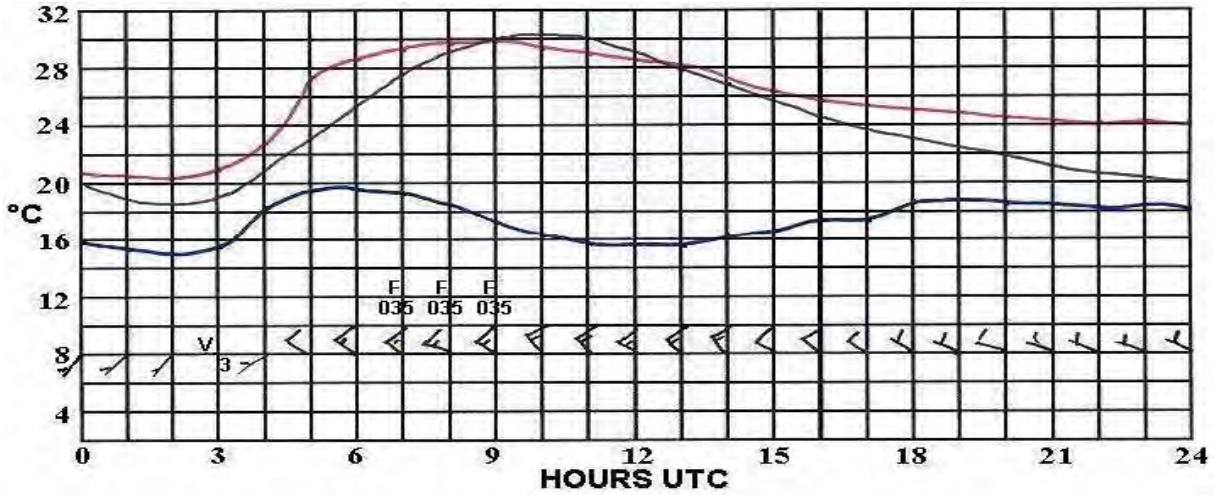

Figure 5.12. As figure 5.9, but for 2003-11-15. The cloud is at 1100 m (3500 ft) AGL.

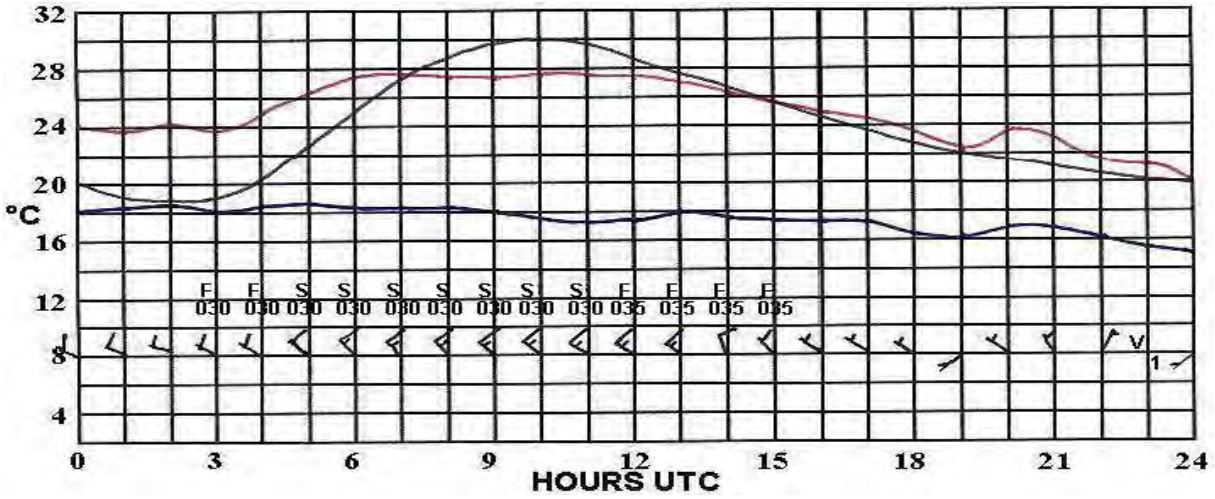

Figure 5.13. As figure 5.9, but for 2003-11-16.The cloud is at 900 – 1100 m (3000 - 3500 ft) AGL.

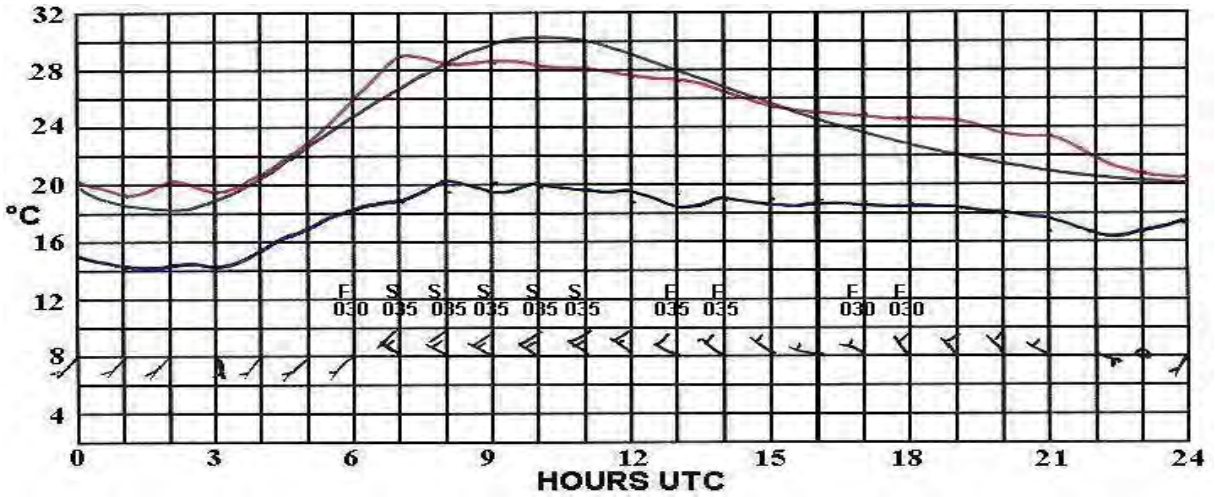

Figure 5.14. As figure 5.9, but for 2003-11-17. The cloud is at 900 – 1100 m (3000 - 3500 ft) AGL.

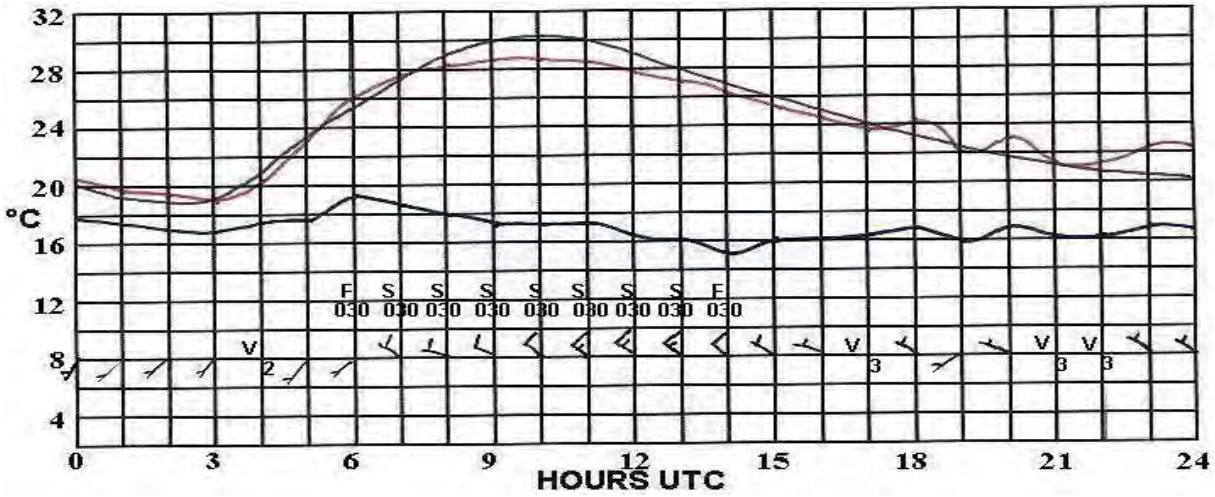

Figure 5.15. As figure 5.9, but for 2003-11-18. The cloud is at 900 m (3000 ft) AGL.

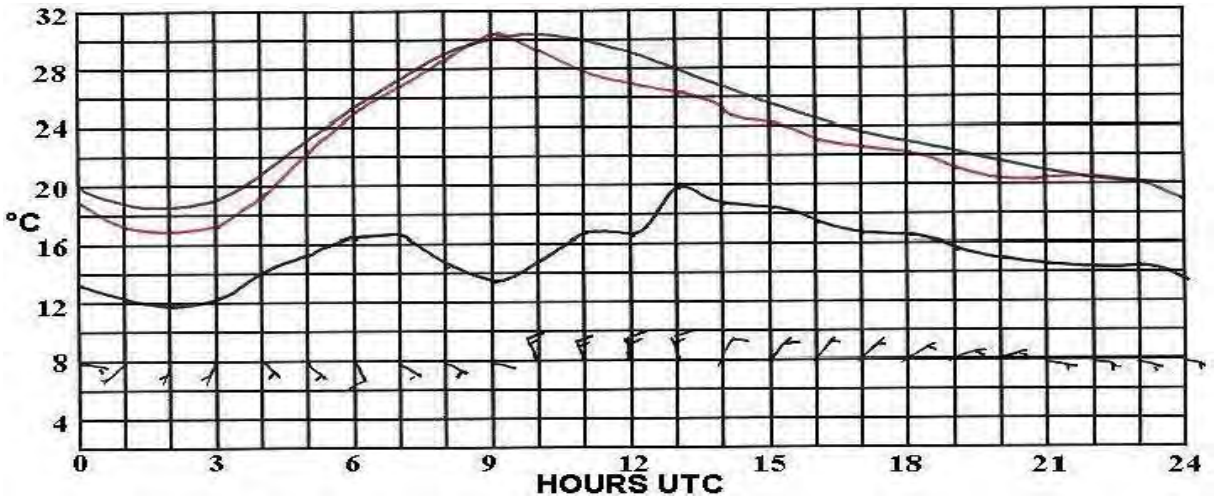

Figure 5.16. As figure 5.9, but for 2003-11-20.

During this Shamal event, low cloud occurred on most days when the wind was from the north-west with a longer path over the Gulf Sea, but it is absent on the 20th when the wind was from the land to the north (figure 5.16). With enough moisture and impetus cloud also forms further inland, such as at Al Ain low cloud during the day from the 16th to the 19th.

In the winter months it is routine for the Shamal to cause scattered to broken stratocumulus to form along the coastal belt. This was clearly illustrated by the analysis of Shamal days with winds greater than 15 knots and cloud days in figure 5.1. The percentage likelihood of cloud with the Shamal is less than 15% in the summer months, increasing to over 90% in December and January. This can be attributed to cooler and stable air over the warm Gulf becoming unstable and mechanical turbulence being strong enough to raise moisture to the lower lifted condensation level in the cooler winter conditions (Taha, et al 1981), but insufficient during the much hotter and drier summer months, in spite of the more humid surface conditions. Daytime convection heating also plays a role, as the cloud is more prevalent during the late morning and afternoon with the cloud dissipating later in the afternoon and early evening.

Figure 5.17. Winter Shamal Stratocumulus arriving over Abu Dhabi from the Gulf Sea.

5.5.5 ATMOSPHERIC SOUNDINGS

The three atmospheric soundings at 0000 UTC and 1200 UTC on the 14th (figure 5.18) and 0000 UTC on the 15th (figure 5.19), based on personal experience, were chosen as being representative of the profiles that occur during winter Shamal conditions. The first morning sounding was made on a night when the wind remained from the north-west overnight and the second morning sounding when the wind turned to south-westerly.

What is immediately apparent when comparing the two morning temperature profiles is the reduced surface radiation cooling inversion when the wind remained onshore north-westerly, than when it was offshore from the south-west on the morning of the 15th.

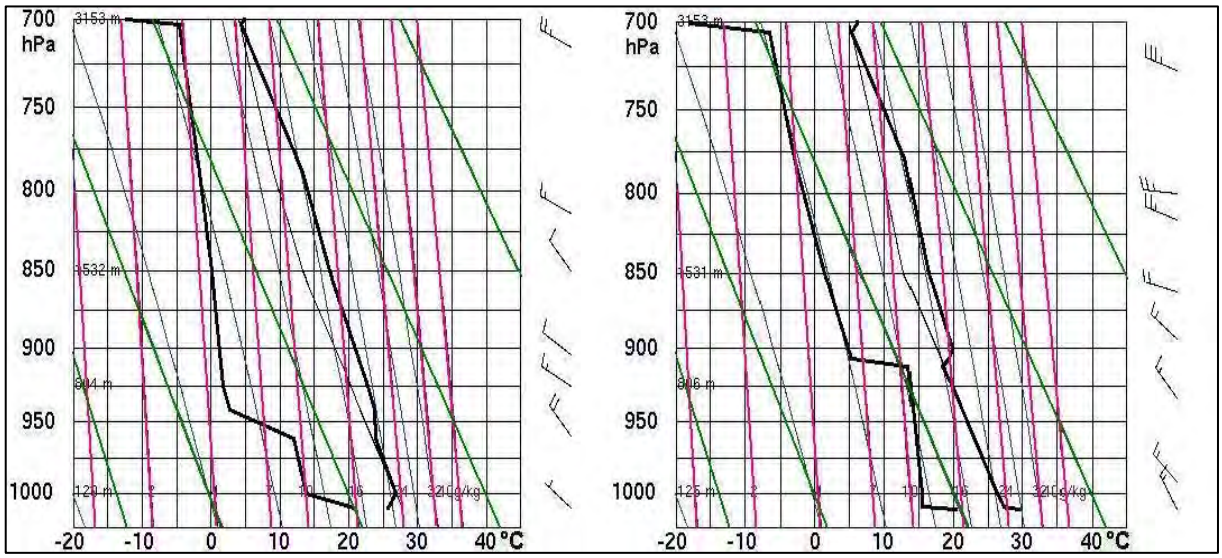

Figure 5.18. Atmospheric soundings at ADIA 2003-11-14 at 0000 UTC on the left and 1200 UTC on the right. The dry adiabatic lapse rate lines are in green and the mixing ratio lines in pink (courtesy of the University of Wyoming).

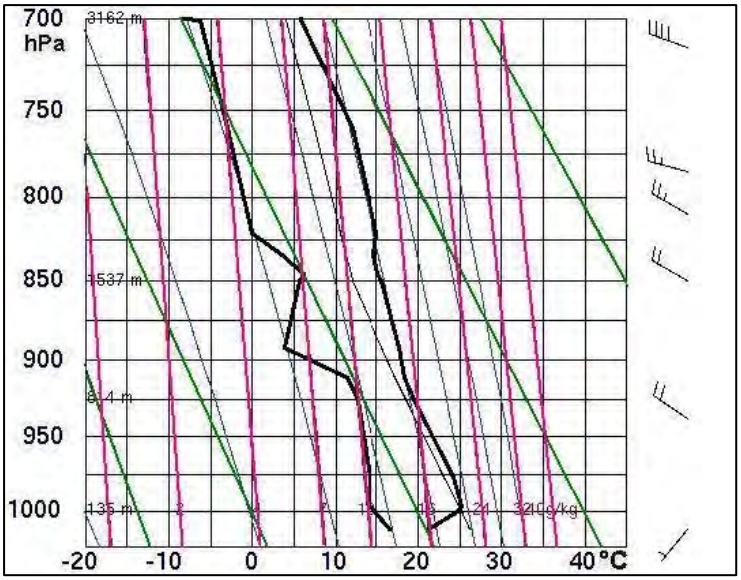

Figure 5.19. As figure 5.18 but for 2003-11-15 at 0000 UTC (courtesy of the University of Wyoming).

Furthermore, the DALR temperature lines and the constant mixing ratio dew point profiles below 960 hPa on the morning of the 14th (figure 5.18 left) and 910 hPa in the other two soundings (1200 UTC in figure 5.18 right and 0000 UTC figure 5.19) clearly indicate efficient turbulent mixing of the atmosphere (Stull 2000). Generally, mixing occurred to a depth of about 900 m to 1200 m MSL (table 5.1) where a temperature inversion was present on most of the afternoon soundings.

The strength of the low level winds at 0000 UTC in table 5.1 bear testimony to the robust turbulent mixing and emphasise why fog does not occur at ADIA in Shamal conditions. Notice the change from the south-easterly desert wind associated with the anticyclone that was to the north-east of the UAE on the 10th and 11th before the Shamal started.

Table 5.1. Winds at 150 m and 900 m above MSL at ADIA on 10th to 20th November 2003 and temperature inversions in metres above t MSL.

	0000 UTC		**1200 UTC**		
	150 m	**300 m**	**150 m**	**300 m**	**Inversion**
10th	140°26	135°18			
11th	125°12	145°12	360°02	010°02	
12th	355°08	355°11	300°11	315°13	
13th	305°13	305°14	300°15	295°16	Not available
14th	315°18	315°18	315°14	320°15	919 m
15th	255°10	270°13	320°18	315°17	No inversion
16th			315°15	320°16	977 m
17th	335°10	335°11	305°17	310°18	1170 m
18th	340°08	340°09	320°17	320°17	1210 m
19th	320°13	325°14	330°12	330°13	907 m
20th			335°15	345°11	

5.6 SUMMER SHAMAL: 28TH APRIL TO 2ND MAY 2003

5.6.1 INTRODUCTION

In summer, high temperatures over the Asian continent and the Arabian Peninsula create a marked surface “heat low,” which is enhanced by the movement of the equatorial low

pressure belt northward to the Gulf. When there is a ridge of high pressure over northern Saudi Arabia, the north to south pressure gradient is strengthened and the resultant north-westerly wind can persist over the Gulf for extended periods. The phenomenon is known locally as the "forty day Shamal." As the time the air spends over the Gulf is relatively short, the Shamal is rather dry, apart from the surface moisture trapped beneath a subsidence inversion, which causes the very humid summer weather over the UAE. Weather associated with mid-latitude systems seldom reaches the UAE in summer, but the associated Shamal often brings dust from the deserts of Saudi Arabia, Kuwait and Iraq.

The summer Shamal has many characteristics similar to the winter Shamal described above. What is significantly different is the drier air in circulation as depicted by the NWP model analysis and prognosis. Another notable aspect is the markedly lower temperatures experienced at Abu Dhabi with the onset of the summer Shamal.

As in the winter study, the research indicated that the summer Shamal wind was caused by the approach of a ridge of high pressure from the west over Saudi Arabia. This resulted in a 6 hPa to 8 hPa pressure gradient over the Gulf between the ridge and a low pressure cell over the Strait of Hormuz. And, as before, the Eta NWP model gave good advance warning of the onset of the 20 to 30 knots Shamal over the Gulf.

5.6.2 SEQUENCE OF EVENTS AND OFFSHORE CONDITIONS

Day 1: 28th April

On the 28th surface high pressure intensified over north-western Saudi Arabia and began to ridge south-eastward, east of the Gulf Sea. The wind over the Gulf at this time was generally north-easterly 5 to 10 knots due to a weak low pressure cell at the surface to the south of the UAE and the sea waves in the Gulf were low at 0.5 m. Along the coast of the UAE a 10 to 15 knots north-westerly sea breeze developed during the afternoon, decreasing to 5 knots inland. At about 1800 UTC, over the northern Gulf, north of Qatar, the north-westerly Shamal began to blow at 15 to 25 knots and the wind waves in the area began to increase.

Day 2: 29th April

By 0000 UTC on the 29th, the wind was blowing at 20 to 30 knots over the Gulf with sea waves 1.5 m to 2.1 m. Thirty minutes later the Shamal, at 10 knots, reached Abu Dhabi Airport. By 0300 UTC (0700 UAE time) it was blowing at 10 to 15 knots along the UAE coast, but reached 25 knots along the western part of the coast. During the day the wind reached 30 knots over the Gulf Sea creating 3 to 4m. Unfortunately the GFS NWP model slightly underestimated the wind by predicting not more than 25 knots over the southern Gulf.

Although the eastern Gulf tends to be sheltered from the Shamal, by 0900 UTC the eastern part of the Gulf had a west-north-west wind in excess of 20 knots and 3 m wind waves. By 1200 UTC (1600 UAE time) all the offshore oilrigs and island reports gave 3 to 4 m wind waves. The wind speed quickly moderated once it crossed the coast, decreasing to 10 to 15 knots, but, it was still strong and turbulent enough to lift sand and reduce the visibility further inland to 6000 metres.

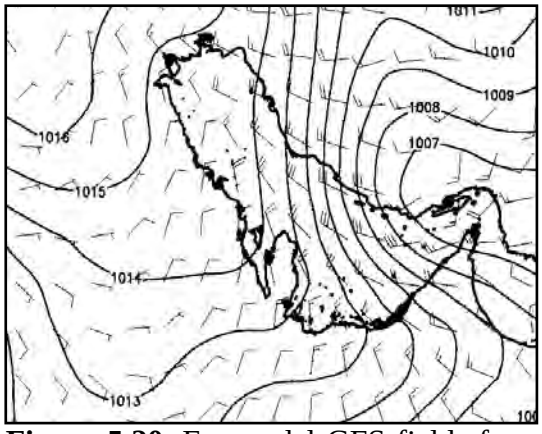

Figure 5.20. Eta model GFS fields for 2003-04-30 1200 UTC. Surface pressure (hPa) and wind (knots) are plotted. A strong pressure gradient with a near gale Shamal is indicated.

Overnight, on the 29th to the 30th, the wind along the coast decreased to 5 to 10 knots due to the land breeze effect and even backed to south-westerly along the coast from Dubai and further eastward to the Musandam Peninsula.

Day 3: 30th

The wind blew at 20 to 30 knots on the 30th with deep-sea wind waves of 2 to 3 m and up to 3 to 4 m at oilrigs in the middle of the Gulf. The Eta NWP model correctly predicted the 6 to 7 hPa pressure gradient across the Gulf and a 30 knots westerly wind extending into the eastern part of the southern Gulf (figure 5.20). Throughout the night of the 30th the wind was 25 to 30 knots and occasionally reached 35 knots in the north. Due to the opposing land breeze effect, along the UAE coast the wind decreased to 10 knots and backed to its original direction of south-west east of Dubai. Inland it decreased to 5 knots.

Day 4: 1st May

The strong to gale force wind persisted over the sea and by 0600 UTC (1200 UAE time) the wind speed was 15 knots at ADIA, averaging 18 to 20 knots in the afternoon with gusts up to 25 knots and the visibility down to 7 km. Inland at Al Ain the wind picked up to 15 knots in the afternoon with similar gusts as at ADIA, but in this sandy environment the visibility went down to 4500 m.

Day 5: 2nd

By the 2nd, the ridge of high pressure had weakened considerably, but the approach of a surface tropical low pressure cell from the east over Oman, maintained a large enough pressure gradient to cause a 15 to 20 knots Shamal over the Gulf Sea and 10 to 15 knots inland. The wind waves decreased to 1 to 2 m, but remained 2 to 2.5 m in the deep-sea.

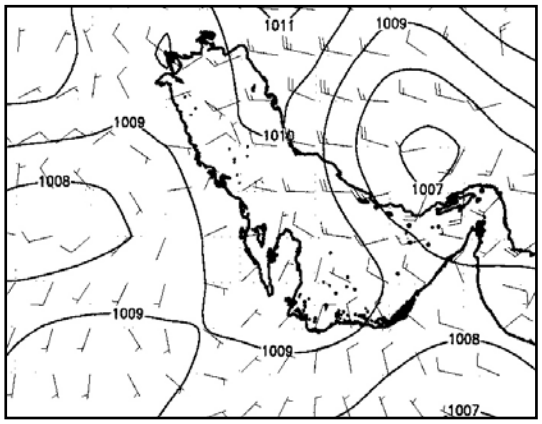

Figure 5.21. As figure 5.20, but for 2003-05-04 1200 UTC.

Days 6 and 7: 3rd and 4th

Theoretically the 3rd and 4th are post-Shamal days, because the wind had dropped to about 10 knots over the sea, while the wind waves fell to 0.5 m inshore and 1 m in the deep-sea. The surface pressure pattern, albeit a weak pressure gradient, remained more or less the same. Now the ridge was further to the east than before and resulted in a weak pressure gradient was over the eastern Gulf (figure 5.21). This gradient that was weak enough for an easterly to south-easterly land breeze to overcome the Shamal in the early hours of the morning.

5.6.3 NWP MODEL DATA

Although the Shamal brings cooler air from the north and, apart from low level moisture that evaporates into the air during its passage over the Gulf, it remains dry continental air. The NWP model prognostic time cross sections at Abu Dhabi on the 28th and the 29th correctly reflect the dry conditions that prevailed prior to the Shamal, as well as the increase and persistence in surface moisture after its onset on the 29th (figure 5.22). Comparison of these time cross-sections with those in the previous winter study (figures 5.2a and 5.2b) clearly show the different conditions, while, about 150 kilometres inland. At Al Ain, the air is even drier than at the coast (figure 5.23).

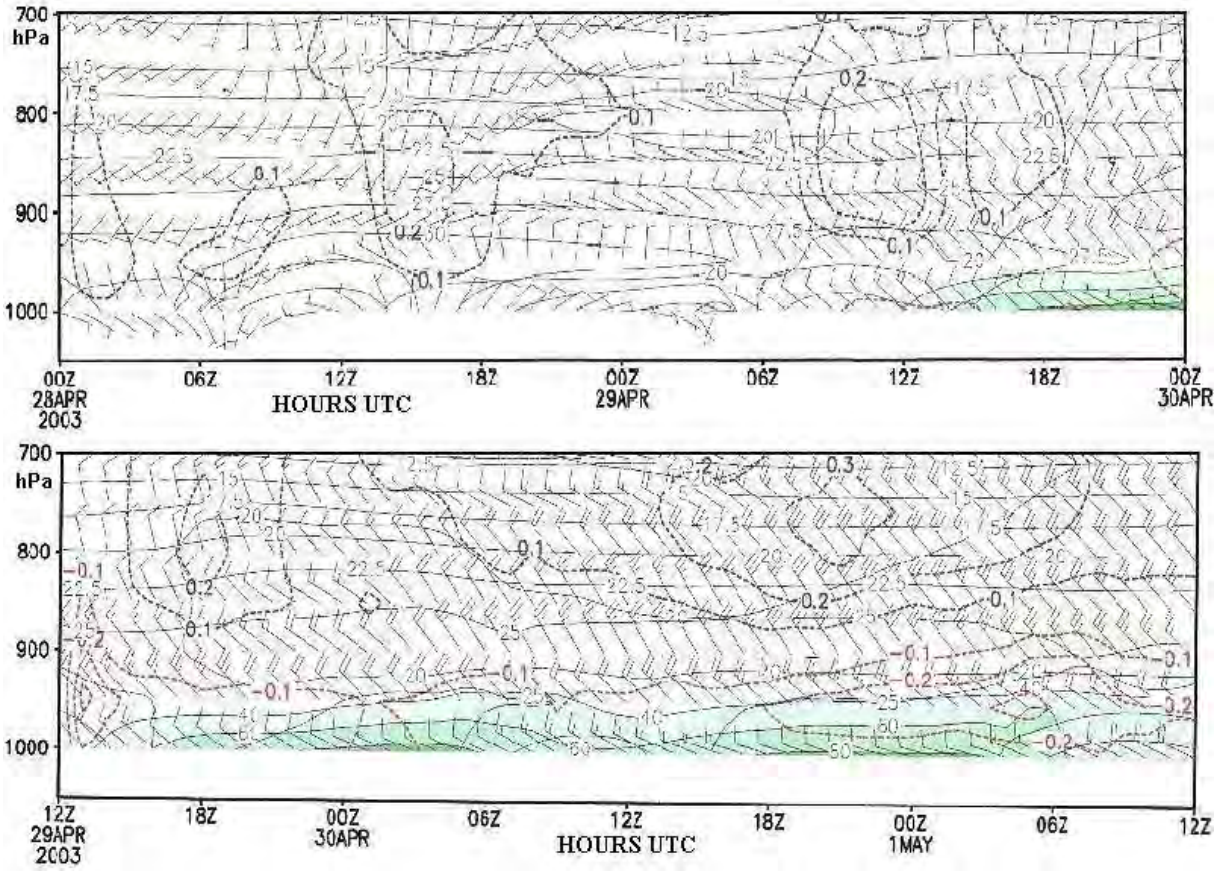

Figure 5.22. Time cross-sections of wind, dew point and vertical motion at ADIA from 2003-05-28 to 2003-05-01 extracted from Eta model runs. Notice the persistence and depth of the Shamal from the 29th, and dryness.

5.6.4 SURFACE OBSERVATIONS

As in winter months, the Shamal brings cooler and moister air from the Gulf Sea. However, due to the very high temperatures, there is not usually much relief from the heat and the increased surface moisture simply helps to make the weather even more humid and unbearable.

On the 28th, when the dry (pre-Shamal) southerly flow was dying, air temperatures reached into the low forties, while dew point temperatures were below 14°C and off the bottom of the chart (figure 5.24). Even though they increased during the afternoon sea breeze they still were not high enough to appear on the chart except at 1700 UTC at 16˚C.

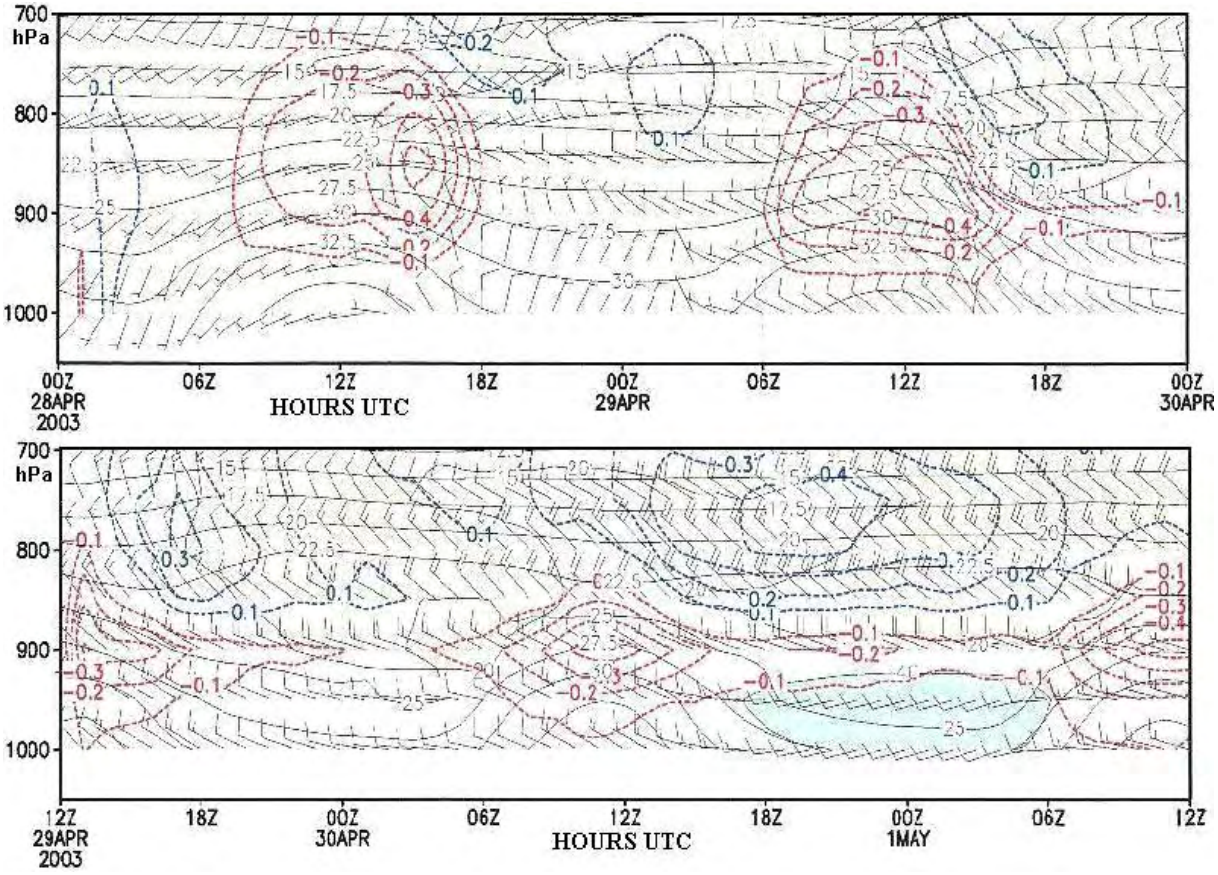

Figure 5.23. As figure 5.22, but at Al Ain for 2003-05-28 to 2003-05-01. Notice the even drier air at Al Ain than at ADIA.

The effect of the Shamal can be seen the following day (the 29th) when there was an immediate jump in the dew point temperature to about 20˚C, about 11°C lower day temperatures and hazy conditions that reduced the visibility to 8000 metres (figure 5.25). The temperature and dew point traces on the 30th and the 1st (figures 5.26 and 5.27) are almost carbon copies of each other. The difference being the wind which was strong enough on the 1st May to raise dust and reduce the visibility to 7000 metres even though the airport is only about 15 kilometres inland (figure 5.27).

Note the total absence of low level cloud that was so evident in the winter study, due to the hotter and drier continental air (Rao, et al 2003).

5.6.5 ATMOSPHERIC SOUNDINGS

Unfortunately, only the soundings at 0000 UTC on the 29th and the 30th at ADIA are available during this summer Shamal event (figure 5.28). Both soundings, the one immediately prior to the Shamal reaching the airport and the one during the Shamal, typify the summer atmospheric profile in that the air is very dry, apart from a shallow surface layer of moist air brought from the Gulf by the Shamal. A comparison of these soundings with those in the previous winter event (figures 5.18 and 5.19) clearly show the difference in moisture above the boundary layer.

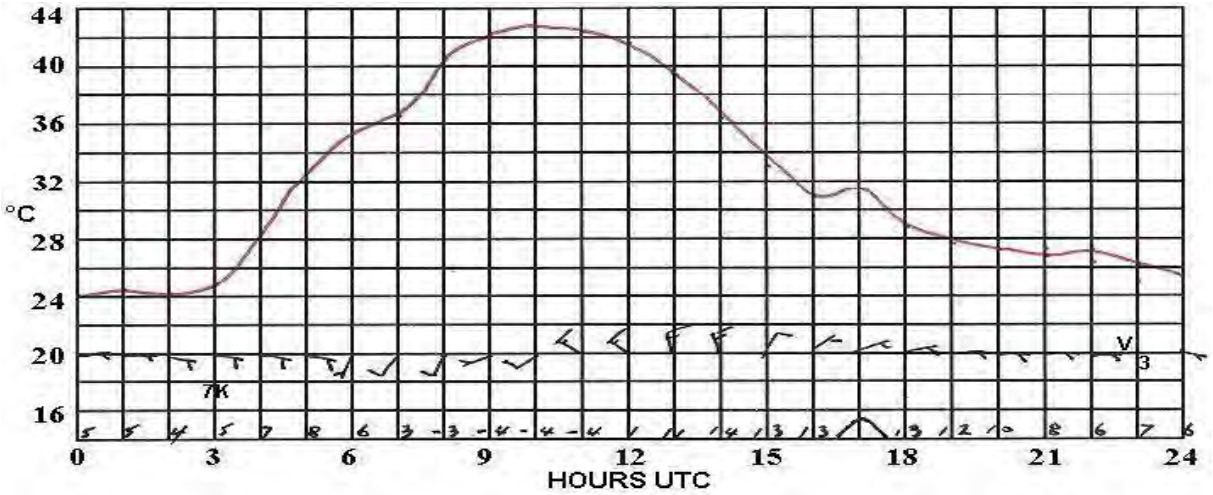

Figure 5.24. Surface observations on 2003-04-28. Air temperature (°C), red line; dew point temperature (°C) written at the bottom of the chart. Wind feathers in tens of knots.

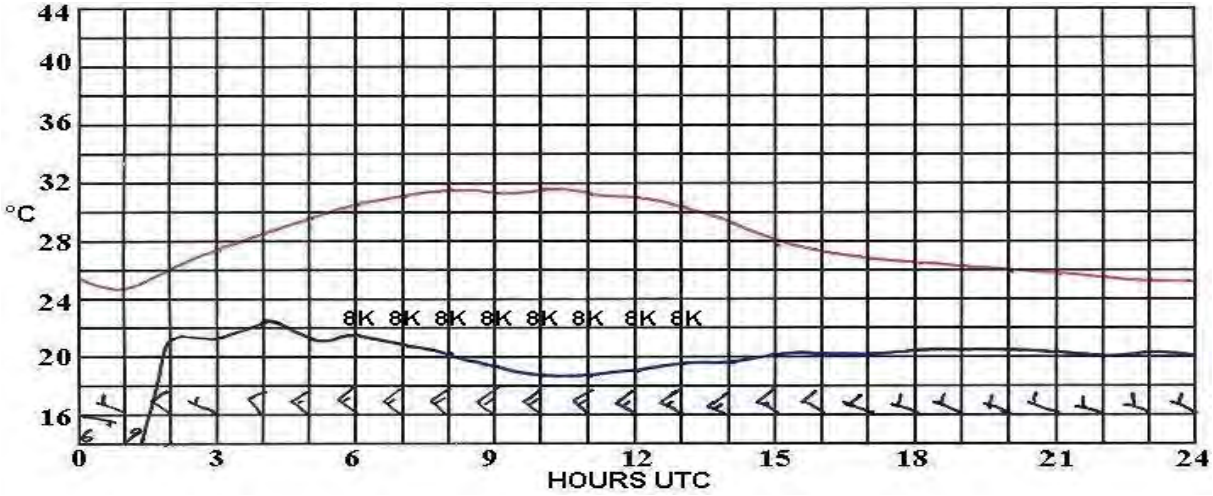

Figure 5.25. As figure 5.24, but for 2003-04-29. Dew point temperature (°C), blue line and visibility in kilometres.

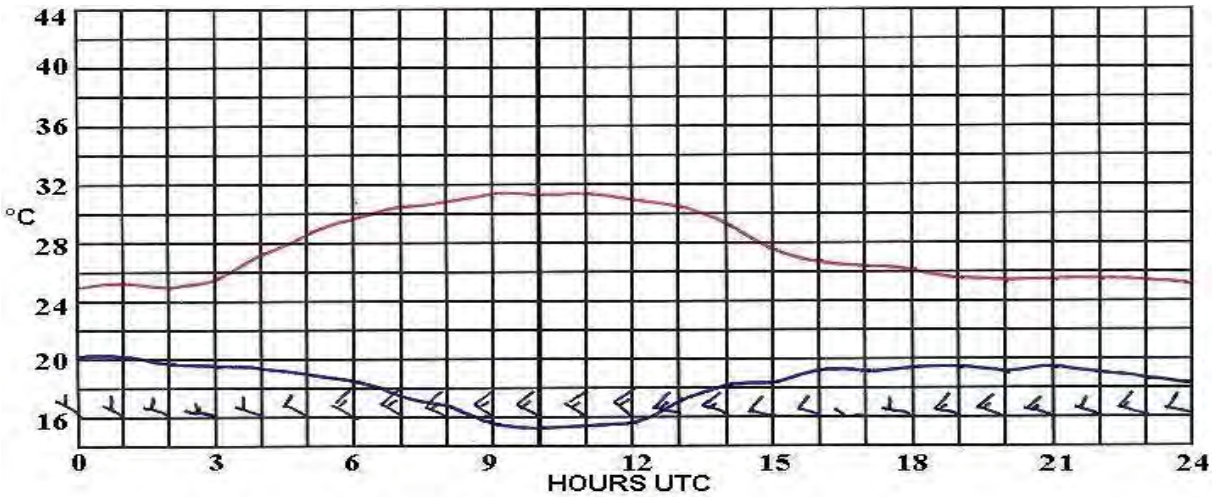

Figure 5.26. As figures 5.24 and 5.25, but for 2003-04-30.

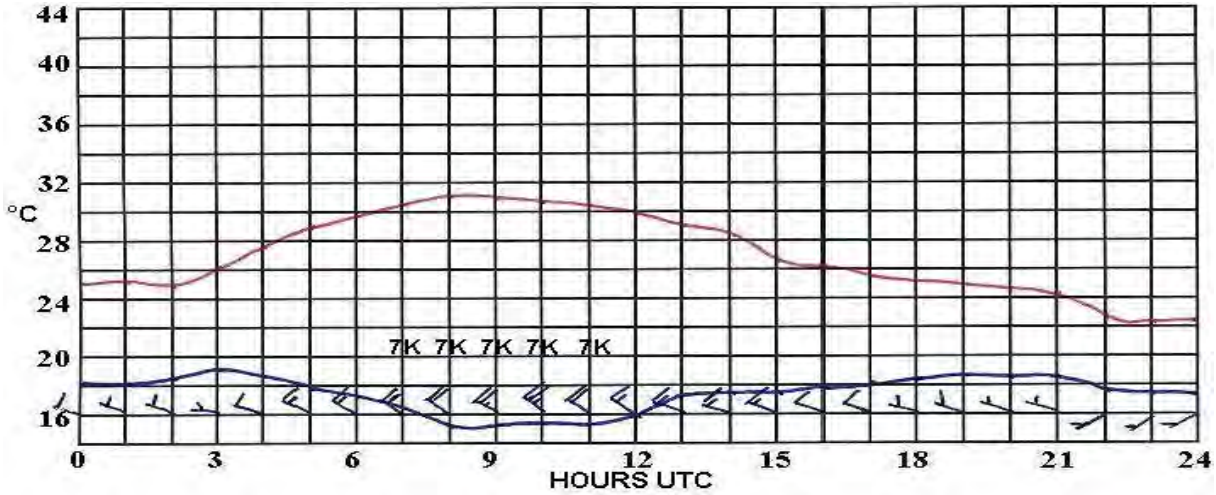

Figure 5.27. As figures 5.24 and 5.25, but for 2003-05-01.

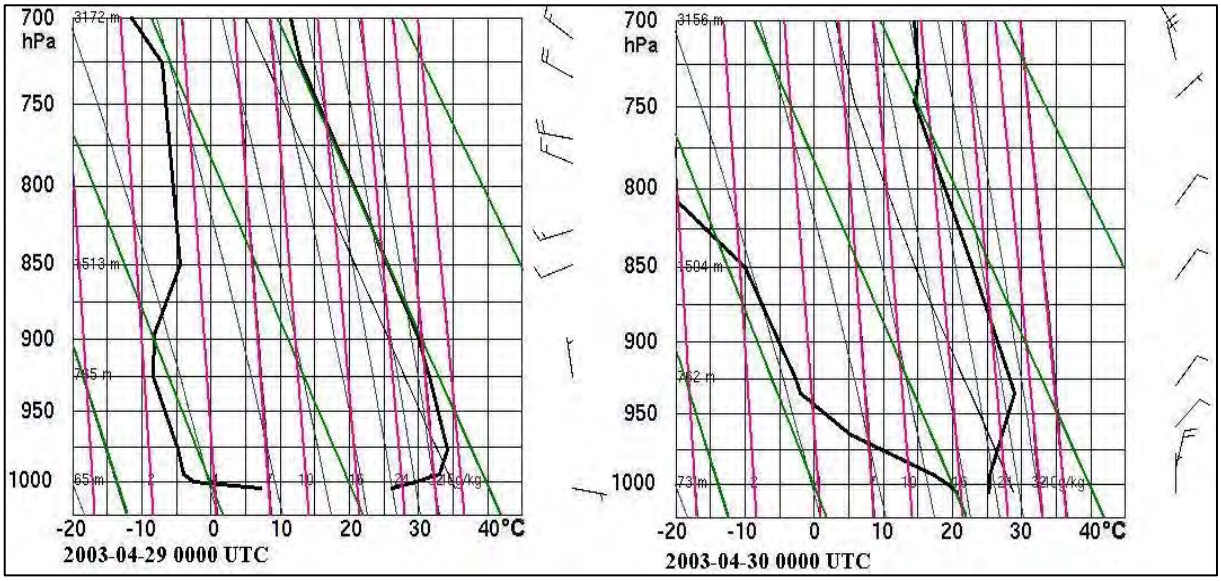

Figure 5.28. As figure 5.18, but for 2003-04-29 and 2003-04-30 (courtesy of the University of Wyoming).

5.7 DISCUSSION

An interesting aspect of the April/May 2003 event was that on the 3rd and 4th May the visibility deteriorated after the wind had abated, but while it was still from the north. The reason for this is that dust, which had been lifted by the northerly wind over Iran, was carried southward to the UAE. Visibility at the oilrigs over the south-western part of the Gulf deteriorated to 6000 to 7000 metres on the 2nd and by the 3rd it was down to 3000 metres at the oilrigs in the east and down to 2000 metres over the land. The following day the visibility was just as bad to start with, but it gradually improved during the day. The deterioration was worst over the eastern part of the UAE where the Gulf narrows to the Strait of Hormuz. In the west, the longer traverse across the sea meant less sand arrived over the western UAE and the visibility did not deteriorate to less than 6000 to 8000 metres.

Another peculiarity of the Shamal (and the sea breeze) is that the wind often blows stronger about 150 kilometres inland at Al Ain in the afternoon than at Abu Dhabi. The wind might blow north-westerly at 15 knots at ADIA, but at Al Ain it can reach and, at times, exceed 20 knots with wind gusts in excess of 30 knots between 0900 and 1300 UTC. Under these conditions sand is whipped up and the visibility can be reduced to 2000 to 3000 metres. Two possible reasons for this phenomenon are proposed. Firstly, the land surface at Al Ain is hotter than at the coast resulting in a near surface super adiabatic temperature lapse rate which in turn promotes convection (producing thermals) that initiates the sea breeze (Hsu 1988 and Riehl 1954) which in turn enhances the Shamal. Secondly solar radiation heating of the Hajar mountain western slope promotes an upslope anabatic wind (Riehl 1954) that will also contribute to the Shamal wind.

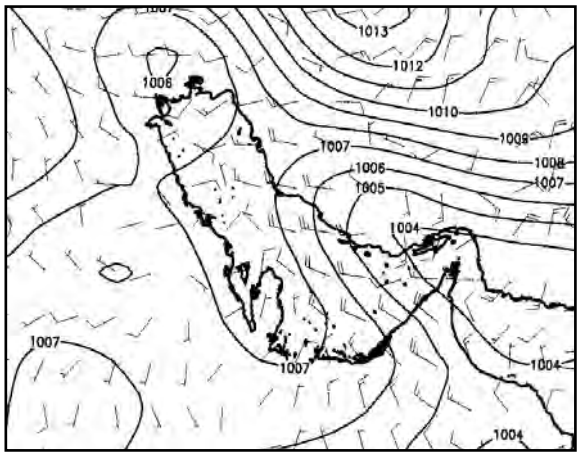

Figure 5.29. As figure 5.20, but for 2003-05-05 1200 UTC.

An example of this occurred during a Shamal on the 5th of May 2003 when a surface ridge the anticyclone over Qatar produced a 4 hPa pressure gradient across the Emirates (figure 5.29).

During intense daytime heating the unstable condition near the surface causes turbulent eddies that transport momentum to the surface. Air below the inversion becomes thoroughly mixed and the surface wind, enhanced by downward flux of momentum and limited only by friction, nears the free air wind speed about 1 km above the ground (Membery 1983). Consequently, the Shamal intensified during the day from about 5 knots before sunrise to an average of 15 knots from the north-north-west and reached 18 knots at its peak at ADIA during the afternoon from 1000 to 1200 UTC. However, at Al Ain, from shortly before 1000 UTC until 1400 UTC, the wind came from the north-west at 15 to 20 knots with wind gusts of up to 35 knots. The visibility was reduced to 4000 metres in blowing sand.

In table 5.2 it can be seen that the wind in the free air at ADIA was 25 to 30 knots at 1000 feet at 0000 UTC and 1200 UTC, respectively. This increase in the wind with altitude to a maximum low level jet at about 300 m, before tapering off up to 900 m, closely resembles the wind profile presented by Membery (1983) in a study of Shamal events at Bahrain during June and July in 1980 (figure 5.30).

Table 5.2. Low level winds at ADIA 5th May 2003.

metres	**0000 UTC**	**1200 UTC**
MSL	**° True/knots**	**°True/knots**
150	290°17	340°21
300	315°25	330°30
600	310°27	315°28
900	305°23	305°24

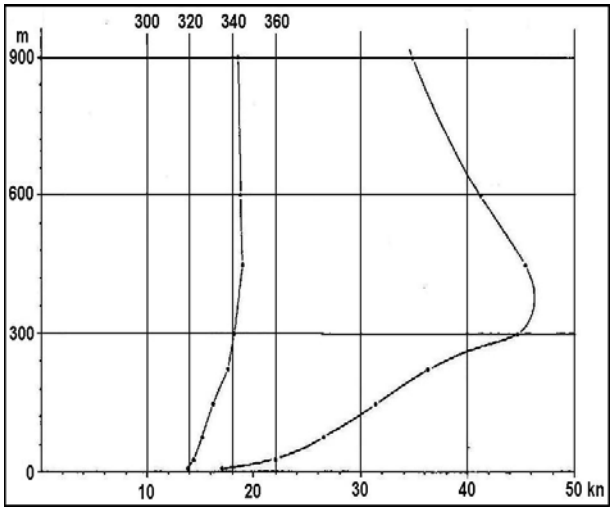

Figure 5.30. Boundary layer wind profile at Bahrain, June and July 1980 (Membery 1983).

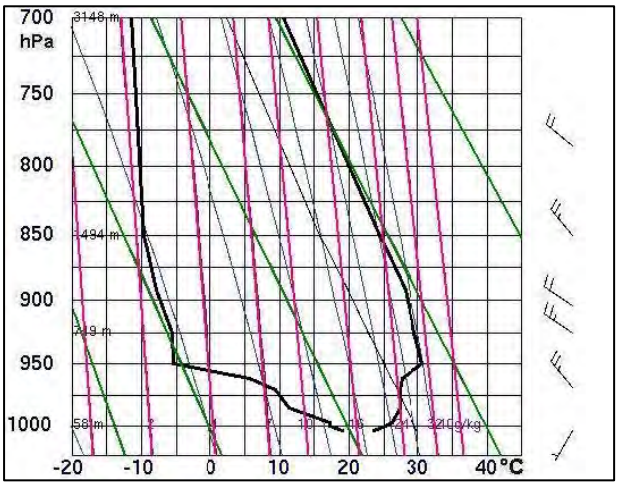

Figure 5.31. As figure 5.18, but for 2003-05-05 0000 (courtesy of Wyoming).

Unfortunately no 2003-05-05 1200 UTC atmospheric temperature sounding is available inland at Al Ain, but the atmospheric sounding at ADIA at 0000 UTC shows that the air was stable with a marked surface temperature inversion (figure 5.31), but with sufficient daytime heating the environmental lapse rate would be equal to, or exceed, the dry adiabatic and convection would promoted. The maximum temperature at ADIA during the afternoon was 36°C and at Al Ain 38°C. These temperatures are high enough for dry convection up to about 950 hPa (±460 metres MSL) at ADIA (and probably higher) and about 900 hPa (±900 metres MSL) at Al Ain. 900 metres being adequate depth of convection required to encourage sea breeze development (UKMO 1997).

The result was that, apart from the wind being retarded to some extent by surface friction over the land (Riehl 1954), it became stronger during the day approaching the free air speed at 300 metres at the top of the turbulent layer. The convection enhanced sea breeze plus the anabatic upslope wind against the Hajar Mountains contributed to make the wind stronger and gustier at Al Ain. This turbulent wind lifted sand from the desert floor and caused the poor visibility.

As ADIA is not more than about 15 kilometres from the coast, the onshore wind travelled a short distance over the desert sand before reaching the airport. The wind did not have enough time to lift the dust off the desert floor before reaching ADIA. For this reason the visibility remained better than at Al Ain. However, if the wind is strong enough, usually about 20 knots, or more, the visibility becomes drastically reduced at ADIA, irrespective of the stability of the atmosphere (see table 6.6 in chapter 6 on dust storms,).

In the NWP data section 5.5.2 in the winter case study, reference was made about fog not forming along the coast under Shamal conditions, but that this is not always valid inland. On the 24th December 2003 Shamal conditions developed during the afternoon and intensified the following day (figure 5.32). As usual the model indicated high surface moisture (95% relative humidity, or greater) along the coast at 0300 UTC (0700 local time) on the 25th, as well as inland, particularly toward the Liwa Oasis region and Empty Quarter (figure 5.33). Also as usual, fog did not form along the coast, but it did occur inland at Al Ain and Radoum (which is part of the Liwa Oasis).

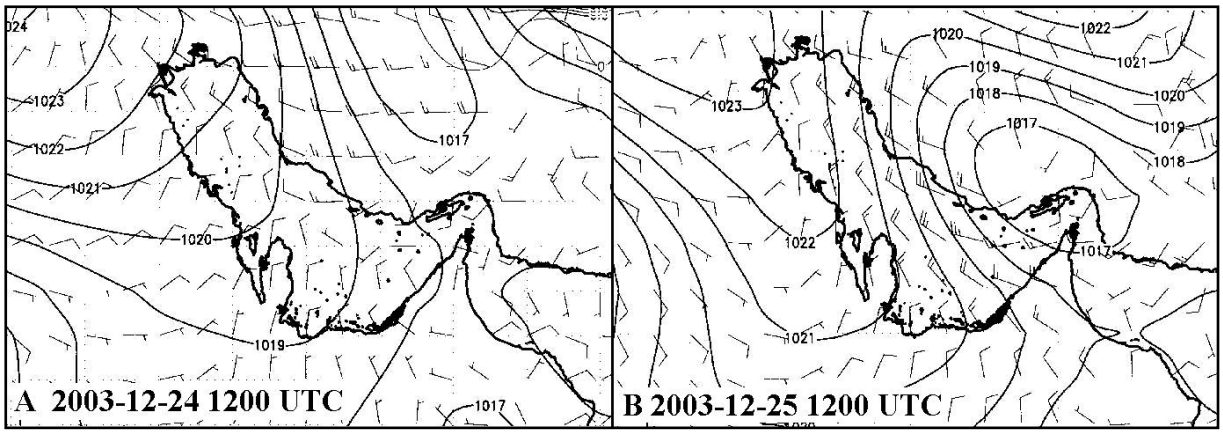

Figure 5.32. 1200 UTC Eta GFS surface pressure (hPa) and wind (knots) fields on the 24th and 25th December 2003.

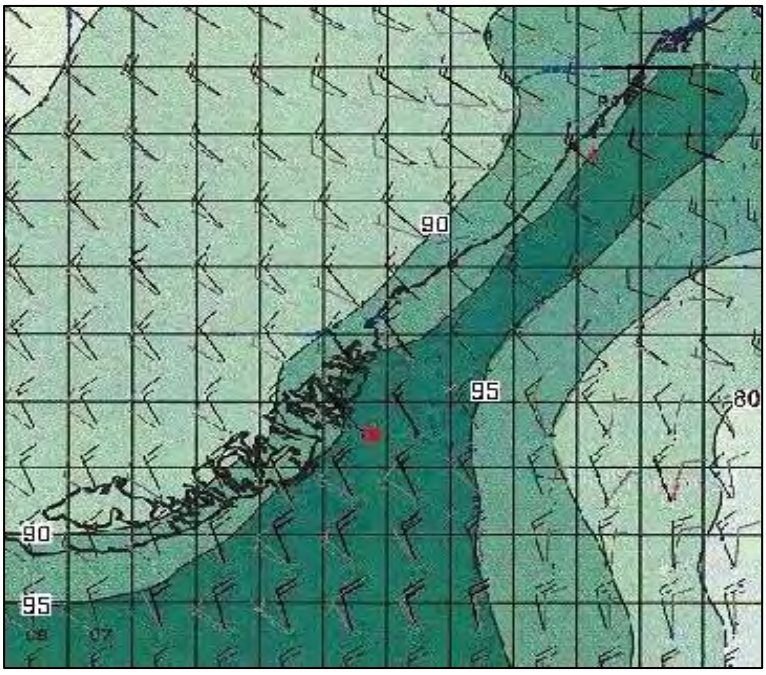

Figure 5.33. Eta model prognoses of surface relative humidity and wind (knots) at 10 metres (black) and 950 hPa (grey) with downward vertical motion (blue lines) for 2003-12-25 0300 UTC.

The fog began to form at Al Ain in a light north-westerly wind between 1930 UTC and 2000 UTC (2330 to 2400 UAE local time). The visibility remained below 1000 metres until 0200 UTC (06:00 local time) and being down to 100 metres for about 2 hours. Observations at Radoum are not received during the night, the first observation being the one at 0300 UTC when fog was reported with a light north-westerly wind and 800 metres visibility.

As a matter of interest, during his first crossing of the Empty Quarter, Thesiger (1994), in the Liwa area at Bir Balagh, noted that the camp was enveloped in thick mist in the morning (±15th 16th December 1946) and that "the cloak which had covered my sleeping-bag was drenched. Each night for the past week we had had this soaking dew, the result of the northerly winds which carried the moisture inland from the Persian Gulf."

5.8 SUMMARY

The Shamal at ADIA is markedly more prevalent during the spring and summer months especially from May to July. Diurnally it blows the strongest during the afternoon and evening from 1300 to 1900 local time (0900 to 1500 UTC) and is at its lightest overnight.

Markedly lower temperatures are experienced after the Shamal begins, although in summer it brings little in the way of relief from the very hot and humid weather. Apart from shallow

surface moisture the air aloft remains very dry in summer. This is in contrast to the winter months when the air is moister, a contrast that is clearly anticipated by the NWP models.

The Shamal is most likely when a surface anticyclone approaches from the west and/or deepening of the surface low over Iran. The NWP models give ample warning of the beginning and duration of the Shamal events with a good indication of the pressure gradients and wind velocities to be expected across the Gulf.

Typically a $\geq$ 5 hPa pressure gradient across the UAE produces wind speeds >20 knots and a wind of 20 to 25 knots over the sea quickly decreases to about 10 to 15 knots when it crosses the coast. A pressure gradient of this strength is strong enough to maintain a north-westerly to west-north-westerly wind during the night. Although, more often than not the wind tends to back to south-westerly and become lighter, due to the influence of the overnight land breeze effect. When this happens, a low level jet of stronger winds up to 30 knots to 40 knots at about 300 metres (1000 feet) MSL can develop with attendant wind shear. The NWP model is not inclined to identify the backing of the wind and usually incorrectly maintains a north-westerly wind throughout the night.

The wind can be stronger and gustier inland at Al Ain in the afternoon than at ADIA. It is suggested that this is due to the hotter conditions inland with increased instability producing stronger thermals and a stronger sea breeze as well as an anabatic effect associated with the Hajar Mountains to the east of Al Ain. Both help to overcome the retarding friction effect of the land as the air moves inland from the sea and produce a strong and gusty wind that lifts sand and reduces the visibility.

Under strong Shamal conditions the wind can carry dust from further afield, such as from Iran, resulting in poor visibility over the Gulf and the UAE. During the summer event discussed in this chapter the visibility was worst over the eastern Gulf Sea and the eastern part of the UAE where there was a shorter sea traverse and less time for the sand to fall out of the atmosphere before reaching the islands and oilrigs offshore and the UAE coast. This resulted in the visibility decreasing to 2000 to 3000 metres in the east as opposed to 6000 to 7000 metres in the west. Dust carried by the Shamal is also discussed in the chapter on dust and sand storms.

Strong winds and very rough seas hamper helicopter operations to the oil rigs. The wind is strongest with the biggest waves over the western part of the Gulf where there is a longer fetch and no protection from the land to the north in Iran. Wind waves quickly build up to 2 to 3 m with wind speeds of 20 to 25 knots and readily reach 4 m at times such as during the winter Shamal of the 13th to 19th November 2003 when the wind speed was 20 to 30 knots. A lighter wind with a smaller wind waves occur in the lee of the Iranian coast in the eastern Gulf Sea.

Low cloud associated with the Shamal forms as a result of turbulent mixing of the maritime air beneath a temperature inversion that varies from about 900 metres to 1200 metres above the surface. In the winter months it is routine for scattered to broken stratocumulus to occur at ADIA. The percentage likelihood of cloud is over 90% during December and January and decreases to less than 15% in the summer months. This can be attributed to mechanical turbulence being strong enough to raise moisture to the lifted condensation level in the cooler winter conditions, but during the much hotter summer months, in spite of the more humid surface conditions, drier air entrainment above prevents condensation from taking place.

Although there is an accumulation of surface moisture inland from the coast, marked turbulent mixing near the surface prevents fog from occurring at Abu Dhabi during Shamal conditions. There is less certainty whether this is also valid further inland when the Shamal drops sufficiently overnight, as there is sufficient reason to believe that further inland toward the Liwa Oasis and the Empty Quarter fog occurs more often than is reported.

5.9 FORECAST CHECKLIST

The Eta NWP model post processing products give ample evidence to identify Shamal winds. Of particular use to identify Shamal conditions are the Eta model surface wind and pressure patterns and pressure gradient and the GRADS surface time cross sections at ADIA and Al Ain.

Important considerations when forecasting a Shamal are:

- Wind speed ≥ 17 knots.
- ≥ 5 hPa pressure gradient across the UAE.
- A surface low, or trough, passing to the east.
- A surface anticyclone approaching from the west and/or deepening of the surface low over Iran.
- Friction effect. 20 - 25 knots over the sea decelerates to 10 - 15 knots when it crosses the coast
- The Eta model does not always identify backing of the wind to south-westerly overnight.
- Wind shear. A 30 – 40 knot low level jet ± 300 metres (1000 feet) MSL can develop during the night.
- Poor visibility. A strong Shamal can carry dust from far away in Saudi Arabia and Iran. See the chapter on dust storms.

CHAPTER 6

DUST STORMS AND DUST

6.1 INTRODUCTION

Estimates have been made that, worldwide, annually up to about two billion metric tons of dust are carried up into the atmosphere, mainly by dust storms. One dust storm can lift and deposit more than 200 metric tons of dust (Griffin et al 2002). The Arabian Peninsula has been listed as one of five major dust producing regions (Idso 1976), while Goudie (1983) added that dust storms are frequent in the area.

Apart from being a hazard and nuisance to the general public, dust storms and sand storms and their attendant poor visibility and gusty winds are a danger to aircraft landing and taking off. This can lead to diverted flights, delayed departures and attendant airport operational problems. Other effects include the scouring of aircraft surfaces and damage to engines as well as hampering ground operations.

A dust storm, or sand storm, is a collection of particles of dust, or sand, vigorously lifted to a great height by a strong and turbulent wind and the visibility is reduced to below 1000 metres (UKMO 1991). The visibility is most likely to be at its worst during daylight hours when the wind is at its strongest (UKMO 1994).

Criteria for defining a dust storm, or sand storm, in the region vary. At ADIA the definition is that the 10-metre wind must be in excess of 17 knots and the surface horizontal visibility below 1000 metres. Safar (1985) uses the same stipulations, but adds that when the visibility falls below 200 metres, the storm is classified as severe.

6.2 SCOPE OF THE STUDY

To the author's knowledge no research results as to when dust events and dust storms occur at ADIA have been published. This chapter examines the weather conditions when dust storms occurred at ADIA from 1994 to 2003 by means of a brief statistical analysis as well as case studies and a methodology for forecasting these events is proposed. In addition, all dust events observed at ADIA when the visibility was reduced to 5000 metres, or less, were included in the statistics.

6.3 METHOD

Dust storm events are researched using surface weather observations at ADIA, as well as 1200 UTC and 0000 UTC atmospheric soundings at ADIA and Eta GFS NWP model data.

6.4 DYNAMICS

Although weather observers may make little distinction whether the cause of the poor visibility is dust or sand, there is a significant difference. The diameter of grains of desert sand usually varies from 0.15 mm to 0.3 mm with the lower limit being 0.08 mm. A diameter below 0.08 mm is defined as dust. Dust is more likely to be found in and around inhabited areas where human and vehicular activity tends to break and crush sandy soil to produce finer sand or dust (UKMO 1994).

The conditions that allow dust to be raised in suspension in the atmosphere for prolonged periods are dry soil, strong winds and a deep and well-mixed boundary layer with a nearly dry adiabatic lapse rate (Jauregui 1989, Safar 1985 and Blair 1957). Over the UAE the extremely dry soil conditions, especially during summer, merely require strong turbulent wind to raise dust and sand.

Wind turbulence, forced by the terrain, is normally too weak to raise grains of sand more than about a metre above the ground until the 10-metre wind speed reaches 20 knots. Sand lifted by the wind is then carried across the surface, but tends to fall back to the ground where they bounce back into the air and in the process disturb other grains of sand on the ground, a process known as saltation. The sand quickly settles to the ground when the wind drops and the visibility immediately improves. Dust, on the other hand, can be easily raised to great heights and, long after the surface wind has dropped, be held in suspension in the atmosphere for hours and even days before settling. Dust grains begin to be lifted when the 10-metre wind speed reaches 15 knots. Larger particles, in falling back to the ground, also disturb smaller particles, which are lifted higher into the air by turbulence and remain in suspension longer (UKMO 1994).

Two atmospheric mechanisms that provide a wind strong enough to lift dust and sand are the outflow from thunderstorms downdrafts and the synoptic situation when there is a strong pressure gradient between an anticyclone and a cyclone (Wheaton and Chakravarti 1990, WMO 1983). Below a thunderstorm dust is raised by the ascent of air in convective thermal currents, as well as in the zone of severe turbulence where the strong downdraft induced wind creates the storms gust front. This mesoscale phenomenon is virtually impossible to predict by coarse grid numerical models (Miller et al 2008). In the synoptic scale strong pressure gradient situation, stable thermal stratification at the edge of the anticyclone normally exists. Lifting of the dust is to due turbulence and vertical motion caused by the steep pressure gradient induced wind. Raised dust permeates upwards in small turbulent eddies that move up through one thermal layer of the atmosphere to the next. Dust raised this way is much more extensive than that lifted by thunderstorms and can cover over a million square kilometres (WMO 1983). Dust storms are also known by the Arabic word Haboob (see Appendix A, Glossasry), a name initially used in the Sudan, but its use is now becoming more widespread (Miller et al 2008).

6.5 STATISTICS

Observational records kept at ADIA from 1982 to 2001 show that while haze, due to dust, commercial pollutants, or moisture, is very common and occurs on average on 242 days per year, dust storms are far less frequent, the average being 3 per year with the maximum being 8 in 2003. By way of comparison, inland at Al Ain and using data from 1994 to 2001, haze

occurs on an average of 304 days per year while dust storms average 4 days per year with a maximum of 7 in 1994. A total of 173 events (141 dust and 32 dust storms) were identified during the period from 1994 to 2003 (table 6.1).

Table 6.1. Events when dust haze, or dust storms were observed at ADIA and the visibility was ≤ 5000 metres from 1994 to 2003.

YEAR	DUST EVENTS	DUST STORMS	TOTAL
1994	10	5	15
1995	16	2	18
1996	13	1	14
1997	10	2	12
1998	12	2	14
1999	18	7	25
2000	15	3	18
2001	10	0	10
2002	17	2	19
2003	20	8	28
TOTAL	141	32	173

These events were divided into 3 groups according to when the wind direction was from the south-east (SE) to west-south-westerly (WSW), or from the west (W) to north-north-west (NNW), or northerly (N) to east-south-east (ESE) (table 6.2). The logic behind these divisions being that wind from the SE to WSW blows from the desert areas to the south-east to south-west. It also blows when a low pressure cell, or trough approaches from the west. Wind from the W to WNW has a track mainly down the longer length of the Arabian Gulf during post trough, or low pressure situations and high pressure building to the west. While that from the N to E either comes from the mainland of Iran to the north and NE, or had to come across the Gulf of Oman Sea and over the peninsula to the east. N-ESE events were difficult to categorise. These winds are most likely when low pressure/trough systems and the building anticyclone are more to the north-east, or east of the UAE. There were borderline instances that were difficult to categorise, such as when the wind blew from a northerly direction and it was possible that the wind was a north-westerly Shamal that with time veered to the north. The Shamal is defined in chapter 5.1.

The visibility was most often reduced at ADIA when the wind was from the south-east to west-south-west. This wind, referred to as a Kaus wind by the U.A.E. Ministry of communications **(**1996), has a long track off the desert. The visibility is less often reduced when the wind arrives from across the length of Gulf Sea to the north-west, or the Gulf of Oman. to the east. This is also the case at the much narrower sea in the vicinity of the Strait of Hormuz to the north-east (table 6.2), whence the cold and dry Nashi wind comes (section 6.6.3). It is interesting to compare the events when the visibility was less than 5000 metres listed in table 6.2 with the number of dust event observations when the visibility limit is raised to less than 8000 metres, as depicted in figures 6.3 to 6.5. The total 95 SE-WSW events in figure 6.2 constitute 45% of the total 211 observations. Similarly 42 W-WNW events out of 103 observations represent 41% and 36 out of 57 N-ESE events equals 63%. These statistics indicate that dust events from the N-ESE are far more frequent than previously thought. The simple fact is that, in this desert region, if the wind blows strong enough across the land dust haze and dust storms must be expected.

There is a close association between dust in suspension and vertical instability (Chepil and Woodruff 1957). It is therefore not surprising to note that there were many instances when a dust storm was associated with the presence of a thunderstorm Cumulonimbus (CB), or Cumulus Congestus (CU), with a high base (±5000 feet). Consequently, the wind direction and high speed was often of a short duration as was the poor visibility. Of the 32 dust storms, convective cloud was present on 15 occasions, most often during N-ESE winds (table 6.3).

Table 6.2. Direction frequency of dust events and sand storms during the period 1994 to 2003 when visibility was reduced to below 5000 m.

DIRECTION	DUST EVENTS	DUST STORMS	TOTAL
SE-WSW	83	12	95
W-NNW	33	9	42
N-ESE	25	11	36
TOTAL	141	32	173

Table 6.3. Direction frequency of dust storms associated with convective cloud during the period 1994 to 2003 when visibility was reduced to below 1000 m.

	SE-WSW	W-NW	N-ESE
Dust storm with CB	2	2	6
Dust storm with CU	1	3	1

The average duration (to the nearest 5 minutes) of visibility at, or below, 1000 metres at ADIA in a dust storm was found to be 1 hour and 15 minutes with the maximum time being 4 hours 30 minutes. The average time when the visibility is at, or below, 3000 metres is 3 hours 45 minutes with the longest time being 15 hours. Taking all 173 dust events into consideration the average time when the visibility was at, or below, 5000 metres is 3 hours 30 minutes and the most 21 hours. On average thunderstorm gusts reduce the visibility to dust storm levels for 37 minutes with the longest time being nearly 60 minutes. These poor visibility periods due to dust during thunderstorms could be longer, because observations when rain was present with dust during a thunderstorm were excluded and it is impossible to determine form the data which of the two was the prime cause of the poor visibility.

Dust reduction of the visibility to below 5000 m, with SE to WSW winds, was most frequent during the morning and most of the afternoon, as depicted by figure 6.1 and where it should be remembered that UAE local time is 4 hours ahead of UTC. This coincides with the regular morning land breeze that would reinforce any southerly flow due to the synoptic pressure pattern, such as when low pressure systems are present to the west. Conversely, dust reduced visibility associated with a W-NW flow, was most likely during the mid and later afternoon when a north-westerly Shamal would be strengthened by the sea breeze. An explanation for the peak of N-ESE events in the late afternoon and early evening is that at this time the sea breeze begins to veer towards the east. More likely, this increased frequency is due to increased wind speed caused by deepening of the diurnal heat low over the Empty Quarter to the south-west (Rao et al 2003).

There is a marked frequency peak in dust reduced visibility by midday and a decrease soon after sunset (figure 6.1). Night cooling of the ground and the air immediately above it by radiation, results in increased stability that suppresses the vertical movement of wind eddies, uncouples the surface wind from the stronger wind aloft, and allows surface friction to further

reduce the near surface wind speed. Dust is therefore given time to settle. During the day increased heating and thermally induced turbulent eddies reduces stability and increases mixing with the air aloft, which increases the wind speed and lifts dust (Kessler 1985).

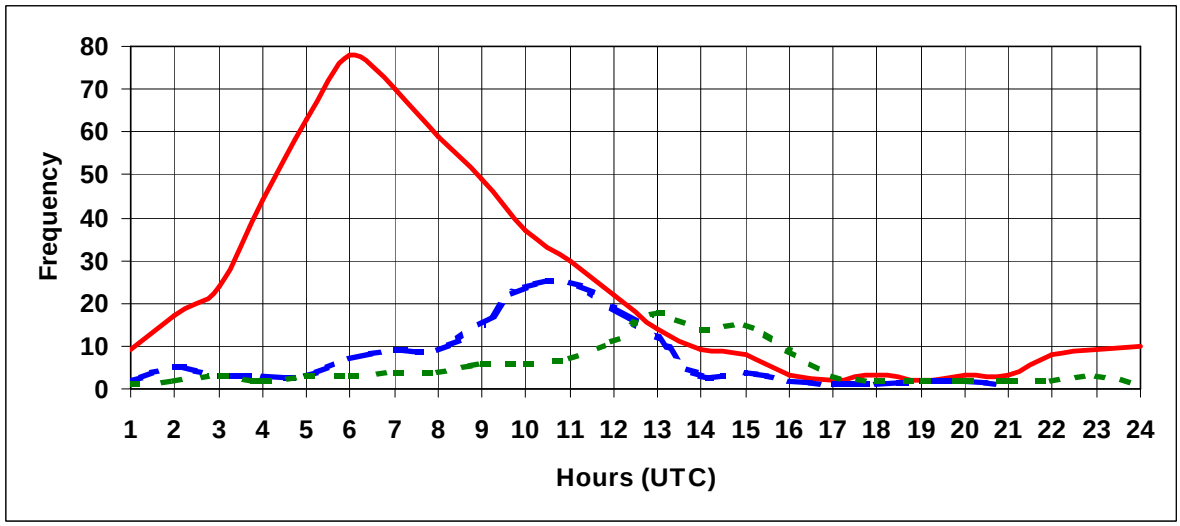

Figure 6.1. Diurnal frequency of dust events (visibility ≤ 5000 metres) from 1994 to 2003, inclusive. SE-WSW wind events – solid red line, W-NNW – blue long dashed line, N-ESE – green short dashed line. Local time is UTC plus 4 hours. Annually the sunrise varies from ±0530 in summer to 0700 in winter (0130 to 0300 UTC) and sunset from 1900 in summer to 1730 in winter (1500 to 1330 UTC).

Correlation between wind speed and visibility was difficult to establish as the scatter graph depicting the relationship for the 32 dust storms events shows (figure 6.2). This is attributed to the visibility remaining poor due to dust remaining in suspension in the atmosphere after the wind has dropped, as well as poor visibility in low sun conditions, particularly at sunrise. Another contributing factor is dust brought aloft from afar by a synoptic system. Such as the trough that caused by a persistent 5-day Shamal from the 16th to 20th May 2003 (section 6.6.2), which carried dust from eastern Saudi Arabia, across the Gulf Sea to Abu Dhabi and reduced the visibility to 3000 metres. Nevertheless, the Pearson product-moment coefficient of correlation (Harper 1977) yields a negative correlation of 0.64.

Viewing figure 6.2 it is clear that the greatest concentration of points lie in an area where the wind speed exceeds 15 knots and the visibility is less than 3000 metres. Below 15 knots most of the pixels are in an area where the visibility is greater than 4000 metres. Although a considerable number are present in an area where the visibility is greater than 4000 metres and the wind is between 15 to 20 knots. Bear in mind that wind direction, such as a shorter track off the sea, has not been taken into consideration. However, there are some loose deductions that can be made;-

i Above 15 knots the visibility can be below 8000 metres and is often less than 5000 metres.
ii Above 20 knots the visibility will be less than 5000 metres and is often less than 2000 metres, but most likely below 1000 metres.
iii Above 25 knots the visibility will be less than 2000 metres and is more likely below 1000 metres.
iv Above 30 knots the visibility will be less than 1000 metres.

Scatter graphs were compiled of dust events during 2003 according to the three wind direction groups. Of the 28 identified during the year, 17 were associated with the southerly sector, 8 from the north-west sector and 3 from the north-east sector (figures 6.3, 6.4 and 6.5).

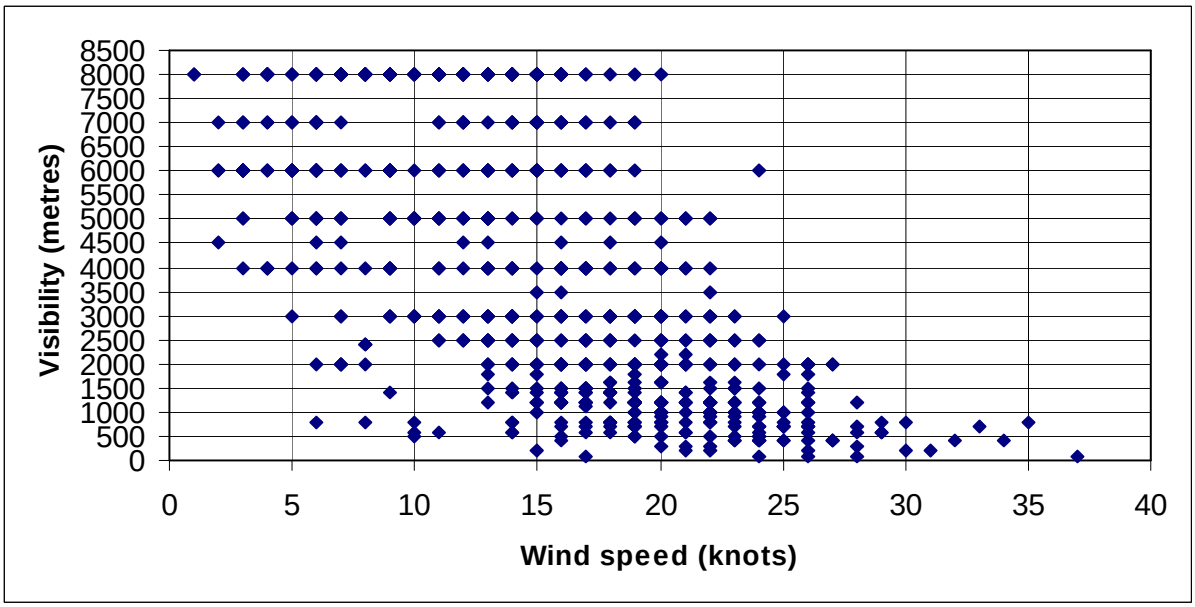

Figure 6.2. Scatter graph of visibility and wind speed recorded (715 observations) during dust storms in ten years from 1994 to 2003 when the visibility was ≤ 8000 metres. Correlation -0.64.

Of the three wind direction groups, the best correlation between the wind and visibility existed when there was a southerly desert wind, the correlation being –0.67 (figure 6.3). For the most part at 5 knots the visibility was never below 6000 metres and at 10 knots the minimum visibility was 3000 metres. A wind speed above 15 knots accounted for most of the observations when the visibility was below 3000 metres. Above 20 knots the visibility was below 1000 metres.

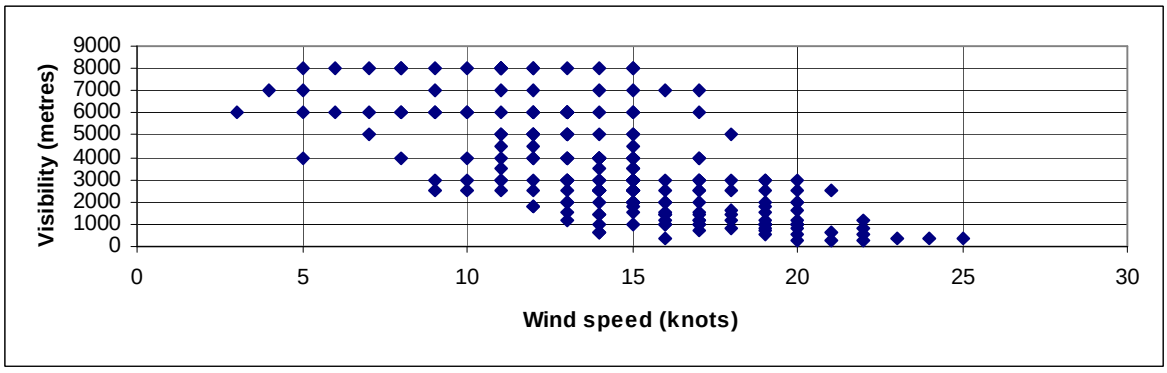

Figure 6.3. Scatter graph of visibility and wind speed recorded (211 observations) during dust events in 2003 when the wind was SE to WSW and the visibility was ≤ 8000 metres. Correlation -0.67.

The correlation between visibility and wind speed for north-westerly winds was poor, namely, -0.4 (figure 6.4). The most probable explanation is that the dust arrived after passing

over a broad expanse of water. The visibility was therefore more dependent on how much dust was still in suspension and not the wind speed.

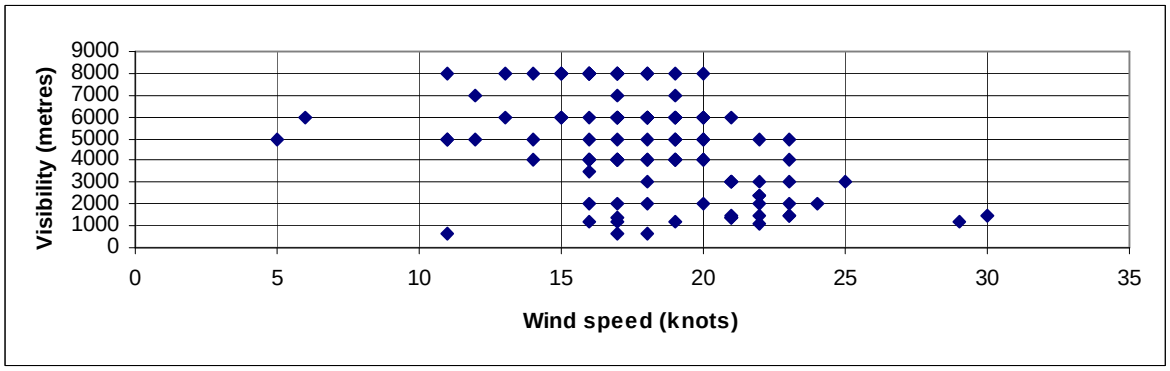

Figure 6.4. Scatter graph of visibility and wind speed recorded (103 observations) during dust events in 2003 when the wind was W to NNW and the visibility was ≤ 8000 metres. Correlation -0.41.

Strictly speaking there were too few events for a reasonable analysis to be made of the north-easterly wind group (figure 6.5). Nevertheless, the scatter graph is interesting. Note, although classified as two calendar day events, two consecutive days were associated with dust that arrived from the north-east after travelling a considerable distance from Iran (13th and 14th December 2003), the so-called Nashi wind. The wind at ADIA was never more than about 13 knots (with one observation of 17 knots). Winds below this speed do not usually cause serious visibility reduction. However, in this instance there were numerous observations when the visibility was below 5000 metres and even less than 1500 metres with the wind below 7 knots. Clearly the dust was not raised locally, but brought from far afield at Iran. This is discussed in section 6.6.3. Another interesting aspect of the graph is that all the winds above 17 knots were observed during brief periods of less than half an hour when there were thunderstorms near to and at the airport. In these instances the dust was clearly locally generated by outflow from the thunderstorms.

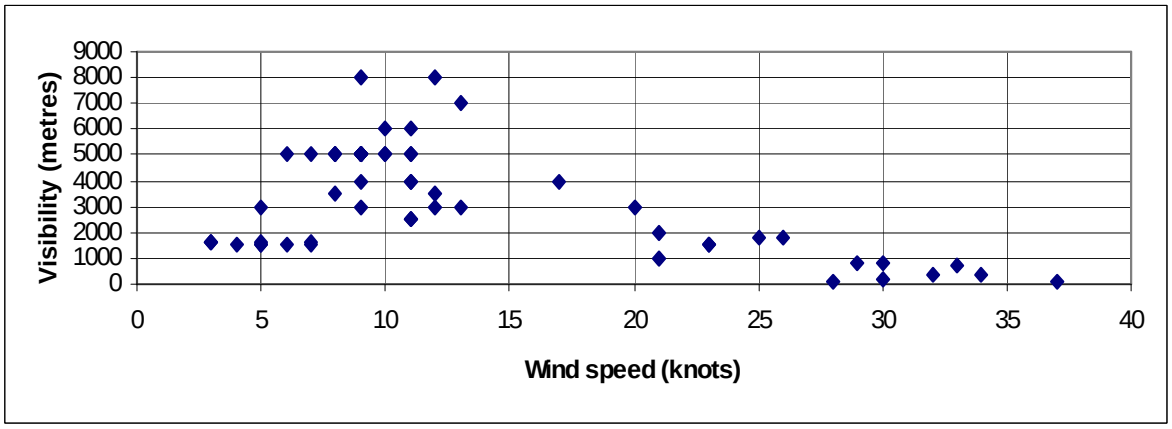

Figure 6.5. Scatter graph of visibility and wind speed recorded (57 observations) during dust events in 2003 when the wind was N to ESE and the visibility was ≤ 8000 metres. Correlation, -0.53.

6.6 STUDY OF DUST STORM EVENTS AT ABU DHABI AIRPORT

Three examples will be presented, one each according to the three wind categories that have been mentioned. An example of a dust storm associated with a thunderstorm will not be discussed, as this will be provided in the section on thunderstorms in chapter 8 and in particular a thunderstorm that occurred on the 18th March 2002.

6.6.1 THE DUST STORM OF THE 12TH AND 13TH MARCH 2003

6.6.1.1 Introduction

A particularly severe dust storm occurred on the 12th and 13th March 2003 when a well developed surface low pressure cell passed close by to the north of the UAE. Apart from the poor visibility experienced, the event was also noteworthy in that the storm lasted for two days. Usually the system moves through fast enough for the storm not to last longer than the daylight hours of one day. More often than not, diurnal land and sea radiation heating differential causes the afternoon sea breeze from the north to overcome the southerly desert wind. It was therefore unusual, during the evening of the first day, to see blurred street and vehicle lights through a haze caused by dust rather than the more usual humidity haze.

Visibility on the 12th at ADIA deteriorated to 1000 metres in a southerly wind that averaged 15 to 20 knots. At Al Ain International Airport the visibility fell to 3500 metres in a gusty wind that reached an average speed of 25 knots.

On the second day at Abu Dhabi the average wind was 20 to 25 knots and the observed visibility intermittently reduced to between 300 and 600 metres for nearly 7 hours during daylight (figure 6.6). At Al Ain the still gusty wind reached 29 knots with the visibility down to 1200 metres.

Figure 6.6. Central Abu Dhabi during the dust storm on the 13th March 2003.

The wind off the hot and dry desert caused the temperature to peak at 42°C and 41°C on the first and second day respectively at Abu Dhabi, with the relative humidity down to 5% and never above 20% during the day. Meanwhile at Al Ain the peak temperature was 39°C and 38°C on the two days, respectively and the daytime relative humidity was between 13% and 20%. The mean maximum temperature in the UAE in March is about 30˚C, so the weather was certainly considerably hotter than normal.

Finally, late on the 13th, the northerly Shamal in the wake of the low brought clear and more humid air from the Gulf Sea and a considerable drop in temperature. The maximum

temperature on the 14th being 25°C at Abu Dhabi and 26°C at Al Ain. Of interest is the fact that when the Shamal started at Abu Dhabi, the visibility temporarily deteriorated before steadily improving.

6.6.1.2 NWP model data and the synoptic situation

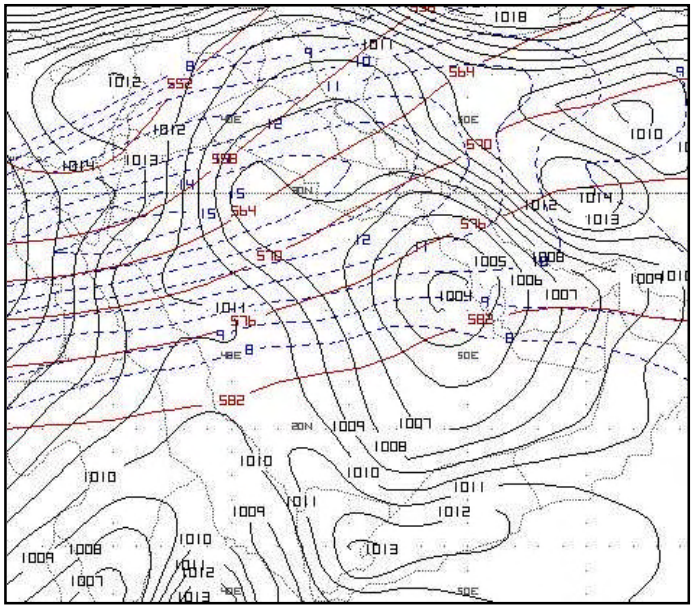

Figure 6.7. Eta GFS analysis at 0000 UTC (T+0) 2003-03-12. Black MSL pressure (hPa), red 500 hPa heights (decametre) and blue 250 hPa wind speed (tens of knots).

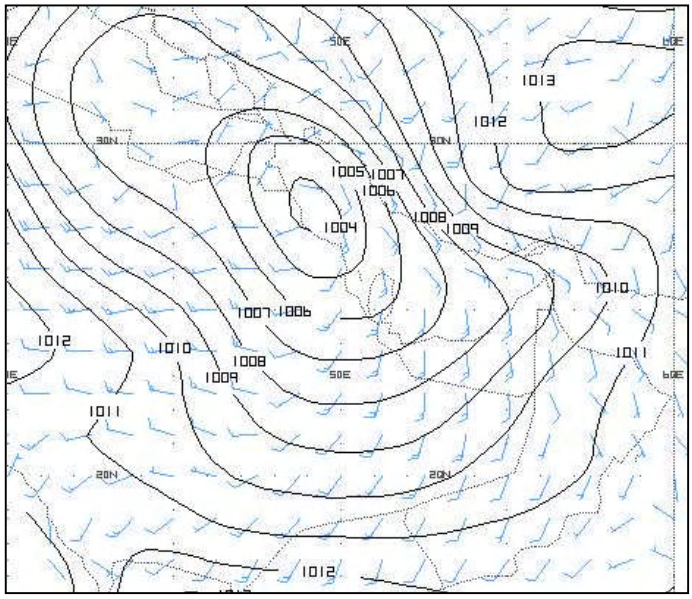

Figure 6.8. Eta GFS MSL pressure (hPa) (black) and 10 metre winds (blue) at 0600 UTC (T+6) 2003-03-12.

The passage of the low pressure cell from west to east was associated with an upper air trough system that was approaching from the west, and to the north, of the Gulf region. The 500 hPa trough was over the eastern Mediterranean Sea and eastern Turkey and at 250 hPa there was a north-westerly jet stream up to 140 knots over the Middle East with the 250 hPa low situated over eastern Turkey (figure 6.7).

The surface low pressure cell began to develop over central Saudi Arabia west of Qatar on the 11th. It had deepened to ±1004 hPa north-west of Qatar by 0600 UTC on the 12th with a 5 hPa pressure gradient across the UAE indicated by the model and a 15 knots southerly wind (figure 6.8). In the event the wind reached 20 knots at ADIA with the visibility down to 1000 metres.

The system moved eastward and by 0600 UTC on the 13th, it was north of ADIA over the Gulf Sea with a 5 hPa pressure gradient straddling the eastern part of the UAE and northern Oman with a wind of up to 25 knots (figure 6.9). It was around this time that the strongest southerly to south-westerly wind and poorest visibility occurred.

At 1800 UTC on the 13th, the cyclone had moved to the Gulf of Oman and a strong Shamal had invaded the UAE with slow visibility improvement (figure 6.10). By the following day it had moved away to the north-east over Iran and was approaching Afghanistan, while Shamal winds continued over the Gulf Sea and the UAE.

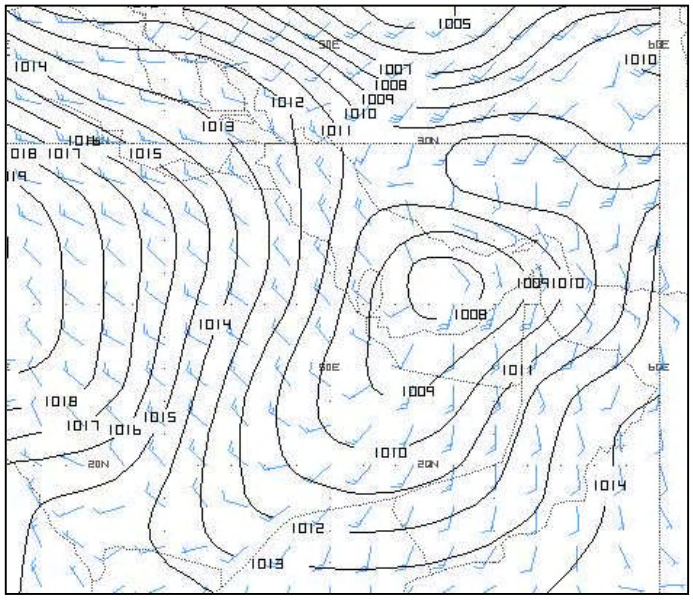

Figure 6.9. As figure 6.8, but at 0600 UTC (T+30) 2003-03-13.

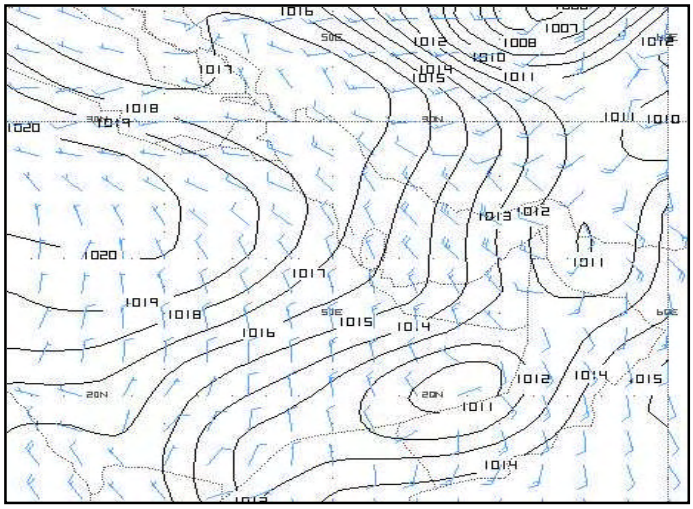

Figure 6.10. As figure 6.8, but at 1800 UTC (T+42) 2003-03-13.

The development of eddies of strong upward currents are necessary to lift dust and fine sand to higher layers of the atmosphere. The upward currents must have vertical speeds that exceed the gravitational falling speed of the particles (WMO Technical Note No.178, 1983). According to the Stokes formula in the WMO Technical Note to lift particles of about 0.1 mm diameter, requires upward currents of 3 to 3.5 ms^{-1}. "The drop in pressure in the centre of the eddy is equal to 1-1.3 hPa, and the rise in wind speed is 10-12 ms^{-1}. The wind speed is almost nil at the height of a few centimetres from the earth, growing quickly in the eddy and reaching l0 m s^{-1} and more at the level of 40-50 metres. The vertical speeds also increase rapidly with height and reach 3-4 ms^{-1}, which allows the eddy to transfer fine sand and dust to a height of up to 1-2 km and even higher".

The Eta GFS time cross section in figure 6.11 clearly shows the correct conditions for dust storm development. Apart from strong winds with little velocity shear up to 850 hPa on both days, indicative of a well mixed boundary layer and the ±5 hPa pressure gradient mentioned earlier, there was also marked upward vertical velocity of up to 3.5 Pa s^{-1} to 700 hPa on the chart ($\omega = dp/dt$ in the x, y, p, t pressure coordinate system, $\omega = -g\rho w$ Holton (1992)). This was associated with the model presenting surface convergence east of the approaching trough system. This indicates that there was sufficient upward motion to carry dust aloft (figure 6.12). Upward motion extended into the middle atmosphere on the 13th when the trough system was closer and there was strong upper air divergence indicated by the model around the 300 hPa level.

The uniform direction and strong winds from the surface to above 5000 feet is depicted by the Eta Grads time cross section on the 12th and the earlier part of the 13th (figure 6.13). Unfortunately, no further model products during this event are available. However, it is worth noting that up to the end of the available data at 0800 UTC on the 13th, the model prognosis was very good and correct in predicting stronger winds for that day.

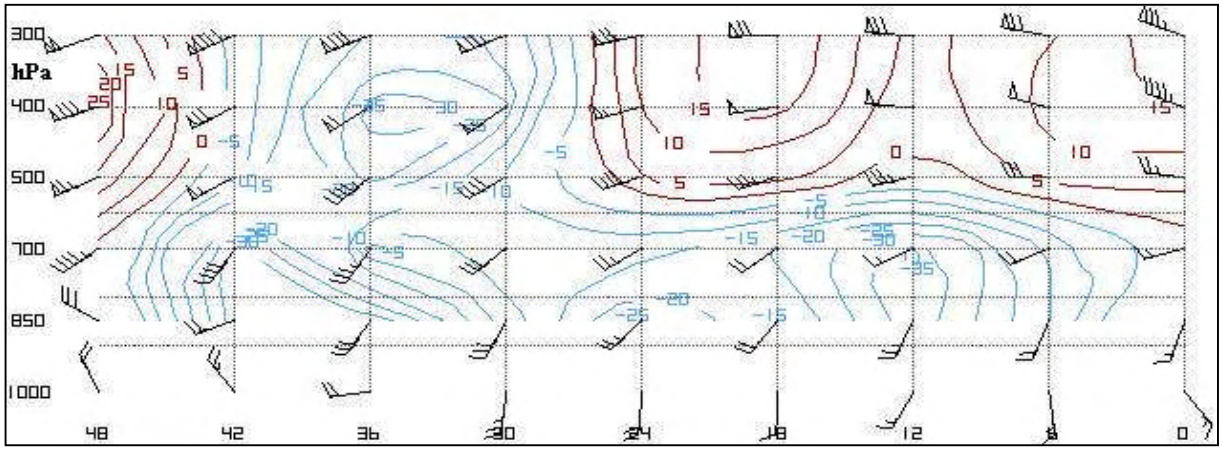

Figure 6.11. Eta GFS vertical time cross-section from 2003-03-12 0000 UTC to 2400 UTC on the 13th. Southerly 15 to 30 knots low level winds are shown up to 850 hPa with upward (blue, negative) vertical velocity of up to 35 micobars s^{-1} (3.5 Pa s^{-1} to 700 hPa).

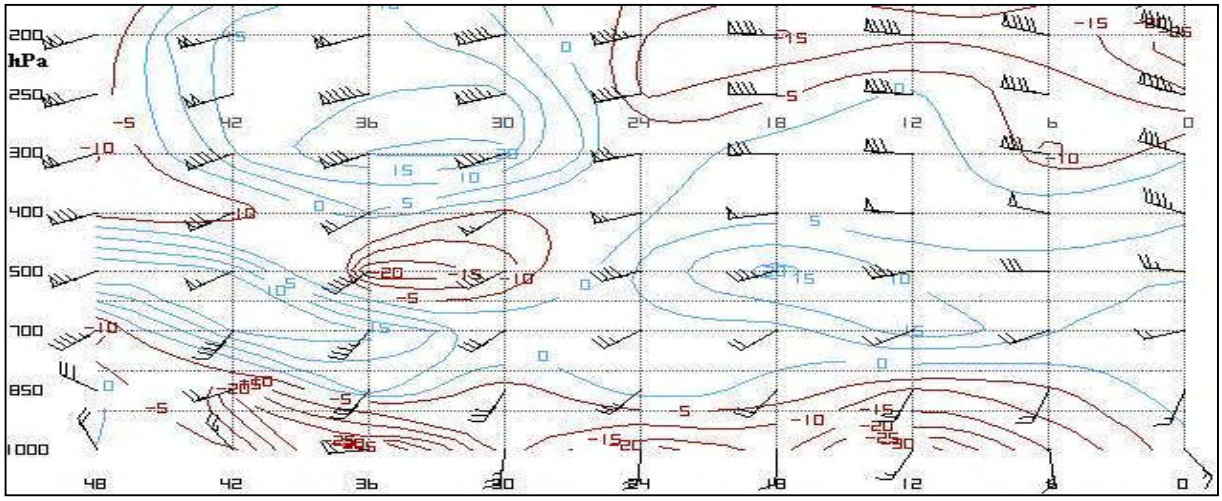

Figure 6.12. Eta GFS divergence time cross-section from 2003-03-12 0000 UTC to 2400 UTC on the 13th. Surface convergence with divergence aloft, coincides with the low level upward vertical velocity in figure 6.11, especially at T+30 to T+36 when the upper air trough was approaching the UAE.

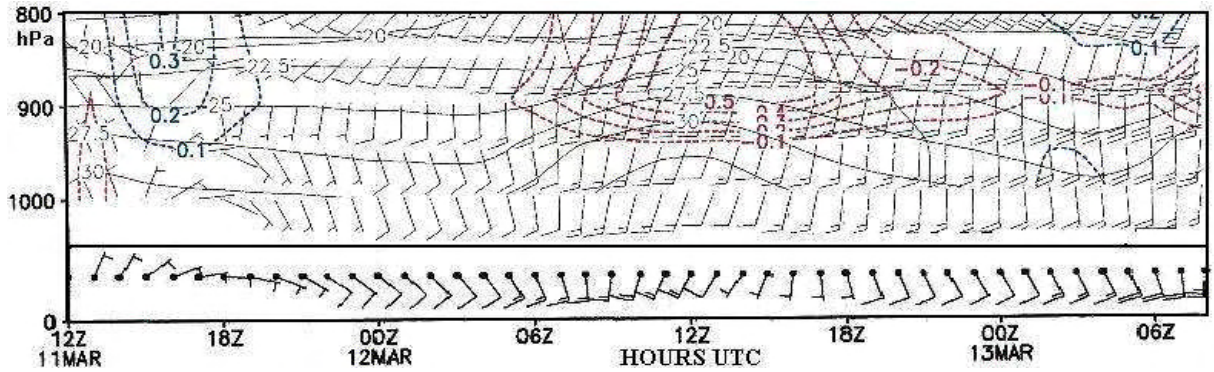

Figure 6.13. Eta GFS prognostic winds at 2003-03-11 1200 UTC. The figure emphasises the steady and strong low level winds, in knots, from the surface up to 800 hPa.

An environmental lapse rate that approaches the dry adiabatic temperature lapse rate facilitates upward motion of sand and dust particles (Safar 1985 and Blair 1943). Prevailing synoptic weather conditions apart, this is most likely in the early afternoon when surface heating is at its maximum and there is unlikely to be a surface temperature inversion. Clear

indication of this happening was provided by the two prognostic vertical profiles at 0300 UTC and 0900 UTC on the 13th (figure 6.14) and verified by the atmospheric soundings carried out at 0000 UTC and 1200 UTC (figure 6.20). The visibility deteriorated from 6000 metres when a surface temperature inversion was still indicated at 0300 UTC, to 300 metres at 1025 UTC when the lapse rate became close to the DALR. These factors being conducive to vertical motion (turbulent mixing) of the surface air at a time when the surface wind increased from 12 knots to over 20 knots, resulting in more dust in suspension.

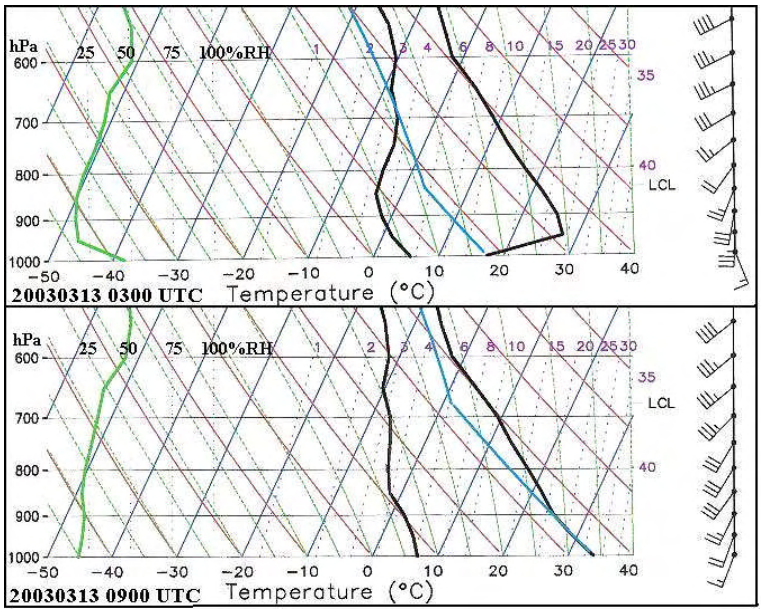

Figure 6.14. Eta GFS prognostic atmosphere profiles at ADIA at 2003-03-12 1200 UTC and 0300 UTC (T+15) on the 13th and 0900 UTC (T+18). DALR, pink lines and mixing ratio, dashed green lines.

6.6.1.3 Surface observations

The 68 observations of wind speed and visibility, from the start to the end of the dust storm, yield a less than encouraging correlation of –0.57. However, if one looks at the scatter graph in figure 6.15, it can be seen that there is a clear negative relationship between wind speed and the visibility. If a visually estimated best fit line is applied to the graph it can be seen that the visibility is about 10 000 metres when the wind is below 10 knots, below 5000 metres at 15 knots and below 1000 metres when the wind exceeds 20 knots. These values are similar to those arrived at in the statistics section (6.5).

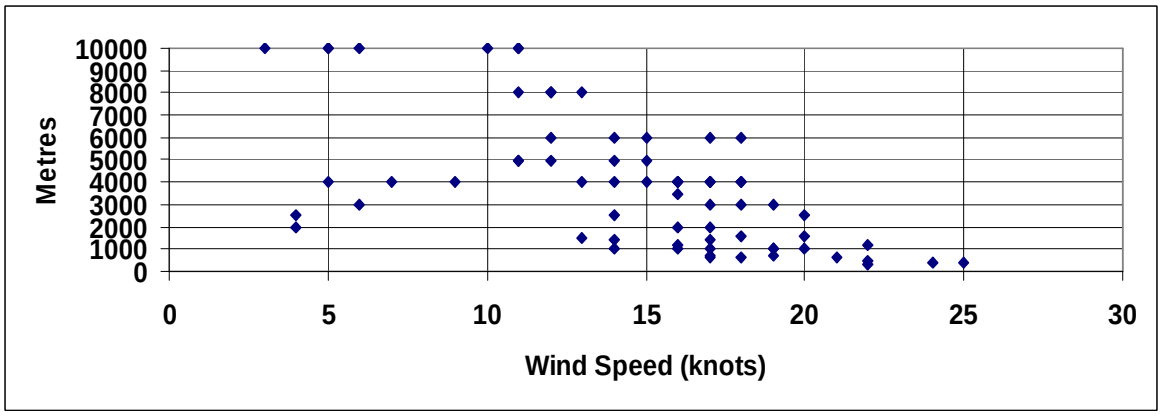

Figure 6.15. Scatter graph of wind speed verses visibility for the 30 hours from 0000 UTC on the 12th March 2003 to 0600 UTC on the 13th.

On the 12th the visibility steadily deteriorated to 1000 metres as the wind, aided by the land breeze, increased to about 20 knots from the south-south-east during the morning and later from the south-south-west during the afternoon (3 to 9 hours UTC in figure 6.16). In the late

afternoon, after 4 pm (1200 UTC), the wind moderated as it rapidly changed to a north-westerly sea breeze and the visibility improved to 5000 metres (figure 6.16). During the night it veered to south-easterly again (and temporarily westerly), became light at times and the visibility improved to 10 000 m, or greater (15 to 24 hours).

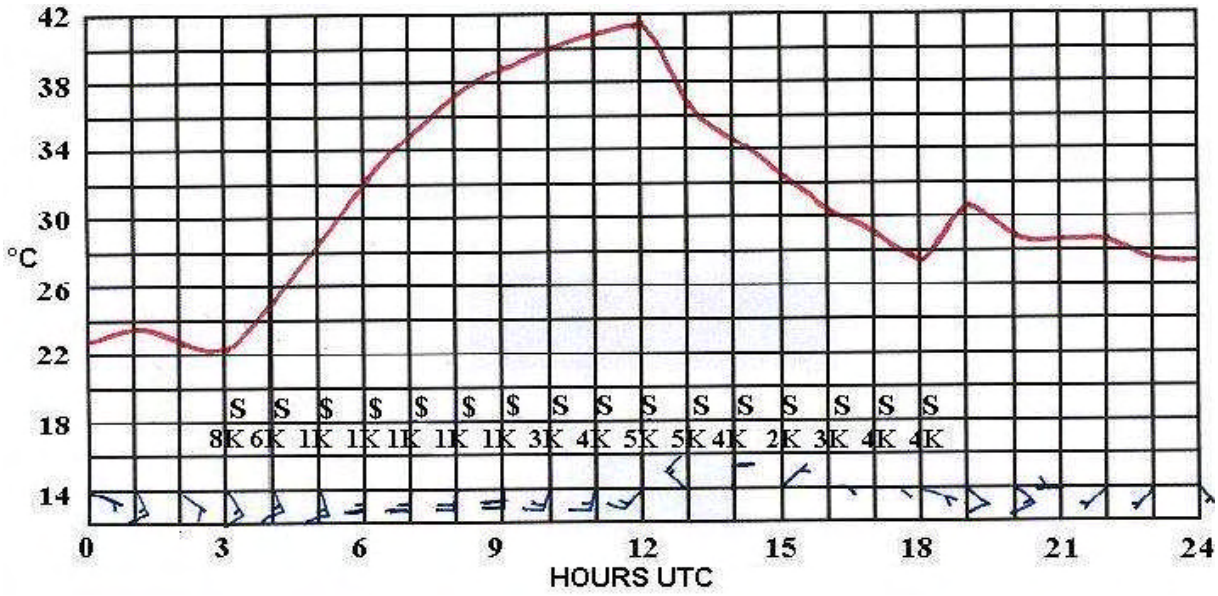

Figure 6.16. Surface observations at ADIA 2003-03-12. The air temperature (°C) is indicated in red, while the dew point temperature is off the bottom of the chart. The wind feathers are in knots (x 10), visibility is indicated in kilometres with dust (S) and blowing dust/sand ($) symbols.

About two hours after sunrise on the 13th (02 to 06 hours in figure 6.18), strengthened by the land breeze, the wind was already up to 20 knots and the visibility down to 500 metres. In the early afternoon it reached 25 knots with the visibility down to 300 metres between 1100 and 1200 hours (figure 6.17). This time it was nearer to 5 pm (1300 UTC) before the wind moderated and swung around to a 15 to 20 knots north-westerly Shamal. Although the sea air caused the visibility to gradually improve, apart from a brief period when the visibility suddenly deteriorated from 3500 metres to 600 metres, it was not until after sunrise on the 14th before the air was again clear enough for the visibility to exceed 5000 metres (figure 6.18). In total the visibility deteriorated to 1000 metres, or less, for about 5 hours on the 12th and 6 hours on the 13th.

The air temperature and dew point temperature graphs reveal very dry and hot desert air with the southerly wind on both days and temporary moister conditions during the intervening night when the wind changed to a north-westerly sea breeze in the evening (figure 6.19). Rapid cooling took place around 4 pm local time on the second day when the Shamal arrived at 36 hours on the chart.

An ambiguity, as mentioned in the introduction (6.6.1), is that on both days the maximum wind was stronger inland at Al Ain than at Abu Dhabi and yet on both days the visibility was

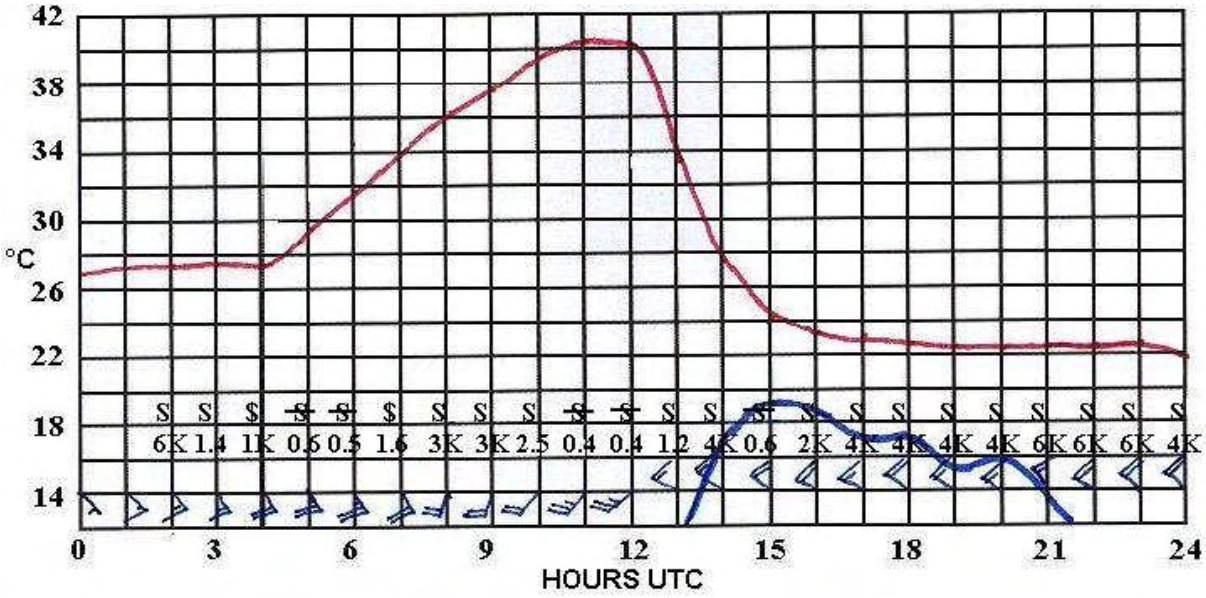

Figure 6.17. As figure 6.16, but for 2003-03-13. S with – strike through = sand storm.

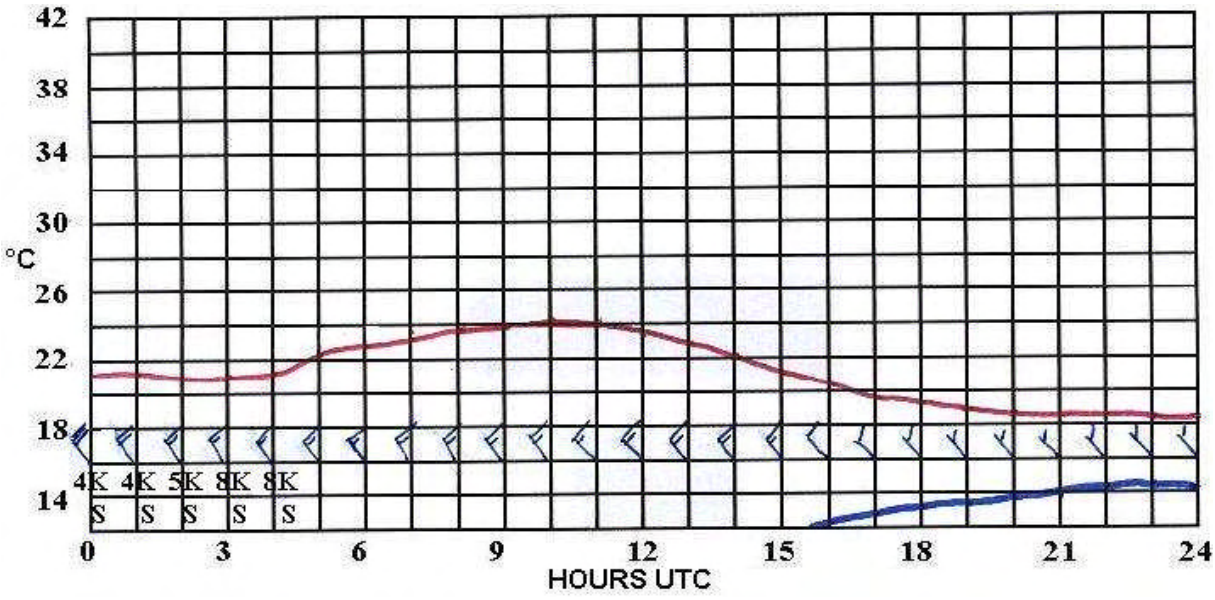

Figure 6.18. As figure 6.16, but for 2003-03-14.

not as poor at Al Ain as at Abu Dhabi. The reason for this is not clear. It could be that the nearby western slope of the Hajar Mountains induced a downward component to the wind, which suppressed the lifting of dust. Another, more likely, explanation is that the sand is different. On trips inland to Al Ain it was noted that the sand is a fine, white and salty dust deposit along a wide coastal strip that becomes a distinct red/brown coloured and much coarser desert sand as one approaches Al Ain. It is, therefore, probable that it is more difficult for the wind to lift the sand at Al Ain than the dust at ADIA. Furthermore, smaller particles, more effectively reduce visibility than larger particles (Robinson 1968), thereby accounting for the poorer visibility at ADIA.

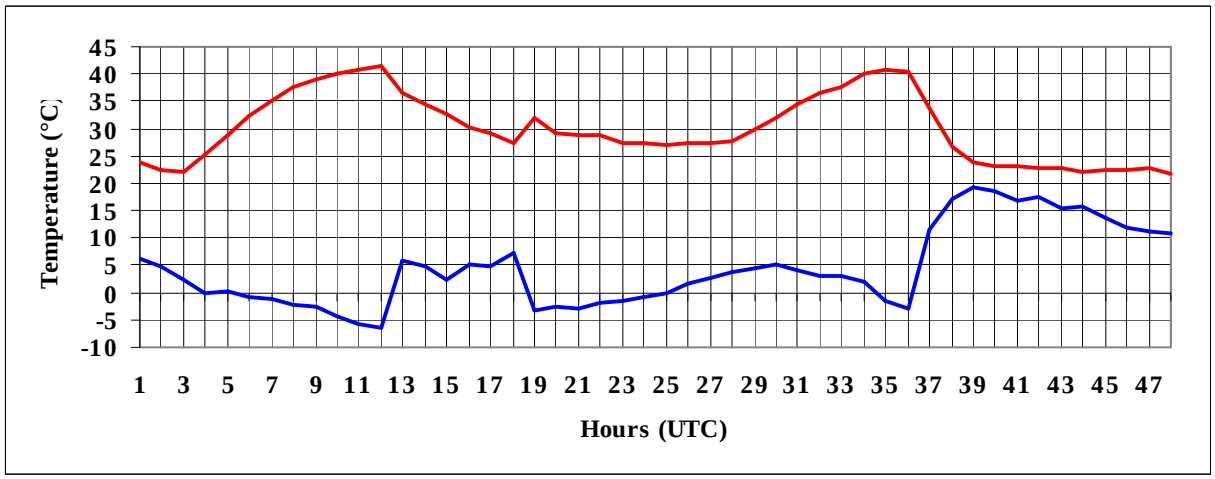

Figure 6.19. Air temperature (red) and dew point temperature (blue) for the 48 hours starting at 0100 UTC on 12-03-2003. The graph shows the extremely dry conditions during the desert wind and much cooler and moister conditions when the Shamal started.

6.6.1.4 Upper air

Table 6.4 gives a clear indication of the change from north-westerly sea breeze conditions on the afternoon of the 11th to a strengthening southerly desert wind during the 12th. The stronger winds, when the low pressure cell in the Gulf Sea was close to ADIA, are also evident on the 13th. Uncoupling of the 10 metre wind at 0000 UTC from the wind higher up is also present due to an overnight radiation cooling surface temperature inversion which developed overnight below 150 metres (500 ft) MSL.

Another noteworthy aspect is the low level nocturnal jet (Blackadder 1957) and wind shear between 150 metres to 610 metres (2000 ft) on the morning of the 13th (table 6.4). Of particular interest is the wind speed shear from 42 knots at 300 metres (1000 ft) to 3 knots at the surface. Weaker wind shear conditions existed on the other mornings.

Table 6.4. Low level winds at ADIA 11th to 14th March 2003.

	11/1200	**12/0000**	**12/1200**	**13/0000**	**13/1200**	**14/0000**
Surface	33009	11007	19015	20003	22024	32018
150 m	34509	12016	19522	18030	22031	32028
300 m	36009	13510	19523	18542	22034	32029
410 m	03509	16019	20522	19037	22037	32530
900 m	09505	18018	20524	20032	21537	32031
1200 m	11508	18019	20525	20530	21539	31522
1500 m	19502	20012	21019	21029	22039	30524

Low level wind shear is a significant hazard to aircraft during landing and take-off. A definite hazard exists if the wind change is sudden enough and big enough to exceed the aircraft's acceleration, or deceleration capacity and large enough to match its airspeed safety margin over the minimum approach, or climb speed (UKMO 1994, ICAO 1987). On the morning of

the 13th, a landing aircraft approaching to land into the wind on runway 13 at ADIA, would experience a rapid loss of airspeed below 150 metres due to the headwind dropping from 30 knots to 3 knots. This translates to loss of lift and rapid sink. If not rapidly counteracted, at the best it results in a hard landing, at the worst a crash landing short of the runway. Taking off on runway 31 with an acceptable 3 knots tailwind results in a tail wind of 30 knots at 150 metres with similar loss of lift effects.

A similar problem exists when there is a large temperature shear such as associated with a surface temperature inversion. On the morning of the 13th the temperature increased by 5°C at 300 metres, but on the morning of the 12th it increased by 8° at 180 metres. An increase in temperature means a decrease in air density, less energy available to the aircraft engines, a loss of lift and aircraft sink (Kermode 1972). Therefore a heavily laden aircraft taking of on runway 31 within ground take-off limits, potentially could have found itself in serious difficulties, if the crew were not aware of the tailwind and higher temperatures aloft.

A similar propensity for danger exists in any situation where strong wind shear and/or strong surface temperature inversions exits, such associated with thunderstorms, land and sea breezes (ICAO 1987) and by implication Shamal conditions in the previous chapter.

The atmospheric soundings at 0000 UTC and 1200 UTC on the 13th are representative of the conditions that prevailed on both days (figure 6.20). The only difference being that the surface temperature inversion was more pronounced on the morning of the 12th. The soundings confirm the Eta model prognostic vertical profiles in figure 6.15.

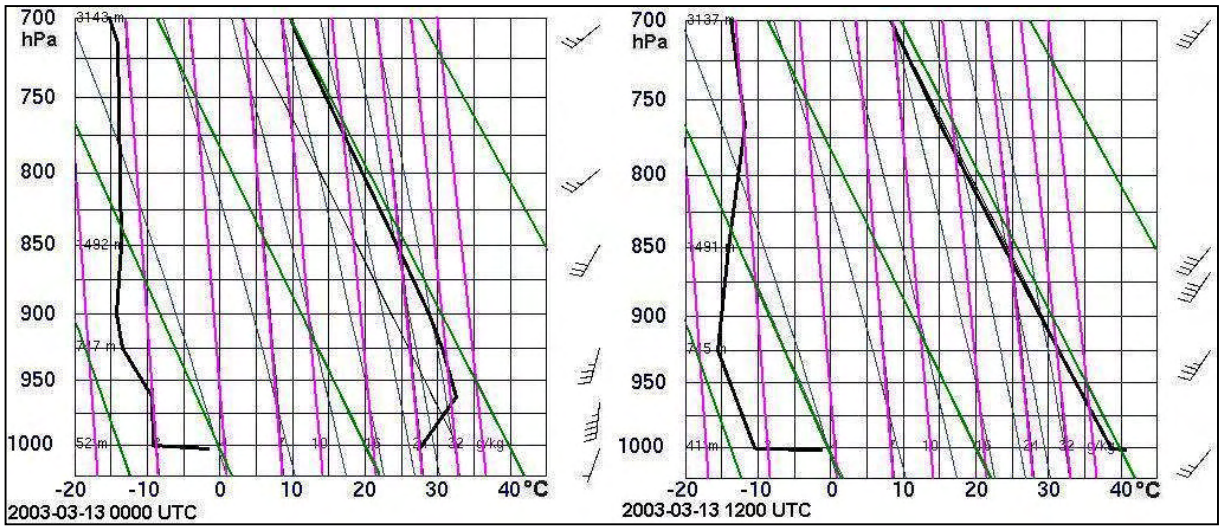

Figure 6.20. Atmospheric soundings at ADIA 2003-03-13 at 0000 UTC and 1200 UTC. The dry adiabatic lapse rate lines are in green and the mixing ratio lines in pink (courtesy of the University of Wyoming).

6.6.1.5 Summary

The dust storm occurred when a southerly wind, which lasted for two days, blew at 20 to 25 knots, reducing the visibility to 300 metres at times. The wind developed due to a strong pressure gradient between an anticyclone retreating to the east and a low pressure cell that approached from the west. The strongest winds and worst visibility occurred on the second

day when the low pressure cell passed close by to the north on its passage to the east. Hot and very dry weather accompanied the wind.

The Eta NWP model gave an accurate indication of the wind velocity to be expected and its duration. The event culminating in the beginning of a cooler Shamal wind and change of air mass that is reminiscent of a cold front.

Conditions were ideal for upward transport of dust and poor visibility.

i A well mixed boundary layer with strong winds and little shear existed up to 850 hPa on both days.

ii An environmental lapse rate that approached the dry adiabatic temperature lapse rate resulted in unstable conditions. In this respect, the visibility was worst later in the morning and the early afternoon when the surface heating was at its maximum and destroyed the surface temperature inversion.

iii There was also marked upward motion (ω = -3.5 Pa s^{-1}) up to 700 hPa associated with surface convergence.

In spite of a poor wind speed and visibility correlation factor of -0.57 for the duration of the dust storm, visual inspection of the scatter graphs show that one can generally conclude that below 10 knots the visibility is about 10 000 metres, or better. Above 15 knots the visibility falls below 5000 metres and falls below 1000 metres when the wind exceeds 20 knots. However, when the wind switches from a southerly desert wind to a north-westerly wind off the sea, the visibility slowly improves, even if it continues to blow at 15 to 20 knots.

6.6.2 FIVE DAYS OF DUST: 16TH TO 20TH MAY 2003

6.6.2.1 Introduction

Sometimes widespread dust from the north-west occurs over the area. It is lifted to the north of the UAE and carried southward on a persistent Shamal wind that can last for days. Such an event happened on the 16th to the 20th of May 2003. Strictly speaking this was not a dust storm event, but it is remarkable for its long duration.

6.6.2.2 NWP model data and the synoptic situation

The dust was raised over northern Saudi Arabia on the 15th where the visibility was reduced to 2000 to 5000 metres during the day, but it became as low as 300 to 800 metres at Bahrain at 1500 UTC.

Early on the 16th, at 0000 UTC, the dust in suspension reached the western part of the UAE at Jebel Dhana, where the visibility fell to 3000 metres. Surface winds were generally 5 to 10 knots from the north-west over the entire region, although the wind was up to 10 to 20 knots over the deep-sea part of the Gulf. During the course of the day the wind blown dust spread to the rest of the Emirates, with the visibility as low as 2500 metres. However, at Doha (in

Qatar) the visibility was 800 metres, while at Bahrain it was 600 metres and down to 200 metres at times. The wind over the Gulf region was north-westerly 5 to 10 knots, but up to 20 knots at the Doha offshore oilrigs. Overnight the wind was lighter, with 2500 to 4000 metres visibility. Figure 6.21 shows the pressure pattern and surface wind at 1200 UTC on the 16th (T+12).

There was little change in the weather on the 17th and the 18th when the wind was 5 to 15 knots from the north-west, but up to 20 knots offshore on the 18th. However, further offshore to the west it reached 25 knots at the Doha oilrigs. The surface pressure and wind analysis at 1200 UTC on the 18th (T+00) is shown in figure 6.22.

At ADIA the wind was generally 10 to 15 knots from the north-west and briefly, for two hours, reached 19 knots on the 16th. The minimum visibility on each day, shortly after sunrise, was 4000 metres on the 16th, 3000 metres on the 17th, 1800 metres on the 18th, 6000 metres on the 19th and 5000 metres on the 20th.

On all days the Shamal penetrated to Al Ain and blew stronger than at the coast on all days and the visibility was worse on most days. This peculiarity of the Shamal and sea breeze wind blowing stronger inland at Al Ain was discussed in the previous chapter in section 5.7. On the 16th it reached 20 to 25 knots with gusts approaching 40 knots and 2500 metres visibility. On the 17th it blew at 15 knots with gusts of 25 knots with 3000 metres visibility. The wind averaged up to 18 knots on the 18th and up to 17 knots on the 19 with 2500 metres visibility on both days. On the 20th it blew up to an average of 19 knots with gusts to around 30 knots and the visibility down to 3000 metres.

After the 20th the visibility continued to improve. The wind remained predominantly north-westerly until the 25th, but by now it had moderated to the point that it was more of a sea breeze than a true Shamal.

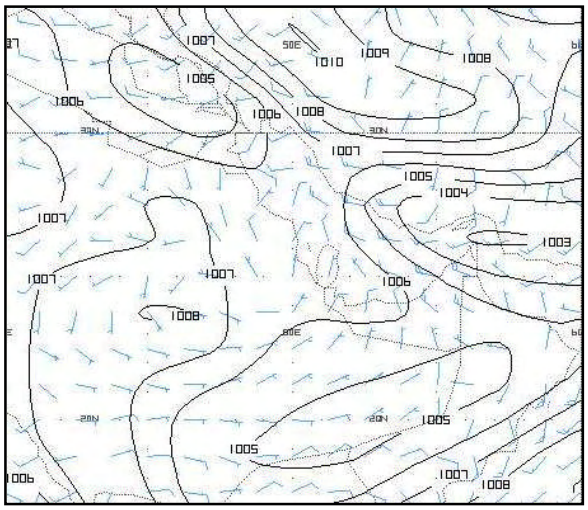

Figure 6.21. As figure 6.8, but at 1200 UTC (T+12) 2003-05-16.

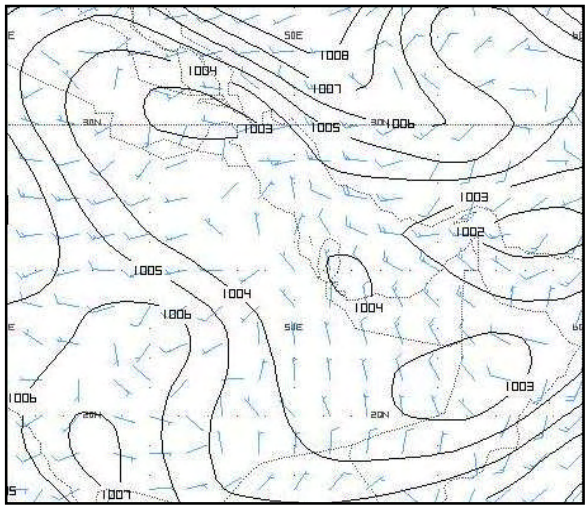

Figure 6.22. As figure 6.8, but at 1200 UTC (T+0) 2003-05-18.

In the previous event (6.6.1) the Eta NWP model indicated that there was low level convergence and upward motion east of the trough. This is to be expected in this region and it

would facilitate the raising of dust. In this event, as is normal in a post-trough circulation, subsiding air (figures 6.23 and 6.24) and low level divergence (figures 6.25 and 6.26) was present (Hess 1959). This is not conducive to the raising of dust.

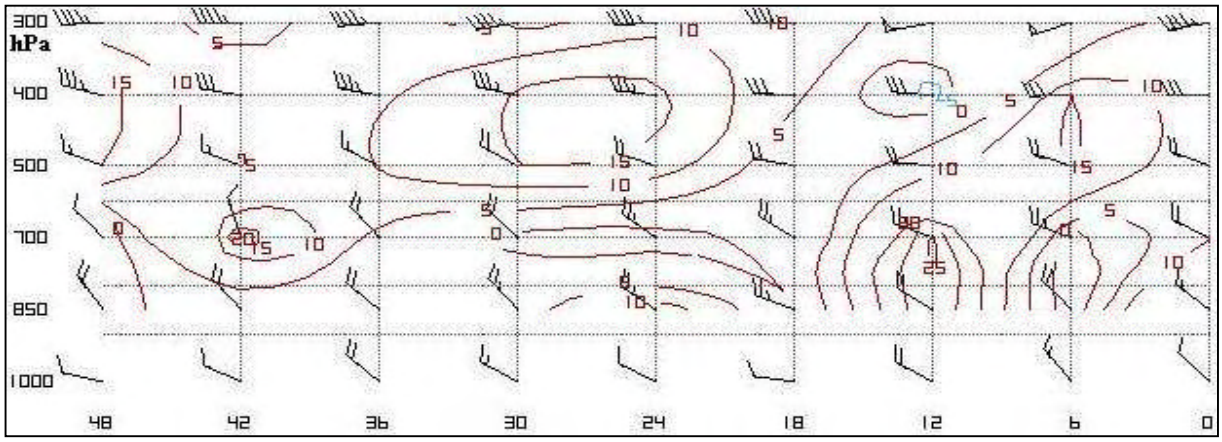

Figure 6.23. Eta GFS vertical velocity (ω) time cross-section 2003-05-16 0000 UTC to T+48 at 0000 UTC on the 18th. Post-trough subsiding air is indicated by the downward motion (ω>0, red) in microbars per second. The wind feathers are in tens of knots.

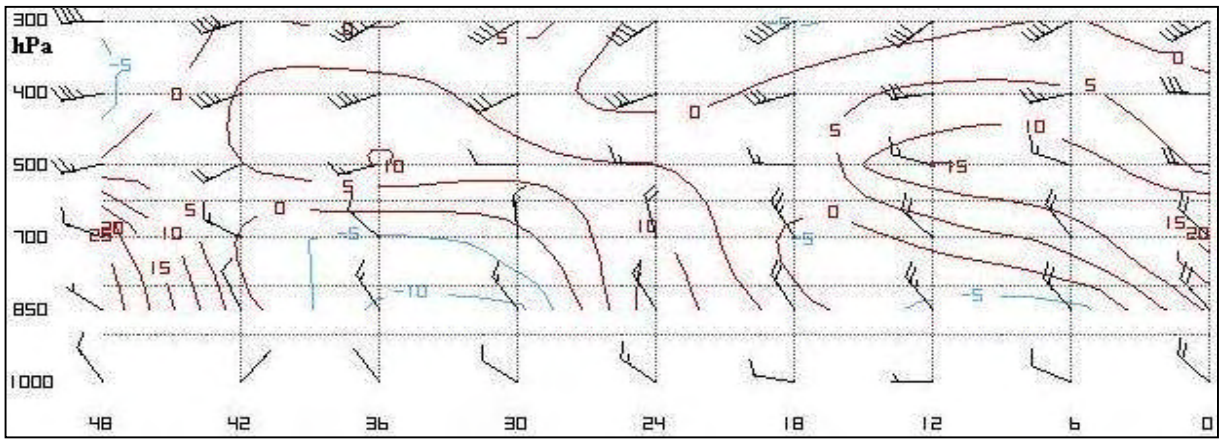

Figure 6.24. As figure 6.23, but for 2003-05-18 1200 UTC to T+48 at 1200 UTC on the 20th. Upward motion shown by blue, negative lines.

The Eta model average wind fields for the 850 hPa to 700 hPa layer at 1200 UTC (T+12) on the 16th (figure 6.27) and 1200 UTC (T+60) on the 18th (figure 6.28), clearly indicate that the dust would be carried from northern Saudi Arabia, across Qatar and the Gulf and then into the UAE.

6.6.2.3 Surface and upper air wind observations

Wind observations at ADIA, in table 6.5 below, show the persistent north-westerly to westerly winds that brought the dust to the region, the exception being a shallow temporary backing change, below ±300 metres, resulting in a southerly to south-westerly wind at 0000 UTC. This is a typical swing and moderation of the Shamal later in the night. Overnight cooling results in the development of a surface temperature inversion. This, combined with

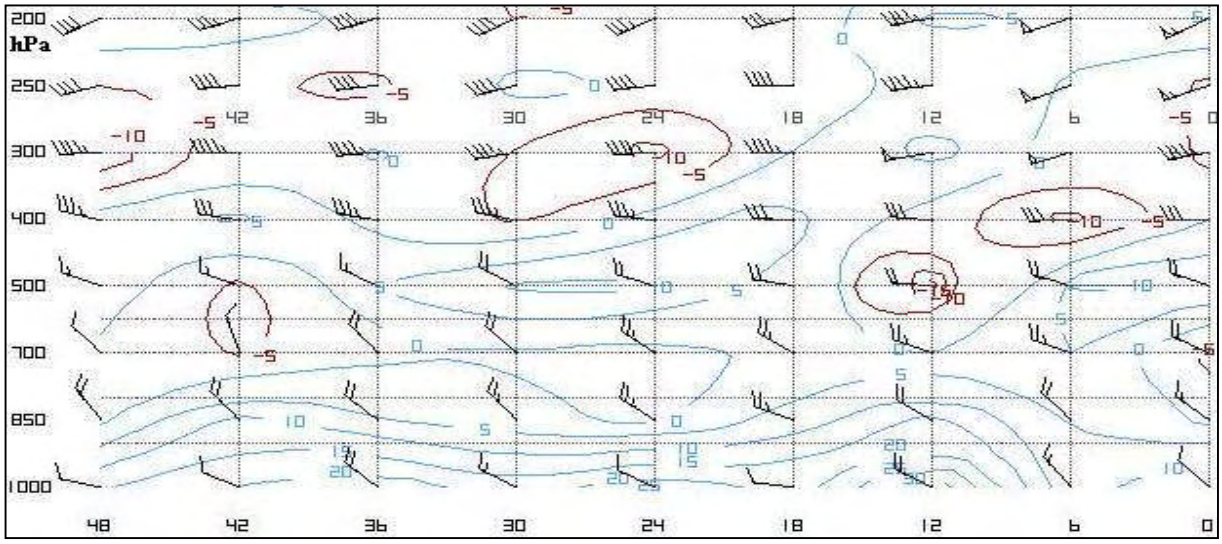

Figure 6.25. Eta GFS divergence time cross-section 2003-05-16 0000 UTC 2400 UTC on the 17th. Surface divergence (positive, blue lines) coincides with subsiding air in figure 6.24.

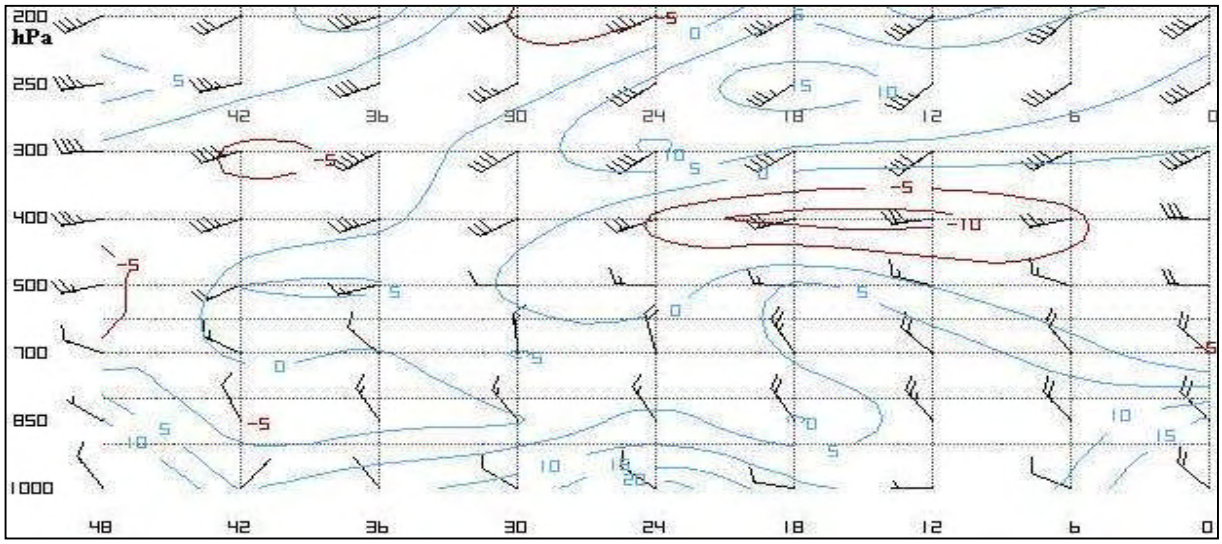

Figure 6.26. As figure 6.25, but for 2003-05-18 1200 to 1200 UTC on the 20th. Surface divergence (positive, blue lines) persists.

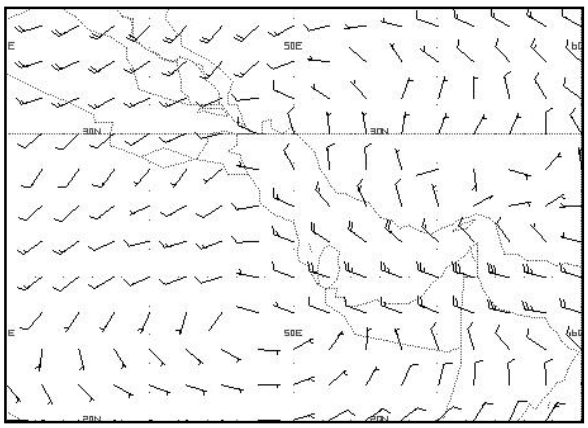

Figure 6.27. Average wind for the 850 hPa to 700 hPa layer on 2003-05-16 1200 UTC (T+12).

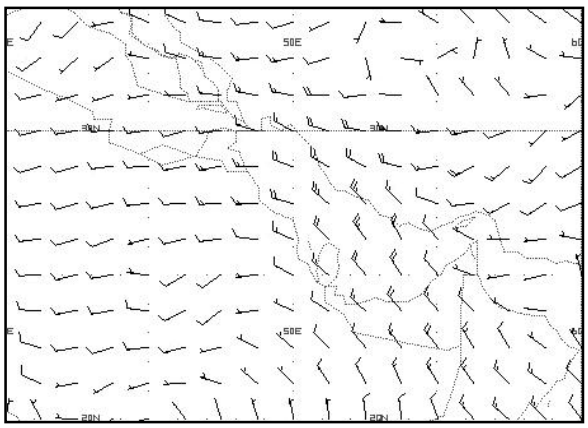

Figure 6.28. As figure 6.27, but for 2003-05-18 1200 UTC (T+60).

the effect of friction, reduces the wind velocity, while the early morning southerly land breeze effect deflects the wind direction (Membery 1983, Riehl 1979 and Hsu 1988).

Table 6.5. Wind observations in metres above sea level at ADIA from 1200 UTC on the 15th May 2003 to the 20th. Wind speed in knots. No observations are available for 0000 UTC on the 16th and the 19th.

DAY	**15th**	**16th**	**17th**	**17th**	**18th**	**18th**	**19th**	**20th**	**20th**
UTC	**1200**	**1200**	**0000**	**1200**	**0000**	**1200**	**1200**	**0000**	**1200**
MSL	330°12	330°15	170°05	350°11	210°06	300°15	300°12	170°03	340°13
300	335°17	325°21	225°10	350°08	280°13	310°18	310°17	280°14	325°17
600	325°10	325°23	265°14	340°08	300°14	315°27	315°19	300°16	325°15
900	005°09	320°21	305°19	325°13	305°16	310°23	315°20	305°18	330°15
1200	340°12	315°20	300°18	325°19	295°19	315°26	320°22	305°18	330°12
1500	335°05	310°25	295°18	320°18	295°23	320°25	325°22	295°16	355°15
2100	280°09	310°34	295°15	300°30	315°23	295°13	345°21	300°18	360°15
3000	290°25	275°26	305°19	305°21	335°17	325°16	340°17	300°20	320°38

6.6.2.4 Summary

The poor visibility was caused by dust in suspension that was transported across the Gulf Sea to the UAE from a considerable distance away to the north-west by a Shamal wind. The wind at Abu Dhabi was generally 10 to 15 knots from the north-west and the visibility was never less than 1800 metres. Inland at Al Ain the wind was stronger, up to 29 knots, but the visibility was never less than 2500 metres. Consequently, this could not be classified as a dust storm event, but it is remarkable for its long duration.

The Eta NWP average wind in the 1000 hPa to 850 hPa layer indicated that the track of the dust would be from northern Saudi Arabia to the UAE, while the prevailing north-westerly to westerly winds aloft at ADIA gave credence to this. The model output was different from the previous event in that post-trough subsidence conditions were present that would not assist the lifting of dust, as opposed to pre-trough upward vertical movement that would have facilitated upward motion.

6.6.3 THE NASHI DUST STORM OF THE 12TH AND 13TH DECEMBER 2003

6.6.3.1 Introduction

The exceptional winter dust storm over the eastern part of the United Arab Emirates (UAE) on the 12th and 13th December 2003 was caused by a cold and dry north-easterly wind known locally as a Nashi wind (UAE Climate 1996). This dust storm caused very low horizontal visibility over the eastern UAE. At Fujairah the visibility remained below 200 metres most of the afternoon of the 12th dropping temporarily to zero metres. On the west coast of the UAE visibility decreased to 1000 metres at Ras Al Khaimah and 500 metres at Dubai and late in the evening, inland at Al Ain, the visibility fell to 2000 metres. This dust reached Abu Dhabi early the following morning where it reduced the visibility to 1500 metres.

In a study of 173 dust events (table 6.2, paragraph 6.5) over the UAE from 1994 to 2003, where the visibility dropped to 5000 metres or less and including dust storms where the visibility drops to below 1000 metres (UKMO 1991), it was found that in 36 (21%) of the events the dust was brought by north-east to easterly winds. Under the same conditions a south-easterly to west-south-westerly wind off the desert accounted for 55% of the events. However, a much higher proportion (31%) of dust storms (visibility less than 1000 metres) came from the north-east. Southerly winds, transporting dust off the desert, accounted for only 13% of the dust storms.

This 'Nashi' dust storm is of considerable interest because of the source region of the dust and the anomalous direction (easterly) from whence it came as well as the very low visibility resulting in extremely hazardous environmental conditions. Furthermore, no other reference or document describing a Nashi dust storm event could be found.

6.6.3.2 NWP model data

The model gave prior warning of a strong anticyclone induced pressure gradient developing over southern Iran on the 12th with 20 to 30 knot easterly to north-easterly winds blowing across the Gulf of Oman and the eastern Gulf Sea into a low pressure cell south of the UAE (figure 6.30). Further to the west, Abu Dhabi was still under the influence of a northerly wind due to a ridge of high pressure extending southward over Saudi Arabia. The wind was the weakened remains of the previous day's Shamal that reached 15 knots when the ridge was more intense.

The wind would still be from the north-east to the east over the UAE on the 13th, but the wind speed much lower due to the retreat of the anticyclone to the east resulting in the collapse of the pressure gradient over the region (figure 6.29). The wind, although still from the east, became even weaker on the 14th.

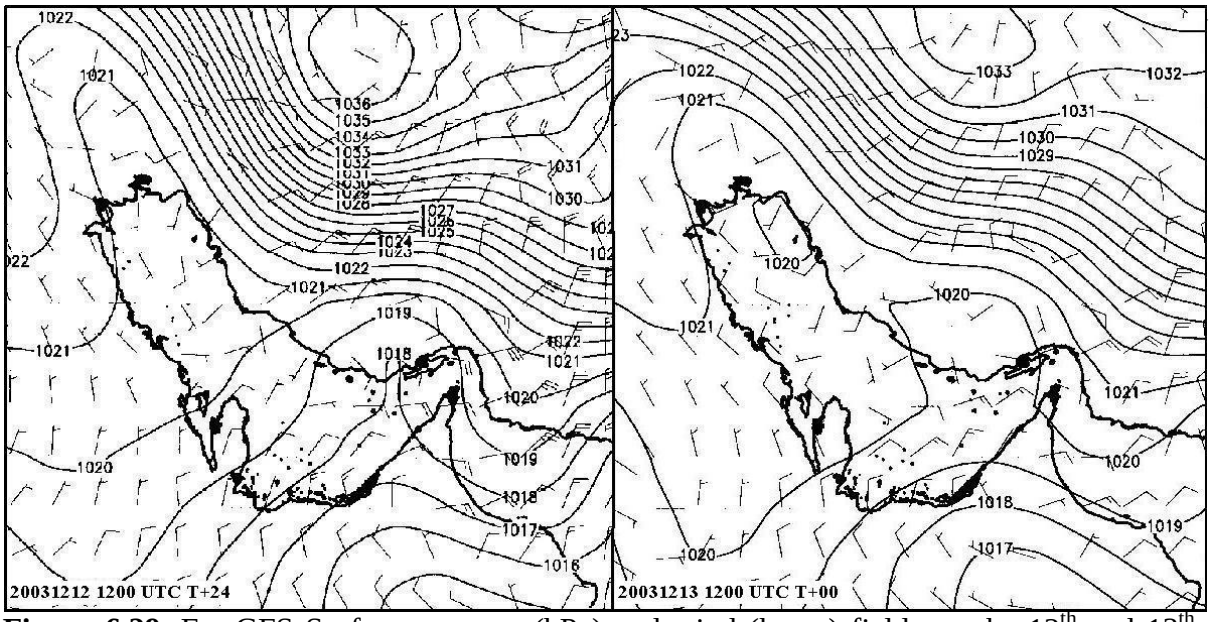

Figure 6.29. Eta GFS Surface pressure (hPa) and wind (knots) fields on the 12th and 13th December 2003. The T+24 field prognoses valid at 1200 UTC indicated that there would be a strong flow from the north-east. The analysis on the 13th shows the weakened flow.

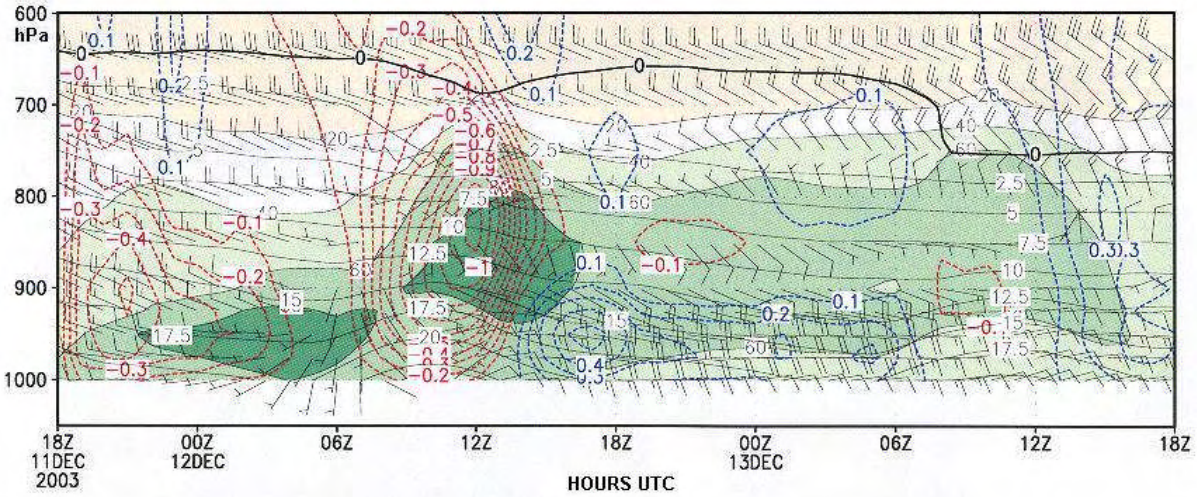

Figure 6.30. Eta GFS time cross-section at Dubai at 2003-12-11 1800 UTC. It shows the distinct atmospheric changes that occurred around 1200 UTC. Warmer air is ascending (red) above colder subsiding air (blue). Note the decrease of the 0°C isotherm height.

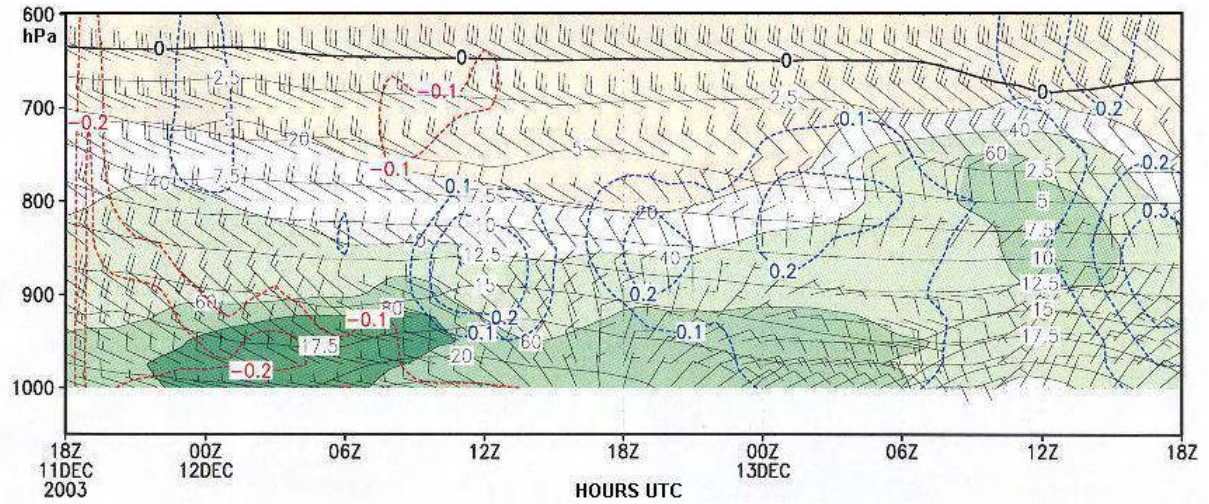

Figure 6.31. As figure 6.30, but at ADIA. The change to a low level easterly winds is indicated nearly 12 hours later than at Dubai with much variation in the vertical of both wind and vertical motion.

6.6.3.3 Surface observations

A strong surface winter anticyclone over Asia, central pressure 1036 hPa, dominated the circulation and maintained a deep, strong, north-easterly to easterly winds from Asia across Iran towards Oman and the UAE. This cold strong turbulent wind picked up dust from the deserts in southern Iran and transported it to the UAE. The wind speed reached 30 knots at Bandar Abbass carrying enough dust to reduce visibility on the Iranian coast to 100 to 300 metres by 0600 UTC on the 12th. The dust crossed the strait to Khasab on the northern tip of the Musandam Peninsula and continued east to the island of Sir Abu Nu'ayr in the Gulf Sea. The dust also crossed the Gulf of Oman to Muscat on the eastern side of the Hajar Mountains where zero visibility was reported.

In figure 6.32 the dashed brown line marks the boundary, at 0600 UTC, of this dust cloud. One hour later the dust cloud reached Fujairah on the Gulf of Oman where visibility fell to 0 metres at the onset and remained below 300 metres for most of the afternoon. During the

course of the afternoon the dust reached Dubai reducing visibility to 500 metres. Surprisingly the general wind over the land remained moderate at 9 to 16 knots, direction east. By 1500 UTC (19:00 local time) all the UAE Weather Offices reported their visibility as having increased to 1000 metres, or better.

The Nashi air came from cold regions near Siberia. Figure 6.32 shows that the air moving across Iran was cold and dry as can be seen from the observation in the top right of the figure where the air temperature was –2°C and the dew-point temperature –8°C. This air, descending to the coast, experienced adiabatic as well as diabatic heating and probably maritime modification by the time it reached the coast in the vicinity of the Strait of Hormuz at Bandar Abbass. Here, at 0600, air temperature was a mild 17˚C but the dew-point temperature -4°C meant dry conditions.

On the 12th the western part of the UAE remained free of this dust. At the Liwa Oasis and Bu Hasah and Al Ain the visibility was more than 6000 metres. This was because it was west of a surface trough axis that maintained a north-westerly Shamal wind that traversed the length of the western Gulf Sea. In summer the Shamal is a hot, dry north-westerly wind that blows over Iraq and the Gulf (UKMO 1991, Rao et al (2001)). On this mid winter day the boundary of the cool air, brought by the Shamal, is marked by the dashed green line in figure 6.32. On the 13th the conditions could no longer be classified as a dust storm. However, the dust did spread further west and the visibility was down to 1500 metres at Abu Dhabi in a 5

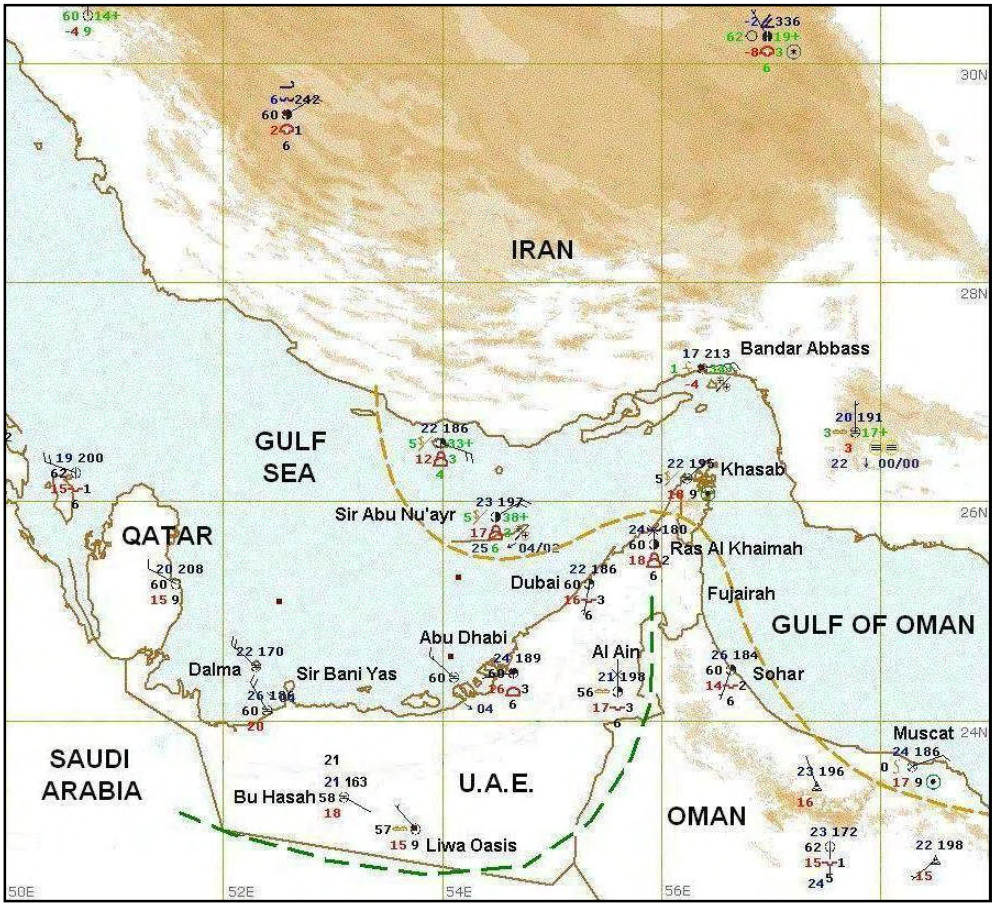

Figure 6.32. Marine surface observation chart at 2003-12-12 0600 UTC. The brown dashed line indicates the dry and colder dust borne Nashi air boundary. The green dashed line indicates the moister Shamal air boundary and the moisture invasion inland.

knots easterly wind by 0400 UTC. By 0600 UTC the dust, in a diluted state, had spread to the western part of the Emirates where the visibility remained greater than 4000 metres at the island of Dalma and at Bu Hasah west of the Liwa Oasis.

6.6.3.4 Satellite image

The invasion of the dust and the contrasting circulation patterns are clearly evident on the remarkable colour enhanced infrared image sensed by the NOAA polar orbiting satellite 17 at 0722 UTC on the 12th (figure 6.33). The image shows how, nearly an hour and a half after the weather observations in figure 6.32, the dust has blown into the eastern part of the Gulf Sea and, having crossed the Gulf of Oman, is now inland of the Fujairah and Oman coasts, but it appears that here its progress inland was hindered by the higher ground of the Musandam Peninsula and the Hajar Mountains.

Figure 6.33 also shows a stream of cloud southward past Qatar over the Gulf Sea. These clouds were formed by the Shamal, which brought cooler air southward over the warm waters of the Gulf Sea. Convection combined with turbulent mixing produced the cloud that penetrated inland as far south as the Liwa Oasis.

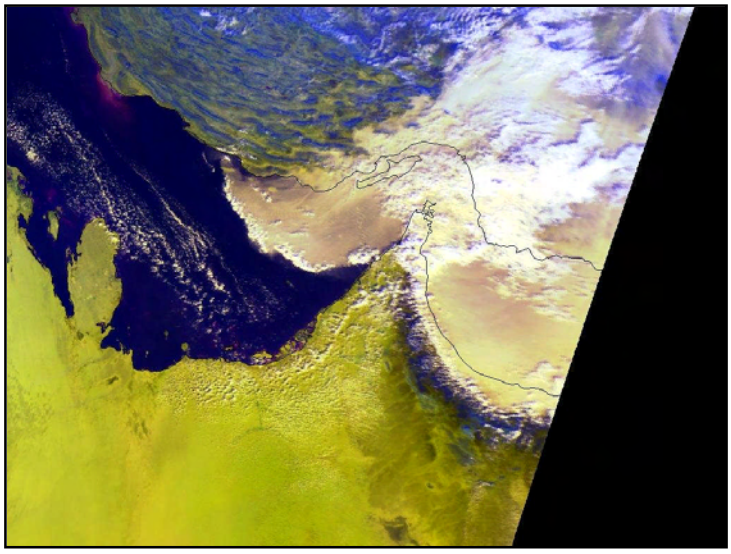

Figure 6.33. NOAA polar orbiting satellite 17 colour enhanced image at 0722 UTC on the 12th.

On the other hand the air brought from the Asian continent by the Nashi wind was cool and very dry. As it moved over the eastern Gulf Sea and the Gulf of Oman it undercut and lifted warmer and moist maritime air ahead of it much as the advance of a cold front would. This resulted in a line of cloud that developed and moved just ahead of the advancing dust front. This is particularly evident over the Gulf Sea and where the anvil head (Cirrus Calvus) remains of short lived thunderstorms can be seen in the strait that developed near and over the northern head of the Musandam Peninsula where the weather station at Khasab reported thunderstorms that had dissipated by 0300 UTC. The storms were probably forced by enhanced convergence of the Nashi and Shamal winds as well as by topographic lifting caused by the Hajar Mountains at the tip of the Musandam Peninsula.

6.6.3.5 Atmospheric soundings

The differences in the air masses invading the eastern UAE is clearly evident in the upper air temperature and dew-point profiles of figure 6.34 obtained from the atmospheric soundings taken at 1200 UTC on the 12th at Bandar Abbass and Abu Dhabi, respectively. At Bandar Abbass the dew-point remains near -10°C from the surface to the 850 hPa level and the dew-

point depression well below 20°C for this layer. This extremely dry air was brought from Iran by a strong east-north-easterly wind prevailing in this layer. In this layer the ambient temperature lapse rate follows the dry adiabatic lapse rate (DALR) while the dew-point follows the constant humidity mixing ratio line. Both these factors indicate air well mixed by turbulence (UKMO 1997). The profile for Abu Dhabi also indicates a well mixed layer up to 925 hPa. But at Abu Dhabi the dew-point depression remained between 8 and 10°C up to this level showing that the north-westerly Shamal air arriving at Abu Dhabi is considerably more humid.

The 850 hPa wet bulb potential temperature is often used to differentiate between air masses (Petterssen 1956, Haurwitz 1941). The air arriving at Bandar Abbass and Abu Dhabi have 850 hPa wet bulb potential temperatures of 280°K and 281°K, respectively. They therefore appear to be parts of the same air mass. However, the profiles in figure 6.34 clearly show the near surface layers had clearly been modified differently. At Bandar Abbass cool and dry continental air is present while at Abu Dhabi the near surface air is modified warmer and moist maritime air.

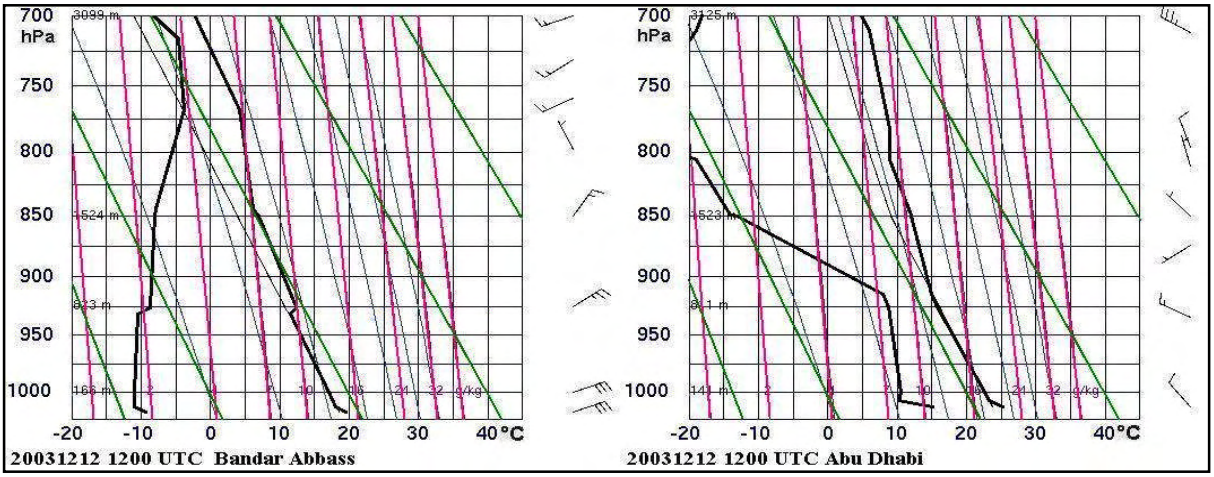

Figure 6.34. Atmospheric soundings at Bandar Abbass, on the Iranian coast, and ADIA at 1200 UTC on the 12th December 2003. Dry adiabatic lapse rate lines in green and mixing ratio lines in pink (courtesy of the University of Wyoming).

6.6.3.6 Summary

The north-easterly to easterly Nashi wind transported dense dust from the deserts of southern Iran to the UAE. Dust brought by the Nashi wind from Asia is less frequent than dust storms over the UAE caused by a southerly wind off the Arabian Desert. Nashi wind dust storms over the UAE tend to be more intense, producing lower visibilities for longer periods. The dust descending over the UAE, resulting in very low visibility, was not accompanied by strong wind. Over Iran, however, wind speed in the lower 1000 metres was 30 to 25 knots very turbulent and kept vast amounts of dust in suspension long enough to reach the UAE.

This Nashi dust storm is also noteworthy because of the contrasting surface weather essentially separated by the Musandam Peninsula on the morning of the 12th. The 850 hPa wet bulb potential temperature indicates that both originated from a single air mass, situated over Asia with fairly uniform characteristics. The route taken to the UAE meant that the

Nashi air had undergone modification as continental air while the Shamal air arrived over the UAE as maritime air. This modification could be clearly identified on the surface synoptic map (figure 6.32) as well as on the satellite image (figure 6.33). Notable also was the cold front like interaction between the cool and dry, but dust laden Nashi air from the north-east with the warmer and moister north-westerly Shamal air over the Gulf Sea and, in the process, producing a marked gust front and thunderstorms.

Model data clearly indicated that the wind was going to be strong in the east with the inference that there would be dust raised and deterioration in the visibility.

6.7 FORECAST CHECKLIST

Use of the Eta NWP model post processing products and satellite imagery gives ample warning of dust and dust storm conditions. Of particular use to initially identify dust storm conditions are the surface wind and pressure fields and the surface wind time cross sections.

Important considerations are;-

- Little or no wind shear.
- An environmental lapse rate that tends to the dry adiabatic lapse rate (instability).
- Dust in suspension is more likely and likely to be more persistent with upward vertical velocity below 700 hPa.
- The dryness of the surface dust/sand.
- Dust and sand storms are most likely with the wind from the south-east to west-south-west. That is, a surface low pressure approaching from the west with a marked southerly pressure gradient.
- The visibility improves when a southerly generating wind veers to north-westerly after the passage of a surface low, or trough, or an afternoon sea breeze develops.
- The visibility improves at night when the wind becomes lighter.
- A low level jet of about 30 knots or more can occur at 150 metres to 600 metres (500 feet to 2000 feet) MSL with attendant wind shear.
- Awareness of dust conditions further afield and dust transport to the UAE.
- Dust from further afield is carried on north-westerly Shamal winds and north-easterly Nashi winds.
- Dust storms with the visibility < 1000 metres last < 2 hours, at the most < 5 hours.
- Dust with the visibility < 3000 metres last < 4 hours, at the most 15 hours.
- Dust and dust storms in southerly winds are most likely between 0300 UTC to 1200 UTC and most prevalent at 0600 UTC.
- Dust and dust storms in a Shamal are most likely between 0800 UTC to 1300 UTC.
- Dust storms are most likely to last about 30 minutes when associated with a thunderstorm and not more than 60 minutes.
- In general, wind speed and visibility relationship in table 6.6 below can be applied.

Table 6.6. Wind speed and visibility relationship at Abu Dhabi

Wind speed	**Visibility**		
> 15 knots	< 8000 metres	often < 5000 metres	
> 20 knots	< 5000 metres	often < 2000 metres	most likely < 1000 metres
> 25 knots	< 2000 metres		most likely < 1000 metres
> 30 knots	< 1000 metres		

CHAPTER 7

LAND AND SEA BREEZES

7.1 INTRODUCTION

A significant wind pattern in the UAE is that of the diurnal land and sea breeze circulation (U.A.E. Climate 1996). This circulation affects most of the country almost on a daily basis, the exception being during the passage of major weather systems, which produce pressure gradients that disrupt and often overwhelm the thermal gradients.

The alignment of the UAE Gulf coast in the east is south-west to north-east, which means that land breezes arrive from a south-easterly direction and sea breezes from the north-west. These are the two dominant wind directions and it is no coincidence that the airport runways in the region are aligned north-west to south-east. For example, 310°/130° at ADIA and 300°/120° at Dubai. To the west of ADIA the coast is oriented west to east and the land and sea breezes tend to be northerly and southerly, respectively.

Numerous references to literature have been made in previous chapters in connection with land and sea breezes at ADIA. These will not be discussed again in this chapter, except where necessity dictates.

7.2 SCOPE OF THE STUDY

This chapter examines land and sea breezes at ADIA during the 12 months from September 2002 to August 2003. Shamal and southerly desert winds due to synoptic pressure systems were ignored, although some were difficult to separate. The dynamics, statistical occurrence (including wind roses at ADIA) and general characteristics of land and sea breezes are discussed with examples and a case study presented. Attention is drawn to their effect inland in the desert at Al Ain, the Abu Dhabi Emirates second international airport, as well as an anabatic and katabatic effect there. Finally, a forecast methodology is proposed.

7.3 DYNAMICS

The coastline marks the boundary between markedly different sea and land temperatures. These differences give rise to land and sea breezes. Bradbury (1989), Hsu (1988) and Riehl (1979), among others, explained how the land/sea breeze is driven by the diurnal diabatic heating/cooling of the land adjacent to the ocean and will not be repeated her. Suffice to say that the diabatic heating of the surface air over the deserts surrounding the Arabian Gulf play an important role in the wind experienced at ADIA.

Land and sea breezes are more common in summer in higher latitudes, but all year round in the tropics (Miller 1966). The latter is especially true along the UAE Gulf Sea coast where land and sea breezes are virtually a daily occurrence.

Sea breezes are strongest when the thermal difference between the land and sea are greatest. This is typically in the early summer period when inland temperatures have begun to increase and sea temperatures, which typically lag behind the air temperature, are still relatively low (Bradbury 1989).

The extent of the circulation varies according to different sources. It may extend about 20 kilometres seaward and 60 to 70 kilometres inland (Miller 1966), or not more than 50 kilometres according to Critchfield (1974), while Hsu (1988) defines the vertical extent as being up to 700 hPa.

Due to thermal stability, usually in the form of a surface temperature inversion, the land breeze is usually very shallow. Ground friction tends to restrict the wind to 2 to 4 knots (about 1 to 2 ms^{-1}), whereas the sea breeze usually attains speeds of 10 to 20 knots (±5 to 10 ms^{-1}). The sea breeze accelerates until ground friction is sufficient to counter the pressure gradient, or the circulation weakens (Riehl 1979).

The prevailing wind has an effect on the land and sea breeze (Bradbury 1989 and Riehl 1979). In the UAE a north-westerly Shamal wind will strengthen the sea breeze, but it will suppress, or obliterate, the land breeze. Similarly, the southerly desert wind, such as east of an approaching low, which can result in a dust storm, will strengthen the morning land breeze.

7.4 STATISTICS AND GENERAL CHARACTERISTICS

The research indicated that on average, during the 12 months, the sea breeze can be expected to start at 0830 UTC (12:30 pm), the average wind speed being 11 knots reaching a maximum at about 1030 UTC (14:30 pm). The lighter land breeze is most likely to begin at 0100 UTC (05:00 am), blow at about 4 knots and reach a maximum at about 0450 UTC (08:50 am).

This normal daily interchange between the land and sea breeze is depicted in figures 4.8 to 4.12 of chapter 4 that details the four days with fog on the 18th to the 22nd July 2002 when fog occurred on four consecutive days under weak surface pressure gradient conditions. Notice the regular and rapid change from a land breeze to sea breeze in about an hour.

Based on weather observations at ADIA from 1995 to 2002, Eager et al (2005) found that sea breezes occur on more than 90% of the days from March to December while land breezes occur on over 90% of the days in May to December. The lowest recorded frequencies of daily sea breezes and land breezes were 77% and 71%, respectively, in February. The consistency of the land and sea breezes during most of the year is evident in the wind roses in figure 7.1. Winds from the north-west and the south-east dominate. What is also apparent is the overall directional dominance of the north-westerly sea breeze and its strengthening by the Shamal. In summer this happens when the Shamal tends to prevail most of the time and in winter when the north-westerly wind is associated with winter troughs (Rao, et al 2001 and Membery 1983). Data for the 12 month study period at ADIA revealed that 73% of the time the land breeze veers from a directly offshore south-easterly to south-west, while 65% of the time sea breeze veers through north to south-east as it subsides in the evening. This is to be expected due to the action of the Coriolis force, which deflects the wind to the right in the

northern hemisphere (Holton 1992). The Coriolis is dependent on the Sinus of the latitude and it is therefore small at the latitude of the UAE (Holton 1992, Bradbury 1989)

By early summer inland desert temperatures have climbed well into the mid 40's. However, sea surface temperature typically lags a month or so behind the rapidly rising air temperatures. Bradbury (1989) stated that sea breezes peak during the early summer when thermal gradients between the land and sea are the greatest. The wind roses in figure 7.1 show that this is equally valid at ADIA with a higher frequency of strong north-westerly to northerly sea breezes in April compared with July.

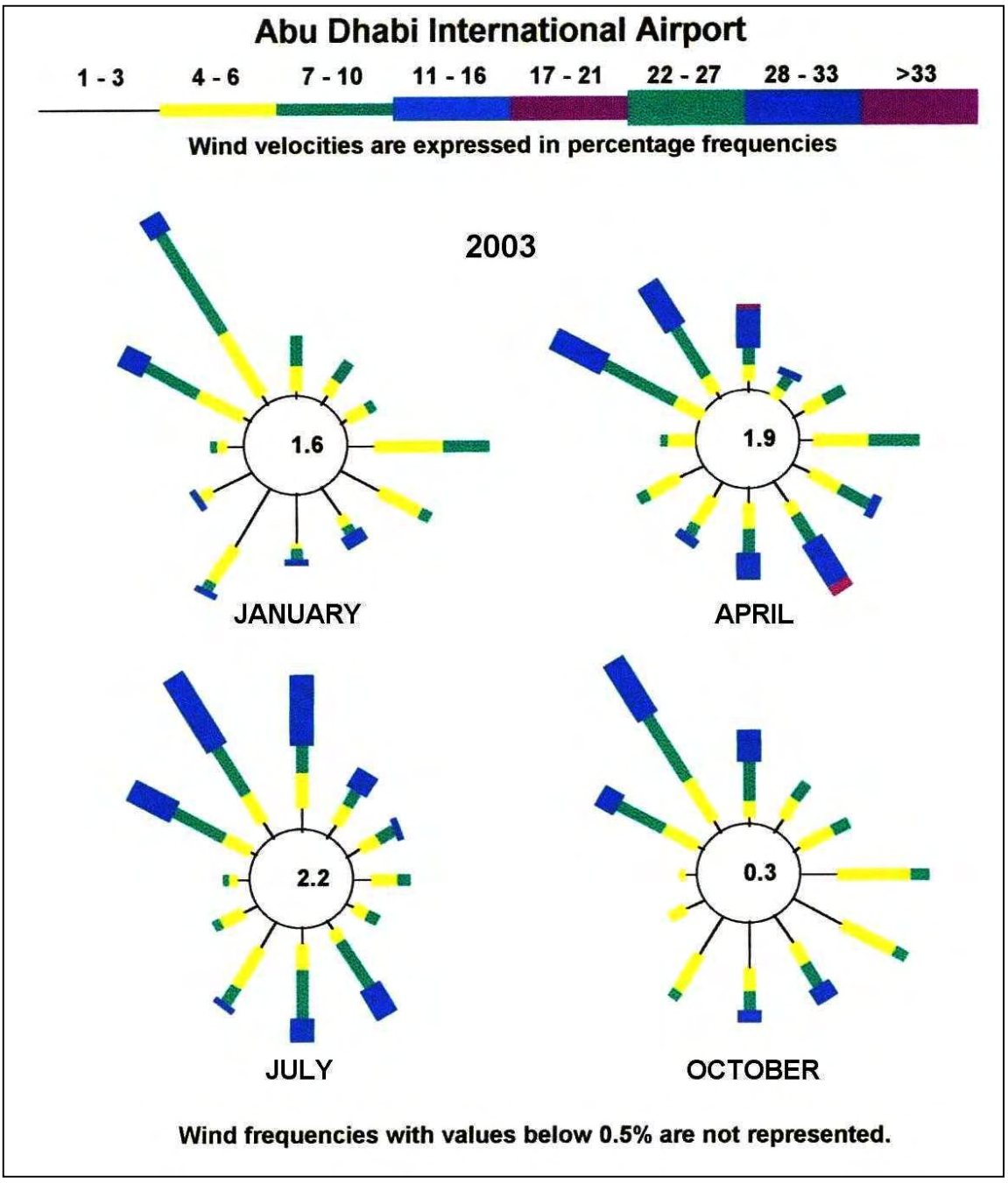

Figure 7.1. Wind roses at ADIA for January, April, July and October, 2003, compiled from hourly observations. The percentages when the wind was calm are entered in the centre circles.

If the sea level pressure is higher south of the UAE, this will enhance the land breeze during the morning and cause higher than normal daytime temperatures. This pressure gradient will also oppose the land/sea thermal gradient due to solar heating of the land heating and therefore delay the onset of the north-westerly sea breeze. Under these circumstances the beginning of the sea breeze can be sudden, strong and gusty. Examples can be seen on the 12th and 13th June 2003 in figures 4.33 and 4.34, chapter 4. The build up of the thermal gradient is sometimes big enough to cause a sea breeze strong enough lift dust and reduce the visibility. Occasionally isolated cumulus clouds will form along the sea breeze gust front as it travels inland.

With high pressure to the south the synoptic scale pressure gradient may on occasions overwhelm the thermal gradient caused by daytime heating of the land surface. The sea breeze is suppressed and a southerly wind continues throughout the day and night. This wind may become light in the evening and overnight, when the lower layer of the atmosphere becomes stable and suppresses the vertical transport of wind momentum. The sea breeze is also suppressed when a surface low pressure cell approaches the UAE from the west. For example, on the 12th and 13th March 2003 (figure 6.17 and 6.18, chapter 6) the synoptic scale pressure gradient was able to suppress the sea breeze for all but the two hours between 1300 and 1500 UTC on the 12th.

On the other hand if the surface pressure increases to the north-west the synoptic scale pressure gradient reverses and the opposite situation applies. If this pressure gradient is strong enough to overcome the overnight thermal gradient, a north-westerly wind may blow throughout the night completely suppressing any land breeze. Under these circumstances, night temperatures tend to be higher than usual, but daytime temperatures tend to be lower due to the advection of maritime air over the land. In the afternoon this pressure gradient will support the thermal gradient and the sea breeze will add its strength to the prevailing onshore flow resulting in an onshore wind speed greater than due to the pressure gradient alone. The case study in chapter 5 on the 15th and 16th November 2003, depicted by figures 5.9 and 5.10 illustrates this phenomenon.

7.5 LAND AND SEA BREEZE: 10TH TO 11TH MAY 2003

Analysis of wind data at both Al Ain and ADIA revealed that the wind inland at Al Ain is sometimes surprisingly stronger than at the coast. This gusty and turbulent wind at Al Ain can be strong enough to raise sand and dust, drastically reducing the visibility at Al Ain. This phenomenon is illustrated by a case study of the land and sea breeze interaction with the synoptic scale flow that happened on the 10th and 11th May 2003. Also of interest is the change in vertical air movement below 700 hPa over the land and sea as indicated by the ETA model data.

7.5.1 SYNOPTIC SITUATION

On the 10th at 1200 UTC (T+12), the Eta NWP model data (figure 7.2) indicated that a surface pressure ridge would develop over Qatar and northward to western Iran, with an area of generally low pressure over the southern Arabian Peninsula. Low pressure cells were also predicted over the Strait of Hormuz with a trough extending to the south of the UAE as well as another to the south-west. A weak 1 to 2 hPa surface pressure gradient is indicated over the

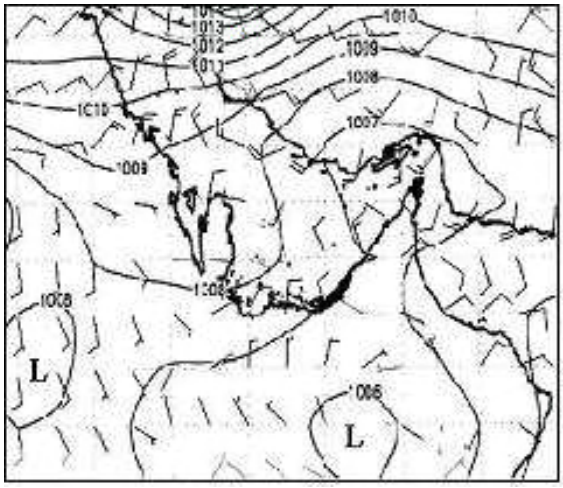

Figure 7.2. 2003-05-10 Eta GFS surface pressure and wind on 2003-05-10 at 1200 UTC (T+12).

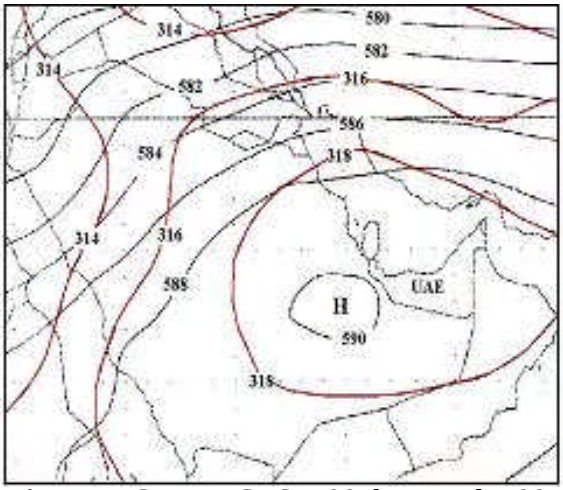

Figure 7.3. Eta GFS 700 hPa and 500 hPa gpm heights in decametres on 2003-05-10 at 1200 UTC (T+12).

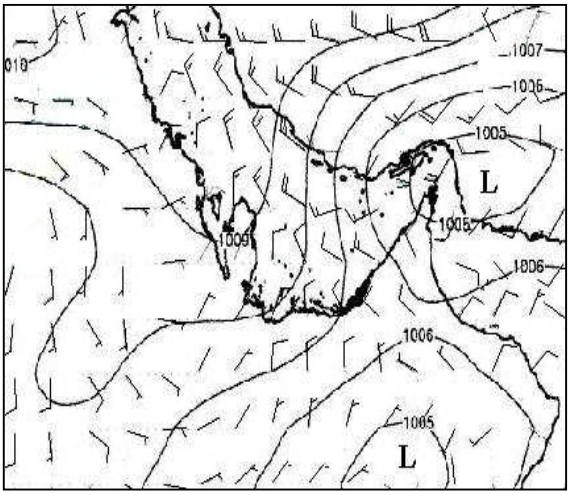

Figure 7.4. As figure 7.2, but for 2003-05-11.

UAE (figure 7.2). Figure 7.3 shows how the anticyclonic circulation supersedes the cyclonic circulation by 500 hPa (U.A.E. Climate, 1996).

Later the following day the model indicated that the upper-air anticyclone would still be over the Emirates, but at the surface an increased pressure gradient, associated with a ridge of high pressure, would develop over the western part of the Gulf and that the low pressure cell over the Strait of Hormuz, as well as the low south of the UAE would deepen somewhat (figure 7.4) and a small col forms in the vicinity of ADIA. This synoptic scale circulation indicates that north-westerly Shamal conditions would develop and strengthen over the western Gulf during the 11th, but that is should not have a significant effect on the land and sea breeze circulation at ADIA. It will be shown that the north-westerly sea breeze was stronger on the 10th, when a weaker pressure gradient existed than on the 11th.

7.5.2 SURFACE OBSERVATIONS

Most of the night of 9th/10th at ADIA, the wind blew from the sea and briefly turned to a light land breeze between 0200 and 0500 UTC (6-9 am) at about 3 knots (figure 7.5). A light variable wind preceded a light to moderate sea breeze that began at 0700 UTC (11 am), reaching a maximum of 14 knots at 1100 UTC (3 pm). Notice the gradual veering change from a sea breeze to a land breeze overnight on the 10th/11th. On the second night the wind veered through north-east to a south-east land breeze and then south-west by 2400 UTC (4 am). Within an hour, at about 0800 UTC (12 noon) the land breeze changed to a sea breeze, reaching a maximum of 13 knots at 1100 UTC (figure 7.6).

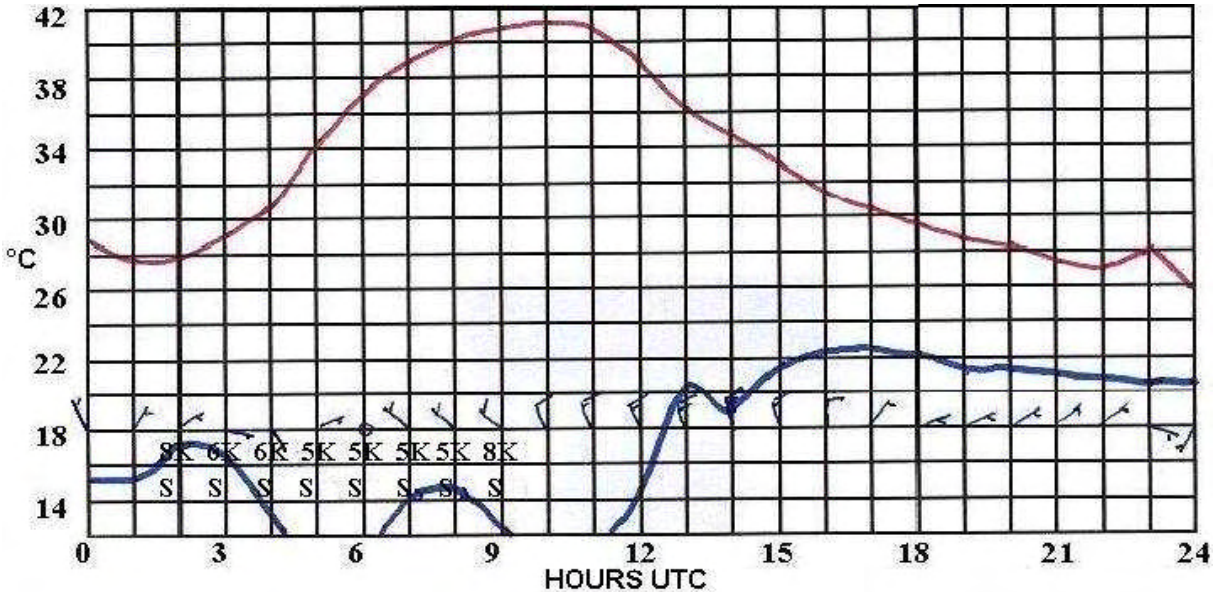

Figure 7.5. Surface observations graph at ADIA on 2003-05-10. The air temperature (°C) is indicated in red, dew point temperature in blue (°C). The wind feathers are in tens of knots with the visibility indicated in kilometres and the dust symbol below.

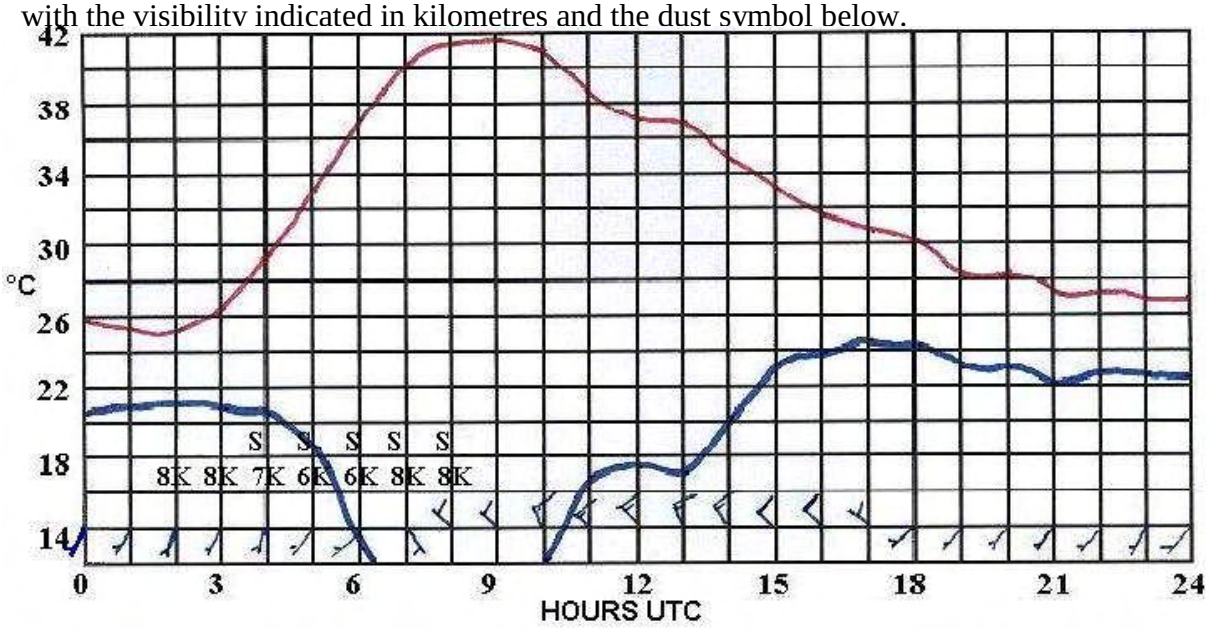

Figure 7.6. As figure 7.5, but for 2003-05-11.

Inland at Al Ain on the 10th the wind was south-easterly to southerly at 3 to 7 knots up to 0700 UTC (1 pm) when it became light variable. On the 11th the wind was north-easterly at 7 to 9 knots for most of the night, becoming south-easterly to southerly at 0400 UTC to 0600 UTC (8-10 am).

Of particular interest is that on both days the land breeze at Al Ain was stronger than at ADIA. The same applied to the sea breeze. The sea breeze reached Al Ain on the 10th at 1300 UTC (5 pm) and blew from 310° at 9 knots and changed to 340° 17 knots by 1336 UTC (5:36 pm) when it was strong enough to lift sand off the desert and reduce the visibility to 4000 metres. As happened at the coast on the 11th, the wind turned to north-westerly earlier in the day. At 0900 UTC (1 pm) it became 330° 9 knots with temporary gusts up to 22 knots at 1100 UTC (3 pm). Thereafter, it averaged 14 to 15 knots with the direction varying through

north between 270° and 060° and the visibility down to 4500 metres. A gusty and directionally variable wind is characteristic of the sea breeze (Miller 1966) and it is usually more so at Al Ain than at ADIA, as evidenced by the above comparative wind and visibility data depicted by figures 7.5 and 7.6.

On both days at ADIA the visibility became unlimited when the clear sea air arrived with the sea breeze. However, there is much more extremely dry desert dust and sand between Al Ain and the coast with ample opportunity for the wind to whip up the dust. When, at about 1600 UTC (8 pm), the wind became light at Al Ain, it enabled the visibility to improve to about 7000 metres, but no better than this due to the amount of dust remaining in suspension in the air.

Bradbury (1989) and Riehl (1979) state that due to the Coriolis force, in middle latitudes the sea breeze is deflected to the right (veers) and to the left (backs) in the northern and southern hemispheres, respectively, to the point that the wind, in time, blows parallel to the coast, thereby limiting sea breeze penetration to about 20 to 50 kilometres inland. Approaching the equator the magnitude of the Coriolis force eventually diminishes to zero. This means that near the equator the wind follows the direction of the pressure gradient and this allows the sea breezes to penetrate further inland in the tropics. This, along with a fairly even desert surface, may account for the penetration of the sea breeze as far Al Ain, which is about 150 km inland. It is worth noting that Eager et al (2005) found that the sea breeze can penetrate up to 130 km inland, while Zhu and Atkinson (2004) found that landward penetration along the UAE coast is over 250 km. On a different occasion, penetration of the sea breeze inland to Al Ain could be tracked inland on Radar by the movement of anomalous propagation echoes caused by refractive index variations at the cooler sea breeze front (figure 7.7).

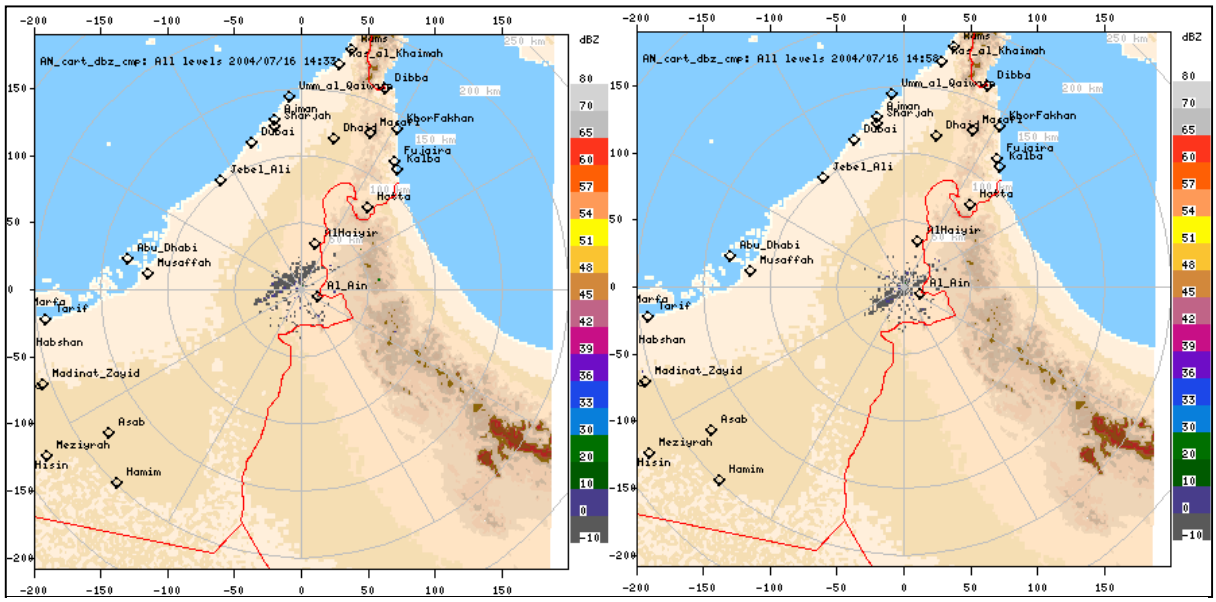

Figure 7.7. Sea breeze approaching Al Ain on 2004-07-16. As seen in the form of clutter (Collier 1989, Rhome 2003) on the UAE Department of Water Resources radar at 1433 UTC (6:38 pm) on the left and 1458 UTC (6:58 pm) on the right. The wind changed from 280° 07 knots at 1400 UTC (6 pm) to 340° 14 knots gusting to 25 knots at 1500 UTC (7 pm).

The Eta surface wind prognosis for ADIA and Al Ain bears testimony to the accuracy of the model data with respect to the onset of the sea breezes (figures 7.8 and 7.9).

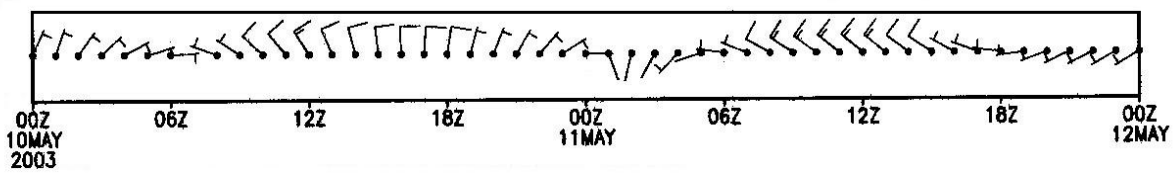

Figure 7.8. Eta GFS 2003-05-10 0000 UTC surface wind prognosis at ADIA up to T+48.

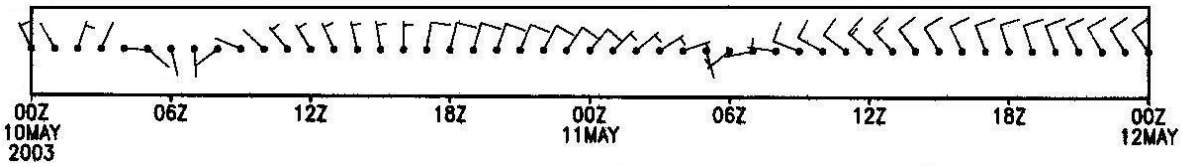

Figure 7.9. As figure 7.8, but for 3002-05-10 at Al Ain.

7.5.3 SEA TEMPERATURE

Sea and land breezes owe their existence to the contrast between land and sea surface temperature (SST) (UKMO 1997, Bradbury 1989, Hsu 1988). There was a marked contrast between surface 1.2 m air temperatures and SST during the days in question. Surface air temperatures reached 42°C and 43°C during the early afternoon at ADIA on the 10th and 11th, respectively. At Al Ain temperatures reached 44°C and 43°C on the two days. Conversely, the Gulf SST adjacent to the UAE were about 28°C to 29°C. Figure 7.10 shows the SST on the 11th. These are very similar to those of the 10th, except the area where the temperature exceeded 28°C, close to the UAE coast, was more prominent than on the 10th.

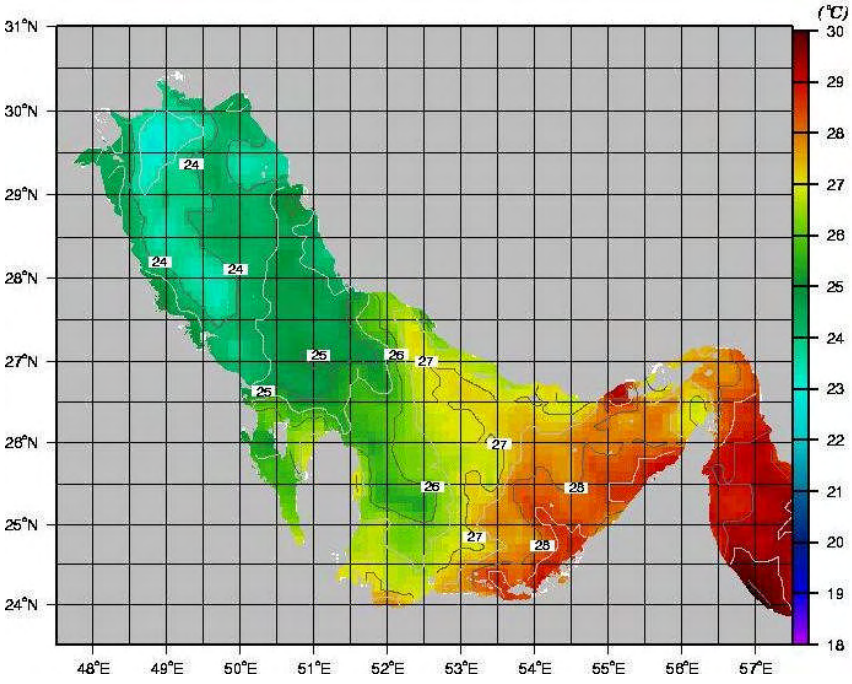

Figure 7.10. Sea surface temperature in the Gulf Sea on 2003-05-11. US Navy Oceanographic Office Multi-Channel Sea Surface Temperature (MCSST) K10 global 1/10th degree grid satellite SST composite updated daily from Polar-orbiting Operational Environmental Satellites.

On the other hand early morning minimum temperatures were very similar to the sea temperature. At Abu Dhabi these were about 28°C on the 10th and 25°C on the 11th (figures 7.5 and 7.6). This probably accounts for a very light land breeze on the first day and slightly stronger wind on the second day. However, it does not explain why the early morning wind was stronger at Al Ain, as stated in the previous section, and where the early morning minimum temperature was 29° and 27°C on the two days.

7.5.4 UPPER AIR

At ADIA the wind changed from a land breeze (of less than 4 knots) to a sea breeze when the surface temperature reached 38°C on the 10th and 41°C on the 11th (figures 7.5 and 7.6, respectively). Based on the morning atmospheric soundings (in the absence of afternoon soundings), this was when the temperature lapse rate from the surface to the top of the surface temperature inversion became dry adiabatic (figures 7.11 and 7.12).

Onset of the north-westerly sea breeze at ADIA was earlier on the 10th than on the 11th. It turned to 310° 5 knots at 0700 UTC and from 1000 UTC increased to 10 to 14 knots from 340°. However, on the 11th it began at 0800 UTC, but decreased to 7 to 12 knots, temporarily reaching 13 knots (figures 7.5 and 7.6). The earlier start of the sea breeze can probably be ascribed to the much shallower surface temperature inversion and the higher minimum temperature on the 10th (figure 7.11) than on the 11th (figure 7.12). On the 10th the inversion top was at 980 hPa (±265 metres MSL) with a minimum temperature of just under 28°C, while on the second day saw the inversion top at 930 hPa (±722 metres MSL) and the minimum temperature was about 25°C. The implication being that less radiation heating was needed to dissipate the inversion on the 10th and allow turbulent mixing with the air above the inversion and the start of the sea breeze than on the 11th.

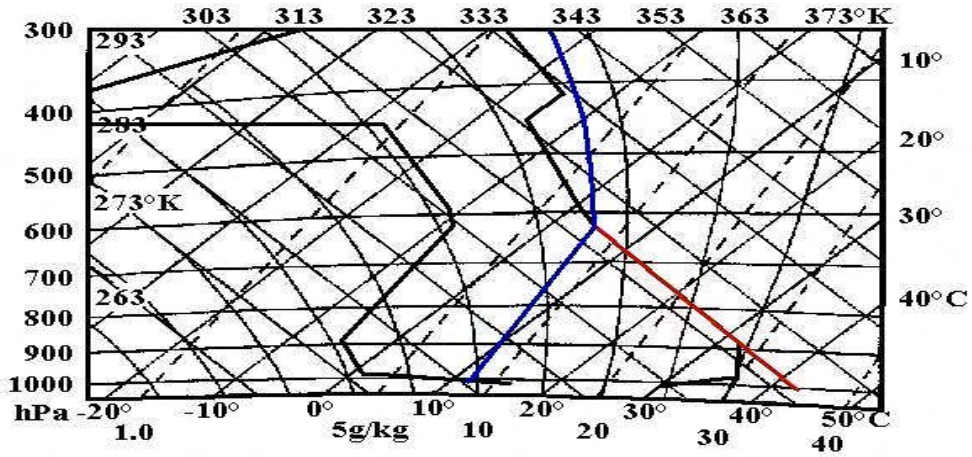

Figure 7.11. Atmospheric profile at ADIA with the low surface temperature inversion on 2003-05-10 0000 UTC. Normand's theorem adiabatic lapse rate line in red and constant mixing ratio in blue below the lifted condensation level at ± 625 hPa.

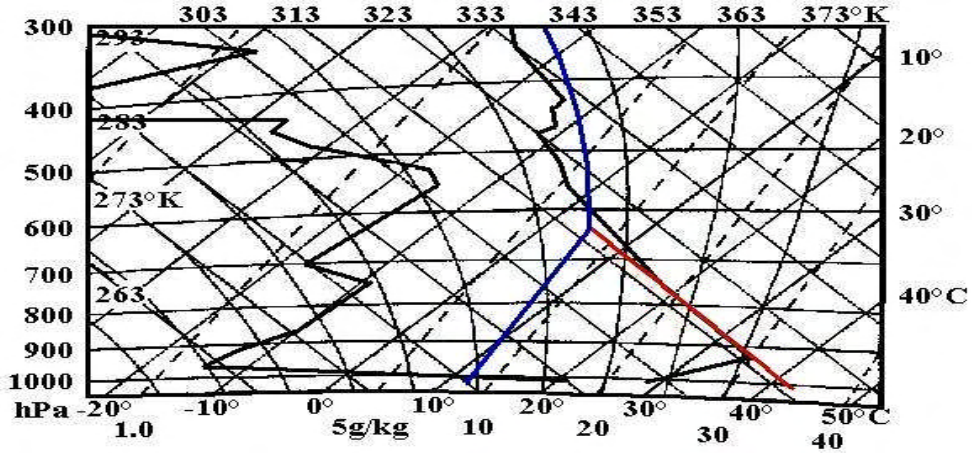

Figure 7.12. As figure 7.11, but for 2003-05-11 0000 UTC. Note the higher surface temperature inversion.

Referring to table 1, lower level winds at ADIA, on the 10th, were from the north to north-east. These appear to have been influenced by the low pressure cell to the south of the UAE with a shallow sea breeze below 500 feet in the afternoon of the 11th. The winds aloft became more northerly on the 11th, probably due to the increasing pressure gradient between the ridge to the west and the low to the east.

Table 7.1. Radiosonde wind observations at ADIA. Wind direction in degrees true and speed in knots.

	2003-05-10		2003-05-11	
metres MSL	**0000 UTC**	**1200 UTC**	**0000 UTC**	**1200 UTC**
150	020°11	050°10	010°15	345°11
300	005°14	055°08	350°18	350°11
600	055°03	225°02	350°09	360°16
900	360°08	130°04	360°10	005°21
1200	330°12	120°02	005°08	010°16

7.5.5 VERTICAL VELOCITY

Bearing in mind that the upper air circulation was anticyclonic and general subsidence could be expected, the time cross section at Al Ain shows that upward vertical velocity (w> 0; w = -gρω and ω = dp/dt (pressure coordinate system)) below 700 hPa was predicted for both afternoons with sinking air overnight (figure 7.13). This is consistent with the land and sea breeze circulation described by Hsu (1988).

The 1000 hPa wind prognosis (figure 7.13) bears testimony to the vertical movement. A northerly sea breeze is indicated in the afternoon from 1200 UTC on the 10th in association with upward motion (ω negative on the figure), changing to an easterly to south-easterly land breeze later in the night and a switch to descending (ω positive) vertical motion. This was followed by a return to a north-westerly sea breeze on the 11th with even stronger upward motion.

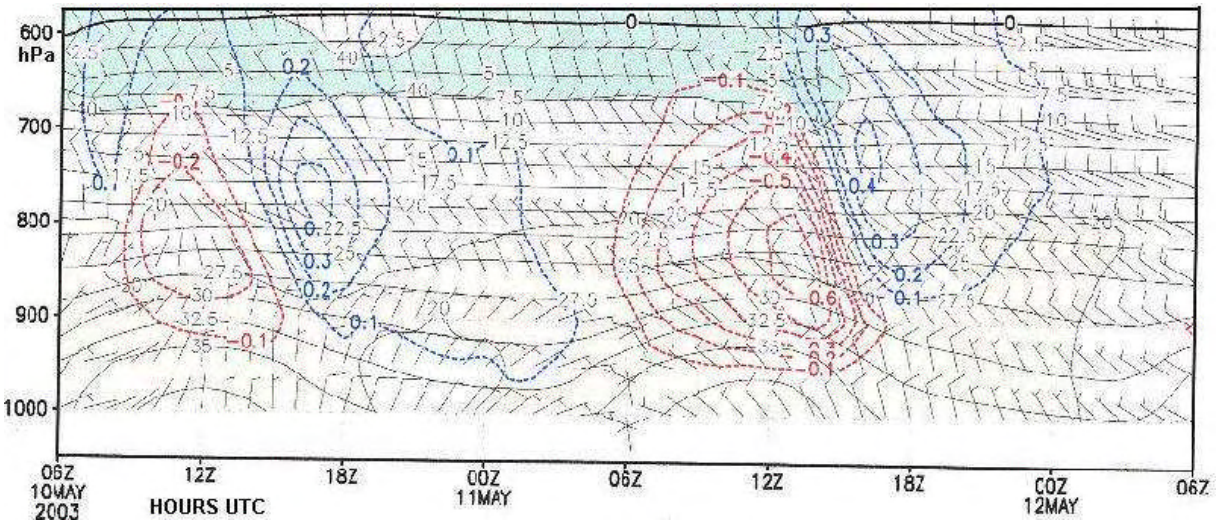

Figure 7.13. Eta GFS model run vertical motion at 2003-05-10 0600 UTC. Upward vertical motion (negative red values) of 0.6 microbars s^{-1} (0.06 Pa s^{-1}) is indicated on both afternoons, with sinking air developing overnight (positive blue lines).

It is worth noting that the model indicated stronger vertical velocity (0.06 Pa s^{-1}) on the afternoon of the 11th than on the 10th (0.02 Pa s^{-1}). This is contrary to what was expected but it should be borne in mind that the magnitude of the vertical motion is a function of the divergence field not dealt with here. On the 11th the predicted vertical velocity for the afternoon was 0.03 Pa s^{-1}. The magnitude of the model derived vertical motion is very small but in phase with the expected secondary (vertical) circulation branch of the land sea breeze system.

North to south cross sections slightly west of ADIA, at 54°E on the 11th, illustrates another view of the land and sea interaction (figures 7.14 and 7.15). The sea is north of 24°N on the cross section. At about an hour and a half after sunrise, at 0300 UTC (figure 7.14), weak upward motion is indicated below 800 hPa accompanied by a 1000 hPa south-easterly to easterly land breeze blowing from inland up to about 1° (100 km) out to sea (right to left). No subsiding air is indicated over the land.

Hsu (1988) claimed that by late afternoon, "because of (wind) velocity divergence and relatively dry air in the upper return flow of the sea breeze, there is a subsidence phenomenon near the coastal area." This is borne out by the subsiding air (positive values) indicated immediately seaward of the coast in the model prognostic cross section at 54°E at 1200 UTC (figure 7.15), with rising air (negative values) over the land south of 24°N. The model also predicted the spread of a 1000 hPa northerly to north-north-westerly sea breeze inland to about 23½°N to 23°N.

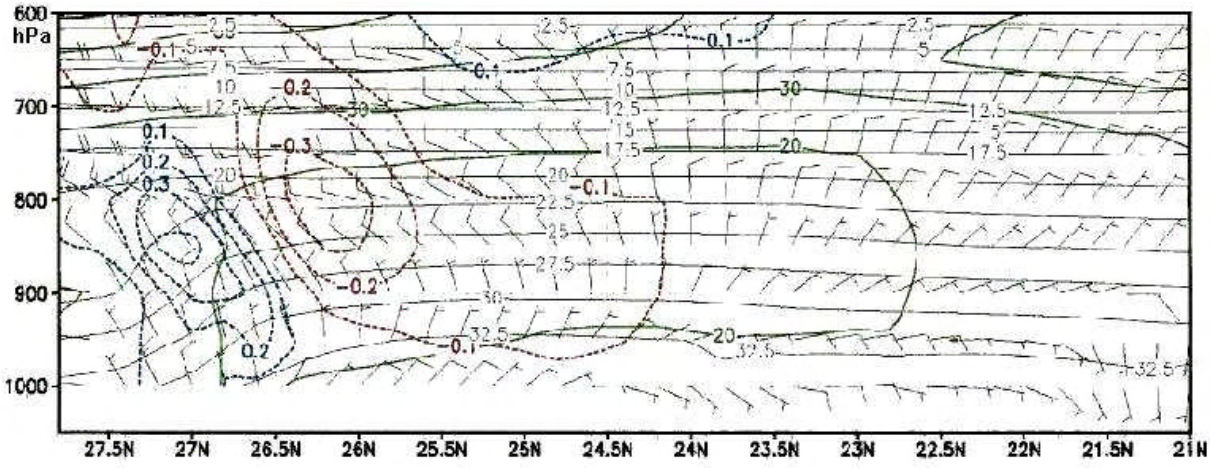

Figure 7.14. Eta GFS 0000 UTC model run cross section at T+3 at 54°E on 2003-05-11. Weak rising air (negative, red) is indicated below 800 hPa north of the coast at 24°N with a 1000 hPa south-easterly to easterly land breeze blowing about 1° out to sea.

7.5.6 INSTABILITY

The depth of the unstable layer has an effect on the distance of inland penetration of the sea breeze. Bradbury (1989) states that the best penetration occurs with dry convection from ±1830 to 2740 metres (6000 to 9000 feet), while the UKMO Source book to the forecaster's reference book (1997) specifies dry convection up to 1500 metres (4000 feet). It goes on to add that if there is a very shallow convection layer, there will be virtually no inland penetration of the sea breeze regardless of the land and sea temperature difference.

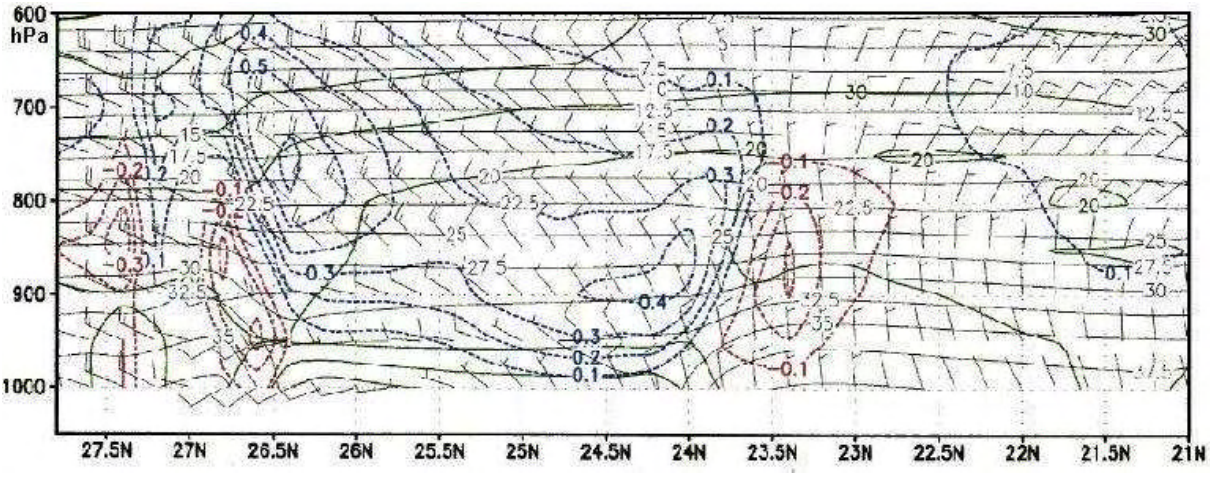

Figure 7.15. Eta GFS 0000 UTC model run cross section at T+12 at 54°E on 2003-05-11. Rising air (negative, red) is indicated below 800 hPa south of the coast at 24°N over the land with weak sinking air over the sea north of the coast.

Consider the model projected tephigrams at 0900 UTC on the 10th (figure 7.16) and 0900 UTC on the 11th (figure 7.17). Both of them reveal that with a surface temperature of 43°C, or 44°C, on either day, it was hot enough for dry air convection up to a lifted condensation level (LCL) of about 650 hPa (±3660 metres,12000 feet). This is considerably more than the limits required for inland penetration of the sea breeze as specified by Bradbury (1989) and the UKMO (1997). Despite this the sea breeze still reached Al Ain. The atmospheric soundings at 0000 UTC on the 10th (figure 7.11) and 11th (figure 7.12) at ADIA confirms this and show that deep instability in very dry air occurred later in the day. On the 10th the LCL was about 625 hPa (±3700 metres), but somewhat lower on the 11th at about 750 hPa (±2500 metres).

The UKMO Source book to the forecaster's reference book (1997) also specifies that inland spread of the sea breeze "is only likely" if the wind is less than 10 knots at 900 metres (3000 feet). This was probably so during this event if one considers the predicted wind at about 900 hPa in figure 7.14 and 7.15 between 25°N and 24°N. The observed winds at 0000 UTC on the 11th were indeed light enough, being 8 to 10 knots between 600 to 1200 metres, with 10 knots already at 900 metres. Furthermore, on the morning of the 10th the winds were 3 to 12 knots with 8 knots at 900 metres (table 7.1).

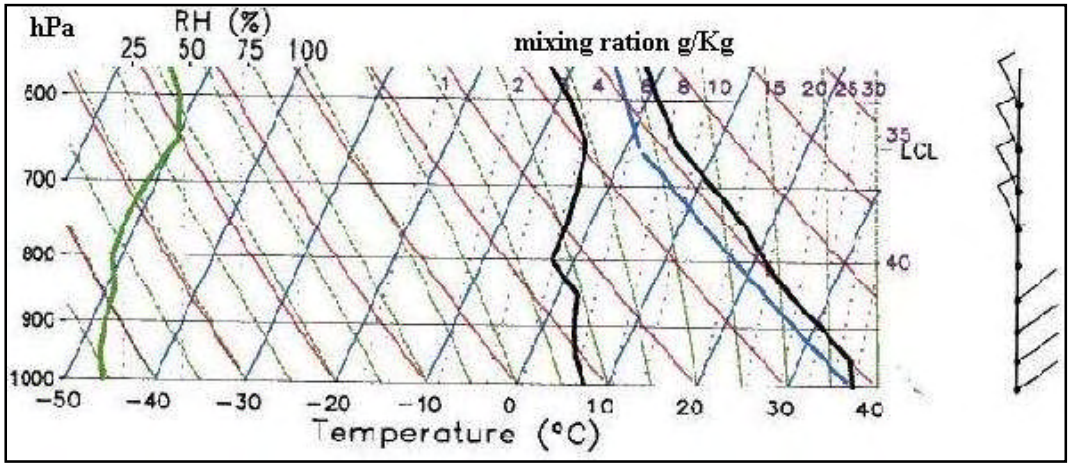

Figure 7.16. Eta GFS 2003-05-11 0600 UTC model projected atmospheric profile at 0900 UTC (T+3).

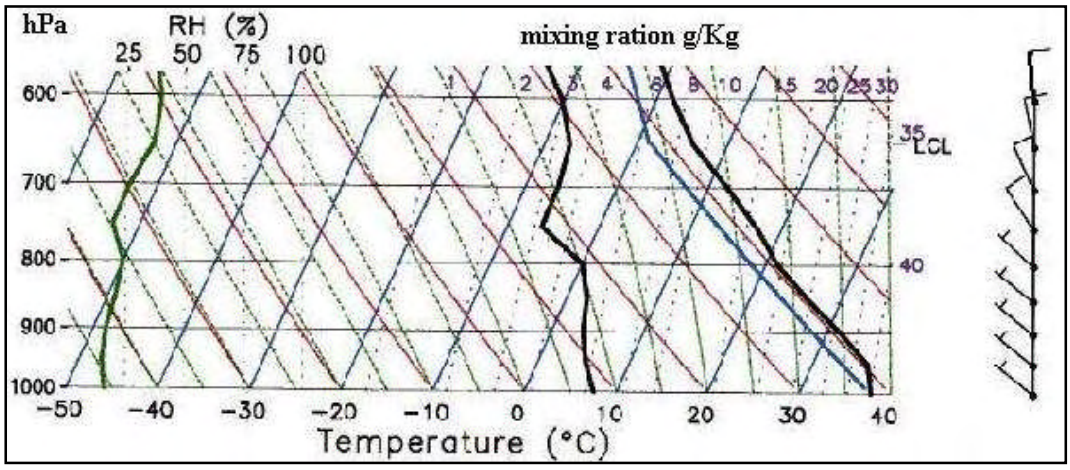

Figure 7.17. Eta GFS 2003-05-11 0000 UTC model projected atmospheric profile at 0900 UTC (T+9).

7.5.7 ANABATIC AND KATABATIC EFFECTS

In section 7.4.2 and 7.4.6 it was pointed out that the land and sea breezes were stronger inland at Al Ain than at Abu Dhabi on the coast. It is unclear to what extent anabatic and katabatic winds on the Hajar Mountain's western slopes influenced the land and sea breeze. Riehl (1954) stated that strong land breezes are common where anabatic, or katabatic, winds reinforce the thermal effect.

About 30 nm to the east of Al Ain are roughly north to south oriented Hajar mountain range. At Al Ain the early morning south-easterly to southerly land breeze was up to 7 to 9 knots while it was no stronger than 3 knots at ADIA. The difference could be due to the katabatic wind (UKMO 1997). Sinking of cool, mountain slope air at night would foster land breeze development at night. While across the flat desert to the coast, ground friction would retard the wind, as would the lack of a significant thermal gradient.

In the afternoon the western slopes of the mountain range are more perpendicularly aligned to the sun's rays than the desert floor. This results in hotter slopes, heated and less dense air in contact with the slope and an up-slope anabatic wind (Miller 1966). This could assist sea breeze penetration and account for the 3 to 4 knots stronger wind with 22 knot gusts experienced at Al Ain as opposed to ADIA.

7.5.8 DRY SEA BREEZE

On occasion the onset of the breeze at ADIA fails to increase the relative humidity. On both the 10th and the 11th the air remained dry (figures 7.5 and 7.6) with the relative humidity remaining below 20% until well after the wind increased to 14 knots and in this case the humidity remained at around 40% until the evening when air temperatures fell. The low relative humidity is attributed to the subsidence taking place in the anticyclonic circulation aloft. The atmospheric soundings at 0000 UTC on the 10th and the 11th indicate that the air was very dry immediately above the surface, particularly on the 11th (figures 7.11 and 7.12) and that this subsiding dry air mixed with the moister maritime air from the Gulf when turbulent mixing began after the demise of the surface inversion. Furthermore, boundary

layer moisture flux fields at 1200 UTC on the 10th and the 11th also confirm that the air was very dry on both days (figures 7.18 and 7.19, respectively). Lee and Shun (2003) explained that it took some time for dry continental air, already in place, to be replaced by moister maritime air.

Another peculiarity that often occurs after the sea breeze begins at ADIA, is that there is a temporary dip in the increasing humidity recorded at ADIA. This dip can be seen in the dew point temperature trace in figure 7.5 and figure 4.9 in chapter 4. An explanation for this is that the convergence zone inland carries dry air aloft and out to sea in the upper part of the circulation, where it sinks and is carried back onshore by the sea breeze (Riehl 1954).

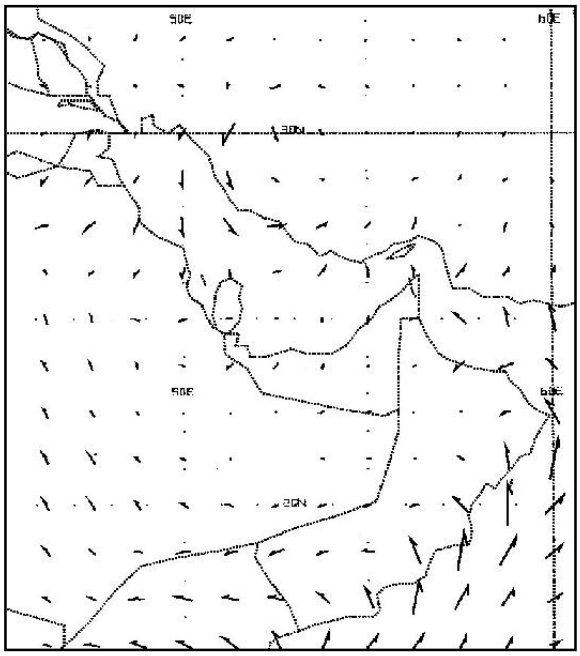

Figure 7.18. Eta GFS surface moisture flux analysis at 1200 UTC (T+00) on 2003-05-10.

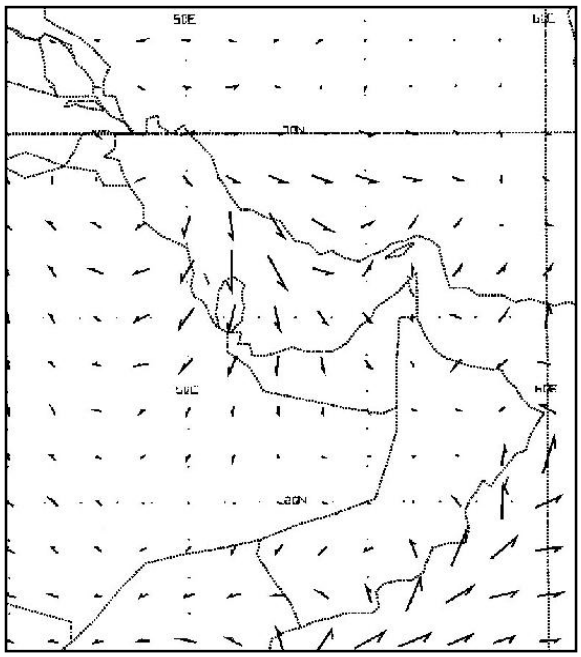

Figure 7.19. Eta GFS 2003-05-10 1200 UTC model run moisture flux prognosis at 1200 UTC (T+24) on the 11th.

7.6 FORECAST CHECKLIST

Use of the Eta NWP model post processing products give ample indication of the onset and demise of land and sea breezes.

Of particular use for forecasting the onset of land, or sea breezes, are the Eta surface wind time cross sections. In this respect the forecaster must be aware of the prevailing synoptic condition and whether this will cause the wind to blow earlier, later, stronger, or weaker.

Important considerations:

The sea breeze.

- The average sea breeze start time is 0830 UTC (12:30 local time).
- It is most likely to blow at 11 knots reaching a maximum at about 1030 UTC (14:30 local time).

- The sea breeze will be strengthened by a northerly flow such as when there is a surface low pressure cell to the east, or an anticyclone approaching from the west and will start earlier. However, under these conditions the land breeze will be weaker, start later and may not occur at all.
- The sea breeze is most likely to veer overnight through easterly to a south-easterly land breeze.
- Night minimum temperature is higher when the north-westerly wind persists throughout the night.
- Dust raised by the land breeze clears when the sea breeze begins.
- The sea breeze penetrates far inland, up to about 150 kilometres to Al Ain. This is probably due to thermal heating and the anabatic effect of the Hajar Mountains.
- The summer sea breeze is usually free of low cloud
- Low cloud that does accompany the sea breeze, more likely in winter, is usually at about 600 to 1167 metres (2000 feet to 3500 feet).

The land breeze.

- The land breeze is most likely to begin at 0100 UTC (05:00 local time)
- It is most likely to blow at about 4 knots and reach a maximum at about 0450 UTC (08:50 local time).
- The land breeze is most likely to veer late morning through south-westerly to a north-westerly sea breeze.
- The land breeze will be strengthened by the southerly flow ahead of a surface low pressure cell to the west and start earlier. However, a sea breeze will then be weaker, start later, or not at all.
- The land breeze is often stronger at Al Ain than at the coast and the sea breeze stronger and gustier. This is probably due to katabatic effect of the Hajar Mountains.

Wind strength, and its effect on the visibility, has been discussed in the chapter on dust storms.

CHAPTER 8

RAIN BEARING TROUGHS, THUNDERSTORMS AND TROPICAL DEPRESSIONS

8.1 INTRODUCTION

The UAE lies in an arid tropical zone that extends across North Africa and rainfall is in short supply, the main supply of water being from desalination plants and underground water. The mean rainfall for the UAE as a whole is around 0.1 mm in May and July in summer, but 0.3 mm in June rising to 11 to 14 mm in the winter months of December and January (UAE Climate 1996).

In winter the passage of upper air troughs from the west are the main producers of cloudy weather and rain in the area. Extensive middle layer cloud with embedded thunderstorm line squalls develop in the south-westerly flow ahead of the trough (Taha, et al 1981). Due to the high cloud base and low mixing ratio conditions below, not much rain reaches the surface, although heavy and persistent rain can occur (Membery 1997) there are more likely to be strong wind gusts with temporary sand storms may (Tantawy 1961). Apart from the aviation hazard caused by thunderstorms, more often than not, these systems drastically reduce visibility by a combination of wind blown sand, or dust and rain.

During summer, when the thermal equator and associated low pressure belt is further north, thunderstorms develop on the Hajar Mountains when an easterly wave, or trough, migrates from east to west from the Arabian Sea over the Gulf of Oman and then over the Emirates. Al-Brashdi (2007) also draws attention to the Arabian Peninsula “heat low” as an important producer of low level moisture from the Gulf of Oman and subsequent convection. The thunderstorms then drift westward from the mountains to the Gulf coast. On the rare occasion a dissipating tropical cyclone may reach ADIA. (Taha, et al 1981).

Needless to say, the occasional thunderstorm that produces about 15 mm of rain is a noteworthy event and reports of heavy rain appear in the press. The Gulf News (2003-04-18), when reporting a late winter trough thunderstorm, told of “heavy lashing downpours” in the UAE that “inundated low-lying residential and commercial areas across the country” and the “municipality pumped water from streets.” The rain recorded at Fujairah was 28 mm, ADIA 13 mm, Sharjah 12.2 mm, Ras Al Khaimah 9 mm and Dubai 4.4 mm.

What is more usual in these storms and does more damage, are strong and gusty winds. During the above event very strong winds uprooted trees, broke electricity cables, blew down billboards, demolished shacks, damaged buildings and caused trouble to vessels at sea. In Dubai two floating restaurants that were “caught up in giant waves” needed assistance. But the most amusing quote is from a farm resident who said "I was trying to cover the ply woods (sic) when one of them suddenly flew away. I quickly backed and saw them fly one by one. I also found myself little above the ground while walking towards my room" (Gulf News, 2003-04-18). A particular danger is that the runoff from a sudden thundershower in the mountains quickly fills the dry wadi beds and can catch the locals and wadi bashing 4x4

Figure 8.1. A wadi in the Hajar Mountains. The dry riverbed on the left and the road both become one and go into a narrow cleft in the rocks ahead of and slightly to the left of the motor car.

drivers unawares (figure 8.1). Wadi bashing is the popular off-road pastime of exploring wadis in luxurious 4x4's and camping in them.

Apart from investigating winter rain bearing trough systems with winter thunderstorms and summer thunderstorms, this chapter also briefly examines rare tropical depressions that occur and proposes a forecast methodology.

8.2 STATISTICS

The winter trough systems have a distinct effect on the rainfall at ADIA with most of the rain falling in the later part of the winter (figure 8.2). While the dominant effect of the middle and upper troposphere anticyclone is clearly evident in the extremely dry summer (Martyn 1992, UAE Climate 1996). The average annual rainfall at ADIA is 84 mm with the highest monthly on record, 202.3 mm, falling in February 1988, 119.9 mm of this fell in less than 24 hours on the 19th during a thunderstorm. Thunderstorms account for most of the rain in tropical deserts (Critchfield 1974) and the U.A.E is no exception.

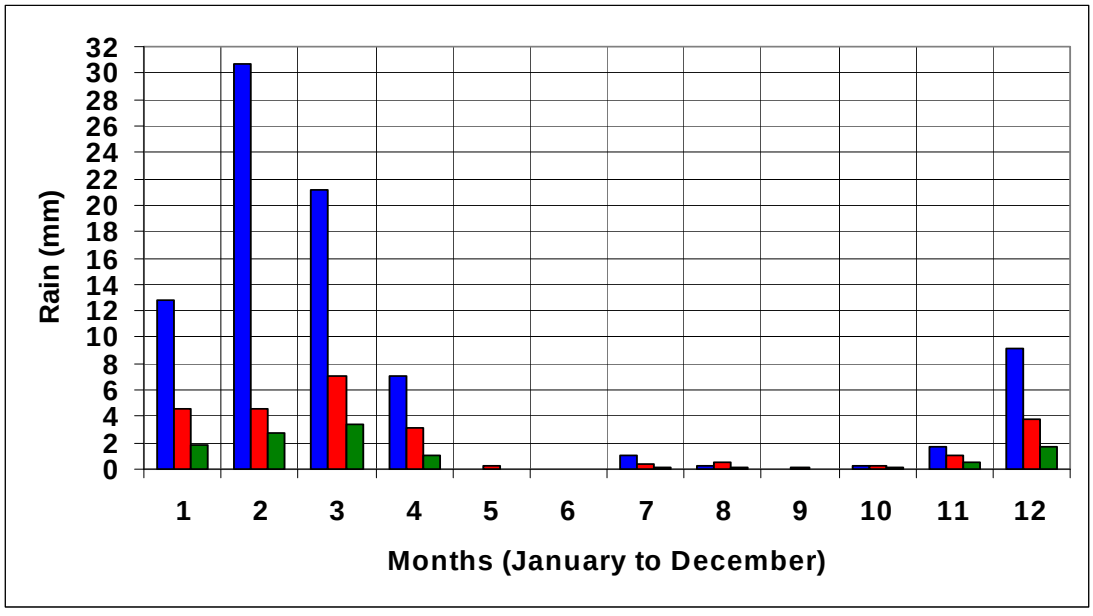

Figure 8.2. Rainfall statistics at ADIA from 1982 to 2001. The blue column depicts the mean rainfall, the red column depicts rain days (including traces) and green column days with >0.2 mm of rain.

The effect of the winter trough systems is also evident in the cloudiness at ADIA. The mean daily cloudiness (if one may be so bold to call it that) from ADIA climate data during 1982 to 2001 is between 2 to 3 oktas (eighths) in the winter months from December to March, with 1.2 oktas at the beginning in November and 1.8 oktas at the end in April. While the summer months of May to October average 0.5 to 0.8 oktas, except for July and August which increase to 1.3 and 1.1 oktas, respectively. The increase in cloud during these two months corresponds with a slight increase in rainfall (figure 8.2) and summer thunder activity (figure 8.3) drifting westward from the Hajar Mountains.

It was also noted that cloudy periods associated with the passage of trough systems at ADIA, usually lasted less than 24 hours, but may last longer. Occasionally cloudiness persisted, as happened in January 2004 when the weather was predominantly cloudy, mainly due to middle layer cloud, from the 14th to the 18th and with a few drops of rain. Thesiger (1990) writing about his epic journey by camel across the Empty Quarter in 1948, from the Oman coast through Saudi Arabia to ADIA, mentions that when west of the Sabkhat Matti, they had cloudy weather for ten days with distant thunder and lightning. It then rained "almost continuously for three days and intermittently for the next four, often with thunderstorms, especially at night."

The seasonal and geographical variation in thunder activity (and paucity) mentioned in the introduction (8.1) is illustrated by the mean thunderstorm days at ADIA on the coast and Al Ain, which is about 150 km inland (in the desert) in the eastern lee of the Hajar Mountains (figure 8.3). ADIA has a winter maximum associated with the passage of winter troughs (blue columns), which have been known to reach a maximum of 8 days in February (red columns), while Al Ain has a winter peak as well as a summer peak due to the passage of summer tropical easterly waves and orograhically induced summer thunderstorms drifting westward off the mountains (green columns). ADIA is too far downstream in the lee to feel the effect of these convection storms.

Hail has not been observed at ADIA, but it does occur, albeit rarely. On the 14th April 2003, during the passage of an upper air trough with embedded thunderstorms, a report was received of a helicopter being damaged by hail while returning from an offshore oilrig. A severe thunderstorm also produced grape size hail at Dubai on the 15th November 2004. Referring again to Thesiger (1990), after crossing the Sabkhat Matti in 1948 and heading toward the Liwa Oasis he saw where, in many hollows between the sand dunes, the rain had formed a crust on the sand and it had been pitted by hailstones.

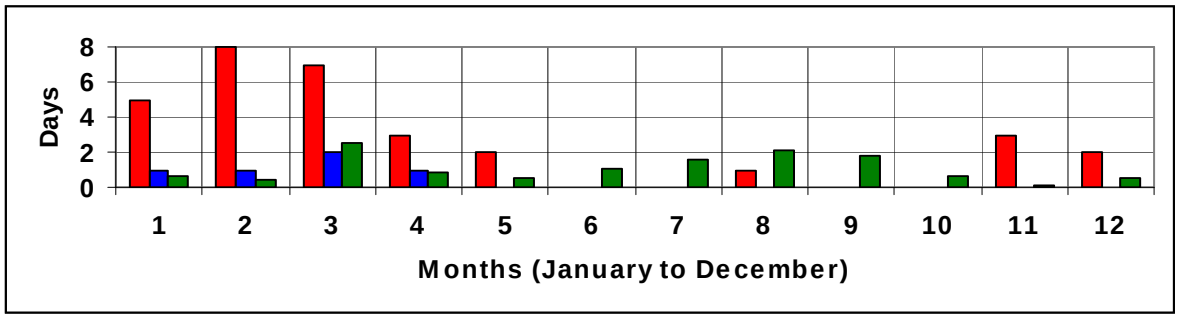

Figure 8.3. Thunderstorm days at ADIA (1982 to 2003) and Al Ain (1994 to 2001). The red columns show the highest thunderstorm days at ADIA and the blue the mean. The green columns are the mean thunderstorm days at Al Ain.

8.3 WINTER TROUGH SYSTEM: 27TH JANUARY 2004

8.3.1 INTRODUCTION

Rain fell when the tail of a baroclinic trough system passed over the Emirates. Most of the rain fell over the northern part toward the Strait of Hormuz where Ras Al Kaimah received 14.5 mm, Sharjah 11.4 mm and Dubai 11 mm. Further south, ADIA had 8.6 mm and Al Ain 4.8 mm. Fujairah, on the east coast and in the lee of the Hajar Mountains, received 1.8 mm. The rain bearing cloud band is shown in figure 8.4.

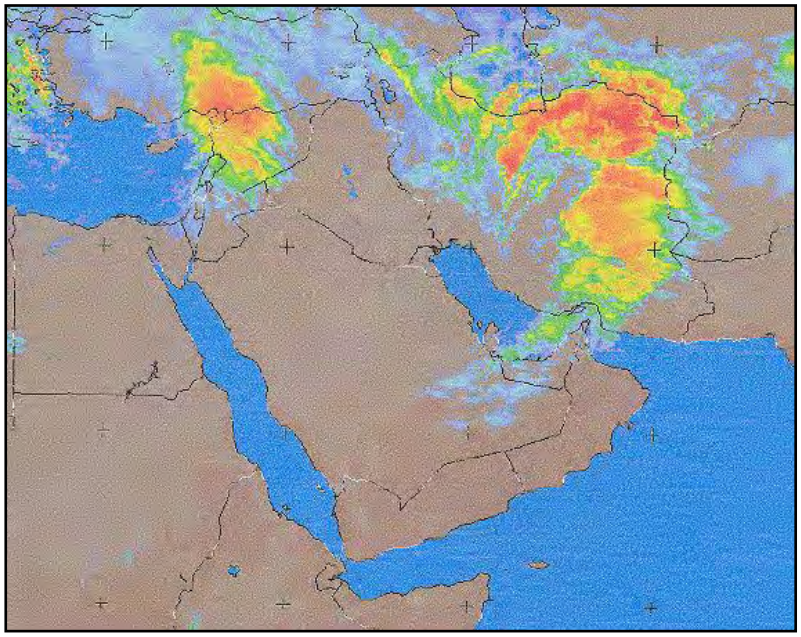

Figure 8.4. Eumetsat infrared image 2004-01-27 0300 UTC.

The significance of this event is that it demonstrates the usually fleeting effect of the systems over the UAE after crossing the Saudi Arabian desert. The cloudy weather lasted for only 9 hours at ADIA and the rain lasted for less than 3 hours. However, a few days earlier the system caused strong wind and dust storms followed by rain at Cairo and Beirut where flights were diverted. Strong winds also caused the Suez Canal to be closed for 12 hours on the 23rd (Gulf News, Saturday 24th January 2004).

8.3.2 GFS NWP MODEL

8.3.2.1 Synoptic situation

A dust event on the morning of the 26th, when visibility fell to 2500 metres in a 15 knot southerly wind, was followed, on the 27th, by a moderate to fresh north-westerly Shamal that blew at 8 to 17 knots at the ADIA following the passing of the surface trough. Figure 8.5 shows GFS model prognosis of the situation on the morning of the 26th and at 0000 UTC on the 27th immediately prior to the wind becoming north-westerly. Note the precipitation indicated over southern Iran in the right hand figure, but none over the UAE. The winds also brought a marked change in the surface air temperature. These were up to 30°C on the 26th in the southerly wind, but barely exceeded 21°C on the 27th when the northerly wind brought colder air, with the cloud aloft blocking the sun.

8.3.2.2 Upper air

At 0000 UTC on the 27th the southern tip of the upper air trough was still west of the UAE with the advance cloud band beginning to pass over the UAE. The cloudy weather, of greater than 4 oktas of middle layer cloud, lasted from 0300 UTC to 1200 UTC with the fell rain from 0530 UTC to 0830 UTC, apart from a brief light shower earlier ADIA at 0300 UTC.

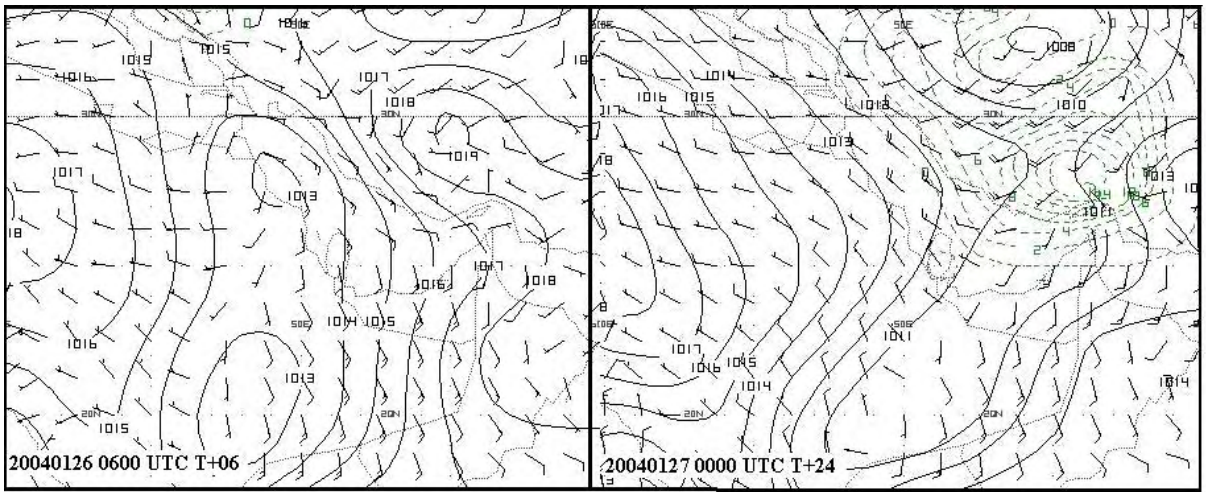

Figure 8.5. Eta NWP surface prognosis 2004-01-26/27. This shows the southerly wind at 0600 UTC on the 26th with an approaching low pressure cell and at 0000 UTC on the 27th immediately prior to the arrival of the surface ridge and north-westerly winds. The dashed green lines indicate precipitation.

Figure 8.6 at 0000 UTC on the 27th, depicts the T+24 GFS NWP model geopotential heights, wind and relative humidity at 700 and 500 hPa, respectively. Eighteen hours later at 1800 UTC the model indicated that moisture would have passed over ADIA and moved to the east. This prognosis turned out to be very good. Indeed, the relative humidity at the 700 hPa and 500 hPa levels was a better indicator of where precipitation would occur than the precipitation field in figure 8.5 at 0000 UTC. The latter showed the rain boundary to be too far to the north, although it was a good indicator where most of the rain and heavier rain fell.

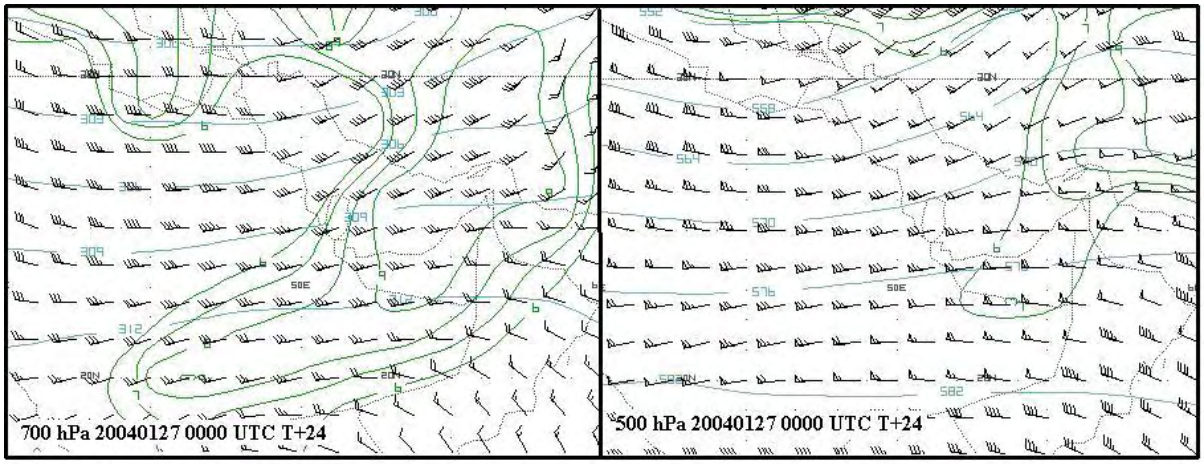

Figure 8.6. Eta GFS model geopotential heights, wind and relative humidity at 700 and 500 hPa, respectively on 2004-01-27 at 0000 UTC.

The vertical velocity and divergence fields also gave a clear indication of the time when most of the weather was to be expected. The zone of maximum upward motion is shown over ADIA at about 0600 UTC (figure 8.7). This corresponds with the predicted maximum divergence aloft at about 300 hPa below a 125 knot jet stream at 250 hPa (figure 8.8). This is nearly in the middle of the period when rain fell from 0530 UTC to 0830 UTC, as well as the cloudy period that lasted from 0300 UTC to 1200 UTC. Apart from the earlier short light rain shower at 0300 UTC, the rain coincided with the time of maximum vertical velocity in the middle troposphere and maximum upper air divergence. This divergence and vertical motion pattern is typical of a mid-latitude baroclinic trough (Membury 1997, Kurz 1994 and Petterssen 1956).

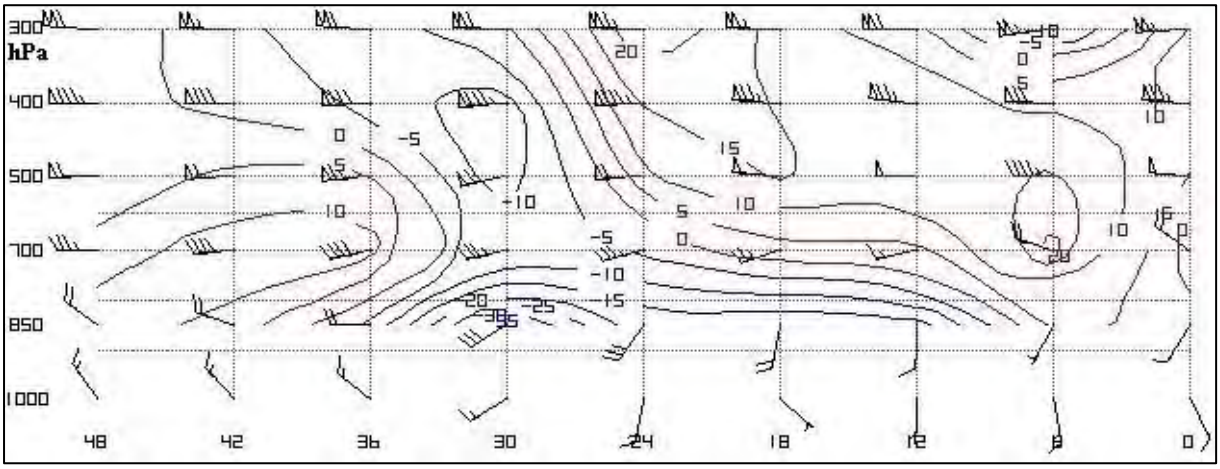

Figure 8.7. Eta vertical velocity (microbars/second) field from 2004-01-26 0000 UTC (T+0) to 2004-01-27 2400 UTC (T+48). The zone of maximum upward (negative) motion (blue) is over ADIA at about 0600 UTC (T+30) on the 27th. Pressure levels (hPa) on the left.

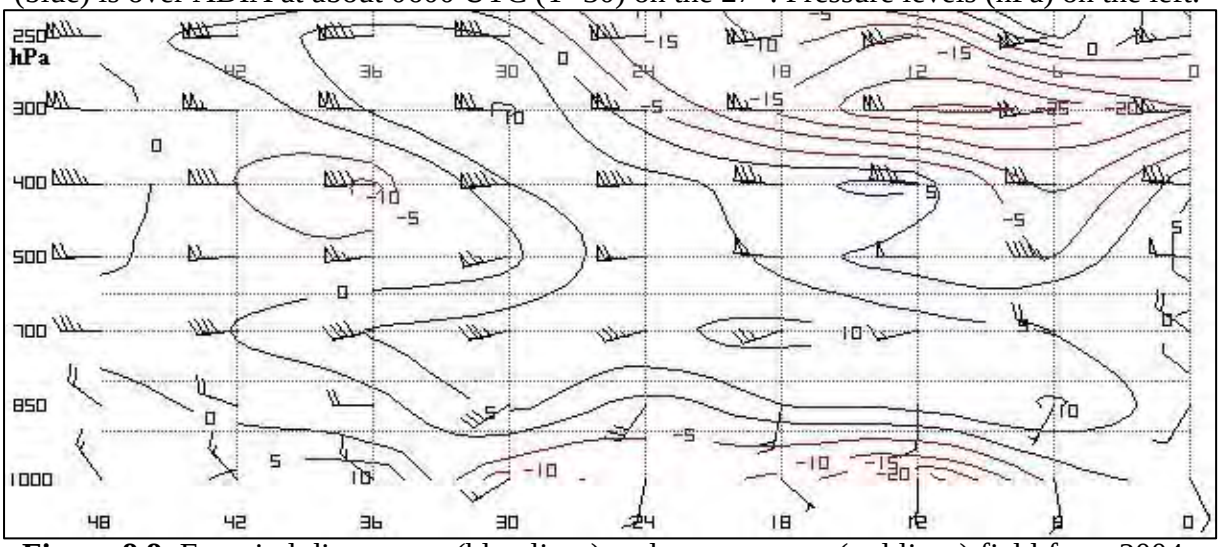

Figure 8.8. Eta wind divergence (blue lines) and convergence (red lines) field from 2004-01-26 0000 UTC (T+0) to 2004-01-27 2400 UTC (T+48). The zone of maximum divergence is shown over ADIA at 300 hPa at about 0600 UTC (T+30) on the 27th.

8.3.3 ATMOSPHERIC SOUNDINGS

That the rain fell from middle layer cloud can be seen in the sequence of atmospheric soundings at ADIA (figure 8.9). These clearly show the increase in moisture in the layer up to

900 hPa where the ambient temperature lapse rate is equal to DARL (unstable) (figure 8.9 and b). Higher conditions remained conditionally unstable with the ambient temperature lapse rate between the DALR and the SALR up to between 6 and 700 hPa. The higher dew-point (relative humidity) in this layer probably indicate the layer cloud was probably down to about 750 hPa with the tops up to nearly 600 hPa. During the passage of most intense part of the cloud band, the cloud layer probably occurred up to 340 hPa.

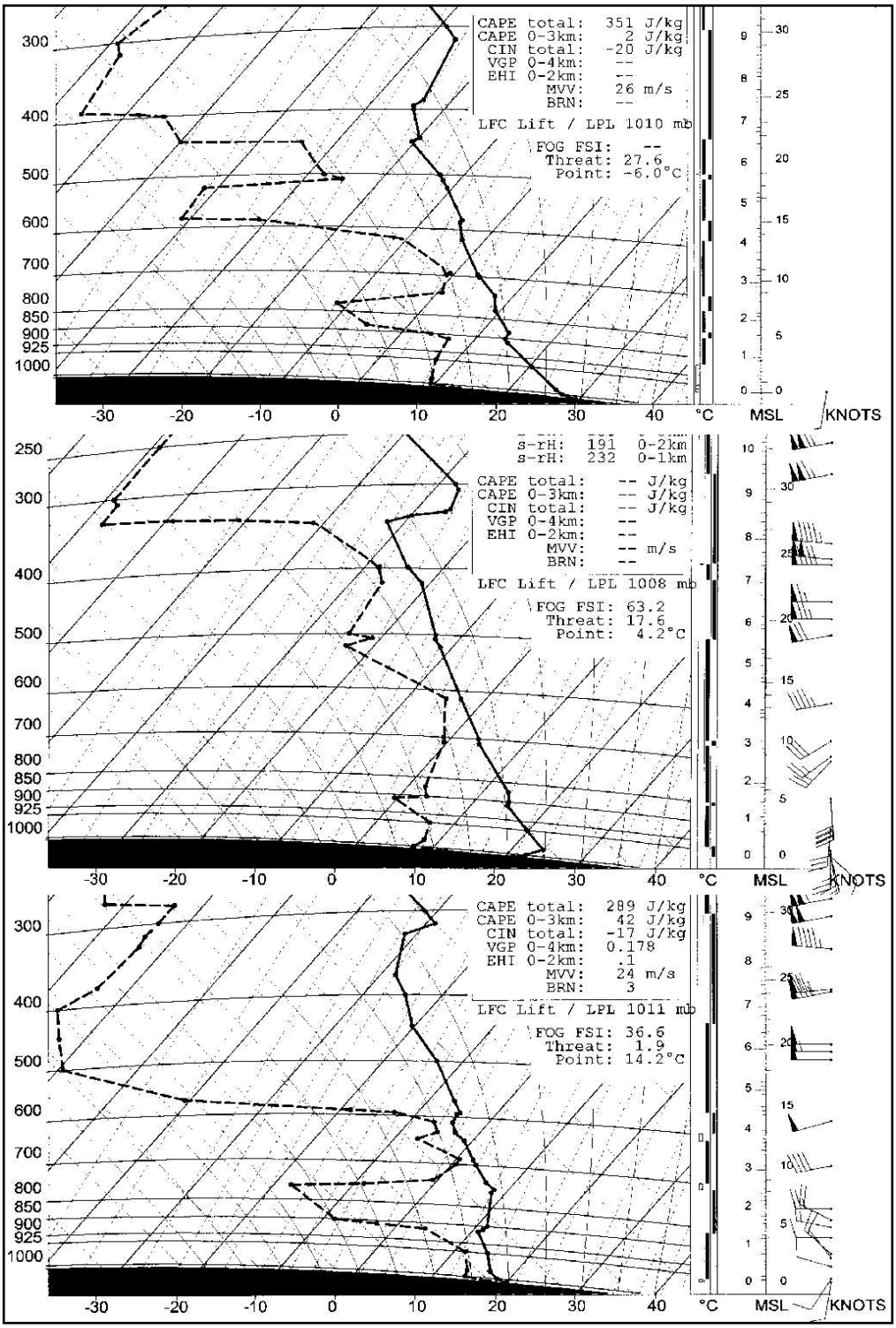

Figure 8.9. The sequence of atmospheric soundings at ADIA from 1200 UTC 2004-01-26 through 0000 UTC to 1200 UTC on the 27th.

8.3.4 RADAR IMAGES

The two images from the weather radar at Al Ain, which show most of the echoes over the northern UAE and the Oman Musandam area and the radar reflectivity data indicate that generally light rain occurred, except for some higher rainfall in the north (figure 8.10).

The fact that most of the radar reflectivity was low at 26 dBZ, with a few cells near to 40 dBZ also suggests that the rain fell mainly from layer cloud and any embedded thunderstorms were light and very isolated (as indicated in the guide in table 8.1). At ADIA portions of thunderstorm clouds and their tops were vaguely observed through layer cloud from time to time to the distant north over the Gulf Sea, but no thunder was heard, nor lightning seen.

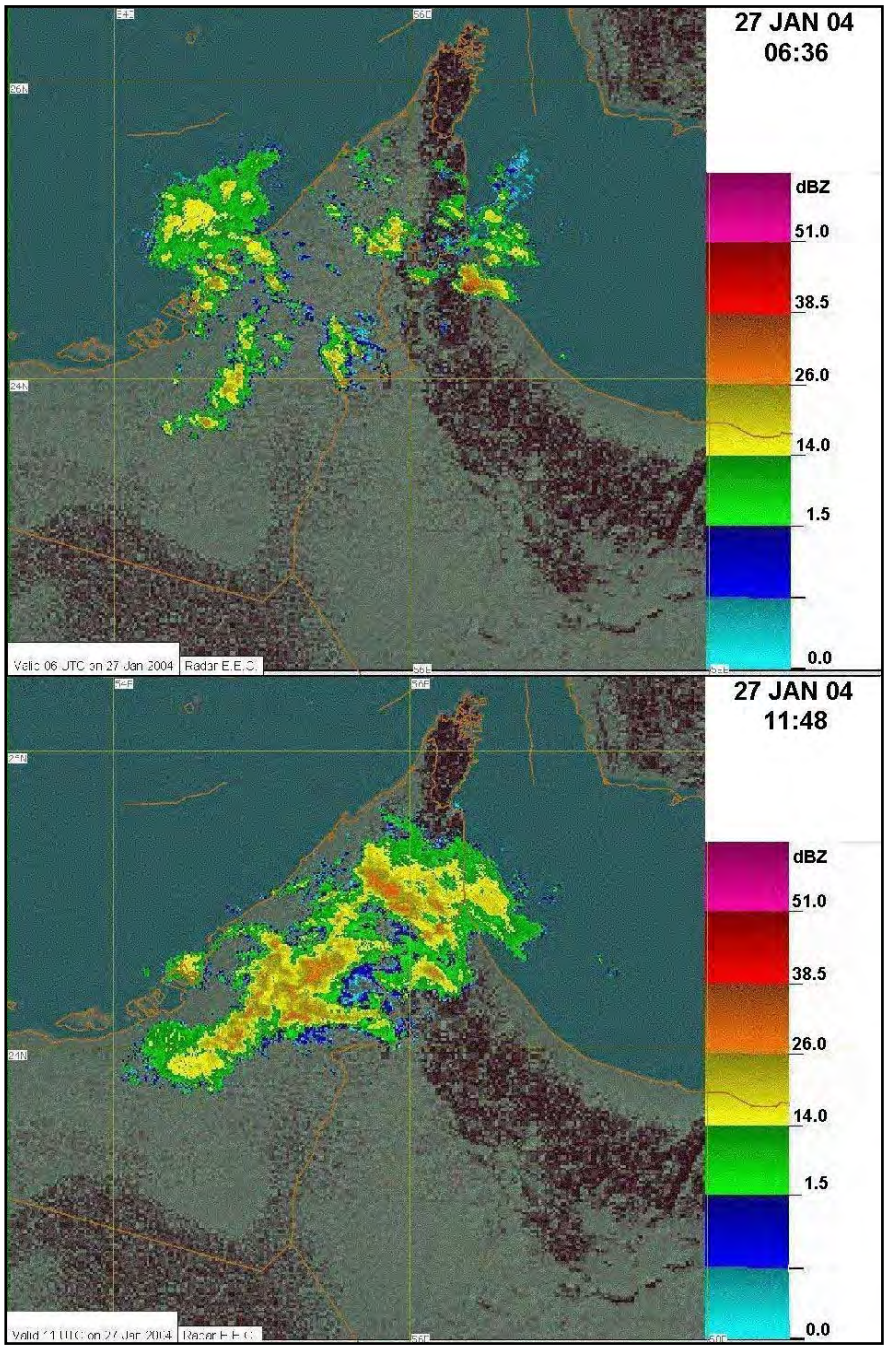

Figure 8.10. Al Ain weather radar PPI reflectivity dBZ images on 2004-01-27. Local times shown (UTC + 4 hours).

Table 8.1. Radar reflectivity dBZ and rainfall rate comparison as used by the National Center of Meteorology and Seismology (2008). The comparative values are a rough guide only.

dBZ	Comments
10	Cloud or rising sand
20	Cloud
25	Chance of light rain
30	Light to moderate rain
40	Moderate to heavy rain
45	Heavy rain
60	Heavy rain. Chance of hail
70	Heavy rain with hail

8.3.5 SUMMARY

The rain occurred when the southern tip of an intense trough system passed quickly over the region. The cloudy weather lasted less than 9 hours at ADIA and the light rain fell in less than 3 hours. The previous day a southerly wind, preceding the trough, raised dust and reduced the visibility to 2500 metres.

Post-processing products of the GFS model data gave the forecaster a good indication of when and where the rain would occur. These were the 700 hPa and 500 hPa relative humidity fields and the time cross-sections of vertical velocity and divergence.

Weather radar data at Al Ain indicated that the light rain fell mainly from layer cloud and the embedded thunderstorms were light and very isolated. This was supported by atmospheric soundings that indicated an increase in middle layer cloud and conditional instability up to the morning of the rain with drier and more stable conditions by the afternoon.

8.4 ABU DHABI WINTER THUNDERSTORM: 18TH MARCH 2002

8.4.1 INTRODUCTION

A particularly severe thunderstorm with strong winds occurred late in the afternoon of the 18th March 2002 at ADIA, in the United Arab Emirates. In the city centre the wind blew over trees and construction boards. There was also a report of large vehicles almost blown off the road. Nearly an hour later, at the airport, strong wind gusts preceding the thunderstorm produced a wall of sand that reduced the visibility to 1000 metres, which was followed by strong sustained wind and rain.

Throughout the previous night a moderate south-easterly wind blew off the desert. By 0330 UTC (07:30 am) the wind was blowing at 20 to 25 knots at ADIA and wind blown sand reduced the visibility to 800 metres. Late in the afternoon, at 1300 UTC, the wind moderated and the visibility improved to 3 kilometres.

A line of developing thunderstorms was detected by weather radar over the south-western part of the UAE about two hours prior to reaching ADIA. The storms produced radar echoes up to 50 dBZ. As a result airport warnings for heavy rain and 30 to 40 knots wind gusts were issued by the weather office more than an hour in advance.

At 1330 UTC the thunderstorm struck the airport and the wind suddenly switched to south-westerly in excess of 30 knots with gusts up to 43 knots. The visibility deteriorated to 1 kilometre in raised sand. At this time the anemometer at the threshold to runway 13 recorded a wind of 234° at 33 knots gusting to 43 knots and at the threshold to runway 31 the wind was 216° 25 knots gusting 34 knots.

Behind the gust front a swirling motion could be seen in the base of the thunderstorm cloud and shortly after this the downburst rain began. In total 9.5 mm of rain fell in 40 minutes. This is a significant amount of rain in this part of the world.

This case study, demonstrates the value of using numerical weather prediction (NWP) model information. As well as the use of some of the more common parameters, or indicators, associated with thunderstorm prediction, to identify and anticipate thunderstorm activity over the United Arab Emirates. Due to the low frequency of thunderstorms, the list of parameters and procedures is by no means comprehensive and deductions made are applicable to this case study only. Furthermore, it does not present any hard and fast rules to be adopted to forecast thunderstorms. Some common thunderstorm indicators were not available for analysis for technical reasons, perhaps the most important being the convective available potential energy (CAPE). Other more complex thermo-dynamical indicators, which produced the same results, for brevity, have not been included.

The NWP model used in this study was the United States of America National Weather Service (NWS) 1° horizontal resolution Global Forecast Service (GFS) model initialised at 0000 UTC on the 18th. Confidence in the model prognoses was raised because the model initialisation, 12 hours earlier at 1200 UTC on the 17th, presented very much the same prognosis with respect to the approaching trough. This model gave more than adequate warning of the impending weather.

8.4.2 SYNOPTIC SITUATION

The severe weather was caused by a marked baroclinic trough system. At the time of the onset of the sand storm, about 10 hours prior to the thunderstorm, a low pressure was to the immediate west and an anticyclone to east of the UAE. The upper air trough extension of the surface low leaned back well to the west and at 500 hPa it was positioned about 10° west of the ADIA. This is a situation conducive to significant upward motion over and ahead of the surface low and with surface cold air advection behind the surface low and below the trough it promotes development of the system (Holton, 1992).

8.4.3 GFS NWP MODEL

8.4.3.1 Surface

Initially, at T+0 (0000 UTC, 0400 UAE local time) the model indicated a west to east surface pressure gradient of 4 hPa across the UAE (±5° latitude) and a southerly wind of 10 to 15 knots at 10 metres. At T+06 (0600 UTC), the prognosis was for a pressure gradient increase to 5 hPa and a southerly wind of 15 to 20 knots (figure 8.11). This is consistent with the observed situation mentioned in the previous section, although the predicted wind speed was was about 5 knots too low. Twelve hours later, at T+12 (1200 UTC), the model indicated a decrease back to a 4 hPa gradient and decrease in wind speed to 10 to 15 knots.

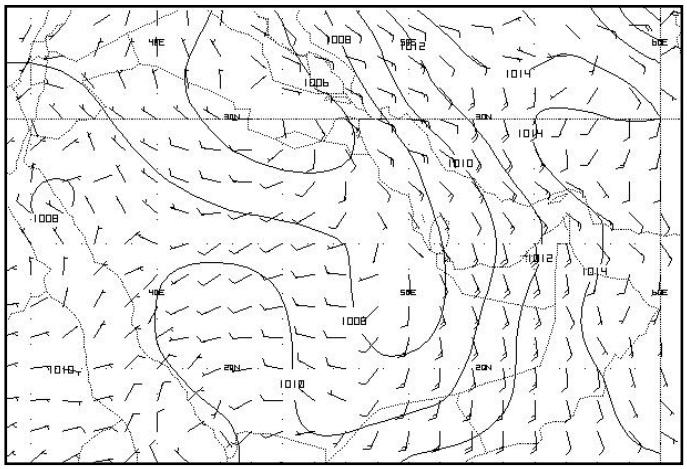

Figure 8.11. Prognosis of surface pressure and 10 metre wind 2002-03-18 at 0600 UTC (T+6). Note the 15 to 20 knots southerly wind over the UAE.

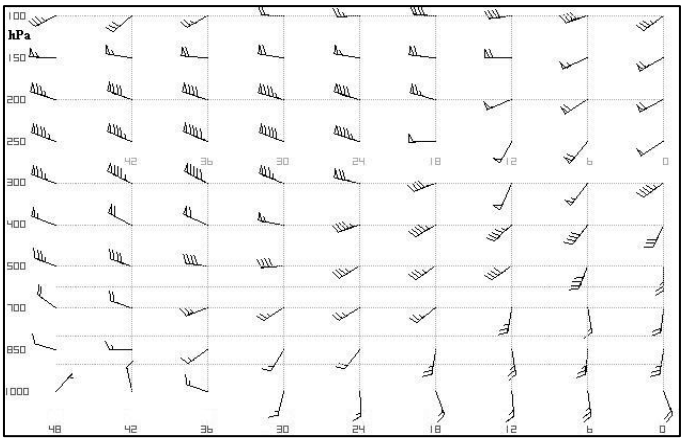

Figure 8.12 Prognostic wind vertical time cross section in knots at ADIA 2002-03-18. Note the 25 to 15 knots southerly wind at 1000 hPa at 0600 and 1200 UTC (T+6 and T+12), respectively, below from the right .

The lower level southerly winds were notable for their consistency of speed and direction, both with respect to those observed by atmospheric sounding and those indicated by the GFS model. The time cross section at ADIA shows the low level wind pattern (figure 8.12). Note, the 1000 hPa wind at 0600 UTC and 1200 UTC was the same as that observed at 10 metres (Figure 8.11)

Although the low level winds were from the south, off the desert and dry, the 1000 hPa dew-point temperature and boundary layer moisture flux fields at 1200 UTC (T+12), figures 8.13 and 8.14 respectively, indicated a marked increase in low level moisture. In this instance the 1000 hPa level was about 120 metres above mean sea level (MSL) at ADIA, compared with surface observations taken at about 27 metres above MSL. Dew-point temperatures over the UAE were expected to reach 16°C (figure 8.14). While earlier and later boundary moisture layer flux fields show that it was transported from the northward from the Arabian Sea, across southern Oman and then over the UAE.

These are in themselves, strictly speaking, not severe weather indicators, but viewed together with the 850 hPa wet-bulb potential

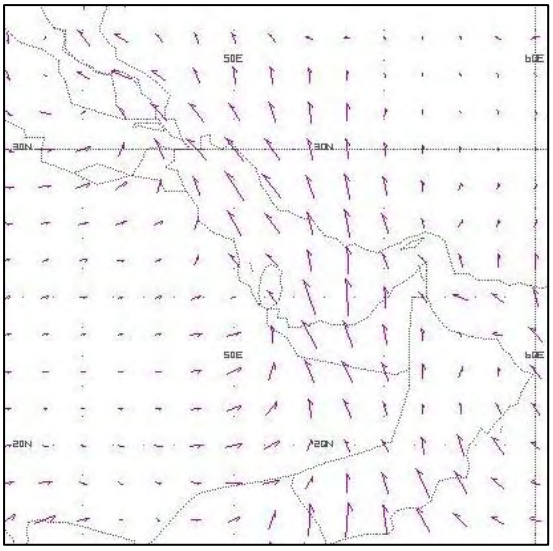

Figure 8.13. Boundary layer moisture flux at 1200 UTC (T+12).

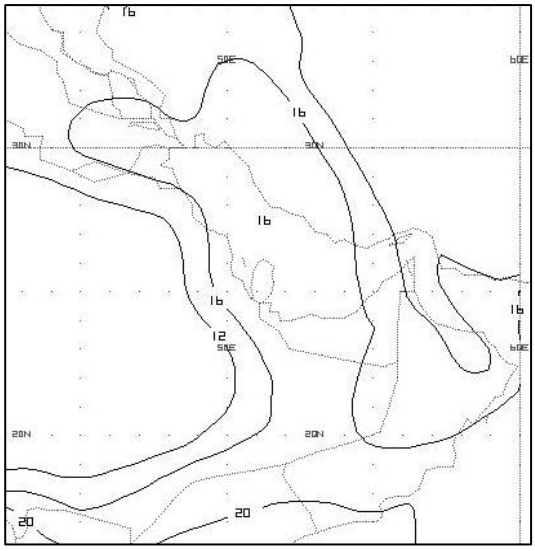

Figure 8.14. Surface dew-point temperature at 1200 UTC (T+12).

temperature (WBPT), they do indicate that enough surface moisture is available to support convective development (Membery 1997). Ample moisture combined with 700 hPa upward motion is a clear sign where deep convection is probable. Thunderstorm development will often be aligned along lines or zones of moisture convergence. Subsequent direction of movement of the storms can frequently be determined from the movement of these zones of moisture convergence. Ridges, or plumes, of higher WBPT often also determine the source region for severe storm development and they frequently develop upstream of the WBPT ridge axis. In this case study higher energy, indicated by increased 850 hPa WBPT, got it right. But, sadly, the predicted low level moisture convergence and 700 hPa upward motion failed to pinpoint the convective development. Only weak convergence was indicated west and east of where the line of thunderstorms developed and the maximum 700 hPa upward motion was predicted over southern Iran (fields not shown).

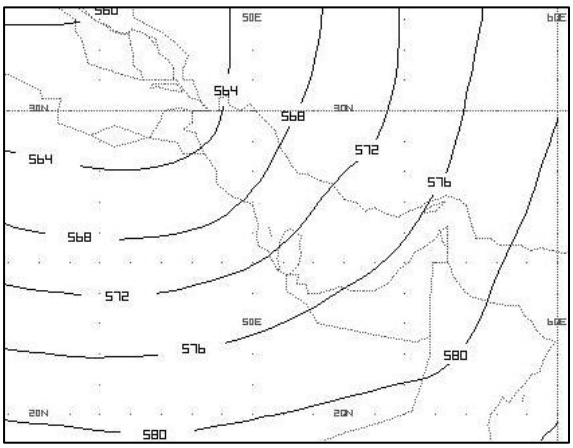

Figure 8.15. 500 hPa circulation at 1200 UTC (T+12) showing the trough west of the UAE.

8.4.3.2 Upper air

The upper air prognostic circulation at T+12 (1200 UTC) at 500 hPa confirmed the marked vertical slope of the system by placing the trough about 10° west of the UAE (figure 8.15). During the following 24 hours, moved to east of the UAE.

The time section graph for vertical velocity, between T+0 and T+12, showed an increase in middle atmosphere upward motion which lowered and became stronger ahead of the approaching trough (figure 8.16). This coincided with an increase in upper air relative humidity and it is indicative of adiabatic cooling (figure 8.17).

Maximum upward motion that continued until 1800 UTC (figure 8.16) was also coincident with areas of maximum low level convergence (negative divergence) and higher level wind divergence indicated by the model prognoses at 1200 UTC and 1800 UTC (T+12 to T+18) (figure 8.18). Convective development occurred in the south-westerly airflow ahead of the advancing trough and the prognostic maps along with the observed convective development provide a good example of Dines compensation as described by Membury (1997), Kurz (1994) and Holton (1992).

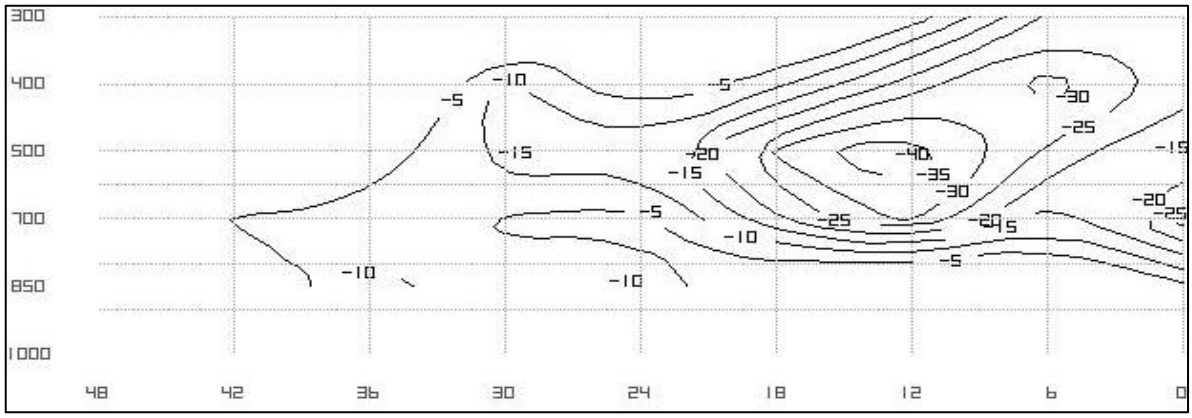

Figure 8.16. Vertical velocity (ω) time cross section at ADIA. Upward, motion (ω<0) increased ahead of the advancing trough, reaching a maximum at the time when the thunderstorm line squall passed ADIA.

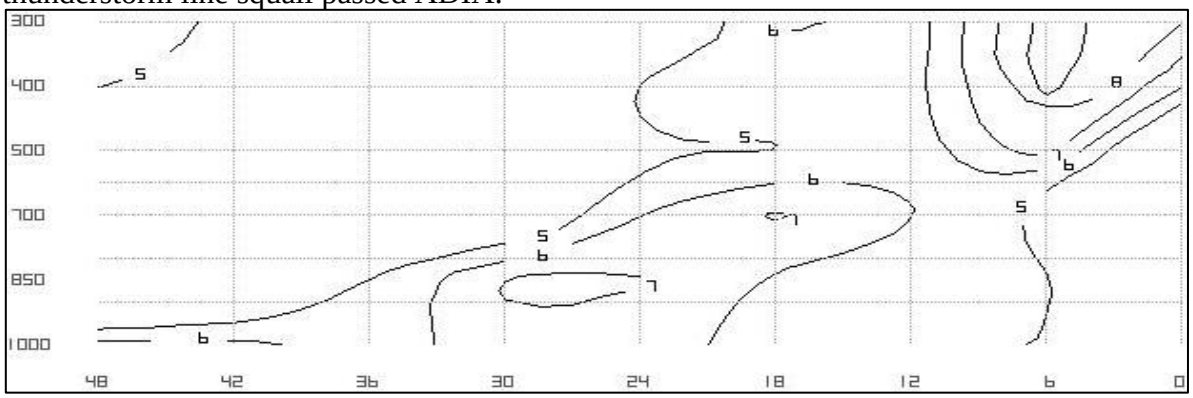

Figure 8.17. Relative humidity time cross section at ADIA. The Eta NWP model indicated increased layer moisture around the time of the thunderstorms.

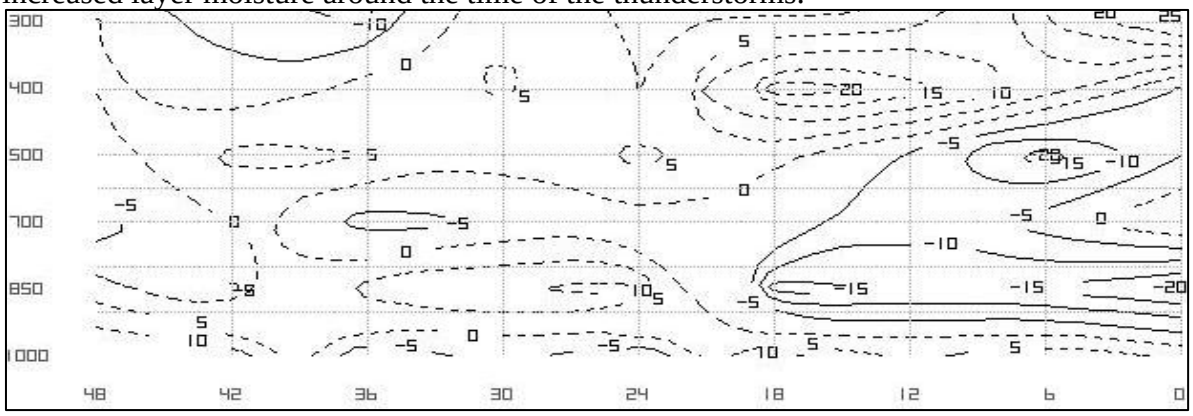

Figure 8.18. Wind divergence time cross section at ADIA, indicating low level convergence (-) and upper level divergence (+). Considering mid-level upward velocity in figure 8.16, this is consistent with the vertical motion field ahead of an upper air trough.

Areas below strong upper troposphere divergence are very favourable regions for severe thunderstorm development, in that they serve to draw air upwards and intensify a thunderstorm up draught (Eagleman 1983).

Figure 8.19 shows that a zone of 500 hPa maximum relative vorticity advection, was over the UAE in the south-westerly circulation ahead of an upper air trough at 1200 UTC (T+12) . Holton (1992) showed that when this happens rapid downwind movement of the trough (toward the UAE) will take place.

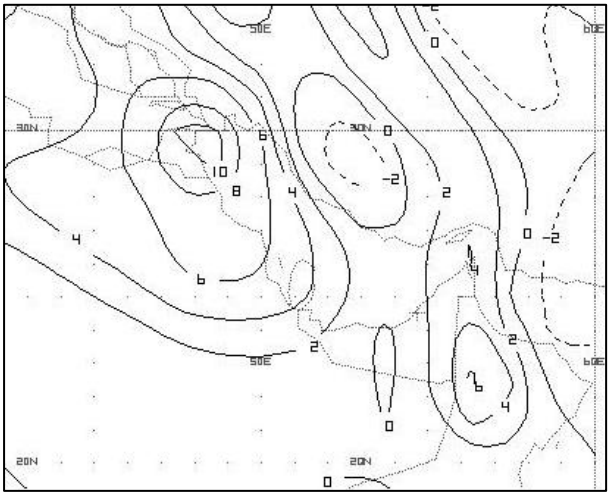

Figure 8.19. 500 hPa vorticity advection at 1200 UTC (T+12) showing a local maximum over eastern UAE and northern Oman.

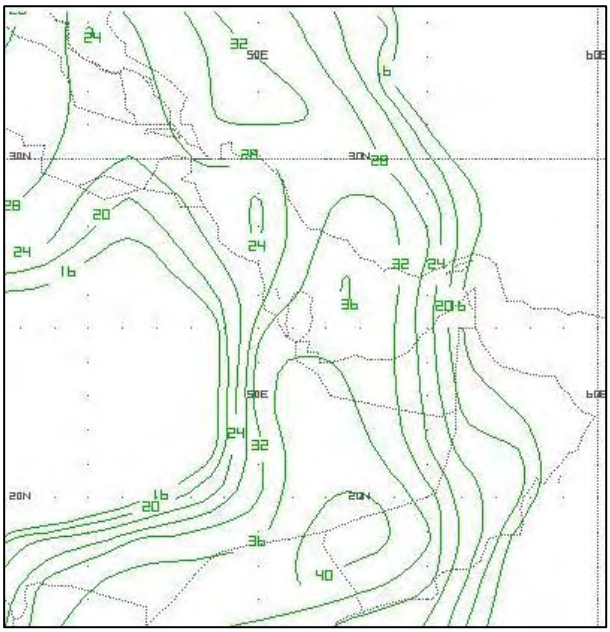

Figure 8.20. A band of increased K Index values positioned over the Gulf and the UAE at 1200. UTC (T+12)

8.4.3.3 Instability Indices

Instability indices,, computed for this day over the UAE, also indicated of the potential for the development and passage of thunderstorms. There was an increase in K Index values of up to 32 to 36 over most of the UAE by 1200 UTC, followed by a decline later as the thunderstorms moved eastward. K index values of 30 to 40 being indicative of moderate thunderstorm potential and heavy rain, while values greater than 40 indicate the high potential of heavy rain (figure 8.20).

The K Index (Appendix A) considers temperature differences between the 850 hPa and 500 hPa levels, as well as 850 hPa dew-point temperatures and 700 hPa dew-point temperature depressions. That is, index values increase with increased moisture. Note dry air at 700 hPa can result in a misleading low value. However, with a lifting mechanism and enough moisture below this level, strong thunderstorms can still occur.

Spatially, maximum Total Totals Index values (Appendix A) lagged slightly behind those of the K index. Values in excess of 30 for the 850 hPa to 500 hPa layer were indicated over the UAE with the highest values of 52 over Qatar and the extreme western part of the UAE (figure 8.21). Index values of 50 and above are indicative of scattered to numerous thunderstorms, while 46 to 49 indicates scattered development.

The index has a bias toward steep lapse rates and determines the 850 hPa to 500 hPa dew-point temperature (moisture) and ambient temperature lapse rates.

A similar spatial discrepancy to the Total Totals Index was noted with respect to the Showalter Index (Appendix A and figure 8.22), with a maximum value of –6 at 1200 UTC, which is just below the strong, or severe, cut-off mark at –7 (Sanders, 1983). This index calculates the lifted condensation level dry adiabatically from the 850 hPa level and then compares the parcel temperature with the environment at 500 hPa to determine instability.

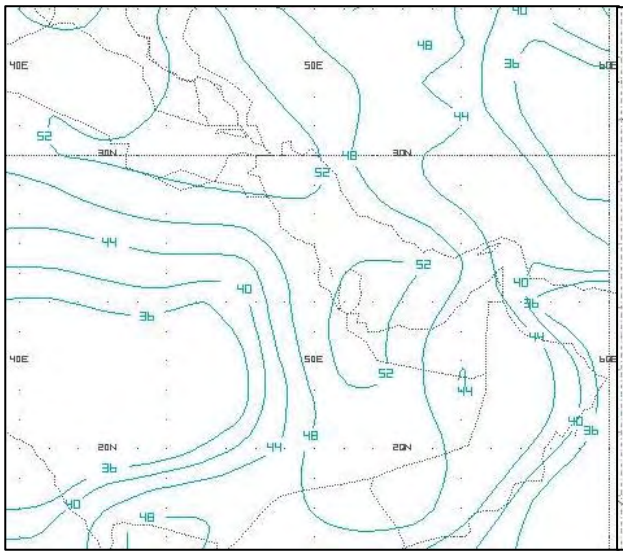

Figure 8.21. Raised Total Totals Index values over western UAE at 1200 UTC (T+12).

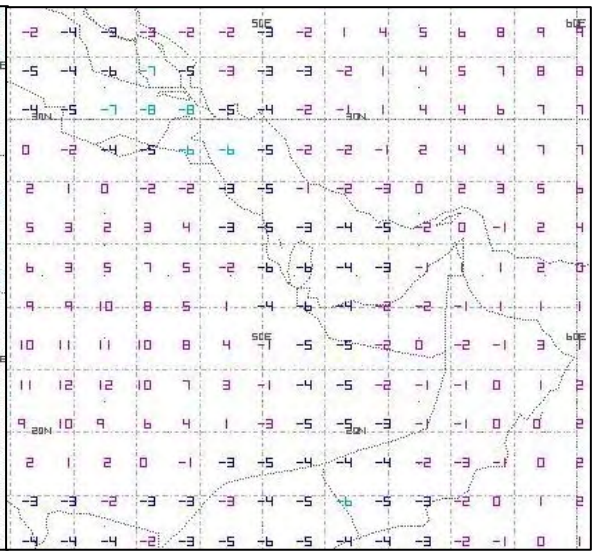

Figure 8.22. Showalter Index at 1200 UTC (T+12). Maximum negative values are over Qatar and the extreme western part of the UAE.

Over the UAE 850 to 500 hPa Lifted Index (LI) values (not shown, Appendix A) of up to –4 were indicated. Conditions are considered moderately unstable between –3 to –5, with more negative LI values indicating strong conditional instability. This index is very similar to the Showalter Index, but differs in that the lower start level can be varied. In this instance the 850 hPa base level is used.

Note, these are all empirical indices, which are adjusted for different parts of the world. Consequently significant values and intensity thresholds will vary from region to region.

8.4.3.4 Relative vorticity and dry line

Cyclonic relative vorticity plumes (positive in the northern hemisphere, negative in the southern hemisphere), particularly along an upper air trough axis, as well as in the lee of the axis, are often present with a plume of drier, colder air. This is often referred to as a dry slot that can be seen on water vapour imagery (Lemon 2001). This cold, dry slot can be entrained into deep convection, where the resultant evaporative cooled downdraughts cause strong wind and gusts at the surface (Sanders 1983). Certainly in this instance, strong winds and gusts were experienced at the airport and in the city.

The dashed lines in figure 8.23 show that a plume of cyclonic relative vorticity was indicated, but it was to the west of the UAE at about the time of thunder activity. Better positioned is the elevated dry line at 4267 metres (14000 ft), indicated by the thick red lines over the

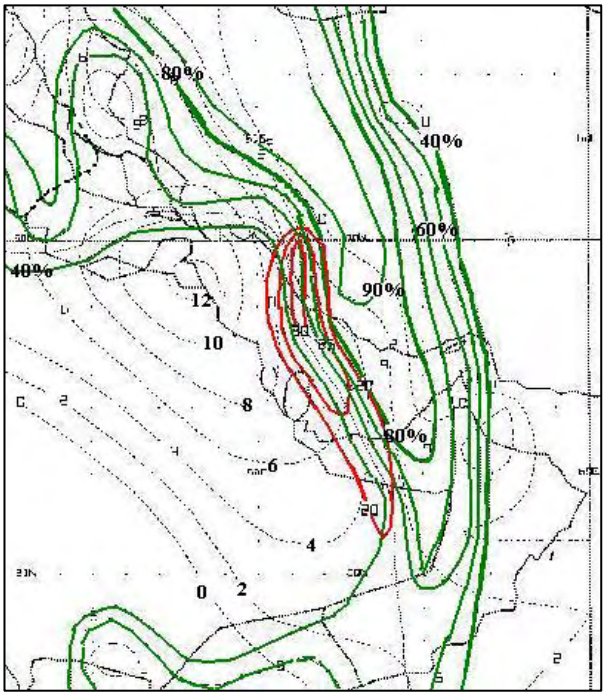

Figure 8.23. Cyclonic vorticity (dashed line), elevated dry line (red) and 600 hPa relative humidity (green) at 1200 UTC (T+12).

western UAE and the central Gulf, as well as the 600 hPa relative humidity shear from 80% to 40% over the western part of the UAE (green lines).

8.4.3.5 Lapse rate

The steeper the lapse rate the greater the atmospheric instability. McCaul (1987) showed that instability in the 850 hPa to 700 hPa layer is a good indicator of the potential for dry microbursts. The closer the ambient temperature lapse rate gets to the dry adiabatic lapse rate (9.8°C/km, 3°C/1000 feet,), the greater the risk of microbursts. When the ambient temperature lapse rate becomes less than 5.5°C/km (±1.7°C/1000 feet) the layer is considered stable.

In this instance the lapse rate was 0.6°C/km (figure 8.24a), indicating conditional instability and almost stable conditions. The stability criteria proved to be correct and valuable because rain accompanied the thunder and there was no evidence of a microburst, dry or otherwise. A strong gusty wind spread ahead of the thunderstorm as a gust front. Wallace and Hobbs (1977) point out that the downdraught is usually strongest and deepest just behind the gust front. Apart from one report of a 40 knot wind on approach to the runway at ADIA, the lack of any aircraft wind shear reports seems to confirm that there was no microburst. However, given the lack of surface observational data the presence of a microburst cannot be ruled out completely.

Mid-level instability, in the 700 hPa to 500 hPa layer, has an effect on hail growth. Moderate instability in this layer favours large hail growth, while strong instability favours stronger upward velocity and the greater risk of dry air entrainment. At about the time of the thunderstorm, the model indicated about 6.4°C/km for the 700 hPa to 500 hPa layer over the UAE and slightly higher to the east (figure 8.24b). In the absence of observed hail, it would seem that the instability present favoured dry air entrainment, rather than hail growth. This in turn supports the evidence presented in the section on relative vorticity and dry line and the strong gusty winds that occurred.

8.4.3.6 Wind shear

In simple terms wind shear tends to destroy up and down draughts and it is not generally conducive to single cell air mass thunderstorm development (Agee 1982, Bennetts, McCullum and Grant 1986, Eagleman 1983). However, in strong up draught forcing, wind shear fosters up draught rotation and storm intensification. The wind shear necessary is generally accepted as having to be >40 to 50 knots within 4 to 6 km AGL (Weisman and Rotunno 2000). Supercell propagation to the left (right) is favoured when the shear vectors turn counter clockwise (clockwise) with height and the shear strengthens (Bunkers 2002, Doswell and Evans 2003). The red lines in figure 8.25 show that higher wind shear values of

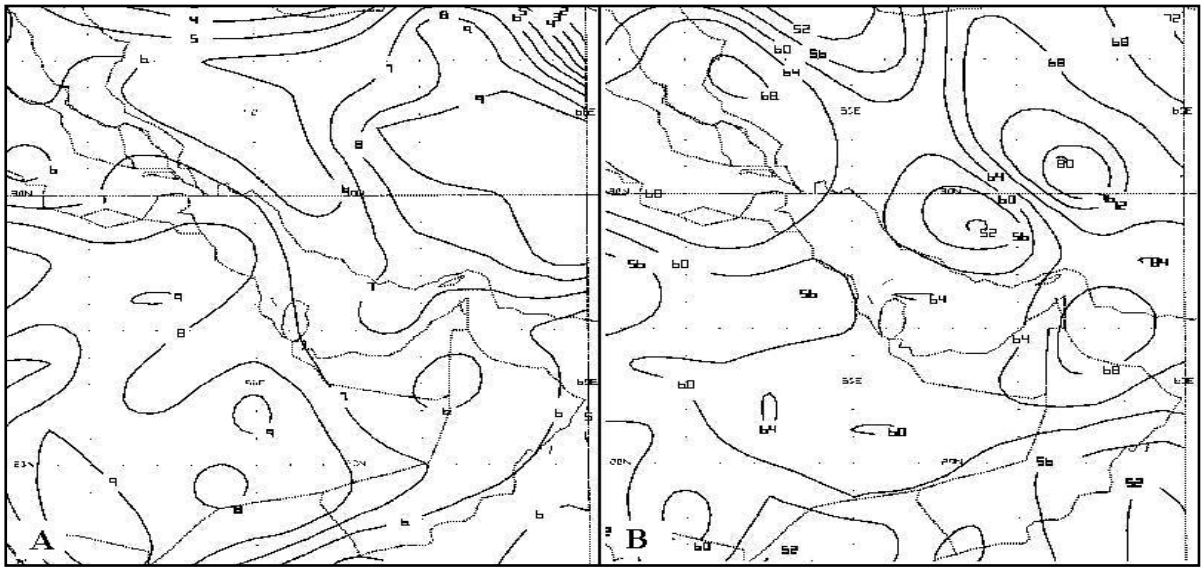

Figure 8.24a and b. Lapse rates (a) 850 hPa to 700 hPa at 1200 UTC (T+12) and (b) 700 hPa to 500 hPa at 1200 UTC (T+12).

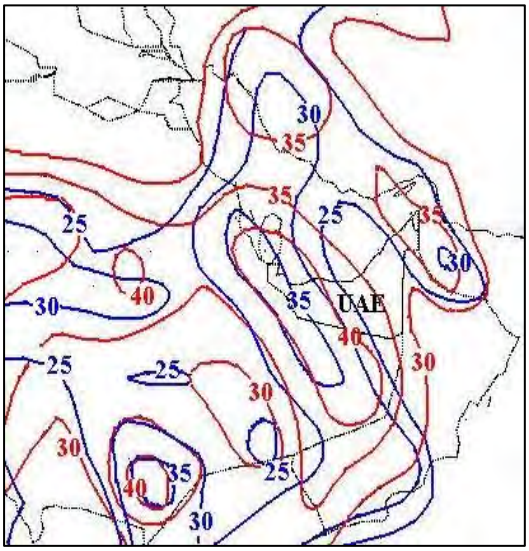

Figure 8.25. Wind shear from the surface to 500 hPa (red lines) and the surface to 600 hPa (blue lines) at 1200 UTC (T+12).

30 to 35 from the surface to 500 hPa were predicted over the UAE, with higher values, up to 40, in the west. Between the surface and 600 hPa (blue lines) values of 25 to 30 were predicted, with up to 35 to the west of the UAE. Marked veering and increased wind speed was also predicted (figure 8.12), although speed increase was only about 25 to 35 knots. Therefore, there was enough wind shear to foster vigorous development, but not enough for a supercell thunderstorm.

8.4.4 SUMMARY

The most important conclusion reached is that the GFS NWP model gave adequate advance warning of the development and passage of a significant baroclinic trough system over the UAE, with thunderstorms. The model also indicated the potential for the thunderstorms to be severe. Considering this desert region and infrequency of thunderstorms, the model prognoses and the derived parameters faired fairly well. The model also predicted the development of the preceding strong southerly winds that gave rise to a dust storm.

Meteorological parameters associated with a synoptic scale baroclinic system, such as vertical velocity, divergence and relative vorticity and humidity, also correctly indicated the development of convection in the south-westerly flow ahead of an advancing trough. Instability indices, notably the K Index, Lifted Index, Total Totals Index and Showalter Index, all served to warn that thunderstorm development was imminent and significant, although, the Total Totals Index and Showalter Index indicated convection spatially slightly to the west of the area where the maximum development occurred. The elevated dry line and

600 hPa moisture shear gave a clue to the potential for strong and gusty wind conditions as did the instability of the 700 hPa to 500 hPa lapse rate.

This convective system had all the ingredients to produce heavy rain described by Membury (1997). Namely, low level flow anticyclonic flow of moist air advected from the Arabian Sea with upward motion under a strong jet stream ahead of an eastward moving mid-tropospheric trough. Under more favourable conditions, that is, greater instability and higher humidity, this system could well have produced the copious rain mentioned in his study when a slow moving trough system produced 131 mm at Dubai and 283 mm fell at Khasab in December 1995.

8.5 SUMMER THUNDERSTORM: 7TH SEPTEMBER 2003

8.5.1 INTRODUCTION

In summer an area of surface low pressure exists over Arabia, the Arabian Sea and across to northern India, which is a trough extension of the summer heat low pressure area centred over the Asian continent (Rao, et al 2003). This generates the general south-west Monsoon flow (the Khareef) over southern Arabia toward the Indian continent, seen here in the surface analysis at 0600 UTC on the 14th August 2003 (figure 8.26), that is, nearly a month earlier than the case study about to be discussed.

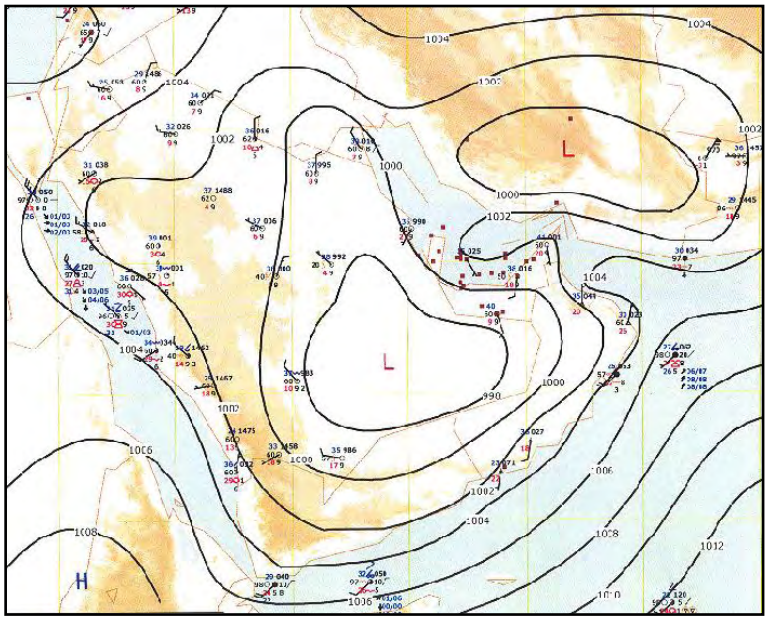

Figure 8.26. Surface analysis at 0600 UTC on the 14th August 2003.

Above 700 hPa a well developed anticyclonic circulation over northern Arabia replaces the winter westerly circulation over the region with a summer easterly to north-easterly flow, particularly at 500 hPa and 300 hPa (Hastenrath 1985). The anticyclone maintains strongly stable and subsiding conditions (UAE Climate 1992, Garbell 1947). Summer thunderstorms are triggered by the Hajar Mountains protruding into this easterly flow. The mountains being both an elevated diurnal radiation heat source and causing topographic uplifting as the air is forced to rise over the mountains (Bradbury 1989). The thunderstorms that develop are then steered to the Gulf coast by the 500 hPa easterly steering winds (UKMO 1997). This is particularly so when a low pressure cell, or easterly wave, migrates from east to west from the Arabian Sea over the Gulf of Oman and then over the Emirates.

The Hajar Mountains are subdivided into the north-south oriented Western Hajar Mountains in the north and the north-west to south-east oriented Eastern Hajar Mountains further to the south-east in Oman. The thunderstorms that form on the Western Hajar Mountains are the ones that influence the weather over the UAE.

8.5.2 GFS NWP MODEL

On the 7th the GFS NWP model indicated that thunderstorms were a distinct possibility. Low level moisture advection was indicated within an area of higher 850 hPa potential temperature and 700 hPa upward motion (figure 8.27a). All were concentrated over the mountains and northern Oman. Other parameters concentrated in the same area and favourable for development were the Total Totals index, the K index (figure 8.27b) and the Showalter index (figure 8.27c). Due to the parcel method used by the Showalter Index this product always indicates raised negative values over the warm Gulf Sea and these are ignored, unless they are supported by other criteria.

Lower winds over the UAE are usually south-westerly due to the thermal low over the Arabian Peninsula (figure 8.26). Ascending, the thermal low is replaced by an anticyclone and the wind backs to north-easterly becoming easterly above 700 hPa. In these conditions, thunderstorms that develop on the mountains slopes would tend to remain there, or drift to the west, or south-west, in these steering winds (Bennetts, McCallum and Grant 1986). The thunderstorms that develop in the north-easterly flow above 700 hPa tend to remain on the Oman part of the mountains, especially where the Hajar Mountain curve to the east and are almost perpendicularly oriented to the upper airflow. On the 7th, the predicted wind circulation at 700 hPa and 500 hPa (figures 8.27d and 8.27d) was 5-10 kn north-westerly and 10 kn northerly, respectively. Therefore, the thunderstorms were expected to either remain over the mountains, or drift southward away from the UAE to Oman.

Further factors promoting thunderstorm development on the mountains is found in the time vertical motion cross section at Al Ain (figure 8.28). Marked upward vertical velocity is indicated in a south-westerly flow toward the mountains at 1200 UTC on the 7th enhanced by topographic lift against the mountains. Note the veering of the wind to north-north-easterly at 500 hPa. The change in wind direction with height from the surface was very similar to the synoptic situation nearly a month earlier, on the 14th August 2003 (figure 8.26), when isolated thunderstorms also developed on the Hajar Mountains.

8.5.3 RADAR IMAGES

Thunderstorms developed on the western Hajar Mountains from 1000 UTC. The radar images from about 1420 UTC to 1630 UTC (figure 8.29) show the position of isolated cells, some of which had cores of around 40 dBZ. The images also show the most common location of the cells. That is, mainly on the Hajar Mountains in Oman, although they do develop further north into the Musandam Peninsula section of the mountains. Of note, in chapter 6, is the satellite image during the dust storm on the 12th December 2003 that shows the remnants of a thunderstorm on the northern tip of the peninsula (figure 6.33).

These thunderstorms tend to develop after 1000 UTC (14:00 local time) and have usually dissipated by 1500 UTC (19:00 local time). The cells tend, for the most part, to be very

isolated and not very intense. Although radar echoes of up to 50 dBZ are not uncommon, it is speculated that dust contamination contributes to the stronger reflected radar signal, as the rainfall measurements often do not reveal heavy precipitation. Observations also indicate that the storms are usually sparse and generate more dust than rain at ADIA.

As is often the case, the storms shown in the radar images were semi-stationary in the vicinity of the mountains. If the steering winds at 700 hPa and 500 hPa are easterly, and the thunderstorms drift toward the Gulf coast, more often than not they collapse shortly after leaving the highlands and Altocumulus and Cirrus anvil remnants drift to the Gulf Sea coast. Evidence of this is the higher incidence of summer thunderstorms at Al Ain, near to the foothills of the mountains, than at ADIA on the coast (figure 8.2). Sometimes they drift to Ras Al Kaimah, Dubai and Sharjah on the west coast and even more rarely, to ADIA. They do not reach the western part of the UAE, that is, most of the Abu Dhabi Emirate.

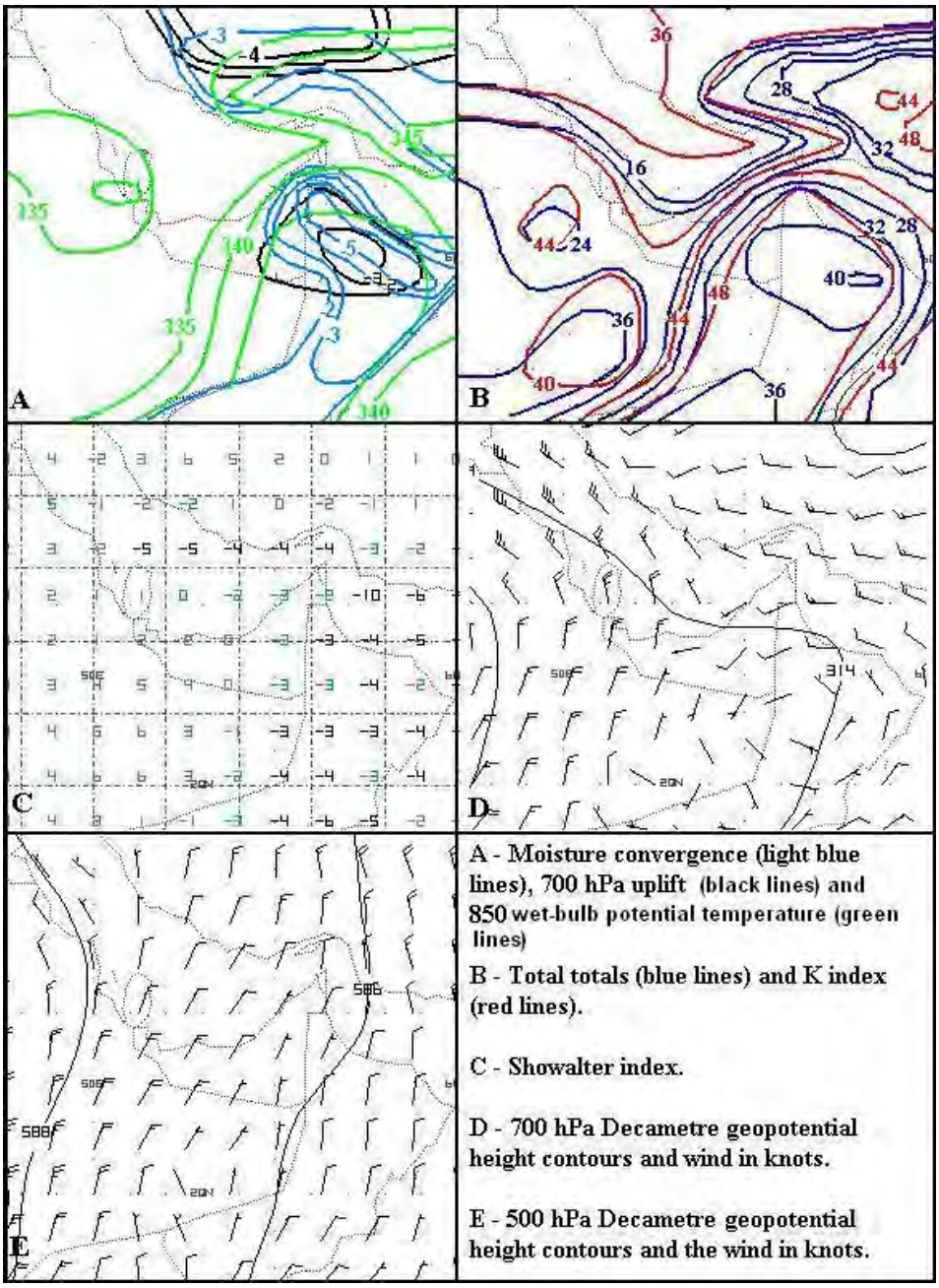

Figure 8.27. Eta NWP model T+12 fields at 1200 UTC on 2003-09-07.

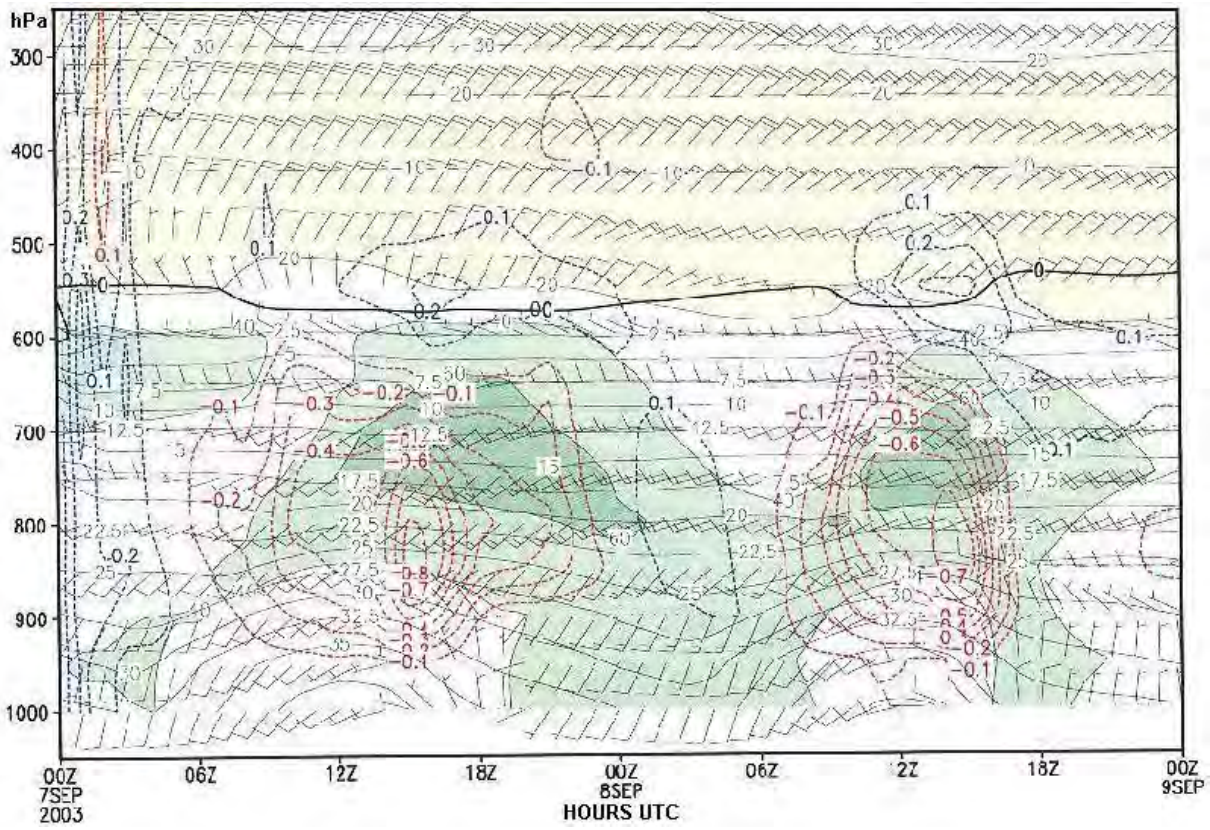

Figure 8.28. Eta NWP model time cross section at Al Ain. The 0000 UTC 2003-09-7 model run indicates marked upward velocity (negative red lines) after 1200 UTC with 60% to 80% relative humidity (dark green) above 800 hPa.

Two isolated cells developed on the higher ground east of and slightly away from the mountain range in the vicinity of Dhaid (figure 8.29). It is suspected that the afternoon sea breeze gust front from the Gulf Sea against higher ground added impetus to their development (Riehl 1978). The development of these cells prompted the forecaster at Dubai to amend the Terminal Area Forecast (TAF) for the airport. In this instance the observed base of the storms was around 1500 metres (5000 ft) AGL and tops were estimated to be about 13716 metres (45000 ft). If thunderstorms are steered by the wind at one third of its base this would be the wind at about 5800 metres (19000 ft), or approximately 500 hPa (UKMO 1997). At this level the forecast and observed winds were north-north-easterly and given the prognostic south-westerly winds lower down (figure 8.28), there was no chance of these storms drifting to the coast. Rather, any movement would be into the desert to the south-south-west. Indeed, figure 8.29 shows that the storms developed and died where they were.

The base height of these storms supported the findings of Al-Brashdi (2007). From a study of 04:00 atmospheric soundings at Seeb Airport, near Muscat in the Sultanate of Oman (figure 2.2), during July 2004, he found that the lifted condensation level (LCL) needs to be below 1800 m above MSL. He also found that the mean mixed layer mixing ratio (ratio of the mass of water vapour to the mass of dry air) must be above 12g/kg in a flow of low level moisture from the Gulf of Oman westward to the surface heat low over the Arabian Peninsula.

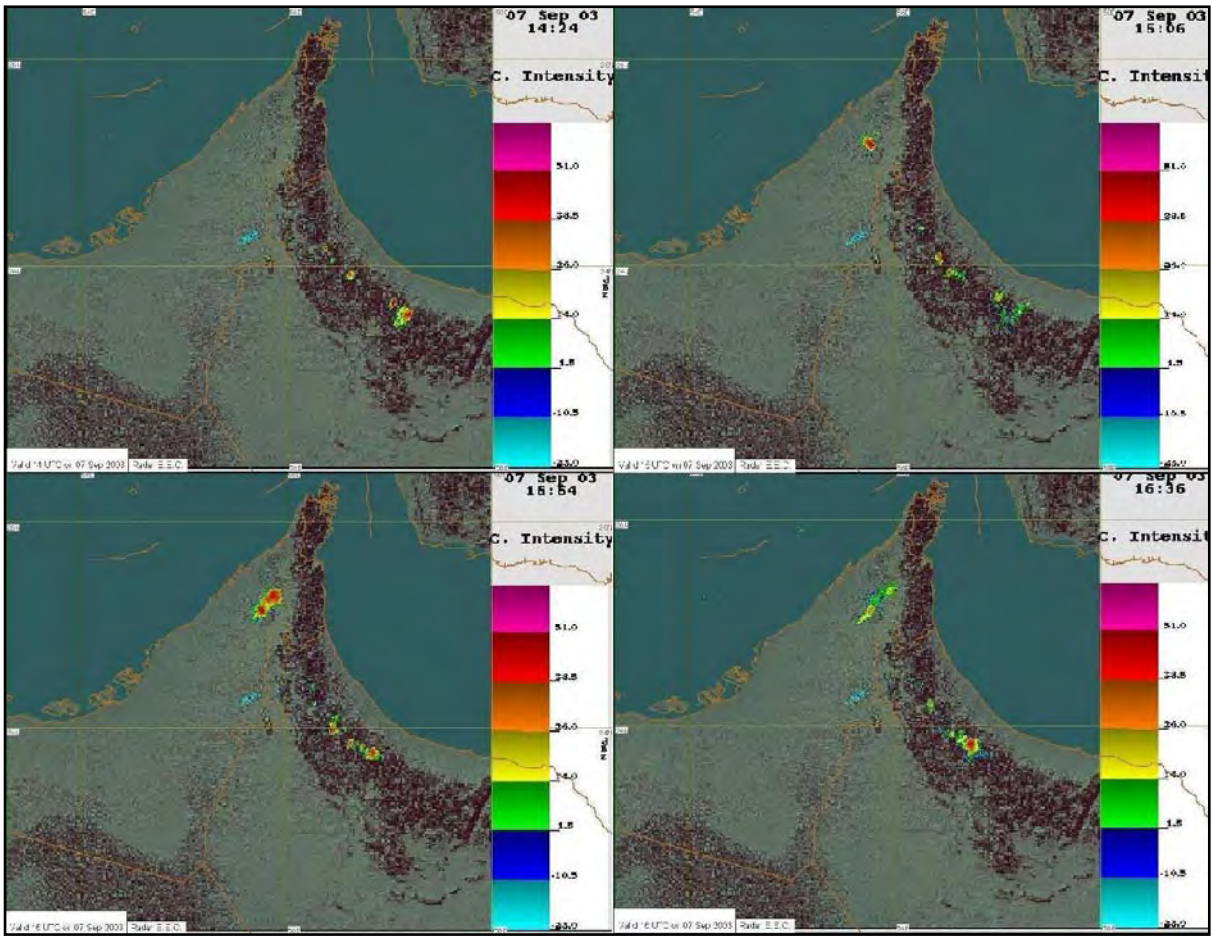

Figure 8.29. Al Ain weather radar PPI dBZ reflectivity images from about 1420 UTC to 1630 UTC, clockwise from the top left, on the 7th September 2003.

8.5.4 SUMMARY

Diurnal thermal heating and topographic forcing of humid air from the Gulf of Oman, in an easterly flow, cause summer thunderstorms to develop in the afternoon on the Hajar Mountains. The thunderstorms develop after 1000 UTC and have usually dissipated by 1500 UTC. They tend, for the most part, to be very isolated and not very intense, although radar echoes of up to 50 dBZ are not uncommon. Rainfall is sparse and the storms usually generate more dust than rain.

The thunderstorms also develop in a north-easterly steering flow above 700 hPa along the eastern edge of an upper air anticyclone situated to the north and west of the UAE. In the UAE these steering winds are around the 500 hPa level. The thunderstorms tend to predominate on the Oman part of the mountains where the mountains are more perpendicularly oriented to the airflow. By virtue of the north-easterly steering winds what little distance they drift, before collapsing, is to the south-west and do not have an effect on the UAE. However, sometimes they develop far enough to the north that they occasionally pass over Al Ain, or close to it.

Sometimes the storms develop far enough north on the mountains in the Musandam Peninsula in an easterly steering wind and the storms to drift to Ras Al Kaimah, Dubai and

Sharjah on the west coast and very rarely, to ADIA. They are more likely at Al Ain, which is nearly in the foothills of the mountains, than at ADIA on the coast. They do not reach the central and western parts of the UAE, that is, most of the Abu Dhabi Emirate.

The GFS NWP model, through fields such as moisture convergence, 850 hPa potential temperature, 700 hPa uplift, Total Totals index, the K index and the Showalter index, gives clear indication whether thunderstorms are likely, or not. Differential relative vorticity advection, which forces upward motion, was not found to be a good indicator as a pronounced upper trough system is not often present. Time cross-sections, such as at Al Ain, provide details of upward vertical velocity and the availability of moisture for thunderstorm development. The wind fields from this product as well as the 700 hPa and 500 hPa wind fields are essential to determine the movement of thunderstorms away from the source region. Particularly whether they will drift eastward to ADIA and Al Ain airport, or drift to the south to south-west into the desert. The weather radar at Al Ain is especially useful for identifying the position of cells and their track away from the mountains.

8.6 TROPICAL DEPRESSIONS

Over the Arabian Sea tropical cyclones, or cyclones as they are known in the region, average 2.3 per year, ⅔ of which occur in the post-monsoon period of October to November and ⅓ in the pre-monsoon period of May to June. Only about 33% of the tropical depressions, found over this part of the Indian Ocean, develop into tropical storms or cyclones (Taha, et al 1981, Koteswaram 1962, Bruintjies and Yates 2003). Tropical depressions are an even rarer event over the Gulf of Oman and the UAE (Martyn 1992), mostly because dry air entrainment from the desert leads to their rapid demise as soon as they move close to the Arabian Peninsula. It is worth noting that Membery (1985) documented a most unusual out of season cyclonic storm that, during August 1985, moved well north of the usual track from the Arabian Sea across northern Oman and the UAE to Rub Al Khali (The Empty Quarter) in eastern Saudi Arabia. The classification of deep tropical depressions and cyclones, by the India Meteorological Department, is listed in table 8.2.

Table 8.2. India Meteorological Department cyclone Classification.

10 minute sustained winds	**Category**
Knots (km/h)	
28-33 (52-61)	Deep Depression
34-47 (62-87 km/h)	Cyclonic Storm
48-63 (88-117 km/h)	Severe Cyclonic Storm
64-119 (118-167 km/h)	Very Severe Cyclonic Storm
≥ 120 (222)	Super Cyclonic Storm

During the period from the beginning of 2002 to mid-2007 only one, classified as a tropical depression (number 01-A) reached the UAE in a much depleted state, but, although it brought some wind damage (Gulf News, 12th May 2002), it did provide welcome rain and one tropical cyclone, 02-A (Gonu) passed close to Muscat.

The tropical depression (01-A) of 2002 had begun to move north-eastward from the Arabian Sea and crossed the coast on the 10th May in the vicinity of Salalah on the south coast of

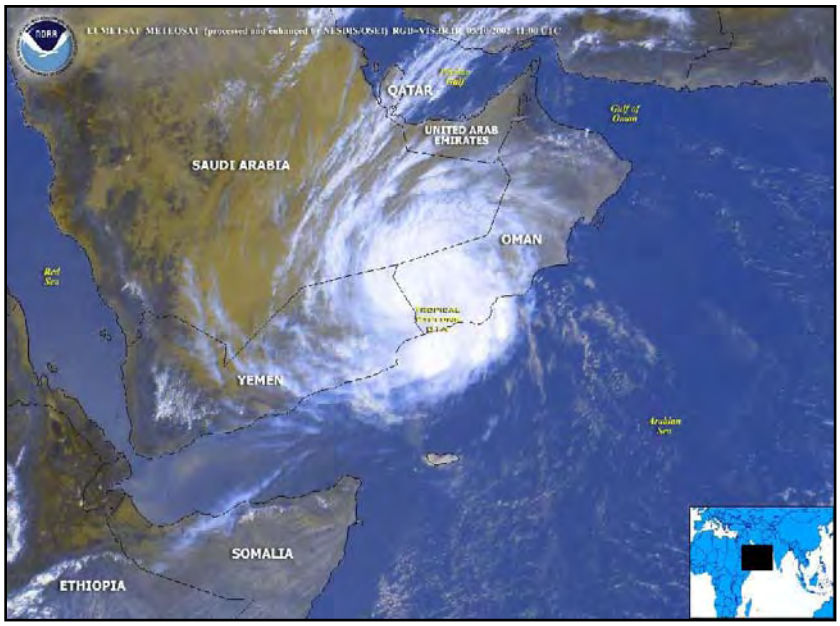

Figure 8.30. Tropical depression 01-A at 1100 UTC 2002-05-10. EUMETSAT METEOSAT image processed and enhanced by NOAA NEDSIS/OSEI. At 0600 UTC it was over southern Oman near 16.5N 56.6E, moving to the NW at 10 knots, with a sustained wind of 40 knots and 50 knot gusts.

Oman (figure 8.30). The wind reached 40 knots (about 78 kilometres per hour) in the Governorate of Dhofar where flash floods killed three people (Gulf News 13th May 2002) and Salalah received about 60 mm of rain. Salalah is on the coast in the south-west corner of Oman. It was immediately west of where the centre of the depression crossed the coast.

In the UAE, the system was preceded by a strong southerly wind that reached 29 knots and reduced the visibility to 600 metres at 1900 UTC on the 10th, followed by a thunderstorm at 2000 UTC. Cloudy weather, mainly in the form of middle layer cloud, with patches of low cloud at 1067 metres (3500 ft) AGL, lasted until 0800 UTC on the 12th. A thunderstorm at 1400 UTC on the 11th brought some rain that lasted until 1600 UTC with another isolated rain shower at 2200 UTC and 0300 UTC to 0500 UTC on the 12th. Cloud, consisting of Stratus patches during the rain, was never lower than 460 metres (1500 ft) AGL.

More recently, on the 6th of June 2007, the centre of tropical cyclone, 02-A (Gonu) passed close to Muscat in the Sultanate of Oman before moving away to the north. This event had very little effect on ADIA, but it is worth mentioning, because it was the first recorded tropical cyclone to enter the Gulf of Oman.

On the 27th May an area of widespread convection was identified on satellite imagery over the south-eastern Arabian Sea and by the 31st it had developed into an organized tropical disturbance with significant cyclonic circulation extending to mid-troposphere levels by the 1st June. It then moved west-north-westward along the south-western edge of a mid-level high pressure situated over north-western India. On the 2nd the Joint Typhoon Warning Center (JTWC 2007) classified it as a Tropical Cyclone 02A. At this time it was 685 km south-west of Mumbai, India and the India Meteorological Department (IMD, 2007) graded it a Cyclonic Storm named Gonu (which means a bag made from palm leaves in the Maldivian language). By the 3rd a typical and well defined eye developed in Gonu, which was clearly seen on satellite imagery and the IMD classified the storm as Very Severe Cyclonic Storm Gonu. It reached its maximum intensity late on the 4th and early 5th with an estimated central surface pressure of 920 hPa and a maximum one minute sustained wind of 135 knots (250 km/h) gusting to 165 knots (306 km/h). It was now classified as Super Cyclonic Storm Gonu by the IMD. However, later on the 5th it was downgraded to a very severe cyclone as it weakened due to the increased entrainment of dry desert air from the Arabian Peninsula, as

well as moving over cooler water that decreased the latent heat available from the ocean (Gray 1968, 1979, Bowditch 2002). At this time the steering mid-level high pressure cell had moved to central India and a second high pressure cell was positioned over the Arabian Peninsula. This combined with a mid-latitude trough approaching to the north of the UAE, created a trough between the high pressure systems and this meant that the cyclone was now steered in a north-westerly direction. So that instead of following the original predicted track over Sur and then inland to the west of Muscat, it eventually passed seaward to the east of Sur and Muscat on the 6th (figure 8.31). By the time it passed about 96 kilometres to the east of Muscat on the 6th it had been downgraded to a severe cyclonic storm with the maximum sustained wind down to 70 knots (130 km/h) gusting to 85 knots (157 km/h) (figure 8.32). Early on the 7th, as it neared the coast of south-eastern Iran, increased land interaction and increasing vertical wind shear (Gray 1968, 1979) took its toll and the cyclone had weakened to 25 knots (46 km/h) maximum sustained wind gusting to 35 knots (65 km/h) and it was reclassified as a tropical depression (JTWC, 2007).

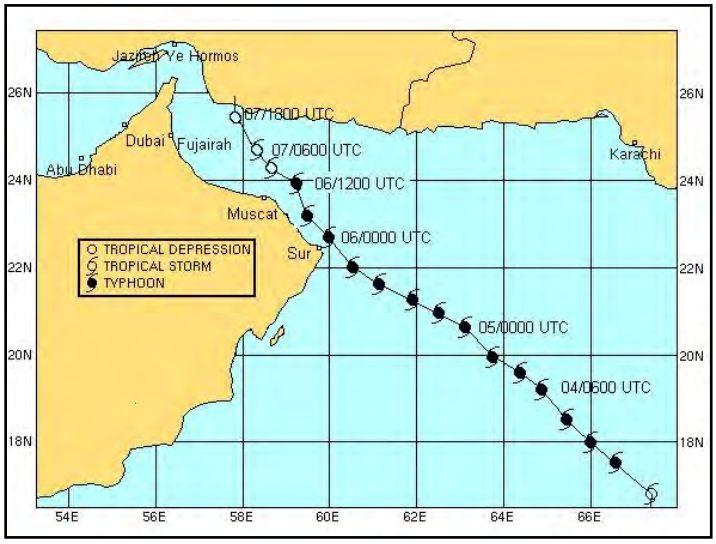

Figure 8.31. The track of Cyclone 02-A Gonu from data supplied by the Joint Typhoon Warning Centre.

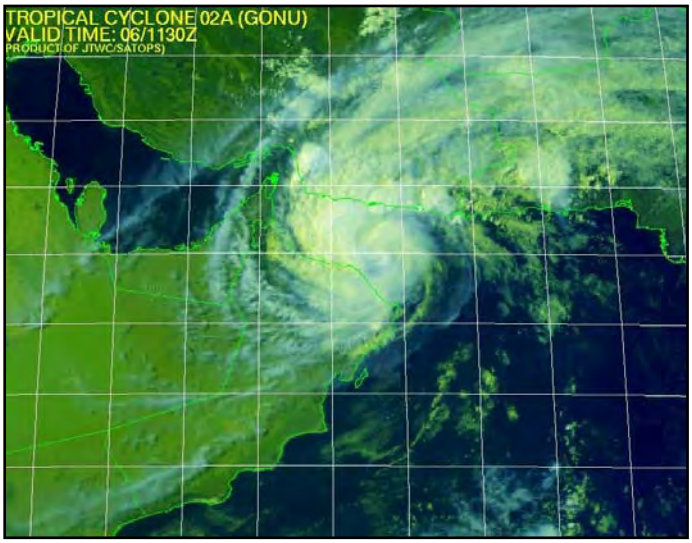

Figure 8.32. Cyclone 02-A Gonu in the Gulf of Oman and passing Muscat (Image courtesy of the Joint Typhoon Warning Centre).

At its peak the maximum significant wave height was estimated as 43 feet at 0000 UTC on the 5th, but by the time it passed along the Oman coast on the 6th it was estimated to be 28 feet decreasing to 26 ft (JTWC, 2007). Nevertheless, the still strong wind and heavy sea caused flooded coastal roads with power and telephone failure across the eastern part of Oman northward from Sur. At Muscat's Seeb airport the visibility was reduced to 300 to 500 metres in rain and thundershowers during the afternoon and evening of the 6th. The wind averaged between 25 to 30 knots with 45 to 50 knots gusts and a total of 70 millimetres of rain fell in the 18 hour period up to 1800 UTC on the 6th. 32 people were reported dead. The airport was closed for about 24 hours. Fortunately, little damage was done to the nation's oil fields and the oil exporting harbour was closed for only 4 days (Arabian Business 2007).

In the UAE along the Fujairah coast some light rain fell, but the storm surge forced water ashore and roads were closed, such as the coastal

road between Kalba and Fujairah. ADIA to the west of the Hajar Mountains was far removed from the action and at its worst experienced a north-easterly to northerly wind that reached 20 knots and caused blowing sand to reduce the visibility to as low as 2000 metres between 1000 to 1200 UTC. At Al Ain the wind reached 19 knots from the north-east with the visibility reduced to 4000 metres in blowing sand.

8.7 FORECAST CHECKLIST

Use of the GFS NWP model post processing products give ample warning of impending rain bearing trough systems and tropical depressions and greatly facilitated the means to predict thunderstorms. Satellite, radar imagery and observational data are vital to pinpoint and track these storms after they appear.

Important general considerations:

- Rain bearing baroclinic upper air troughs occur in winter.
- Their associated weather usually last less than 24 hours, but may rarely persist up to 4 days.
- Rain, from Ac and As cloud, is usually light and isolated. Heavy rain does occur, albeit rarely, from isolated thunderstorms.
- Primary indicators are the 700 hPa and 500 hPa relative humidity and upward (negative) vertical velocity fields.
- Tropical depressions are extremely rare and move from the south-east over Oman and the eastern Empty Quarter.

Winter Thunderstorms:

- A baroclinic trough system advancing from the west.
- Low level moisture, advected from the south to south-east, reflected by increasing moisture at 850 hPa.
- Increasing middle atmosphere upward motion accompanied by increasing 700 hPa and 500 hPa relative humidity.
- Plumes of cyclonic relative vorticity along an upper air trough axis, near a clear slot indicated by the Meteosat Geostationary Satellite water vapour (0.62 micron) channel.
- The presence of an elevated dry line at about 600 hPa.
- Steep ambient temperature lapse rate in the 850-700 hPa layer (indicative of surface wind gusts and potential microburst).
- Raised instability indices, such as KI (>30), Total Totals (>44), Lifted (<-3) and Showalter (-3 to <-6).
- Steep ambient temperature lapse rate in the 700-500 hPa layer (potential hail development).
- Wind direction veering with height and speed shear (25-30 kn) with higher values indicative of possible Supercell development.

Summer Thunderstorms:

- A low level easterly wave moving westwards from the Gulf of Oman.
- Deepening Arabian Peninsula heat low.
- Lower level moisture moving from the Gulf Sea towards the Hajar mountains. (Mean mixed layer mixing ratio ≥12g/kg and LCL <1800m above MSL.)
- Upward motion below the 800 hPa level identified by time cross sections of predicted vertical motion.

CHAPTER 9

CONCLUSION

9.1 GENERAL

The principal objective of this thesis is to provide comprehensive documented forecast material for aviation forecasters in the Emirates and in particular at ADIA. With this in mind, significant weather phenomena and systems of the region have been identified, their development described and researched through case studies and the results summarised in each chapter. Based on the research, forecast methodologies, or checklists, were developed and presented at the end of each relevant chapter. These are summarised in the sections in 9.3 that follow.

Post-processing macros were developed to identify and assess the particular weather phenomena and their use was instituted in the ADIA forecast office in 2002 to 2004.

The secondary objective was to describe the general seasonal climate sequence in the UAE and its immediate surroundings. This was achieved in chapter 3. The main climate factors are summarised in paragraph 9.2.

9.2 GENERAL CIRCULATION: A SUMMARY

The weather experienced in the Arabian Peninsula, is strongly influenced by the summer and winter Monsoon over Asia and the annual reversal of trans-equatorial flow of air at the surface and the upper troposphere, as well as associated changes in velocity divergence and convergence. The primary effect is the surface transition from winter high pressure to summer low pressure.

In winter the passage of mid-latitude low pressure cells in association with upper air troughs, are important weather and rain and thunderstorm producers. Interspersed with the passing lows, latitudinal movement of the surface anticyclonic cell over Arabia results in alternating dry and hot southerly to south-easterly winds and cooler northerly Shamal winds.

The summer circulation, dominated by the position of the Asia low, results in a consistent northerly to north-westerly Shamal wind with high temperatures. While water vapour advection, into the low from the Arabian Gulf causes very humid conditions and can provide enough water vapour for the development of thunderstorms, which are driven to the UAE west coast by the mid-level easterly circulation.

In spring rapid land surface heating causes the development of shallow cyclonic circulation systems. They accentuate the shallow, near sub-synoptic depressions arriving from north-west Africa. These shallow low pressure cells are preceded by southerly winds with intense heat waves and sandstorms.

By virtue of its location straddling the Tropic of Cancer, the subtropical anticyclone in the lower atmosphere dominates the weather and climate of the UAE. This results in predominantly weak pressure gradients and subsiding air. Combined with the warm Gulf Sea and marked land/sea temperature differences, this makes the region ideal for consistent land and sea breeze conditions and overnight fog. In early summer, large daytime temperature difference between the land and the still lower Gulf Sea temperatures, cause intensified land and sea breeze circulation. The lower sea temperature is also influential in increased fog.

9.3 SIGNIFICANT WEATHER PHENOMENA AND SYSTEMS

To the author's knowledge documented aviation weather research, indeed any research, in the UAE and ADIA in particular, is non-existent. The little aviation forecast information that was available was anecdotal and limited to a few pages of notes. Research that does exist relates to weather further afield and it is not aviation specific. These are Shamal studies done by Membery (1983) at Bahrain and Rao, et al (2001) at Doha in Qatar; sea breezes across the UAE coast (Eager et al, 2005); waterspouts (Jackson, 1987 and Davey, 1987). More relevant, but still not aviation specific is thunderstorm and enhancement of precipitation research in the nearby Hajar Mountains (Breed et al, 2005 and 2002; Jensen et al, 2005; Bruintjes and Yates 2003 and Al-Brashdi, 2007). Therefore, the research in the weather phenomena chapters, for the greater part, covers new ground.

9.3.1 FOG

Fog is the most serious disrupter of aviation activity at ADIA and, although there is a higher frequency in autumn and winter it occurs often enough to be a continual source of concern to the aviation forecaster throughout the year. The fog forms as result of advection and radiation processes. Moist air is advected from the Gulf during the afternoon and evening. During the latter part of the night radiation cooling causes the fog to form over the land. It then expands toward, or drifts over, the airport on its way to the coast, borne by a light early morning land breeze (figure 9.1).

Figure 9.1. Early morning Stratus cloud and fog drifting into the island city of Abu Dhabi from the direction of ADIA further inland (2004-03-07).

Clear night and weak pressure gradient conditions aside, the wind is the most critical factor for determining whether fog will occur or not. Fog is most likely after a Shamal has been blowing for some time and then dies away and veers to a light south-easterly land breeze around sunrise. The ideal situation being after the passage of a trough and a slow moving following anticyclone maintains a north-westerly wind off the Gulf Sea and then settles over

the UAE. Significantly it rarely occurs when the wind backs through westerly during the night with a longer period blowing off the desert to ADIA.

It is equally important to know when fog will not occur. It does not occur when the wind persists from the north-west to north-east, such as during a Shamal, no matter how much water vapour is available. Although not affecting ADIA, prior to this research, it was not known that well inland this wind can become light enough for fog to form at the Liwa Oasis on the edge of the Empty Quarter. Fog also does not occur when the wind persists off the desert, which happens when there is a low pressure to the west. However, the forecaster must also be wary of the sea breeze during the day, bringing increased water vapour, which then ceases with a light land breeze around sunrise.

The fog very quickly becomes thick enough for the visibility to decrease below the CAT3A ILS 200 m minimum, resulting in aircraft diversions. During the winter months fog tends to occur earlier in the night and clear later than in summer. It is so frequent later in the night and around sunrise between 2200 and 0300 UTC (0200 and 0700 local time) that scheduled flights into ADIA virtually cease between these times.

A significant discovery, and contrary to local weather lore, is that fog is unlikely to occur on two, or more, consecutive nights. It does happen, but the likelihood is less than 18% and the risk of fog during four or more consecutive days is 1%. Another research result relates to the local belief that 80% or higher surface relative humidity at 1800 UTC (2200 local time) is a precursor to fog. This factor was found to be a useful, but not an infallible, nowcasting tool, The research showed that 90% of the study fog events occurred when the relative humidity was $\geq$ 73% at this time. On the other hand, the relative humidity also exceeded 80% on some nights and then fog did not form by the next morning. A far more reliable indicator was found to be whether the minimum surface air temperature, later in the night, will drop to, and below, the maximum surface dew-point temperature that occurred late the previous afternoon, or early evening.

A detailed forecast methodology to pursue is provided in chapter 4, but taking everything into consideration the most important fog forecasting criteria at ADIA are:

- Clear sky expected.
- Pressure gradient $\leq$ 1 hPa over the UAE (surface anticyclone or col present).
- Shamal ceases during the afternoon, or evening.
- Very misty evening conditions brought by the sea breeze or Shamal.
- Surface relative humidity $\geq$ 73% by1800 UTC and $\geq$ 90% at 0000 and 0300 UTC.
- $\leq$ 5 knots surface winds and in the atmospheric boundary layer expected.
- Surface wind expected to veer from north-west to south-easterly.
- A surface, or near surface temperature inversion expected overnight, preferably $\leq$ 168 metres (± 550 feet) above MSL.
- $\geq$ 50% relative humidity within ± 100 metres of the surface.
- Forecast minimum temperature lower than, the maximum dew point temperature the previous late afternoon or evening.

9.3.2 SHAMAL

The Shamal is the only wind in the region that can routinely last for several days, brings cooler, but still humid air to ADIA and promotes fog formation. Over the Gulf Sea the Shamal can reach strong to gale force, causing a very rough sea and disrupt helicopter flights to the oil rigs. The wind develops in the northerly flow east of a surface anticyclone that approaches over Saudi Arabia and follows a low pressure cell over southern Iran, or the Strait of Hormuz.

As described by Membery (1983) at Bahrain and Rao, et al (2001) at Doha (Qatar), the wind is most prevalent in summer and most persistent during the summer months of May to July with a secondary maximum in winter from November to March. The wind is strongest during the afternoon from 1000 to 1500 local time when it is reinforced by the sea breeze.

Strong Shamal winds can carry sand from Iran and Saudi Arabia over the Gulf Sea to the UAE and cause poor visibility. The visibility tends to be worst over the eastern UAE where there is a shorter sea traverse and less time for the dust to fall out of the atmosphere before reaching the oilrigs offshore and the UAE coast.

The wind can be stronger and gustier inland at Al Ain in the afternoon than at ADIA. It is suggested that this is probably because of enhanced cyclonic circulation due to the hotter conditions inland and upslope (anabatic) wind along the western slope of the Hajar Mountains to the east of Al Ain. This contribution by the land breeze may also help to overcome the retarding friction effect of the land as the air penetrates inland from the sea. This strong and gusty wind lifts dust and reduces the visibility.

At night, during persistent Shamal conditions, the wind tends to become lighter and may even back to south-westerly, due to the influence of the overnight land breeze effect, but may persist from the north-west, or the west-north-west, when synoptic scale surface pressure gradients dominate.

Strong upper air subsidence above the surface heat low means that this (superior) air is usually too dry for low cloud to develop, but in winter with cooler and moist air off the sea, scattered low cloud often occurs over the coast, but less often further inland. The cloud, formed as a result of turbulent mixing of maritime air beneath a temperature inversion, is usually about 2500 feet to 3000 feet above ground level.

The most important considerations when forecasting a Shamal are:

- Wind speed $\geq$ 17 knots.
- Surface $\geq$ 5 hPa pressure gradient across the UAE.
- A surface low, or trough, passing to the east.
- A surface anticyclone to the west of the UAE and/or a deepening of the surface low over Iran.
- Wind shear. A low level jet developing overnight, 30–40 knots ± 300 metres MSL.
- Poor visibility. The Shamal can carry dust from far away in Saudi Arabia and Iran.

9.3.3 DUST STORMS

Dust storms at ADIA occur either as a result of a thunderstorm gust front, or in the synoptic scale when a strong surface pressure gradient develops over the UAE. This often happens when a low pressure system advances from the west and it is further enhanced by diabatic heating over the desert. The enhanced gradient causes a strong to gale force gusty and turbulent wind and dust may be lifted from afar and transported to the UAE.
Dust storms, when the visibility is below 1000 metres, are not as common as legend would have it. Owing to the geographical location of the UAE, the average is only 3 per year. However, dust events when the visibility is reduced to less than 5000 metres are more common and occurred on 141 occasions from 1994 to 2003.

The duration of dust storms, when the visibility is below 1000 metres, is not long. The average duration was found to be about 1¼ hours and the longest 4½ hours. On average thunderstorm gusts reduce the visibility to dust storm levels for 37 minutes with the longest time being nearly 60 minutes. Dust events, when the visibility is ≤ 3000 metres, last on average 3¾ hours with the maximum duration 15 hours. The longest period, when the visibility remained ≤ 5000 metres due to dust, was 21 hours.

Dust events and dust storms are most likely when the wind blows from the desert to the south. With Shamal conditions the dust has to be transported from the north-west and a considerable distance across the Gulf Sea with the result that the visibility is seldom seriously reduced. Dust storms are even less likely from the north-east, or east. The exceptional Nashi wind dust storm that reached the UAE happens very seldom, and no literature reference to such an event could be found. Weather forecasters need to consider the risk of dust transport to the UAE whenever model prognoses indicates strong turbulent winds over the desert to the south and west as well as over southern Iran.

Poor visibility is most likely when thermally induced eddies reduce stability and increased mixing with the air aloft. This happens most often during the morning and the early afternoon. The peak time is at 0600 UTC (1000 local time). This also coincides with the regular early morning land breeze that reinforces any southerly, pressure gradient forced, wind off the desert. By way of contrast the Shamal, or a strong sea breeze, penetrating inland, is most likely to cause poor visibility during the afternoon.

There is negative correlation between wind speed and dust reduced visibility. As a predictive tool, this correlation is not worth much due to other factors. These include poor visibility due to dust in suspension after the wind has dropped, or dust carried aloft from elsewhere, while the local wind speed remains low and also the effect of a low sun with haze or dust in suspension. Other factors are the dust source region and type, such as finer dust in the vicinity of ADIA and more sandy soil at Al Ain (section 6.6.1.3). However, there are some loose conclusions that can be made. At wind speeds above 15 kn the visibility can generally lower to below 8000 m and it is often reduced to below 5000 m. Above 20 kn the visibility will frequently be less than 2000 m, but most likely be below 1000m. For wind speeds above 30 kn the visibility will be less than 1000 m.

The most important forecasting considerations are;-

- Strong wind from the south-east to west-south-west .

- Strong outflow from thunderstorms creating a turbulent and gusty wind at the outflow leading edge.

These two mechanisms are considerably enhanced when:
- The environmental lapse rate approaches the value of the dry adiabatic in the lower layers.
- The dryness of the surface dust/sand.

However, the visibility improves when:
- The southerly dust generating wind veers to north-westerly after the passage of a surface low system.
- An afternoon sea breeze develops
- At night when the wind speed decreases.

Other factors to be considered are:
- The transport of dust from further afield by the Shamal and north-easterly Nashi.
- Dust and dust storms in southerly winds are most likely between 0300 UTC to 1200 UTC and most prevalent at 0600 UTC.
- Dust and dust storms in a Shamal are most likely between 0800 UTC to 1300 UTC.
- Thunderstorm associated dust storms last ± 30 minutes and hardly ever more than 60 minutes.

9.3.4 LAND AND SEA BREEZES

The very consistent sea breeze at ADIA can be expected to start at 0830 UTC (1230 UAE time) and average about 11 knots, reaching a maximum at about 1030 UTC (1430 UAE time). The equally regular, but much lighter, land breeze is most likely to begin at 0100 UTC (0500 local time), blow at about 4 knots and reach a maximum at about 0450 UTC (0850 local time). The change from a land breeze to sea breeze usually occurs within about an hour, whereas the overnight change from a sea breeze to a land breeze is more gradual. Generally, the Eta GFS NWP model surface wind time section fields give a good indication of the strength and timings of sea and land breezes.

This research revealed that the marked thermal difference between the sea temperature and maximum land temperatures causes the sea breeze to penetrate up to about 150 kilometres inland to Al Ain and the Liwa Oasis. Most references to the extent of sea breezes inland limit this to 20 to 70 kilometres (Bradbury 1989, Riehl 1979, Critchfield 1974 and Millar 1966), while only Eager et al (2005) claimed that they can be penetrate up to 130 kilometres inland.

Another factor that this research revealed was that the sea breeze can be stronger and gustier inland at Al Ain than at ADIA accompanied by worse visibility due to wind blown dust. The stronger wind at Al Ain is considered to be due to the anabatic upslope wind driven by the daytime heated slopes of the Hajar Mountains. The land breeze at Al Ain was also found to be stronger than at the coast. This is probably due to the night time cold air drainage (katabatic effect) of the western slopes of these mountains.

Dry air entrainment from near the top of the boundary layer can maintain low humidity and produce a “dry” sea breeze. A peculiar temporary dip that has been noted in the rising humidity shortly after the sea breeze begins and this is attributed to dry air that is advected to

sea by the upper diverging branch of the inland convergence zone. It then sinks and is carried back onshore by the sea breeze.

Important forecasting considerations:

The sea breeze.

- Will be enhanced and start earlier in a northerly synoptic scale flow. This happens due to the strong gradient between a surface low pressure in the east and or an anticyclone approaching from the west. This pattern suppresses the land breeze. It will be weaker, start later and may not occur at all.
- It is most likely to veer overnight through easterly to become a south-easterly land breeze.
- Dust raised by the land breeze clears when the sea breeze begins.
- It can penetrate up to about 150 kilometres inland.
- In the summer the sea breeze is usually free of low cloud
- In winter low cloud with the sea breeze is more common. The cloud base is generally between about 600 to 1200 metres (2000 feet to 3500 feet).
- At Al Ain the sea breeze is often stronger and gustier.

The land breeze.

- Will be enhanced by the synoptic scale southerly flow when a surface low pressure cell lies to the west. The land breeze will start earlier and in this case the sea breeze will be suppressed, start later, or not at all.
- It is most likely to veer through south-westerly to a north-westerly sea breeze.
- The land breeze is often stronger at Al Ain than at the coast at ADIA, but not as strong and gusty as the sea breeze.

9.3.5 RAIN TROUGHS, THUNDERSTORMS AND TROPICAL DEPRESSIONS

Thunderstorms, embedded in the south-westerly flow ahead of eastward moving upper air troughs in winter, are the main producers of rain in the vicinity of ADIA. Thunderstorm precipitation can be heavy and result in brief flash floods. However, rain depth of around 10 mm to 20 mm is most common. Hail is vary rare with no recorded incidence at ADIA. Wind shear parameters obtained from the Eta NWP model at the time of the 18th March 2002 thunderstorm (Chapter 8.4.3), indicated the potential for enough wind shear to foster vigorous development, but not enough to produce a supercell thunderstorm.

To a lesser extent, diurnal thermal heating and orographic forcing cause afternoon summer thunderstorms to develop on the Hajar Mountains. Echoes of up to 50 dBZ are not uncommon with thunderstorms tops up to about 45000 feet (13716 metres). They develop in a north-easterly steering flow along the eastern edge of an upper air anticyclone situated to the north and west of the UAE. Surface low level moisture is advected from the Arabian Sea and the Gulf of Oman and carried aloft by synoptic scale ascent. Under these circumstances the majority tend to be on the Oman part of the mountains south of Al Ain where the mountains are nearly perpendicularly to the lower level north-easterly flow. Sometimes they develop in the far north on the mountains in the Musandam Peninsula and an easterly 500 hPa steering wind causes the storms drift to Ras Al Khaimah, Dubai and Sharjah on the west coast, but rarely, to ADIA. It is possible that the afternoon sea breeze gust front, meeting

thunderstorms on higher ground toward the mountains, adds impetus to the thunderstorm development.

The passage of a trough system is normally marked by a short period of cloudy weather of less than 24 hours, but, occasionally cloudy periods lasting up to about 8 to 10 days do occur. Intense and slow moving mid-tropospheric trough systems, on occasion, have the potential to produce severe convective weather. When this happens fresh to strong, hot and dry southerly desert winds precede the thunderstorm line squall. Visibility is reduced to below 2000 metres by a combination of wind blown dust and rain. Visibility, below 1000 metres, occurs in the wind blown dust at the thunderstorm gust front and improves in the following rain. Cloud bases remain high enough so that they rarely hamper landing aircraft.

Over the UAE, tropical depressions are very rare severe weather and rain producers. In 2002 one tropical depression (number 01-A) reached the UAE in a much depleted state in and one other rapidly degenerating cyclone 02-A Gonu passed well east of the UAE east coast in 2007.

Important considerations:

- The passage of upper air troughs during winter.
- Thunderstorms are likely to occur embedded in cloud ahead of these troughs.
- Summer thunderstorms are rarely reach ADIA when they drift westward from the Hajar Mountains.
- When the 500 hPa steering winds are from the north-east the summer storms drift away to the Empty Quarter.
- Tropical depressions are extremely rare and move from the south-east over southern Oman, or move northward over the Gulf of Oman.

9.4 GUIDELINES ON THE USE OF THIS THESIS

Apart from a copy of this thesis being made available to the UAE Federal Meteorological Service and to the Abu Dhabi Directorate of Civil Aviation, the recommendation is that copies of the forecast methodologies, or checklists, be placed in a ready reference file and kept at the work station as a decision making tool.

The research detailed in this thesis could also provide the basis for an operations and training manual.

To assist forecasters in decision making, macros, based on this research, currently in operational use, can be updated using new post-processing technology.

9.5 THE FUTURE OF UAE AVIATION WEATHER FORECASTING

One tends to view the desert environment as one with little in the way of weather. The disruption to airport operations and diverted flights due to fog, dust storms, thunderstorms and wind disprove this.

Commercial aviation in the UAE is a rapidly growing and expanding industry, particularly at ADIA and Dubai. Airport passenger and cargo hubs are continually being enlarged with the aim of being global centres. An all new airport, Al Maktoum International Airport at Jebel Ali on the coast near Dubai, will be operational by 2010 and before the recession of 2009, it was projected to be the biggest in the world by 2015. Commercial aircraft flying to and from the UAE, such as the A340-500, already have flight endurance of 19 hours, while the A380 typically carries 525 passengers and can carry up to 555.

Aviation weather forecasting in the UAE will become more important and the emphasis will be on greater forecasting accuracy for longer forecast periods. Better understanding of weather phenomena detrimental to aviation will become more important and the author trusts that this thesis will contribute.

9.6 RECOMMENDED FUTURE RESEARCH

Fog is the most serious form of weather detrimental to aviation in the UAE, particularly along the Gulf Coast. Some fog forecasting indices in use elsewhere in the world, such as Saunders and the Craddock and Pritchard methods (UKMO 1997), were briefly tested during research for this thesis and found to be unsuitable for the weather conditions in the UAE. The surface wet-bulb temperature at 0000 UTC and the 1200 UTC dew point temperature showed promise. The invention of a reliable local fog index would be of great benefit to the forecaster at ADIA and at Dubai.

As producers of severe weather over the UAE, thunderstorms in association with the passage of upper air troughs deserve further research. This also holds for the summer westward displacement of thunderstorms to the Emirates coast by 500 hPa steering winds. Closer scrutiny is recommended of the relationship between low level water vapour flux from the south and south-east and passing trough systems as a thunderstorm rain producer in support of the pioneering research by Al-Brashdi (2007).

The little known Nashi wind is certainly worthy of further statistical and analytical research, as is the role played by the diurnal land and sea breeze effect on the strength and direction of the Shamal.

A useful area of research would be the anabatic and katabatic effects of the Hajar Mountains on the land and sea breezes. As well as the peculiar temporary dip in humidity often noted at ADIA shortly after the onset of the sea breeze. Is this due to dry air carried out to sea aloft, then sinking and brought back to the coast on the sea breeze? Of additional interest is the effect of land and sea temperature differential on the strength and onset of the land and sea breezes and whether the sea breeze penetrates further than 150 km inland.

Although the primary mechanisms of the weather in the UAE are known and understood, there are synoptic and mesoscale characteristics and circulatory systems that need further investigation. For example, the semi-permanence of the winter, surface anticyclonic cell over Arabia and the transitory spring desert depressions with their attendant sand storms. It would also be beneficial to examine the extent to which the zone of 200 hPa convergent air at about 40°E is a compensatory effect for the upward flow at 70°E, as well as to what extent the subsiding air below this convergent zone contributes to the dry summer weather over the Arabian Peninsula.

REFERENCES

Abu Dhabi Explorer. 2001. 2nd Edition. Dubai: Explorer Publishing.

Abu Dhabi Airports Company (ADAC). 2009a. Abu Dhabi International Airport. http://www.abudhabiairport.ae/theairport/index.asp. Accessed 2009-04-24.

Abu Dhabi Airports Company (ADAC). 2009b. A+9m passengers through Abu Dhabi in 2008. Press release 18 January 2009. http://www.adac.ae/. Accessed 2009-04-09.

Agee, E. M. 1982. An introduction to deep convective systems. In Cloud Dynamics, edited by E. M. Agee and T. Asai. Dordrecht: Reidel Publishing Company.

Airbus. 2008. A340-500. The world's longest range airliner. http://www.airbus.com/en/aircraftfamilies/a330a340/a340-500/. Accessed 2008-05-15.

Al-Brashdi, H. A. S. 2007. Forecasting techniques over the Western Hajat Mountains in the Sultanate of Oman. Unpublished MSc dissertation. University of Pretoria.

American Meteorological Society (AMS). 1989. Glossary of Meteorology. Boston: American Meteorological Society.

Arabian Business, 2007. Death toll soars to 32 as Gonu passes Oman. Friday, 08th June 2007. http://www.arabianbusiness.com. Accessed 2007-06-07.

Aviation Business. 2005. Dubai: ITP Business Publishing. January 2005, pp 38.

Bennetts, D. A., McCullum, E., Grant, J. R. 1986. Cumulonimbus clouds: An introductory review. Meteorological Magazine. Volume 115, pp 242 – 256.

Blackadder, A. K. 1957. Boundary layer wind maxima and their significance for the growth of the nocturnal inversion. Bulletin of the American Meteorological Society. Volume 38, pp 283 – 290.

Blair, T. A. 1957. Weather elements. New York: Prentice Hall, Inc. Pp 228 – 229.

Bowditch, N. 2002. The American Practical Navigator, 2002 Bicentenial Edition. Publication Number 9. Chapter 36. Bethesda: National Imagery and mapping Agency (Cay Publications).

Bradbury, T. 1989. Meteorology and flight. London: A and C Black. Pp 58, 113.

Breed, D., Jensen, T., Bruintjes, R., Piketh, S., Al Mangoosh, A., and Al Mandoos, A. 2005. Precipitation development in convective clouds over the eastern Arabian Peninsula (2005 - H20SUPPLY). AMS Conference on Planned and Inadvertent Weather Modification. Volume 16, J10.6, (no page numbers).

Breed, D., Bruintjes, R., Jensen, T., Salazar, V. and Piketh, S. 2002. Aerosol and cloud droplet measurements in the United Arab Emirates (2002 - 11cldphy). AMS Conference on Cloud Physics. Volume 11, P5.11, (no page numbers).

Brown, R., Roach, W. T. 1976. The physics of radiation fog: II – A numerical study. Quarterly Journal of the Royal Meteorological Society. Volume 102, pp. 335 – 354.

Bruintjes, R.T., Yates, D.N. 2003: Report on review and assessment of the potential for cloud seeding to enhance rainfall in the Sultanate of Oman, Research applications program, NCAR, Boulder, Colorado, USA.

Bunkers, M. J. 2002. Vertical Wind Shear Associated with Left-Moving Supercells. Weather and Forecasting. Vol 17, August. Pp 845-855.

Callan, L., Robison, G. 2000. Oman and the United Arab Emirates. Lonely Planet Publications, Melbourne.

Chepil, W. S., Woodruff, N. P. 1957. Sedimentary characteristics of dust storms. II: Visibility and dust concentration. American Journal of Science. New Haven. Volume 255, No. 2, pp 104 – 114.

Collier, C. G. 1989. Applications of weather radar systems: A guide to uses of radar data in meteorology and hydrology. Chichester: Ellis Horwood Limited. Pp 33- 34.

Cotton, W. R., Anthes, R. A. 1989. Storm and cloud dynamics. San Diego: Academic Press, Inc. Pp 306.

Critchfield, H. J. 1974. General climatology. New Jersey: Prentice-Hall Inc. Pp 86, 172.

Croft, J., Darbe, D, L., Garmon, J, F. 1995. Forecasting significant fog in southern Alabama. National Weather Digest. Volume 19, Number 4, July, pp 10-16.

Crowther, H. G. 1993. Tornadoes hit new heights. Weatherwise. Volume 36, number 1, pp 29-37.

Davey, B. J. 1987. Tornadic waterspout at the Jebel Ali Sailing Club. Meteorological Magazine. Volume 116, pp 129 – 137.

de Villiers, M. P. 2003. Meteorological aspects of the wind towers of the United Arab Emirates. Weather. Volume 58, Number 9, pp 319-324.

Doswell, C. A. and Evans, J. S. 2003. Promimity sounding analysis for derechos and supercells: an assessment of similarities and differences. Atmospheric Research. New York: Elsevier. Volume 67-68, pp 117-133.

Dubai International Airport. 2009. Another year of growth and success for Dubai Airports. Press release 25th January 2009. http://www.dubaiairport.com/DIA/English/TopMenu/News+and+Press/Airport+News/Another+year+of+growth+and+success+for+Dubai+Airports.htm. Accessed 2009-11-24.

Dubai International Airport. 2006. Department of Civil Aviation. http://www.dubaiairport.com. 13-03-2006.

Eager, R. E, Raman, S., Childs, P., Boyles, R. P., Reid, J. S. Westphal, D. 2005. Observations and modelling of the coastal meteorology of the United Arab Emirates during the Unified Aerosol Experiment (2004)(2005 – 6 COASTAL). AMS Conference on Coastal Atmospheric and Oceanic Prediction and Processes. Volume 6, 3.4, (no page numbers).

Eager, R. E. and Raman, S. 2005. A climatology of the sea breeze circulation over the southern Arabian Gulf. AMS Symposium on Meteorological Observations and Instrumentation. Volume 13, JP1.8, (no page numbers).

Eagleman, J. R. 1983. Severe weather and unusual weather. New York: van Nostrand Reinhold Company Inc.

Erickson, T. A. 2001. Louisiana and southeast Texas fog research and modelling. National Weather Service. http://www.srh.noaa.gov.lch/research/fogres/htm. Accessed 2003-08-03.

Findlater, J. 1985. Field investigations of radiation fog formation at outstations. Meteorological Magazine. United Kingdom Meteorological Office. No. 114, pp 187 – 201.

Garbell, M. A. 1947. Tropical and Equatorial Meteorology. New York: Pitman Publishing Corporation. Pp 28 – 35.

Galvin, J.F.P. 2004. Radiation fog on 9 and 10 December 2003. Weather. Royal Meteorological Society. July 2004, Volume 59, No. 7, pp177 – 182.

Galvin, J. F. P. 2003. Back to basics: Radiosondes: part 2 – Using and interpreting the data. Weather. Volume 58 No 10, October 2003, pp 387 – 395

Galway, J. G. 1956. The lifted index as a predictor of latent instability. Bulletin of the American Meteorological Society. Volume 37, pp 528 – 529.

George, J. J. 1960. Weather Forecasting for Aeronautics. Burlington: Academic Press, Elsevier Inc. Pp 673.

Gill, A. E. 1982. Atmosphere – Ocean Dynamics. New York; Academic Press, Inc. Pp 404.

Glen, T. 1954. An introduction to climate. McGraw-Hill, New York, Toronto, London, 3rd edition.

Goudie, A. S. 1983. Dust storms in space and time. Progress in Physical Geography. London. Volume 7, No 4, pp 502 - 530.

Gray, W.M. 1979. Hurricanes: Their formation, structure and likely role in the tropical circulation Meteorology Over Tropical Oceans. D. B. Shaw (Ed.). Bracknell: Royal Meteorological Society. Pp155-218.

Gray, W.M. 1968. A global view of the origin of tropical disturbances and storms. Monthly Weather Review. American Meteorological Society. Volume 96, No. 10, October, pp 669-700.

Griffin, D. W., Kellogg, C. A., Garrison, V. H., Shinn, E. A. 2002. The global transport of dust. American Scientist. Volume 90, May-June, pp 220 – 235.

Griffiths, J. F. 1976. Applied climatology. An introduction. Second edition. Oxford: Oxford University Press. Pp 21, 90.

Gulf News. 2004. Suez Canal shut as storms batter the Middle East. 2004. Gulf News. Dubai: Al Nisr Publishing LLC. 2004-01-24.

Gulf News. 2003. Thunderstorms flood low-lying areas. 2003. Gulf News. Dubai: Al Nisr Publishing LLC. 2003-04-18, pp 1.

Gulf News. 2002. Oman floods kill three, wreak havoc. 2002. Gulf News. Dubai: Al Nisr Publishing LLC. 2002-05-13.

Gulf News. 2002. Tropical cyclone brings first summer rains. Gulf News. Dubai: Al Nisr Publishing LLC. 2002-05-12.

Gulf News. 2001. Abu Dhabi airport passenger volume up by 5%. 17-01-2001.

Harper, W. M. 1977. Statistics. Plymouth: Macdonald and Evans Ltd.

Hastenrath, S. 1985. Climate and circulation of the tropics. Reidel Publishing Company.

Hayward, L. Q., Steyn, E. E. 1968. Aeronautical Climatological Summaries. Descriptive memoranda for five South African airports. WB 31. South African Weather Bureau.

Hess, S. L. 1959. Introduction to theoretical meteorology. New York: Henry Holt and Company. Pp 221 – 224, 229 - 234

Holl, W (editor). 1981. World climates. Wissenschaftliche Verlagsgesellschaft mbH, Stuttgart. Pp 54 - 55, 102 - 103.

Holton, J. R. 1992. An Introduction to Dynamic Meteorology. 3rd edition. San Diego: Academic Press. Pp 511.

Hsu, S. A. 1988. Coastal Meteorology. San Diego: Academic Press Inc.

Idso, S. B. 1976. Dust storms. Scientific American. No 4, pp 235.

India Meteorological Department (IMD). 2007. RSMC New Delhi Bulletins. http://www.imd.ernet.in/section/nhac/dynamic/rsmc.htm. Accessed 2007-06-02 to 07.

International Civil Aviation Organization (ICAO). 2004. Meteorological Service for International Air Navigation, Annex 3. Montreal: ICAO.

International Civil Aviation Organization (ICAO). 1987. Wind shear. Circular 186-AN/122. Montreal: ICAO. Pp 21 – 49, 53 – 55.

International Civil Aviation Organization (ICAO). 2007. Meteorological Service for International Air Navigation, Annex 3, amendment 74, attachment A. Montreal: ICAO.

Jackson, C. C. E. 1987. Vortex phenomena in the United Arab Emirates. Weather. Volume 42, pp 302 – 308

Jauregui, E. 1989. The dust storms of Mexico City. International Journal of Climatology. Royal Meteorological Society. Chichester: Wiley. Volume 9, No 2, pp 169 – 180.

Jensen, T., Salazar, V., Breed, D., Bruintjes, R., Piketh, S., Al Mangoosh, A., and Al Mandoos, A. The Relationship between Cloud Droplet Distributions and Ambient Aerosol Populations in a Subtropical Desert Region (2005 - 16WEAMOD). AMS Conference on Planned and Inadvertent Weather Modification. Volume 16, 5.4, (no page numbers).

Joint Typhoon Warning Center (JTWC). 2007. Current Northwest Pacific/North Indian Ocean Tropical Systems. https://metocph.nmci.navy.mil/jtwc.php. Accessed 2007-06-02 to 07.

Kay, S. 1995. Wings over the Gulf. Motivate Publishing, Dubai.

Kendrew, W. G. 1961. The climate of the continents. Oxford University Press, New York, 5th edition.

Kermode, A. C. 1976. Mechanics of flight. London: Pitman Publishing. Pp 25 – 43, 225 – 240.

Kessler, E. 1985. Severe weather. Handbook of applied Meteorology. Ed: Houghton, D. New York: John Wiley & Sons.

King, J. A. 1955. Low cloud at Jan Smuts Airport. South African Weather Bureau Newsletter. No 81, December, pp 3-4.

Korb, G., Zdunkowski. 1970. Distribution of radiative energy in ground fog. Tellus. Volume 22, pp 298 – 320.

Koteswaram, P. 1962. Origin of tropical storms over the Indian Oceam. WMO Inter-Regional Seminar of Tropical Cyclones. Tokyo: World Meteorological Organization. Pp 69 – 71.

Kurz, M. 1994. The role of diagnostic tools in modern weather forecasting. Meteorological Applications. Royal Meteorological Society. Volume 1, No 1, pp 45 – 67.

Lee, O., Shun, C. M. 2003. Observation of sea breeze interactions at and near Hong Kong International Airport. Meteorological Applications. Volume 10, No. 1, pp 1 – 9.

Lemon, L. R. 2001. On the Mesocyclone "dry intrusion" and tornadogenesis. Lockheed Martin Ocean, Radar and Senso Systems Weather and ATC Programs. http://www.rubix.net.au/~cadence/lemon7.htm.

Martyn, D. 1992. Climates of the World. Warszawa: Polish Scientific Publishers.
McCaul, E. W., Jr. 1987: Observations of Hurricane Danny tornado outbreak of 16 August 1985. Monthly. Weather Review. No 115, pp 1206 – 1223.

Membery, D. 1997. Unusually wet weather across Arabia. Weather. Volume 52, pp 166 - 174.

Membery, D. A. 1985. Unique August cyclonic storm crosses Arabia. Weather. Volume 40, pp 108 – 115.

Membery, D. A. 1983. Low level wind profiles during the Gulf Shamal. Weather. Volume 38, pp 18-24.

Miller, S. D., A. P. Kuciauskas, M. Liu, Q. Ji, J. S. Reid, D. W. Breed, A. L. Walker, and A. A. Mandoos. 2008. Haboob dust storms of the southern Arabian Peninsula, Journal of Geophysical Research – Atmospheres. Volume 113, 12 January 2008. Pp 26.

Miller, A. 1966. Meteorology. Charles E. Merrill Books, Inc., Columbus, Ohio.

Miller, R. C. 1972: Notes on analysis and severe storm forecasting procedures of the Air Force Global Weather Central. Tech. Rept. 200(R), Headquarters, Air Weather Service, USAF. Pp 190.

National Center of Meteorology and Seismology. 2008. Interpreting Weather Radar Information. http://das.ae/dbz.htm. United Arab Emirates. Accessed 2008-06-03.

Pal Arya, S. 1988. Introduction to Micrometeorology. San Diego: Academic Press Inc.

Petersen, R.A., Lord, J. M. 1997. Personal Computer based Gridded Interactive Display and Diagnostic System (PCGRIDDS), user's guide. National Weather Service, National Oceanic and Atmospheric Administration, Department of Commerce, United States of America.

Petterssen, S. 1956. Weather analysis and forecasting. Volume 1: Motion and motion systems. Second Edition. New York: McGraw-Hill Book Company, Inc. Pp 196 – 213, 294.

Petterssen, S. 1956. Weather analysis and forecasting. Volume 2: Weather and weather systems. Second edition. New York: McGraw-Hill Book Company Inc.

Pruppacher, H. R. and Klett, J. D. 2003. Microphysics of Clouds and Precipitation. Norwall (USA) and Dordrecht: Kluwer Academic Publishers.

Rao, P. G., Hatwar, H. R., AI-Sulaiti, M. H., AI-Mulla, A. H. 2003. Summer shamals over the Arabian Gulf. Weather. Royal Meteorological Society. Volume 58, No. 12, December, pp 472 - 477.

Rao, P. G., Al-Sulaiti, M. H., Al-Mulla, A. H. 2001. Winter shamals in Quatar, Arabian Gulf. Weather. Royal Meteorological Society. Volume 56, No. 12, December, pp 444 - 451.

Ricks, E. L. 1981. Some empirical rules for forecasting fog and stratus over northern Florida, southern Georgia and adjacent coastal waters. NOAA Technical Memorandum NWS SR-104. National Hurricane Center. Miami, Florida. August

Riehl, H. 1954. Tropical Meteorology. New York: McGraw-Hill Book Company.
Riehl, H. 1979. Climate and weather in the Tropics. London: Academic Press.

Rhome, J. R. 2003. Detecting marine winds from space: An introduction to scatterometry and the current operational scatterometers. Mariners Weather Log. Volume 47, Number 2, December.

Roach, W. T., Brown, R., Caughey, S. J., Garland, B. A., Readings, C. J. 1976. The physics of radiation fog: I – A field study. Quarterly Journal of the Royal meteorological Society. Volume 102, pp 313 – 333.

Roach, W. T. 1994. Back to basics: Fog: Part 1 – Definitions and basic physics. Weather. Volume 49, pp 411 – 415.

Roach, W. T. 1995. Back to basics: Fog: part 2 – The formation and dissipation of land fog. Weather. Volume 50, pp 7 – 11.

Robinson, D. N. 1968. Soil erosion by wind in Licolnshire (England). East Midland Geographer. No 30, pp 351 – 363.

Rudloff, W. 1981. World-Climates. Books of the Journal Naturswissenschaftliche Rundschau. Editor, Holl, W. Wissenschaftliche Verlagsgesellschaft mbH, Stuttgart. Pp. 102 and 103.

Safar. M. I. 1985. Dust and dust storms in Kuwait. Directorate of General Civil Aviation, Meteorological Department. State of Kuwait. Pp. 15.

Salazar, V,. Bruintjes, R. T., Breed, D., Jensen, T., Piketh, S., Ross, K., Al Mangoosh, A. and Al Mandoos, A. 2003. Aerosol-cloud interactions in the -United Arab Emirates (2003 - 5ATCHEM). AMS Conference on Atmospheric Chemistry: Gases, Aerosols, and Clouds. Volume 5, 7.12, (no page numbers).

Sanders, F. 1983. Prediction of severe convection. In Meso-scale Meteorology – Theories, Observations and Models, edited by D. K. Lilly and T. D. Gal-Chen. Dordrecht: Reidel Publishing Company.

Showalter, A. K. 1947: A stability index for forecasting thunderstorms. Bulletin of the American Meteorological Society. Volume 34, pp 250 – 252.

Stull, R. 2000. Meteorology for scientists and engineers, second edition. Pacific Grove, California: Brooks/Cole. Pp 151.

Taha, M. F., Harb, S. A., Nagib, M. K., Tantawy, A. H. 1981. The Climate of the Near East. World Survey of Climatology. Chief editor: Landsberg, H. E. Amsterdam, Oxford, New York: Elsevier Scientific Publishing Company. Pp 183 to 192, 215 - 228, 253 - 255.
Taljaard, J.J. 1994-1996. Atmospheric circulation systems, synoptic climatology and weather phenomena of South Africa, parts 1 to 5. South African Weather Bureau. Technical Notes No 27 to 31. Pretoria: Government Printer.

Taljaard, J.J. 1985. Cut-off lows in the South African region. South Africa. South African Weather Bureau. Technical Note No 14. Pretoria: Government Printer.
Tantawy, A. H. I. 1961. The role of the jet stream in the formation of desert depressions in the Middle East. In High level forecasting for turbine engined aircraft operations over Africa and the Middle East. World Meteorological Organization. Technical Note No. 64, pp 159 - 171.

Taylor, G. I. 1917. The formation of fog and mist. Quarterly Journal of the Royal Meteorological Society. Volume 43, pp 241 – 268.

Thesiger, W. 1990. Arabian Sands. Dubai: Motivate Publishing. Pp 241, 226 - 260.

Triegaardt, D. O., Landman, W. A. 1992. Charts of the mean circulation over the monsoon region of the world. South African Weather Bureau. Government Printer, Pretoria Technical paper No. 25.

Tuson, P. 1990. Records of the Emirates. Primary document 1820 – 1958. Archive edition. Volume 8, 1935 – 1947. Trowbridge: Redland Burn, Ltd. Pp 80.

U.A.E. Climate. 1996. First Edition. Ministry of communications. Abu Dhabi: Cultural Foundation Publications.

United Arab Emirates Yearbook. 2001. London: Trident Press Ltd.

United Kingdom Meteorological Office (UKMO). 1997. Source book to the forecasters' reference book. Met.O.1024. Meteorological Office College.

United Kingdom Meteorological Office (UKMO). 1994. Handbook of Aviation Meteorology. 1994. London: Her Majesty's Stationary Office.

United Kingdom Meteorological Office (UKMO). 1991. Meteorological Glossary. 6th edition. London: Her Majesty's Stationary Office.

Webster, P. J. 1983. Large-scale structure of the tropical atmosphere in Large-scale dynamical process in the atmosphere, edited by Hoskins, B. and Pearce, R. London; Academic Press, Inc. Pp 242.

Wheaton, E. E., Chakravarti, A. K. 1990. Dust storms in the Canadian Prairies. International Journal of Climatology. Royal Meteorological Society. Chichester: Wiley. Volume 10, No 8, pp 829 – 837.

Weisman, M. L. and Rotunno, R. 2000. The use of vertical wind shear versus helicity in interpreting supercell dynamics. Journal of the Atmospheric Sciences. Volume 57, May, pp 1452-1472.

Western, S. A. 1997. Weather forecasting for sport fishing in the United Arab Emirates. Weather. Volume 52, pp 121 – 125.

World Meteorological Organization (WMO). 1995. Manual on Codes. Volume I.1, Annex II, Part A. WMO No 306. 1. Geneva: Secretariat of the World Meteorological Organization.

World Meteorological Organization (WMO). 1983. Meteorological Aspects of Certain Processes Affecting Soil Degradation – Especially Erosion. Technical Note No.178. WMO No. 591. Geneva: Secretariat of the World Meteorological Organization.

Xinmei, H., Lyons, T. J., Pitts, R. O. 1990. Fog formation at Perth Airport. Australian Meteorological Magazine. Volume 38, Number 2, June, pp 99-106.

Yates, D. N., Al Mangoosh, A., Al Malki, M. and Bruintjes, R. T. 2005. Seasonal strategies to enhance groundwater recharge in hyper-arid zones (2005 - H20SUPPLY). AMS Conference on Planned and Inadvertent Weather Modification. Vol.16, J6.2, (no page numbers).

Zhu, M., Atkinson, B. W. 2004. Observed and modelled climatology of the land-sea breeze circulation over the Persian Gulf. International Journal of Climatology. Royal Meteorological Society. Volume 24, number 7, pp 883-905.

APPENDIX A

DEFINITIONS

The definitions below were obtained from the American Meteorological Society (AMS) Glossary of Meteorology (1989), or the United Kingdom Meteorological Office (UKMO) Meteorological Glossary (1991).

Adiabatic (process): A thermodynamic change of the state of a system in which there is no transfer of heat or mass across the boundaries of the system. In this process, compression (as in sinking of air) results in warming, expansion (as in rising air) in cooling and meteorologically speaking the process is often considered to be reversible (AMS 1989).

Advection: The process of transport of an atmospheric property solely by the mass motion of the atmosphere (AMS 1989).

Altimeter: An instrument for determining the altitude (generally of an aircraft) with respect to a datum level. The two main types are a (i) radio altimeter and (ii) a pressure altimeter (UKMO 1991).

Anabatic wind: A local wind that blows up a slope which is heated by sunshine. It is a feature which is much less common than its converse, the Katabatic wind (UKMO 1991).

Backing: The changing of the wind direction in an anticlockwise direction in either hemisphere. The opposite is veering of the wind (UKMO 1991).

Baroclinic: A baroclinic atmosphere is one in which surfaces of pressure and density (or specific volume) intersect at some level or levels. The atmosphere is always, to some extent, baroclinic. Strong baroclinicity implies the presence of large horizontal temperature gradients and thus of strong thermal winds (UKMO 1991).

Barotropic: The hypothetical atmosphere in which surface of pressure and density, or specific volume, coincide at all levels (UKMO 1991).

Boundary layer: That layer of a fluid adjacent to a physical boundary in which the fluid motion is much affected by the boundary and has a mean velocity less than the free-stream value. The depth of the boundary layer in the earth's atmosphere varies markedly with static stability, from a few hundred metres in stable conditions to 1 or 2 kilometres in convective conditions (UKMO 1991).

Col: (Also called saddle point, neutral point.) In meteorology, the point of intersection of a trough and a ridge in the pressure pattern of a weather map. It is the point of relatively lowest pressure between two highs and the point of relatively highest pressure between two lows (AMS 1989).

Convergence: See Divergence.

Coriolis force/parameter: An apparent force on moving particles in a non-inertial co-ordinate system. The Coriolis forces per unit mass arises solely from the earth's rotation and

is equal to **-2Ω x V**, where **Ω** is the angular velocity of the earth and **V** is the relative velocity of the particle. The parameter is twice the component of the earth's angular velocity about the vertical**, 2 Ω sin φ**, where **Ω** is the angular speed of the earth and **φ** is the latitude (AMS 1989).

Dew-point temperature: The temperature to which the air must be cooled in order that it shall be saturated with respect to water at its existing pressure and humidity mixing ratio (UKMO 1991).

Diabatic: A diabatic thermodynamic process is one in which heat enters or leaves the system. Meteorological examples are evaporation, condensation and emission and absorption or radiation. The established term "non-adiabatic" is generally preferred because it emphasises the nature of the process involved (UKMO 1991).

Dines compensation: That property of the atmosphere whereby the sign of the divergence is reversed at least once in a vertical column. This implies that the sign integrated divergence from the earth's surface to the top of the atmosphere, and the associated surface pressure tendency, are small residuals of much larger contributions. In general, a single change of the sign occurs in the troposphere, and regions of convergence and divergence are separated by a level of zero divergence which is usually at around 600 hPa (UKMO 1991).

Diurnal variation: The changes of value, for example of a meteorological element, within the course of a solar day, more specifically the systematic changes that occur within the average day (UKMO 1991).

Divergence: The divergence of the flux of a quantity (e.g. radiation or momentum) expresses the time rate of depletion of the quantity per unit volume. Negative divergence is termed convergence and relates to the rate of accumulation. In meteorology, divergence (or convergence) is mostly used in relation to the velocity vector and so refers to the flux of air particles themselves. The divergence of velocity is a three dimensional property which expresses the time rate of expansion of the air per unit volume (UKMO 1991).

Dry adiabatic lapse rate (DALR): The rate of decrease of temperature with height of a parcel of dry air lifted adiabatically through an atmosphere in hydrostatic equilibrium. The rate is 0.98°C per 100 metres, or approximately, 3°C per 1000 feet (UKMO 1991 and AMS 1989).

Equivalent potential temperature: The (isobaric) equivalent temperature (T_c) of a moist air sample is the temperature that would be attained on the assumption of condensation at constant pressure of all the water vapour in the sample, all the latent heat released in the condensation being used to raise the temperature of the sample. The equivalent potential temperature (θ_e) is found on an aerological diagram by progressing along the dry adiabatic line from T_c to the 1000 hPa level (UKMO 1991).

Environmental lapse rate: The rate of decrease of temperature with elevation (AMS 1989).

Friction layer: The atmospheric layer, extending from the earth's surface to about 600 m (2000 feet) above ground in which the influence of surface friction on air motion is appreciable (UKMO 1991).

Geopotential metre (gpm): Geopotential is the potential energy acquired by a unit mass on being raised through a unit distance in a field of gravitational force of unit strength. Dynamically, a dynamic height unit, on average over the world, is a better measure of height in the atmosphere than is geometric height (UKMO 1991).

Gust: A sudden brief increase in the speed of the wind. This may be vertically or horizontally AMS 1989).

Haboob: Many variant spellings, including habbub, habub, haboub, hubbob, hubbub.) A strong wind and sandstorm or duststorm in northern and central Sudan, especially around Khartoum, where the average number is about 24 a year. The name comes from the Arabic word habb, meaning "wind." Haboobs are most frequent from May through September, especially in June, but they have occurred in every month except November. Their average duration is three hours; they are most severe in April and May when the soil is driest. They may approach from any direction, but most commonly from the north in winter and from the south, southeast, or east in summer. The average maximum wind velocity is over 13 m s^{-1} (30 mph) and a speed of 28 m s^{-1} (62 mph) has been recorded. The sand and dust form a dense whirling wall that may be 1000 m (3000 ft) high; it is often preceded by isolated dust whirls. During these storms, enormous quantities of sand are deposited. Haboobs usually occur after a few days of rising temperature and falling pressure (AMS 1989). Also, the name derived from the Arabian habb meaning to blow, applied to a duststorm in the Sudan north of about 13°N. Such storms occur from about May to September and are most frequent in the afternoon and evening (UKMO 1991).

Hadley circulation: A direct thermally driven and zonally symmetric circulation under the strong influence of the earth's rotation, first proposed by George Hadley in 1735 as an explanation for the trade winds. It consists of the equator ward movement of the trade winds between about latitude 30° and the equator in each hemisphere, with rising wind components near the equator, pole ward flow aloft, and, finally, descending components at about latitude 30° again (AMS 1989).

Hydrostatic equilibrium: The state of a fluid whose surfaces of constant pressure and constant mass (or density) coincides and are horizontal throughout (AMS 1989).

Instrument landing system: (Abbreviated ILS.) A navigational aid used to facilitate the landing of an aircraft in instrument weather at an airport. The instrument landing system consists of two parts: 1) a directional guide to bring the plane to the correct runway; and 2) a glide path to bring the plane down at the correct glide angle or slope to touch the runway at the correct point (AMS 1989).

Isotherm (isothermal): Of equal or constant temperature, with respect to either space or time (AMS 1989).

Jet stream: Relatively strong winds concentrated in a narrow stream in the atmosphere. For the purposes of this dissertation it refers to the jet stream in the upper troposphere. The jet stream as a narrow current of air, generally near the tropopause, thousands of kilometres long, about hundreds of kilometres wide and a few kilometres deep, with strong vertical and horizontal wind shear (UKMO 1991).

Katabatic wind: On a "radiation night" of clear skies and weak pressure gradient, log-wave radiation from the earth's surface causes a layer of cold air to form near the surface of the ground with an associated temperature inversion. If the ground is sloping, the air close to the ground is colder than air at the same level but at a horizontal distance. Down slope gravitational flow of the colder and denser air beneath the warmer and lighter air produces the Katabatic, or drainage, wind (UKMO 1991).

K Index: (Also called George's index, 1960). A stability index that is a measure of thunderstorm potential based on temperature lapse rate, moisture content of the lower troposphere, and the vertical extent of the moist layer. The K index is determined by the following equation:

$$K = (850\ hPa\ T - 500\ hPa\ T) - 850\ hPa\ Td - (700\ hPa\ T - 700\ hPa\ Td),$$

where T is the temperature and Td is the dew-point in degrees Celsius at the pressure levels indicated. The higher (positive) the K index, the greater the likelihood of thunderstorm development (AMS 1989).

Lifted Index: This index, developed by Galway (1956), is

$$L = (T_L - T_{500}),$$

so is nominally identical to the Showalter index, except that the parcel being lifted (dry-adiabatically to saturation and then moist-adiabatically to 500 hPa) is defined by the dry adiabat running through the predicted surface afternoon temperature maximum and the mean mixing ratio in the lowest 900 m of the sounding. If no further heating is expected, as with a sounding taken in the late afternoon, then the mean potential temperature in the lowest 900 m of the sounding defines the dry adiabat used for the parcel. Numerous variations, focused on how the lifted parcel is defined, have been used since the original definition. The values of this index tend to be somewhat lower than those of Showalter, and the interpretation depends to some extent on how the lifted parcel is defined (AMS, 1989).

Nashi: Also spelled N'aschi. The Arabic name for a north-easterly wind that occurs in winter on the Iranian coast of the Arabian Sea, especially near the entrance to the gulf and also on the Makran coast. It is probably of the bora type, though less strong, representing the outflow of cold air from central Asia. The N'aschi is part of the Asiatic monsoon system (AMS, 1989).

Numerical weather prediction (also numerical forecasting): The forecasting of the behaviour of atmospheric disturbances by the numerical solution of the governing fundamental equations of hydrodynamics, subject to observed initial conditions, performed with the aid of high-speed computing devices (AMS 1989).
Okta: Unit, equal to area of one eight of the sky, used in specifying cloud amount (UKMO 1991).

Pascal: The SI derived unit of pressure. One pascal (Pa) is equal to 1 newton m^{-2}. The kilopascal (kPa) is the preferred unit for atmospheric pressure, but the more familiar millibar (mb) is the unit of pressure generally used by meteorologists (in the USA, Author), by international agreement; 1 mb = 1 hPa (hectopascal). For a typical sea level pressure, 102.345 kPa = 1023.45 hPa = 1023.45 mb (AMS, 1989).

Potential temperature: The temperature a parcel of dry air would have if brought adiabatically from its initial state to the (arbitrarily selected) standard pressure of 1000 hPa (AMS 1989).

Runway visual range (RVR): The maximum distance in the direction of take-off, or landing, at which the runway, or the specified lights delineating the runway can be seen from a position on the centreline at a height corresponding to the average eye-level of the pilot at touchdown (UKMO 1991).

Saturated adiabatic lapse rate (SALR): The rate of decrease of temperature with height of a parcel of saturated air lifted in a saturation-adiabatic process through an atmosphere in hydrostatic equilibrium. The saturation-adiabatic process is maintained at saturation by the evaporation or condensation of water substance, the latent heat being supplied by or to the air, respectively. The rate is about half of the DALR, that is, about 1.5°C per 1000 feet (UKMO 1991 and AMS, 1989).

Showalter stability index: An index given by

$$S = (T_{500} - T_L)$$

where T_L is the temperature (°C) of a parcel lifted from 850 hPa to 500 hPa, dry-adiabatically to saturation and moist adiabatically above that. As the index decreases to zero and below, the likelihood of showers and thunderstorms is considered to increase (Showalter, 1947) (AMS, 1989).

Statically stable (static stability): The stability of the atmosphere in hydrostatic equilibrium with respect to vertical displacements. The criterion for stability is that a displaced parcel of air be subjected to a buoyant force opposite to its displacement. For example a parcel displaced upward becomes colder than its new environment and will attempt to sink back to its original level once the disturbing force ceases (AMS 1989).

Stratosphere: The atmosphere above the troposphere and below the mesosphere. It is characterised by stable atmospheric conditions (AMS 1989).

Superadiabatic lapse rate: An environmental lapse rate greater than the dry-adiabatic lapse rate, such that potential temperature decreases with height (AMS 1989).

Temperature inversion: A layer in which temperature increases with altitude. A typical trait is its marked static stability, so that very little turbulent exchange can occur within it. Strong wind shears often occur across inversion layers (AMS 1989).

Total Totals Index: The index is attributable to Miller (1972). It is defined as the sum of two indices:

$$TT = VT + CT$$

Where VT is the Vertical Totals index, defined by

$$VT = T_{850} - T_{500},$$

A value of about 40 corresponds to a dry-adiabatic lapse rate. For a moist adiabatic lapse rate it is about 20 for T_{850} = 15°C, about 30 for T_{850} = 0°C. The Cross Totals index, CT, is defined by

$$CT = D_{850} - T_{500}$$

So it is strongly influenced by the 850 hPa moisture. Showers and thunderstorms become increasingly likely from TT values of about 30, and severe thunderstorms are considered likely for values of 50 or more (AMS 1989).

Tropopause: The boundary between the troposphere and stratosphere, usually characterised by an abrupt change of atmospheric stability. The change is to more stable conditions compared with those below the tropopause (AMS 1989).
Troposphere: The portion of the atmosphere from the earth's surface to the tropopause. This is the lowest 10 to 20 km of the atmosphere (AMS 1989).

Turbulence: A state of fluid flow in which the instantaneous velocities exhibit irregular and apparently random fluctuations. When encountered by an aircraft in flight it results in bumpy and uncomfortable flying conditions. A common cause of turbulence is wind shear (AMS 1989).

Veering: This is the clockwise change of wind direction in either hemisphere. The opposite is backing of the wind (UKMO 1991).

Wet-bulb potential temperature: The wet-bulb potential temperature (θ_w) at any level is obtained on an aerological diagram as that temperature at which the saturated adiabatic through the wet-bulb potential temperature at the level concerned intersects the 1000 hPa isobar. It is, for practical purposes, conservative for processes such as evaporation or condensation and for both dry adiabatic and saturated adiabatic temperature changes. It is therefore a useful property for air-mass analysis (UKMO 1991).

Wind shear: The local variation of the wind vector or any of its components in a given direction. The shear may be in the vertical or horizontal. In other words, wind shear is a marked change in wind speed and/or direction, either vertically or horizontally, spatially and with respect to time (AMS 1989).

APPENDIX B

CONVERSIONS

Conversions from knots to metres per second and feet to metres from the Handbook of Aviation Meteorology, 1994. London: HMSO Publications Centre. Page 355.

KNOTS TO METRES PER SECOND

1 knot = 0.51479 metres per second

Knots	0	1	2	3	4	5	6	7	8	9
	metres per second									
0	0.0	0.5	1.0	1.5	2.1	2.6	3.1	3.6	4.1	4.6
10	5.1	5.7	6.2	6.7	7.2	7.7	8.2	8.8	9.3	9.8
20	10.3	10.8	11.3	11.8	12.4	12.9	13.4	13.9	14.4	14.9
30	15.4	16.0	16.5	17.0	17.5	18.0	18.5	19.0	19.6	20.1
40	20.6	21.1	21.6	22.1	22.7	23.2	23.7	24.2	24.7	25.2
50	25.7	26.3	26.8	27.3	27.8	28.3	28.8	29.3	29.9	30.4
60	30.9	31.4	31.9	32.4	32.9	33.5	34.0	34.5	35.0	35.5
70	36.0	36.6	37.1	37.6	38.1	38.6	39.1	39.6	40.2	40.7
80	41.2	41.7	42.2	42.7	43.2	43.8	44.3	44.8	45.3	45.8
90	46.3	46.8	47.4	47.9	48.4	48.9	49.4	49.9	50.4	51.0
100	51.5	52.0	52.5	53.0	53.5	54.1	54.6	55.1	55.6	56.1

FEET TO METRES

1 foot = 0.3048 metres

1000's of feet	.0	.1	.2	.3	.4	.5	.6	.7	.8	.9
	metres									
0	0	305	610	915	1219	1524	1829	2134	2438	2743
10	3048	3352	3657	3962	4267	4572	4877	5182	5486	5791
20	6096	6401	6706	7011	7351	7620	7924	8229	8534	8839
	kilometres									
30	9.1	9.5	9.8	10.1	10.4	10.7	11.0	11.3	11.6	11.9
40	12.2	12.5	12.8	13.1	13.4	13.7	14.0	14.3	14.6	14.9
50	15.2	15.5	15.9	16.2	16.5	16.8	17.1	17.4	17.7	18.0
60	18.3	18.6	18.9	19.2	19.5	19.8	20.1	20.4	20.7	21.0
70	21.3	21.6	22.0	22.3	22.6	22.9	23.2	23.5	23.8	24.1
80	24.4	24.7	25.0	25.3	25.6	25.9	26.2	26.5	26.8	27.1
90	27.4	27.7	28.0	28.4	28.7	29.0	29.3	29.6	29.9	30.2
100	30.5									

Note: Metres are rounded off to the nearest whole metre; kilometres are rounded off to the nearest tenth of a kilometre; 500 feet = 152 metres.

Microbar

1 microbar = one millionth of a bar
1 bar = 100 000 Pascals (Pa)
100 Pascals = 1 hectopascal (hPa)
Examples; 0.6 microbars = 0.06 Pa, 35 microbars = 3.5 Pa.

APPENDIX C

FOG INDICES

1 SAUNDERS' METHOD OF CALCULATION OF RADIATION FOG POINT (UKMO 1997).

The method takes account of moisture throughout the cooling layer; it is based on Mk. llb radiosonde profiles; Mk. ill *Td* data may differ.

(i) Select a representative upper-air sounding and find the condensation level from the maximum temperature and the dew point at that time, using Normand's theorem.

(ii) Find the humidity mixing ratio at the condensation level and read off the temperature where the humidity mixing ratio line cuts the surface isobar. This is the expected fog-point temperature.

This procedure needs modification to allow for different types of sounding (see figure below):

(a) *Type I* has a constant dew-point lapse rate except near the ground where the surface dew-point lies on, or to the right of, a downward extension of the upper dew-point curve. *T* is the maximum temperature and Td is the surface dew-point. If there is a superadiabatic, use the value *Tc* instead of *T* to eliminate the superadiabatic section. The pecked lines through *Tc* and the dew point Td meet at the condensation level A. The humidity mixing ratio at this level is at B and the fog point is at C.

(b) In *Type II* the dew-point lapse rate increases aloft. Point B is found by extrapolating the lower part of the dew point curve above the point at which the lapse rate increases.

(c) In *Type III* the surface dew point lies to the left of the downward extension of the upper dew-point curve, two possibilities are illustrated:

(i) If the temperature lapse in the lowest layers is less than a dry adiabatic, the construction follows the basic principles as for *Type l.*

(ii) If the temperature lapse rate in the lowest layer is equal to or greater than a dry adiabat, then no Normand construction is drawn and the fog point is taken to equal the dew-point.

Normally, if the boundary layer is mixed at the time of the midday sounding, extending the mean mixing-ratio through the boundary layer to the surface will give an acceptable fog point. As a rough guide, the afternoon dew point at screen level minus 2˚C gives a good first guess for Tr>- 2˚C.

Notes:
(i) If a subsidence inversion has brought dry air down to within 30 hPa of the ground, use the dew point *(Td)* as the fog-point.
(ii) If rain falls during the afternoon leaving the ground wet, the actual fog point may be higher than the calculated value.

(iii) If a sea-breeze reaches the area later in the day, the fog point may be much higher than calculated; use the coastal dew point.
(iv) The dew-point temperature 60 hPa above the surface nearly always gives a fog-point value close to Saunders' value, exception being *Type /lIb* when the surface dew-point is used.
(v) If the calculated temperature is ≤0˚C, then the actual fog point may well be lower (due to deposition by hoar frost).

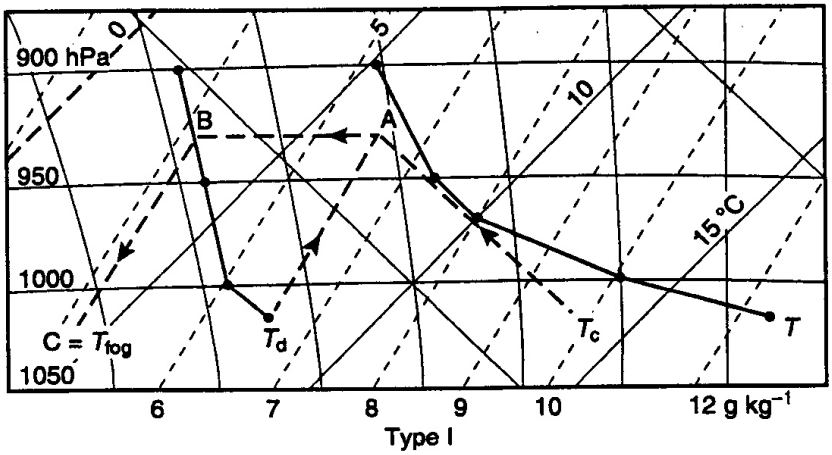

Type I

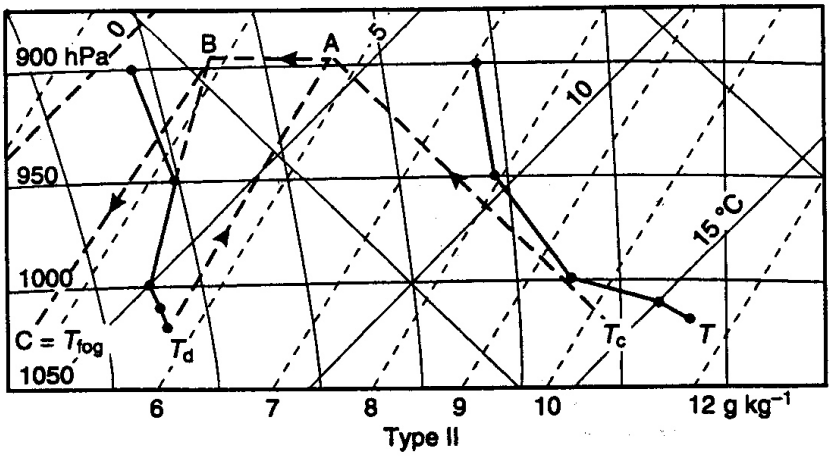

Type II

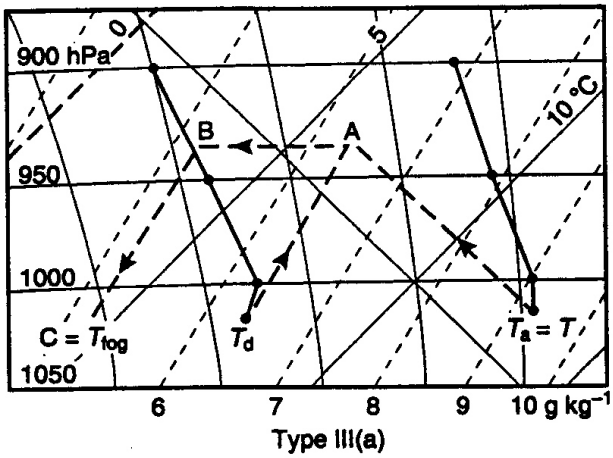

Type III(a)

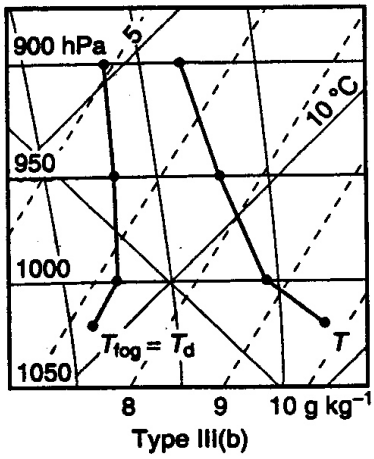

Type III(b)

2 CRADDOCK AND PRITCHARD METHOD (UKMO 1997)

If T_f is the fog point, T_{12} is the screen temperature at 1200 UTC, and T_{d12} is the dew point at 1200 UTC, then

$$T_f = 0.044\ (T_{12}) + 0.844\ (T_{d12}) - 0.55 + A = Y + A.$$

Table 1. Values of Y (°C) corresponding to the observed values of T_{12} and T_{d12}

	T_{12}								
T_{d12}	30	25	20	15	10	5	0	-5	-10
20	17.7	17.4	17.2						
18	16.0	15.7	15.5						
16	14.3	14.1	13.8						
14	12.6	12.4	12.1	11.9					
12	10.9	10.7	10.5	10.2					
10	9.2	9.0	8.8	8.6	8.3				
8	7.5	7.3	7.1	6.9	6.6				
6	5.8	5.6	5.4	5.2	5.0				
4	4.1	3.9	3.7	3.5	3.3	3.0			
2	2.5	2.2	2.0	1.8	1.6	1.4			
0	0.8	0.6	0.3	0.1	-0.1	-0.3	-0.6		
-2	-0.9	-1.1	-1.4	-1.6	-1.8	-2.0	-2.2		
-4	-2.6	-2.8	-3.0	-3.3	-3.5	-3.7	-3.9		
-6	-4.3	-4.5	-4.7	-5.0	-5.2	-5.4	-5.6	-5.8	
-8	-6.0	-6.2	-6.4	-6.6	-6.9	-7.1	-7.3	-7.5	
-10	-7.7	-7.9	-8.1	-8.3	-8.6	-8.8	-9.0	-9.2	-9.4

Table 2. The number A (°C) is an adjustment which depends upon the forecast cloud amount and geostrophic wind speed, as tabulated below.

*Mean cloud amount (oktas)	*Mean geostrophic wind speed (kn)	
	0 - 12	13 - 25
0 – 2	0.0	-1.5
2 – 4	0.0	0.0
4 – 6	+1.0	+0.5
6 – 8	+1.0	+0.5

*Mean of forecast values for 1800, 0000 and 0600 UTC.

Notes:

(a) The equation for T_f was derived from the combined data for 13 widely separated stations in England. There was considerable variation from station to station in their proximity to major smoke sources.

(b). Account was not taken of variations in atmospheric pollution so that, in effect, an average degree of pollution is assumed in using this technique (in contrast to Saunders' method which refers mainly to fog in clean air).

(c). If the minimum temperature is predicted using Craddock and Pritchard' s method it is suggested That:

(i) if T_f is 1 °C or more above T min, forecast fog;

(ii) if T_f is 0.5 °C above to 1.5 °C below T min, forecast a risk of fog;
(iii) if T_f is 2 °C or more below T min, do not forecast fog.

(d). When forecasting for a region, rather than a specific airfield, allow a larger safety margin, since there is always more low-level moisture present near streams and in lush valleys than over flat airfields with trimmed grass.

3 TEST SAMPLE OF FOG INDICES

Table 1. Summer event 2002-07-18/22 and winter 2003-01-08/11 using fog indices. Temperatures rounded to whole degrees

Key:
Saunders = Saunders method.
C & P = Craddock & Pritchard.
850WBPT = 850 wet-bulb potential temperature.
12T/Td = 1200 UTC surface wet-bulb temperature (12T/Td).
00T/12Td = Surface wet-bulb temperature using 0000 UTC temperature and 1200 UTC dew point temperature.
FogT = Temperature at which the fog began.
MnT = Early morning minimum temperature.
V = Calculated fog index temperature.
D = Difference from the temperature at which the fog began.

Date	Saunders		C & P		850WBPT		12 T/Td		00T/12Td		FogT	MnT
	V	D	V	D	V	D	V	D	V	D		
2002-7												
18/19	10	-19	26	-3	20	-9	31	+2	32	+3	29	29
19/20	-8	-39	25	-6	19	-12	31	0	29	-2	31	30
20/21	21	-10	26	-5	19	-12	31	+0	30	-1	31	29
21/22	-5	-34	23	-6	14	-15	28	-1	28	-1	29	29
2003-01												
08/09	9	-3	14	+2	10	- 2	18	+6	15	+3	12	11
09/10	0	-14	12	-3	11	- 4	18	+3	14	-1	15	14
10/11	3	-12	14	-1	14	- 1	18	+3	15	0	15	12